

Effects of changing N:P supply on phytoplankton in the eastern tropical Pacific and Atlantic Ocean

Dissertation
zur Erlangung des Doktorgrades
der Mathematisch-Naturwissenschaftlichen Fakultät
der Christian-Albrechts-Universität zu Kiel

vorgelegt von
Jasmin Maria Seraphine Franz

Kiel 2012

Referent/in: Prof. Dr. Ulf Riebesell

Koreferent/in: Prof. Dr. Ulrich Sommer

Table of contents

Zusammenfassung	3
Summary	5
I. Introduction	7
Oxygen minimum zones and climate change	7
Coastal upwelling areas	11
Cyanobacteria of the tropical oligotrophic ocean	15
Controls of phytoplankton stoichiometry	16
Nutrient limitation of phytoplankton	18
Major objectives and thesis outline	19
II. Manuscripts	23
Study 1. Dynamics and stoichiometry of nutrients and phytoplankton in waters influenced by the oxygen minimum zone in the tropical eastern Pacific	23
Study 2. Changes in N:P stoichiometry influence taxonomic composition and nutritional quality of phytoplankton in the Peruvian upwelling	51
Study 3. Effect of variable nutrient enrichment on the functional composition of a phytoplankton community in the eastern tropical Atlantic	75
Study 4. Production, partitioning and stoichiometry of organic matter under variable nutrient supply during mesocosm experiments in the tropical Pacific and Atlantic Ocean	97
III. Synthesis and future perspectives	119
Nitrogen as primary limiting nutrient for phytoplankton growth	120
N ₂ -fixation in the realm of coastal upwelling areas	122
Multiple controls of cellular N:P stoichiometry	124
Ecological implications for coastal upwelling areas	125
Perspectives	127
References	131
Contribution of authors	149
Danksagung	151
Eidesstattliche Erklärung	153

Zusammenfassung

Steigende Temperaturen der Meeresoberfläche im Zuge der globalen Klimaveränderung fördern durch eine verstärkte Schichtung der Wassersäule und eine reduzierte Sauerstofflöslichkeit die Ausbreitung von intermediären Wasserschichten mit niedrigem Sauerstoffgehalt, und verändern hierdurch die redox-sensitiven Nährstoffreservoirs. Marine Sauerstoffminimumzonen (SMZ) treten vornehmlich in den östlichen Gebieten des tropischen Pazifiks und Atlantiks auf, wo der Auftrieb kalter, nährstoffreicher Wassermassen an der Küste eine hohe Primär- und indirekt auch eine hohe Sekundärproduktion ermöglicht. SMZ fördern den Netto-Verlust an anorganischem Stickstoff (N), begünstigen jedoch gleichzeitig die Freisetzung von anorganischem Phosphor (P) aus dem Schelfsediment in die Wassersäule. Sauerstoffarmes Wasser, das durch Auftrieb in die Oberflächenschicht zu den Primärproduzenten transportiert wird, hat somit eine relativ niedrige N:P Nährstoffzusammensetzung. Aufgrund der erwarteten Ausbreitung tropischer SMZ wurde die Reaktion von Phytoplankton auf Veränderungen im N:P-Nährstoffangebot hinsichtlich Produktion, Artenzusammensetzung der Gemeinschaft und elementarer Stöchiometrie im tropischen Ostpazifik und –atlantik untersucht.

Während Nährstoffanreicherungs-Experimente, die in Mesokosmen an Deck im Rahmen dreier Forschungsausfahrten durchgeführt wurden, war die Gesamtprimärproduktion jeweils ausschließlich durch den Eintrag von N kontrolliert. Kombinierte Zugaben von N und P konnten keinen weiteren Anstieg in der Biomasseproduktion hervorrufen. Für diese Reaktion waren vorwiegend Diatomeen verantwortlich, da diese die Phytoplanktongemeinschaft in den Mesokosmen nach der Nährstoffzugabe in allen Experimenten dominiert haben. Jedoch konnte ein Einfluss der Nährstoffanreicherung auf die Artenzusammensetzung innerhalb der Phytoplanktongemeinschaft festgestellt werden, wobei einige flagellate Photoautotrophe (*Phaeocystis globosa*, *Heterosigma* sp.) bevorzugt bei niedrigen N:P-Verhältnissen auftraten. Im Gegensatz zu Model-Simulationen zeigten weder die Mesokosmenexperimente noch eine biogeochemische Feldstudie vor der Küste Perus eine Wachstumsstimulierung von stickstofffixierenden Cyanobakterien unter niedrigen N:P-Verhältnissen. Ein Überschuss an P erscheint ein notwendiger aber nicht hinreichender Faktor für die Entwicklung von diazotrophem Phytoplankton zu sein. Spezifische Phytopigmente und funktionelle Gene in den Experimenten weisen allerdings auf eine Entwicklung von stickstofffixierenden Cyanobakterien in Sukzession zu Diatomeenblüten nach Nährstofferschöpfung hin.

Die N:P-Stöchiometrie von Phytoplankton war unter nährstoffarmen Bedingungen sehr flexibel und korrelierte mit dem N:P-Verhältnis des Nährstoffeintrags während der Experimente. Demzufolge ist die elementare Zusammensetzung des Phytoplanktons stark von der gegenwärtigen Wachstumsphase abhängig. Zudem wurde eine große Variabilität in der N:P-Zusammensetzung unterschiedlicher funktioneller Phytoplanktongruppen beobachtet. Große,

exponentiell wachsende Mikroalgen (z.B. Diatomeen) der eutrophen Schelfgewässer besaßen niedrige N:P-Verhältnisse ($\sim 10:1$), bedingt durch ihren P-reichen auf schnellen Zellaufbau ausgerichteten Metabolismus. Picoplanktonische Algen (z.B. *Prochlorococcus*) im oligotrophen offenen Ozean zeichneten sich durch hohe N:P-Verhältnisse ($>20:1$) aus, was wiederum auf ihren hohen Proteingehalt, der für die effiziente Ressourcenbeschaffung benötigt wird, zurückzuführen ist. Somit weisen meine Ergebnisse auf eine multiple Kontrolle der N:P-Zusammensetzung in Phytoplankton durch das Nährstoffangebot, die Wachstumsphase sowie der klassenspezifischen Wachstumsstrategie hin.

Resultate dieser Studie deuten auf einen abnehmenden Trend von diatomeen-dominierte Primärproduktion und auf eine potentielle Verschiebung der Zusammensetzung der Phytoplanktongemeinschaft auf dem Schelf von großen mikrop planktonischen Arten hin zu Nanoplankton hin. Diese Veränderung des Größenspektrums hätte unmittelbare Konsequenzen für das gesamte Nahrungsnetz des Auftriebssystems. Ferner spielen Diatomeen eine Schlüsselrolle im Transport von organischem Material in die Tiefe, folglich könnte die Sauerstoffverarmung die Bindung von Kohlenstoffdioxid im Ozean auf indirektem Weg reduzieren. Ergebnisse dieser Arbeit konnten die auf Modellen basierende Hypothese über den stimulierenden Wachstumseffekt niedriger N:P-Nährstoffverhältnisse auf diazotrophe Cyanobakterien nicht bestätigen. Stattdessen deuten sie auf eine Entkopplung von N-Verlust und der Kompensierung des N-Defizits über die Stickstofffixierung durch Cyanobakterien hin. Dennoch suggeriert die Aufeinanderfolge von Diatomeen und Diazotrophen, dass, zusätzlich zu den üblichen Verbreitungsgebieten von Stickstofffixierern im oligotrophen offenen Ozean, Schelfgewässer das Wachstum von diazotrophen Cyanobakterien nach Aufzehrung von N durch Diatomeen im Anschluß an Auftriebsevents begünstigen.

Summary

Rising sea surface temperatures in the course of global climate change promote expansion of oxygen-depleted intermediate waters due to strengthened water column stratification and reduced oxygen solubility, thereby modifying the redox-sensitive nutrient inventories. Marine oxygen minimum zones (OMZ) occur primarily on the eastern margins of the tropical Pacific and Atlantic Ocean, where cold nutrient-rich water is transported into the surface layer via coastal upwelling, enabling high primary and indirectly also high secondary production. OMZs facilitate net loss of inorganic nitrogen (N), but simultaneously promote the release of inorganic phosphorus (P) from the shelf sediment. O₂-deficient water supplied to primary producers in the surface layer via upwelling has consequently a relatively low N:P nutrient composition. Based on the predicted expansion of tropical OMZs, the response of phytoplankton to changes in N:P supply with regard to production, community composition and elemental stoichiometry in the eastern boundary regions of the tropical Pacific and Atlantic Ocean was investigated.

Total primary production during nutrient enrichment experiments performed in shipboard mesocosms on three cruises was solely controlled by N supply. Combined addition of N and P could not stimulate a further increase in biomass production. Diatoms were the main contributors to this overall response, as they dominated the phytoplankton community in the mesocosms after nutrient enrichment within all experiments. Yet, a different effect of nutrient enrichment was detected within the phytoplankton community, as some nanoflagellates (*Phaeocystis globosa*, *Heterosigma* sp.) were favoured by low N:P supply ratios. Contrary to model simulations, neither mesocosm experiments nor a biogeochemical field survey off the coast of Peru could show a stimulation of growth of nitrogen-fixing cyanobacteria under low N:P conditions. Excess P appears to be a necessary but not sufficient factor for development of diazotrophic phytoplankton. However, diagnostic phytopigments and functional genes in the experiments suggest development of nitrogen-fixing cyanobacteria under nutrient exhaustion in succession to diatom blooms.

The N:P stoichiometry of phytoplankton was highly flexible under nutrient depletion and correlated with the N:P supply ratio during the experiments. Thus, phytoplankton elemental composition is strongly constrained by the current growth phase. Furthermore, a large variability in the N:P composition according to functional types of phytoplankton was observed. Large blooming microalgae (e.g. diatoms) of the eutrophic shelf waters featured low N:P ratios owing to their P-rich metabolism optimized for fast cell assembly. Picoplankton algae (e.g. *Prochlorococcus*) of the oligotrophic open ocean was characterized by a high N:P composition, caused by large amounts of proteins required for efficient resource acquisition. Hence, these results indicate a multiple control of phytoplankton N:P stoichiometry by nutrient supply, the current growth phase and the group-specific growth strategy.

Findings from this thesis suggest a declining trend in diatom-dominated primary production and a potential shift in the taxonomic composition of the shelf phytoplankton community from large microplanktonic species towards nanoplankton. Consequences of a change in food size spectra can be expected to propagate along the entire food web of the upwelling system. Furthermore, diatoms are a key control of the downward export of organic matter, thus deoxygenation may indirectly reduce the biological sequestration of carbon dioxide in the ocean. Results from this thesis could not confirm the model-based hypothesis about a stimulating growth effect on diazotrophic cyanobacteria by low nutrient N:P, but indicate rather a decoupling of N loss and compensation of the N-deficit via cyanobacterial N_2 -fixation. Yet, succession of diatoms and diazotrophs suggests that, in addition to the common distribution of N_2 -fixers in the oligotrophic open ocean, shelf waters may facilitate growth of diazotrophic cyanobacteria after N depletion by diatoms subsequent to upwelling events.

I Introduction

Oxygen minimum zones and climate change

Like most living environments on earth, the ocean faces times of strong change as a result of enhanced anthropogenic activity since the beginning of industrialization in the 18th century. Above all, the combustion of fossil fuels had and still has a tremendous impact not only on global climate (IPCC, 2007), but also on the world's oceans. Increasing emissions of greenhouse gases such as carbon dioxide (CO₂) and nitrous oxide (N₂O) have caused a net increase in sea surface temperature particularly in the last 60 years (Levitus et al., 2000). Rising temperatures in the atmosphere as in the sea have an apparent impact on high latitude hydrology by promoting melting of sea ice and icebergs. But ocean warming has also a significant effect on the hydrography of the low latitude ocean by intensifying stratification of the upper water body. Vertical expansion of the thermocline increasingly impedes ventilation of the subjacent water parcel, reducing supply of dissolved oxygen (O₂) into the ocean's interior (Keeling and Garcia, 2002; Matear and Hirst, 2003). Rising water temperatures are further promoting a general seawater deoxygenation by lowering O₂ solubility (Shaffer et al., 2009). The so-called oxygen minimum zones (OMZs), located below the euphotic zone between about 100–900 m depth, are major characteristics of eastern boundary current systems in the Atlantic and Pacific Ocean (Karstensen et al., 2008; Fuenzalida et al., 2009), as well as of the monsoon-influenced regions of the Arabian Sea and the Bay of Bengal in the Indian Ocean (Helly and Levin, 2004) (Fig. I.1).

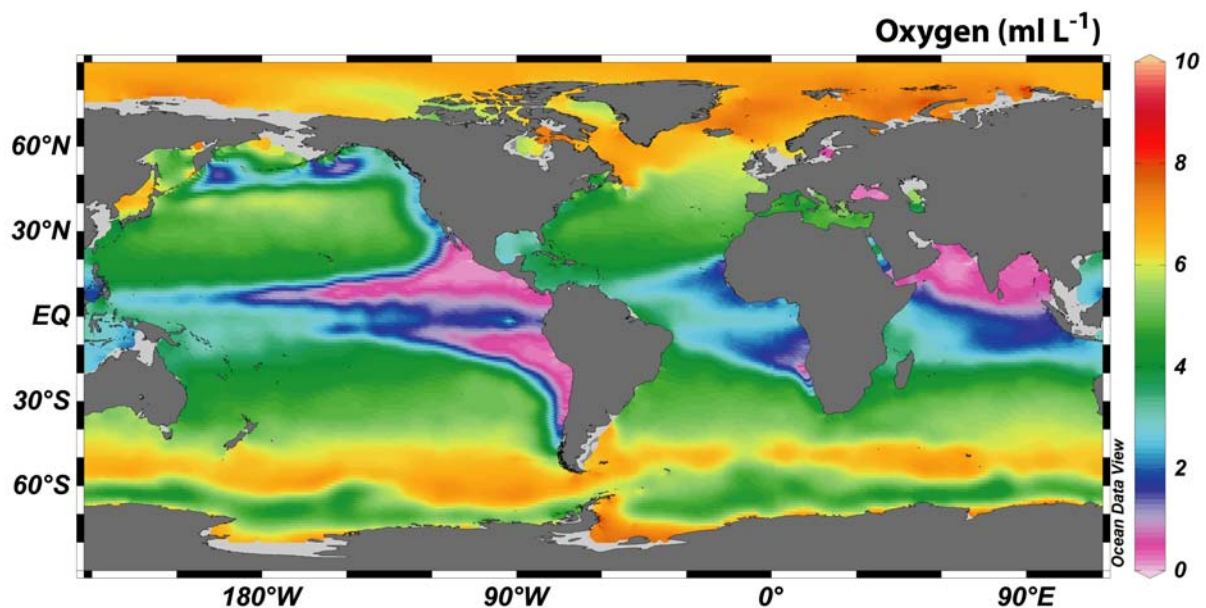


Figure I.1. Mean annual global distribution of dissolved oxygen at 200 m depth (from World Ocean Atlas (WOA) 2009; Garcia et al., 2010a).

Tropical OMZs are commonly situated in high productivity eastern boundary upwelling areas. Microbial degradation of large amounts of exported organic material contributes additionally to the subsurface O_2 -deficit (Helly and Levin, 2004). Human-induced eutrophication of coastal seas via run-off and atmospheric deposition of nutrients with industrial or agricultural origin are further enhancing the imbalance between O_2 demands and resupply (Rabalais et al., 2010).

Seawater O_2 concentrations below $20 \mu\text{mol kg}^{-1}$ are typical for the center of the OMZs in the East Pacific and the Indian Ocean, but even complete absence of measurable O_2 has been frequently observed (Karstensen et al., 2008). The East Atlantic OMZs, in contrast, appear rather moderate in terms of O_2 -deficiency with minimum levels of $40 \mu\text{mol O}_2 \text{ kg}^{-1}$.

Deoxygenation of the ocean's interior has multiple implications on nutrient cycling, ecosystem productivity and marine life. Key fluxes of N and P in the realm of the OMZ are illustrated in Fig. I.2. Sub- or anoxic conditions, in the water-column as well as in the sediment, provide an ideal environment for a unique microbial community consisting amongst others of denitrifiers, chemolithotrophs, nitrifiers, sulphur bacteria and proteobacteria (Stevens and Ulloa, 2008; Stewart et al., 2011).

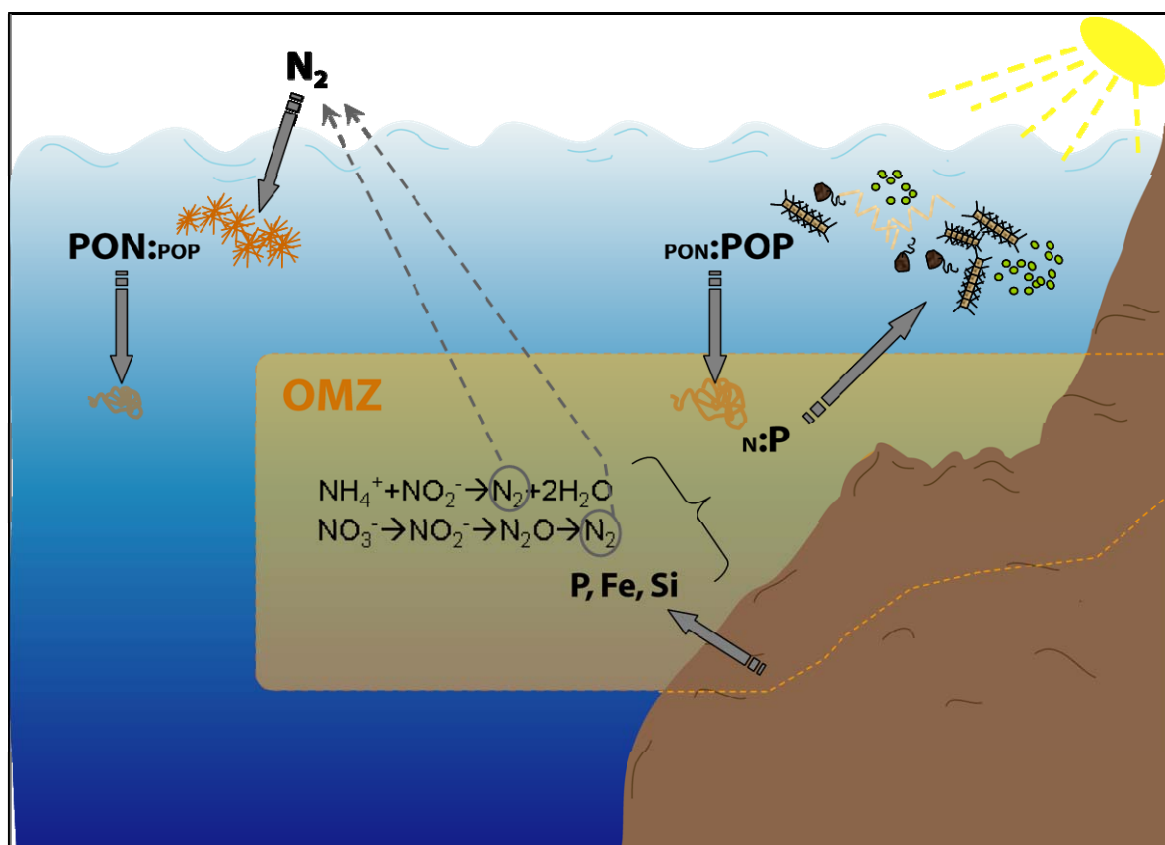


Figure I.2. Scheme of redox-dependent fluxes of N and P in the realm of the OMZ

The microbial pathways of denitrification (Codispoti and Christensen, 1985) and anaerobic ammonium oxidation (anammox) (Kuypers et al., 2005; Hamersley et al., 2007) are key processes of the nitrogen cycle, as large amounts of biologically available nitrogen (N) in form of nitrate (NO_3^-) and ammonium (NH_4^+) are transformed into dinitrogen (N_2) or N_2O , and are consequently lost for the autotrophic system (Fig. I.2). A scientific debate about the contribution of each process to total N loss in the individual OMZs is in progress. Anammox seems to be the prevalent reaction for N loss in the OMZ off Peru (Hamersley et al., 2007; Lam et al., 2009) and in the Benguela upwelling off Namibia (Kuypers et al., 2005). The OMZ off Northwest Africa appears to be devoid of both processes, at least within the water column (Ryabenko et al., 2011). Whereas tropical OMZs are a net sink for N, they represent a major source for inorganic phosphorus (P) once converging with the continental shelf (Fig. I.2). P associated to metal oxides such as iron (Fe) oxide and buried in the sediment is released back into the water column under reducing redox-conditions (Ingall and Jahnke, 1994). This reaction delivers simultaneously large amounts of bioavailable Fe(II) from the shelf sediment into the water column. The pelagic pool of P is further enlarged through dissolution of apatite-containing fish debris in the shelf sediments, which applies especially to the high fish production areas of the Peruvian upwelling (Suess, 1981; Van Cappellen and Berner, 1988).

As a consequence of O_2 -deficiency, intermediate nutrient-rich waters are featuring a low inorganic N:P stoichiometry, expressed as an N-deficit relative to the concentration of P ($\text{N}^* = \text{N} - 16 \cdot \text{P}$) (see Fig. I.3). Extreme anoxia in the Pacific OMZ causes strongly reduced N:P ratios compared to the canonical Redfield ratio of 16:1 (Redfield, 1958), generating high negative values of N^* . The relatively moderate O_2 -depletion in the East Atlantic precludes large-scale N loss processes, preserving N:P conditions around Redfield's 16:1 (Moore et al., 2008).

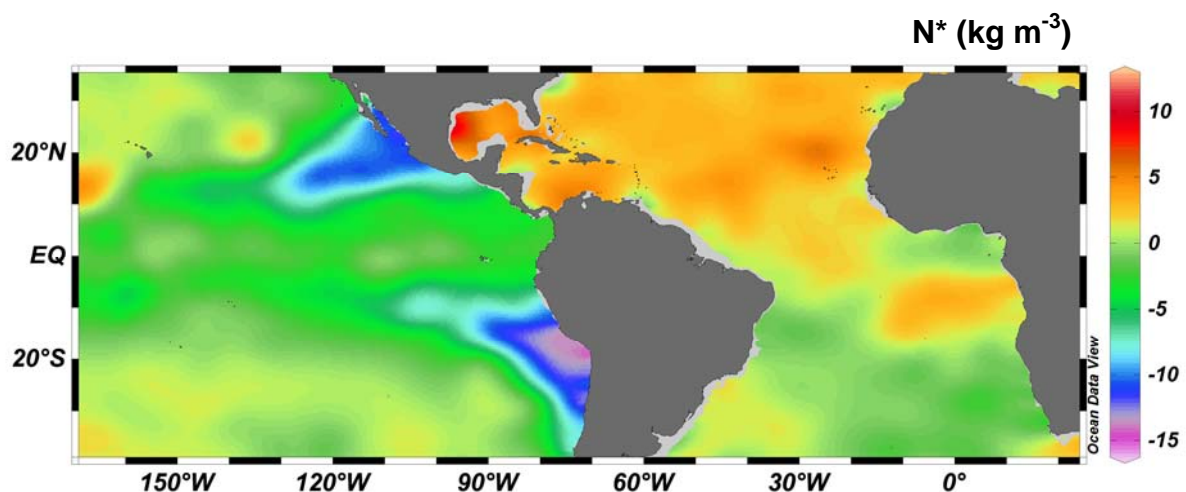


Figure I.3. Mean annual distribution of N^* at 200 m depth in the Pacific and Atlantic Ocean calculated according to Gruber and Sarmiento (1997). Positive N^* indicates inorganic N:P ratios larger Redfield (16:1), negative N^* indicate $\text{N:P} < 16:1$. Data used for calculation of N^* was taken from WOA 2009 (Garcia et al., 2010b).

Expansion of OMZs, expected as a result of global warming-induced changes in ocean stratification and O_2 gas solubility, is already confirmed by observational data. Time series data from the last 50 years shown in Fig. I.4 revealed a vertical expansion of O_2 -deficient intermediate zones in the tropical Pacific and Atlantic Ocean (Stramma et al., 2008) and climate models predict a further general decline in oceanic O_2 concentrations (Bopp et al., 2002; Matear and Hirst, 2003). Furthermore, model simulations predict an increase in O_2 -consumption as a result of increased respiration under elevated CO_2 -levels (Schneider et al., 2004; Oschlies et al., 2008). In particular the O_2 -sensitive nitrogen cycle could be significantly affected by this development in the course of climate change, as habitats exhibiting O_2 concentrations below the threshold for microbial N loss processes are likely to increase. The ‘moderate’ OMZ in the eastern tropical North Atlantic experienced with an average annual O_2 decline of $0.34 \mu\text{mol kg}^{-1}$ over the last 50 years the strongest trend in ocean deoxygenation among the tropical OMZs and may thus have the largest potential for broadening of O_2 -deficient waters (Stramma et al., 2008). Quite recently dead-zone eddies, which are water masses without detectable O_2 concentrations, have been recorded at the Cape Verde Ocean Observatory in the ETNA (Karstensen, pers. comm.). These are clear signals for a progression of deoxygenation in the tropical Atlantic. Hence, absence of water column denitrification and anammox off the coast of Northwest Africa might soon belong to the past, amplifying the global N-deficit to currently unknown dimensions.

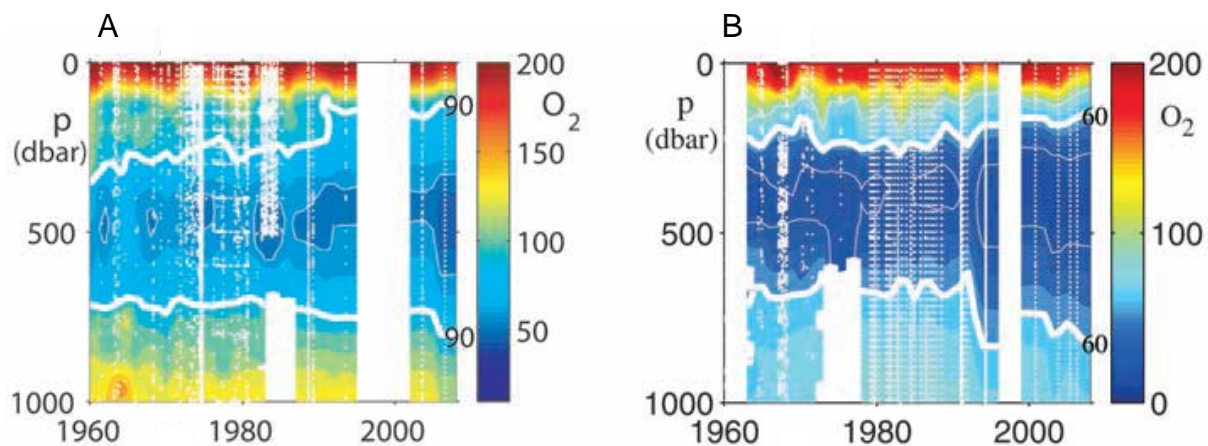


Figure I.4. Dissolved oxygen concentration (in $\mu\text{mol kg}^{-1}$) plotted versus time (1960-2008) and pressure (1 dbar \sim 1 m). White dots represent sample locations. (A) The eastern tropical North Atlantic (10° to 14°N and 20° to 30°W), with thick white contour line at $90 \mu\text{mol kg}^{-1} O_2$. (B) The eastern equatorial Pacific Ocean (5°S to 5°N and 105° to 115°W), with thick white contour line at $60 \mu\text{mol kg}^{-1} O_2$. (from Stramma et al., 2008)

N-deficiency associated with excess amounts of P in surface waters influenced by the OMZ could provide an ecological niche for phytoplankton N₂-fixation (Deutsch et al., 2007). However, Fe limitation of N₂-fixation may inhibit the compensation for extensive N loss (Moore and Doney, 2007). Since N limits primary production, changes in the ocean's N inventory due to widespread anoxia will likely affect the magnitude of CO₂-sequestration in the ocean via the biological pump (Falkowski, 1997; Codispoti et al., 2001).

Coastal upwelling areas

Coastal upwelling is defined as the trade winds-mediated upward transport of cold and nutrient-rich intermediate water into the surface layer on the continental shelf. Wind-driven and equatorward flowing currents running parallel to the coast (e.g. Peru Current, Benguela Current, Canary Current) are diverted by the Coriolis force in a 90° angle to the left (Southern Hemisphere) or to the right (Northern Hemisphere). This 90° net movement of the surface layer due to wind forcings is called Ekman transport (Ekman, 1905). The resulting offshore flowing surface water is replaced by colder and usually nutrient-rich deep water. As a consequence, surface waters off the coast of Peru in the Pacific and off Mauretania and Namibia in the Atlantic are featuring relatively low temperatures for these in general warm regions of the tropical and subtropical ocean. The relatively cool surface water parcels contain large amounts of nutrients like nitrate (NO₃⁻), phosphate (PO₄³⁻), silicate (Si(OH)₄) and iron (Fe), representing a marine oasis in the generally oligotrophic deserts of the blue tropical surface ocean (see Fig. I.5). In particular on the Peruvian shelf constant upwelling supports the formation of vast nutrient plumes that are stretching far out into the Pacific Ocean.

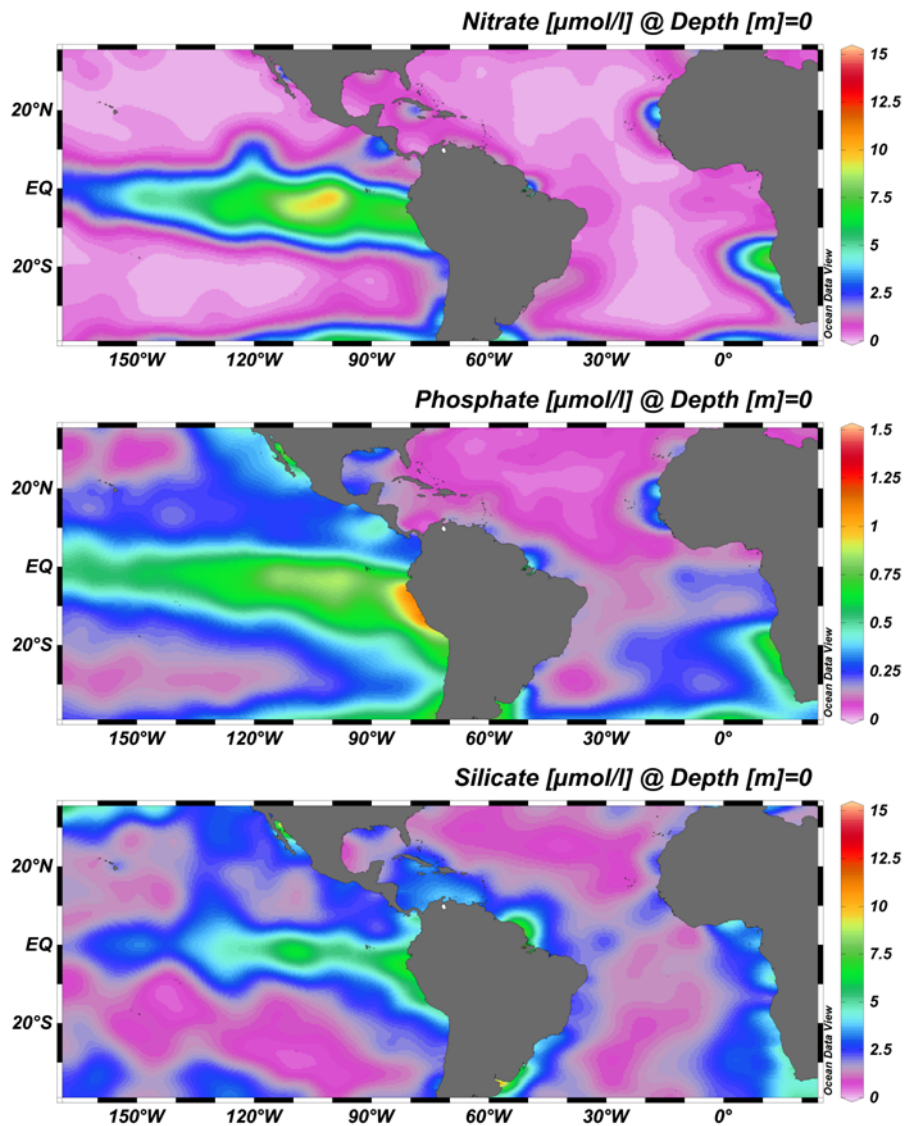


Figure I.5. Mean annual surface concentrations of (A) nitrate, (B) phosphate and (C) silicate in the Pacific and Atlantic Ocean (from WOA 2009, Garcia et al., 2010b).

In contrast to the commonly poor productivity of the tropical ocean due to stable stratification of the upper water body, diapycnal transport of deep water loaded with nutrients into the euphotic layer enables extremely high primary production rates. The resulting large phytoplankton standing stocks in shelf waters represent the foundation for the high ocean productivity in eastern boundary current systems (Chavez, 1995; Pennington et al., 2006). Even though upwelling areas contribute only ~0.2% to the global ocean, they are providing 34% of global marine primary production (see biomass index chlorophyll *a* in Fig. I.6) and up to 58% of the global marine fish catch (Pauly and Christensen, 1995). This extremely large fish production is not only a result of enhanced primary productivity. Eutrophic conditions favour especially growth of large phytoplankton which facilitates short food chains, resulting in high ecological energy transfer efficiencies, and therewith exponentiating total fish yield (Ryther, 1969; Cushing, 1989).

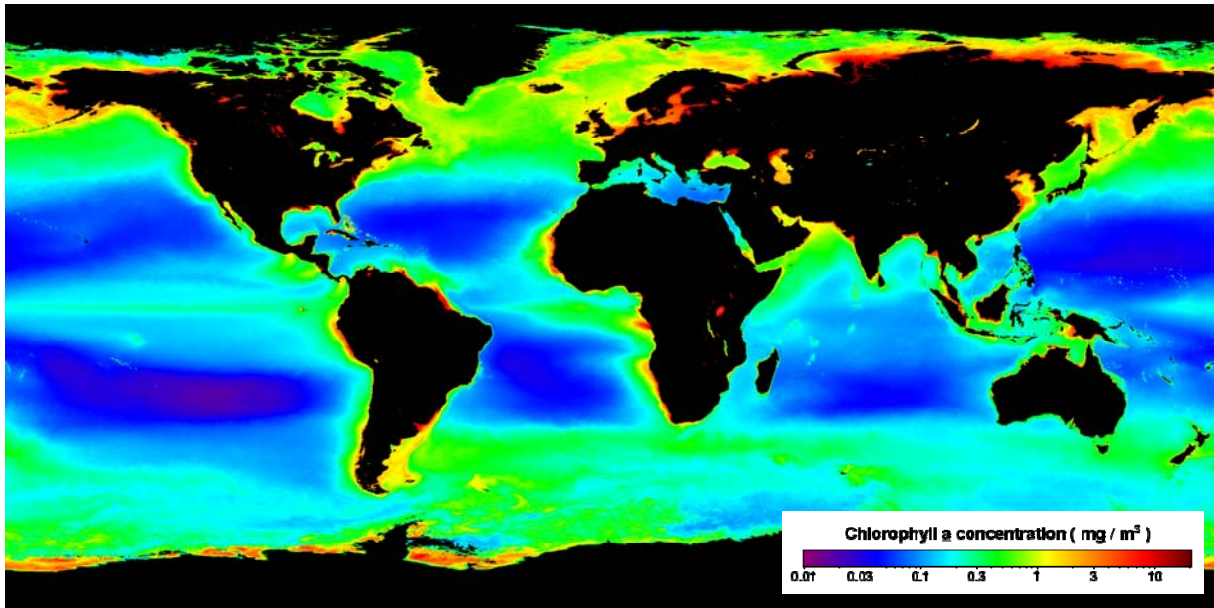


Figure I.6. Mean annual surface ocean chlorophyll *a* concentration between 1997-2010 (SeaWiFS, <http://oceancolor.gsfc.nasa.gov/>).

Diatoms play an important role in global biogeochemical cycles by accounting for 40% of primary production in the ocean (Smetacek, 1999) and by controlling export production into the deep ocean via their fast-sinking silica frustules (Buesseler, 1998). Yet, diatoms are absolutely dominating the photoautotrophic community in upwelling areas of the eastern margins (Rojas de Mendiola, 1981; Wilkerson et al., 2000) (see Fig. I.7A). Large cell size (up to 200 μm) (Hasle and Syvertsen, 1997), high nutrient storage capacity (Sunda and Huntsman, 1995) and high growth rates under nutrient saturation (reviewed in Sarthou et al., 2005) are perfect adaptations of this phytoplankton group for successful blooming after episodic pulses of nutrients from the deep. Fawcett and Ward (2011) observed a very fast metabolic response of diatoms on sudden nutrient input, which may be the key advantage to overgrow and out-compete other photoautotrophic species right from the start. *Phaeocystis globosa* and dinoflagellates are further phytoplankton abundant in upwelling areas (Margaelf, 1978), but in terms of biomass they play a minor role compared to diatoms.

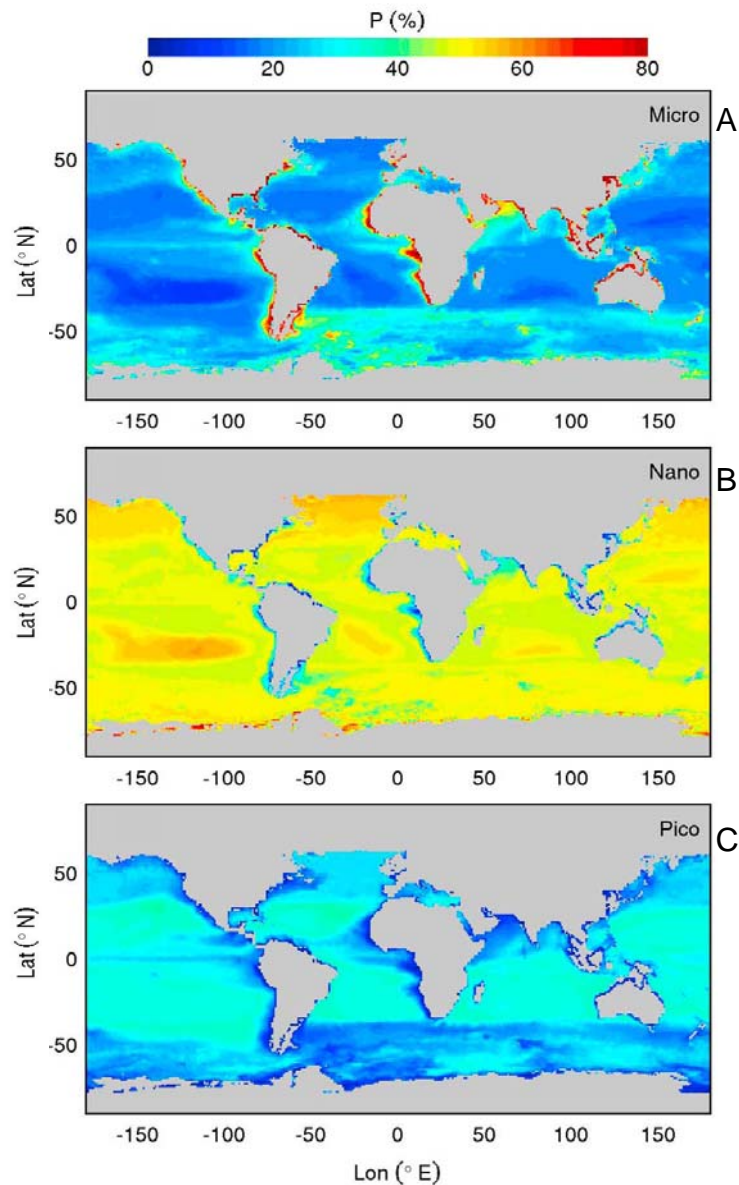


Figure I.7. Seasonal climatology (1998-2007) for the Dec-Feb period showing the percentage contribution of size-class-specific phytoplankton production to total primary production. The three size-classes (A) micro-, (B) nano- and (C) picophytoplankton are based on phytopigment composition (from Uitz et al., 2010).

As large-sized, fast growing phytoplankton is the major producer of sinking particulate material (Michaels and Silver, 1988), it represents a key factor in the export of photoautotrophically fixed carbon to the deep ocean, namely the biological pump (Dugdale and Wilkerson, 1998). Consequently, downward carbon fluxes will likely react sensitive to shifts in the planktonic community structure of diatom-dominated assemblages abundant in coastal upwelling areas (Boyd and Newton, 1998).

Due to their large variability in size and shape, diatoms represent an important food source for a wide spectrum of pelagic organisms, consisting of micro- and mesozooplankton and planktivorous fish. The enormous production of small pelagic fish like anchoveta and sardines in

the Peruvian upwelling is principally fuelled by periodic blooming of large diatoms (Ryther, 1969; Smetacek, 1999). Changes in the abundance of diatoms could potentially have serious implications on the distribution of these swarm-building fish.

Coastal upwelling areas represent from an ecological as well as from an economical perspective highly valuable marine systems, which rely on the permanent nutrient supply through vertical advection on the shelf. Changes in nutrient inventories and stoichiometry, as will likely occur in the course of expanding OMZs, may not only affect primary production significantly. In a bottom-up controlled system with short food chains, changes on the primary producer level may have a direct impact on the whole food web up to large predatory fish.

Cyanobacteria of the tropical oligotrophic ocean

Marine life in continental shelf areas of eastern boundary regimes benefits from episodic vertical intrusions of 'fresh' nutrients. Open ocean regions, in contrast, encounter very stable and constant hydrographic conditions. Weak seasonality in low latitude regions cause a pronounced year-round stratification of the upper ocean which inhibits exchange with the underlying nutrient-enriched water body, resulting in a nutrient-impoverished surface layer. Large phytoplankton dominating the eutrophic waters of coastal upwelling areas (see Fig. 1.7A) are disadvantaged under nutrient-depleted conditions, as their low surface-to-volume-ratio is unfavourable for nutrient uptake at low concentrations (Chisholm, 1992). Pico- and nanoplanktonic cells, primarily of the cyanobacterial genus *Synechococcus* und *Prochlorococcus*, tend to dominate primary production in most oligotrophic waters of the tropical ocean (Partensky et al., 1999; Uitz et al., 2010) (see Fig. 1.7B and C). In contrast to the episodic appearance of large blooming algae in eutrophic systems, small oceanic phytoplankton pursues the strategy of sustaining constant net growth, since nutrient conditions hardly change throughout the year. Cell abundances of *Synechococcus*, which can also occur in meso-/eutrophic areas closer to the coast, are lower in strongly nutrient-depleted areas, while *Prochlorococcus* abundance is considerably higher in oceanic 'deserts'. This is primarily a result of the higher genetic variability of *Prochlorococcus* that facilitates colonization of different light regimes (Ferris and Palenik, 1998). *Prochlorococcus* contains a specialized photosystem, which can collect photons efficiently even at very low irradiances down to 200 m depth (Moore et al., 1995). The photosynthetic adaptation allows growth in the deep layers below the thermocline, where diffusion and advection of nutrients from underlying water allows for establishment of a deep chlorophyll maximum. This vertical flexibility of *Prochlorococcus* across the water column is representing a major advantage compared to most other commonly light-limited photoautotrophs that are bound to the light-flooded but nutrient-impoverished surface layer.

Beside *Synechococcus* and *Prochlorococcus*, both lacking the ability to fix N_2 , a variety of diazotrophic cyanobacteria are abundant in the oligotrophic ocean of the tropics and subtropics. The filamentous colony-forming *Trichodesmium* (Capone et al., 1997; Carpenter et al., 1999), unicellular species such as *Crocospaera* (Zehr et al., 2001), recently discovered unicellular heterotrophic cyanobacteria (Zehr et al., 2008), and symbiotic diazotrophs associated with diatoms (Carpenter et al., 1999; Foster and Zehr, 2006) occur in the tropical and subtropical open ocean. For a long time marine diazotrophy was primarily linked to the abundant cyanobacterium *Trichodesmium* (Carpenter and Romans, 1991; Falkowski, 1997), which is able to form extensive surface blooms under favourable conditions like water temperatures $>25^{\circ}\text{C}$ and calm sea (Breitbarth et al., 2007). High water temperatures between $25\text{--}34^{\circ}\text{C}$ appear to be a key factor in controlling distribution of *Trichodesmium* (reviewed by Stal, 2009). In the last decade unicellular cyanobacteria, auto- as well as heterotrophic, gained increasing attention as they were discovered to equal or even exceed abundance and N_2 -fixation rates of filamentous *Trichodesmium* (Zehr et al., 2001; Montoya et al., 2004; Langlois et al., 2008). Unicellular *Crocospaera* ($3\text{--}8\text{ }\mu\text{m}$) has with $22\text{--}36^{\circ}\text{C}$ a much broader temperature spectrum (Webb et al., 2009), implying a larger geographic distribution than *Trichodesmium* (Moisander et al., 2010). Recently discovered heterotrophic unicellular cyanobacteria named 'Group A' are even found in cooler waters with temperatures down to 15°C (Needoba et al., 2007; Langlois et al., 2008). Therefore colder waters ($\text{SST} < 25^{\circ}\text{C}$) of the subtropical and even temperate ocean or close to upwelling hotspots, previously not considered as common areas of N_2 -fixation, may provide favourable conditions for diazotrophic phytoplankton. Unicellular 'Group A' cells ($<1\text{ }\mu\text{m}$) represent a unique group of cyanobacteria, as they completely lack photosystem II and enzymes for carbon fixation; consequently they have been classified as photoheterotroph (Zehr et al., 2008; Tripp et al., 2010). Another special form of cyanobacteria in the tropical ocean are the diatom-diazotroph associations (DDA). Autotrophic cyanobacteria *Richelia intracellularis* or *Calothrix* live in a symbiotic relationship with the diatoms *Hemiaulus*, *Rhizosolenia* or *Chaetoceros* (Foster and Zehr, 2006).

Diazotrophic cyanobacteria play a critical part in biogeochemistry of the tropical ocean, as N_2 -fixation represents the only process with the potential to counterbalance the deficit in the marine N-budget.

Controls of phytoplankton stoichiometry

The composition of essential elements for microalgal nutrition in the ocean (carbon, nitrogen and phosphorus) is highly similar to the elemental stoichiometry of phytoplankton. This was first discovered by Redfield (1958), who suggested a tight mutual regulation of nutrient and organic matter stoichiometry. This “they are what they eat” theory was pursued in many studies, declaring the nutrient supply ratio as the major control of cellular chemical composition (Rhee, 1978; Sterner and Elser, 2002). Yet, Goldman et al. (1979) observed in culture experiments a tight correlation of phytoplankton stoichiometry with growth rate, regardless of the medium N:P ratio. The growth phase, either exponential (nutrient saturation) or stationary (nutrient depletion), seems to be highly relevant for the biochemical composition of the cell (Klausmeier et al., 2004a; 2004b; 2008). Under replete nutrient supply, phytoplankton consumes nutrients in a fixed ratio closely matching its specific optimal uptake ratio. Whereas algae assimilate nearly all the residual nutrients in the medium under nutrient starvation, hence cells “are what they eat” or “eat what they are served”, respectively, matching the nutrient supply ratio (Sterner and Elser, 2002).

As described in the two previous chapters, the community of marine phytoplankton is composed of a variety of functional types and size spectra (see Fig. I.7) that pursue different strategies of growth based on the prevailing conditions of hydrography and nutrient distribution. Broadly classified, there are large microalgae specialized on blooming in high-nutrient regions close to the coast, and there are picoplanktonic species adapted to survive in nutrient-poor waters of the open ocean. Phytoplankton stoichiometry is suggested to be highly influenced by the predominant metabolic machinery (Klausmeier, 2004a; Arrigo, 2005; Loladze and Elser, 2011), since cellular compartments are characterized by quite different chemical compositions (Geider and LaRoche, 2002). Blooming phytoplankton like diatoms have typically a relatively low N:P composition (~10:1), since cell assembly requires synthesis of increased amounts of P-rich ribosomes. Picoplankton is forced to accumulate N-rich proteins for resource (nutrients, light) acquisition in the oligotrophic waters, consequently cellular N:P is high (>20:1).

Regardless of whether growth rate, growth strategy or the nutrient supply ratio are ultimately regulating phytoplankton elemental composition, the impact of dissolved organic compounds is regularly ignored. Banse (1974) already described uptake and release of dissolved organic nitrogen (DON) and dissolved organic phosphorus (DOP) by phytoplankton as a significant process influencing the stoichiometry of algal biomass. Certain constituents of DON and/or DOP are not exclusively utilized by heterotrophic bacteria, but represent additional nutrient sources for a multitude of phytoplankton species (reviewed by Bronk et al., 2007; Dyhrham and Ruttenberg, 2006; Dyhrham et al., 2006; Ranhofer et al., 2009). Dissolved organic compounds are generally transformed into bioavailable molecules by extracellular enzymes released from the algae. DON and/or DOP as potential substitute sources for phytoplankton nutrition may play

a crucial role in nutrient and organic matter cycling, specifically in the context of changing nutrient inventories induced by expanding OMZs.

Nutrient limitation of phytoplankton

A multitude of different concepts for phytoplankton nutrient limitation can be found in literature. Famous Liebig's law of the minimum states existence of a single limiting nutrient, ultimately controlling total biomass yield by its availability (Liebig, 1855). Rate limitation, also known as Blackman limitation, describes the impact of a limiting nutrient on growth rate rather than on absolute biomass (Blackman, 1905). Both concepts are originally based on the decisive factor of a single limiting nutrient, whereas availability of other nutrients is irrelevant. However, co-limitation, limitation by multiple elements, can frequently be observed due to the simultaneous deficiency of several nutrients in the surface ocean (Saito et al., 2008). Co-limitation appears often in conjunction with micronutrients (trace metals), induced either by two micronutrients (e.g. Fe, Zn, Co, Mn) (Saito et al., 2002), or by one trace metal in combination with a macronutrient (N, P, Si) (DiTullio et al., 1993).

The general complexity of nutrient limitation can be well demonstrated using the study by Mills et al. (2004) conducted in the eastern tropical North Atlantic (ETNA). Bioassay experiments revealed a general N limitation of total primary production, whereas N₂-fixation was co-limited by Fe and P. N limitation of the photoautotrophic system in the tropical North Atlantic may be a prerequisite for high N₂-fixation. Large Fe and potentially also P supply by dust deposition from the African continent (Gao et al., 2001) facilitates oceanic diazotrophy, turning the tropical North Atlantic into one of the most important areas of marine N₂-fixation world-wide (Gruber and Sarmiento, 1997). Diazotrophic cyanobacteria require supplemental amounts of Fe for synthesis of the Fe-containing protein nitrogenase that is catalyzing the reaction of N₂-fixation (reviewed by Howard and Rees, 1996). Cell growth and N₂-fixation of cyanobacteria are thus especially prone to Fe limitation (Paerl et al., 1994; Berman-Frank et al., 2007; Okin et al., 2011). However, Fe has been questioned being the key nutrient regulating marine N₂-fixation, suggesting P as a further important control of diazotrophic phytoplankton growth (Sañudo-Wilhelmy et al., 2001). A variety of studies in limnetic (Smith, 1983; Vrede et al., 2009), brackish (Niemi, 1979) and marine (Michaels et al., 1996) systems discovered blooming of cyanobacteria initiated by low seawater N:P stoichiometry. The question is whether N depletion, high P supply or a combination of both are favouring cyanobacterial growth. Based on the N:P Redfield ratio of 16:1, excess supply of P generated within OMZs is expected to stimulate growth of diazotrophic phytoplankton and N₂-fixation (Deutsch et al., 2007), thereby potentially compensating for the extensive N loss from the anaerobic processes anammox and denitrification. This scenario is based on nutrient uptake by non-diazotrophic phytoplankton

according to Redfield. However, numerous studies, based on data from the field as well as from culture experiments, already reported on non-Redfieldian N:P utilization by phytoplankton. According to the concept of growth strategy described in the previous chapter, blooming species are commonly consuming nutrients with an N:P below Redfields' 16:1 (Arrigo et al., 2005; Klausmeier et al., 2004a), while picocyanobacteria abundant in oligotrophic waters are characterized by high N:P uptake ratios (Bertilsson et al., 2003; Klausmeier et al., 2004a). Low N:P assimilation of fast-growing phytoplankton in coastal upwelling areas may therefore reduce P availability for N₂-fixing species abundant in off-shelf waters (Mills and Arrigo, 2010).

The micronutrient Fe is also a crucial factor in controlling in particular blooming of diatoms (Hutchins and Bruland, 1998; Coale et al., 1996). For example, generally productive upwelling areas on the Peruvian shelf in the Pacific can be transferred into HNLC (high nutrients low chlorophyll) regions if diatom growth is restricted by the availability of Fe (Bruland et al., 2005). Diatoms, with their exclusive requirement for Si(OH)₄ (with the exception of the negligible group of silicoflagellates), rely further on the supply of Si(OH)₄ and their development is constrained by availability of this macronutrient. Beside N and Fe, autotrophic production in upwelling systems could thus be additionally limited by Si(OH)₄ (Dugdale et al., 1995; White and Dugdale, 1997).

The debate about the ultimate limiting nutrient of marine primary production on a global scale goes back to Redfield in 1958. Based on the theory that potential N-deficits in the ocean could be fully compensated by N₂-fixation, he concluded net organic production to be limited by the supply of P. However, this proposition could only arise by neglecting considerations about potential limitation of N₂-fixation itself. More than 10 years later Ryther and Dunstan (1971) possibly approved overall P limitation on geological time scales, but claimed N as the critical and proximate factor limiting phytoplankton growth in coastal waters. Today, diatoms as the largest contributors to primary production in eutrophic waters (Blain et al., 1997; Smetacek, 1999) and bulk phytoplankton in the oligotrophic North Atlantic (Graziano et al., 1996; Mills et al., 2004; Moore et al., 2008) are known to be limited by N availability. Falkowski (1997) considered the general N limitation of marine primary production as a consequence of low Fe supply limiting N₂-fixation over large areas of the surface ocean.

Major objectives and thesis outline

As a consequence of climate change, O₂-deficient areas in the tropical ocean are expected to expand, leading most likely to a universal decrease in the N:P ratio of nutrients supplied to the surface ocean from the deep. These predictions encouraged me to investigate how phytoplankton in coastal upwelling areas overlying OMZs is responding to changes in the N:P supply ratio in terms of (i) total production, (ii) community structure and (iii) elemental stoichiometry. Based on the specific question whether N:P composition of photoautotrophic biomass in upwelling areas will follow the deoxygenation-induced decrease in nutrient N:P stoichiometry, I investigated (iiii) whether nutrient N:P is reflected in the microalgal N:P composition in general.

The first study of the thesis is based on a hydrographic and biogeochemical field survey along an east-west transect at 10°S in the eastern tropical South Pacific (ETSP), stretching from the upwelling area above the narrow Peruvian continental shelf to the stable stratified open ocean. Links between vertical and horizontal gradients of nutrients, phytoplankton species composition and phytoplankton N:P stoichiometry were examined.

A close to nature experimental approach was used for testing community biogeochemical responses to variable N:P supply ratios in study 2, 3 and 4. Nutrient enrichment experiments with natural phytoplankton communities in shipboard mesocosms were conducted in the Peruvian upwelling and in the waters off Northwest Africa. Study 2 (off Peru) and 3 (off NW Africa) tested the effect of different nutrient fertilization on growth and taxonomical structure of the phytoplankton community.

Study 4 represents a synthesis of the results from all three mesocosm experiments, investigating the impact of nutrient supply and nutrient stoichiometry on production, partitioning and elemental composition of phytoplankton-derived organic matter.

Work for this dissertation was conducted in the framework of the Sonderforschungsbereich SFB 754 "Climate-Biogeochemistry Interactions in the Tropical Ocean" funded by the German Science Foundation (DFG) and included participation in three cruises on board of German *R/V Meteor* to the study sites in the tropical Atlantic and Pacific Ocean. Cruise M77-3 was carried out in the ETSP from Guayaquil (Ecuador) to Callao (Peru) in Dec./Jan. 2008/09, M80-2 in the oceanic ETNA from Mindelo (São Vicente/Cape Verde) to Dakar (Senegal) in Nov./Dec. 2009 and M83-1 again in the ETNA from Las Palmas (Gran Canary/Spain) to Mindelo (São Vicente/Cape Verde) in Oct./Nov. 2010 (Fig. I.8).

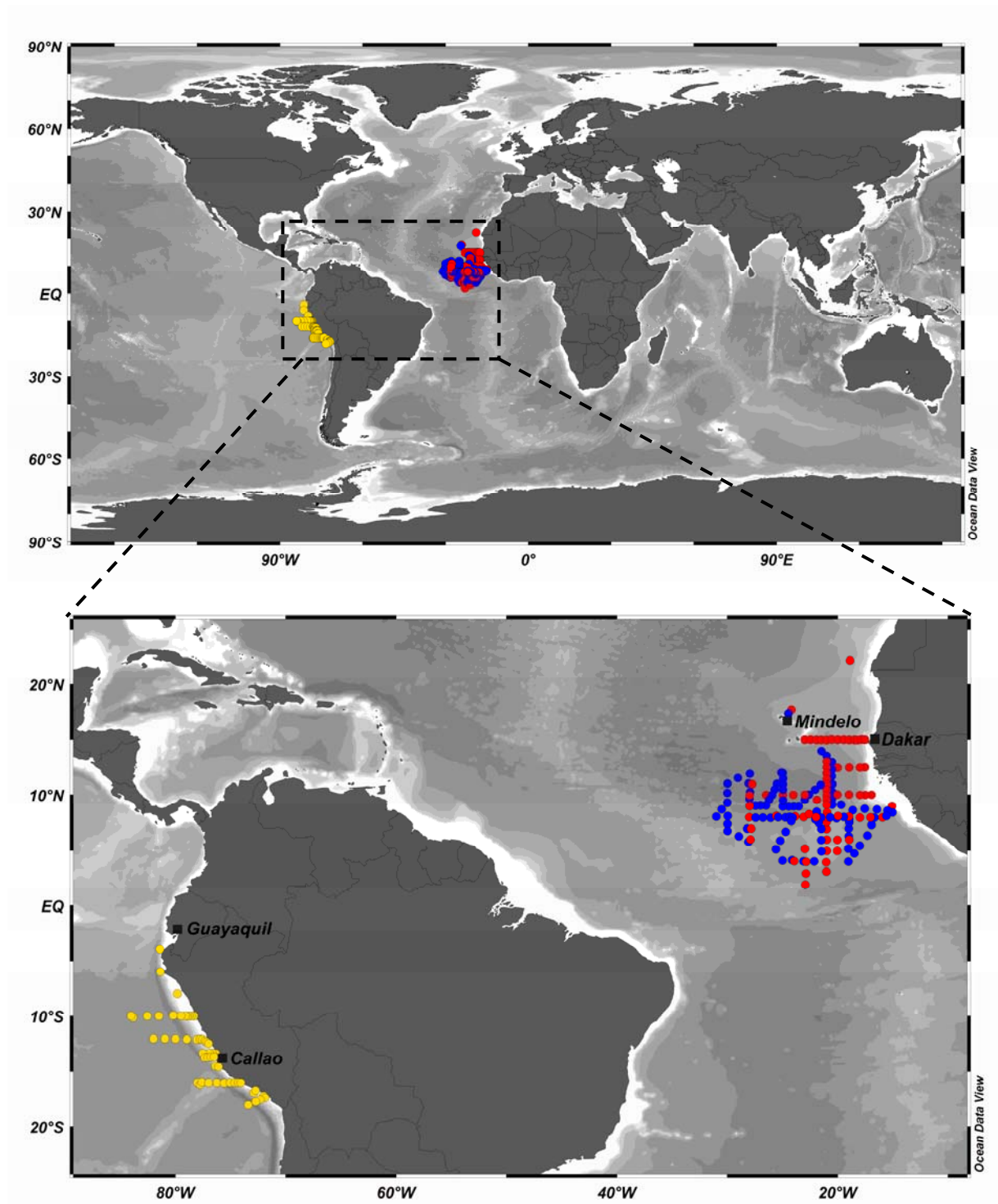


Figure I.8. Maps showing sampling stations of *R/V Meteor* cruises M77-3 (yellow), M80-2 (blue) and M83-1 (red).

Study 1.**Dynamics and stoichiometry of nutrients and phytoplankton in waters influenced by the oxygen minimum zone in the tropical eastern Pacific**

Jasmin Franz^{1*}, Gerd Krahmann¹, Gaute Lavik², Patricia Grasse¹, Thorsten Dittmar³ and Ulf Riebesell¹

¹Helmholtz Centre for Ocean Research Kiel (GEOMAR), Düsternbrooker Weg 20, 24105 Kiel, Germany

²Max Planck Institute for Marine Microbiology, Celsiusstr. 1, 28359 Bremen, Germany

³Max Planck Research Group for Marine Geochemistry, Carl-von-Ossietzky-Str. 9-11, ICBM, 26129 Oldenburg, Germany

*corresponding author:

Jasmin Franz, Helmholtz Centre for Ocean Research (GEOMAR), Düsternbrooker Weg 20, 24105 Kiel, Germany, jfranz@geomar.de, Phone: +49 431 6004290, Fax: +49 431 6004446

Abstract

The tropical South East Pacific is characterized by strong coastal upwelling on the narrow continental shelf and an intense oxygen minimum zone (OMZ) in the intermediate water layer. These hydrographic properties are responsible for a permanent supply of intermediate water masses to the surface rich in nutrients and with a remarkably low inorganic N:P stoichiometry. To investigate the impact of OMZ-influenced upwelling waters on phytoplankton growth, elemental, and taxonomical composition we measured hydrographic and biogeochemical parameters along an east-west transect at 10°S in the tropical South East Pacific, stretching from the upwelling region above the narrow continental shelf to the well-stratified oceanic section of the eastern boundary regime. New production in the area of coastal upwelling was driven by large-sized phytoplankton (e.g. diatoms) with generally low N:P ratios (<16:1). While nitrate and phosphate concentrations were at levels not limiting phytoplankton growth along the entire transect, silicate depletion prohibited diatom growth further off-shore. A deep chlorophyll *a* maximum consisting of pico-/nano- (*Synechococcus*, flagellates) and microphytoplankton occurred within a pronounced thermocline in subsurface waters above the shelf break and showed intermediate N:P ratios close to Redfield proportions. High PON:POP (>20:1) ratios were observed in the stratified open ocean section of the transect, coinciding with the abundance of two strains of the pico-cyanobacterium *Prochlorococcus*; a high-light adapted strain in the surface layer and a low-light adapted strain occurring along the oxic-anoxic transition zone below the thermocline. Excess phosphate present along the entire transect did not appear to stimulate growth of nitrogen-fixing phytoplankton, as pigment fingerprinting did not indicate the presence of diazotrophic cyanobacteria at any of our sampling stations. Instead, a large fraction of the excess phosphate generated within the oxygen minimum zone was consumed by non-Redfield production of large phytoplankton in shelf surface waters.

1. Introduction

The tropical and subtropical South East Pacific is oceanographically a highly diverse region. Coastal upwelling driven by alongshore winds is the dominant physical mechanism along the coast forming the basis for one of the most productive marine food webs worldwide (Ryther, 1969). An oxygen-deficient intermediate water body occurs from approximately 100 m down to 900 m depth, where concentrations of dissolved oxygen (O_2) can drop below $20 \mu\text{mol kg}^{-1}$ (Helly and Levin, 2004; Karstensen et al., 2008; Stramma et al., 2008; Fuenzalida et al., 2009). These oxygen minimum zones (OMZs) are caused by a pronounced stratification of the water column in the region off the continental shelf, which impedes ventilation of the intermediate water parcel (Reid, 1965). In addition, high primary production in the surface waters of the shelf area, induced by upwelling of nutrient-loaded water masses previously in contact with shelf sediments, enhances the O_2 -deficit via bacterial degradation of organic matter in the intermediate water layer (Helly and Levin, 2004). This deoxygenation has crucial implications on cycling of the macronutrients nitrogen (N) and phosphorus (P). The microbial processes anammox (anaerobic ammonium oxidation) (Kuypers et al., 2005; Hamersley et al., 2007; Galan et al., 2009), heterotrophic denitrification (Codispoti and Christensen, 1985) and DNRA (dissimilatory nitrate reduction to ammonium) (Lam et al., 2009) can occur within these OMZs. Anammox and denitrification both represent large sinks of inorganic N in anoxic or suboxic waters close to the shelf, thereby lowering N:P stoichiometry and driving the autotrophic system ultimately into N limitation. Furthermore, anoxic conditions in shelf sediments and shelf bottom waters enhance the release of reactive phosphate into the water column formerly associated to iron hydroxides (Ingall and Jahnke, 1994), further enhancing the negative deviation from the Redfield N:P ratio of 16:1 (Redfield, 1958). The resulting excess phosphate (P^*) may provide a niche for N-fixing cyanobacteria (Deutsch et al., 2007). Consequently, diazotrophic cyanobacteria could be the beneficiary of expanding OMZs and might have the potential to replenish the inorganic N-deficit caused by deoxygenation, reconstituting 'Redfieldian' nutrient stoichiometry. The underlying assumption for this concept is an N:P assimilation by non-diazotrophic phytoplankton according to Redfield.

Similar to the deviations in nutrient stoichiometry, also primary producers can diverge in their elemental composition from the canonical Redfield ratio. Recent studies argue that this non-Redfield behavior originates in the specific growth strategy of the microalgae, which determines its cellular nutrient requirements (Klausmeier et al., 2004; Arrigo, 2005; Mills and Arrigo, 2010). According to this, phytoplankton can be broadly divided into two groups, the 'bloomers' and the 'survivalists', a classification that seems to be seeded in their phylogenetic background (Quigg et al., 2003). 'Bloomers' are characterized by large phytoplankton belonging to the red plastid superfamily like diatoms and dinoflagellates that are flourishing especially in eutrophic upwelling systems. They are adapted to exponential growth and possess a cellular assembly machinery

rich in low N:P-containing RNA. At the other end of the spectrum are the 'survivalists', predominantly pico- and nanoplankton, with eukaryotic phyla originating from the green plastid superfamily. The 'survivalists' can sustain net growth even under nutrient scarcity. With the aim of expanding their capacity for scavenging nutrients at low concentrations they synthesize large amounts of N:P-rich proteins.

Based on these concepts, two opposing hypotheses about the dynamics of N:P stoichiometry above the Peruvian OMZ can be formulated. According to the first hypothesis (*sensu* Deutsch et al. 2007) inorganic nutrients in upwelled waters are utilized in Redfield proportions by non-diazotrophic phytoplankton, creating a niche for N-fixing cyanobacteria through the availability of P^* . This scenario would be particularly relevant in the course of expanding OMZs and the accompanied increase in the local N-deficit. The second hypothesis (*sensu* Arrigo, 2005; Mills and Arrigo, 2010) allows for non-'Redfieldian' nutrient assimilation depending on the growth strategy of the phytoplankton species, possibly leading to consumption of P^* by non-diazotrophic phytoplankton. To date the two hypotheses are based primarily on theoretical grounds, as empirical data from O_2 -deficient eastern boundary regions suited for their rigorous testing are scarce. To examine the dynamics of N:P stoichiometry in OMZ-influenced waters and to test for the two opposing hypotheses, we have conducted vertical high-resolution profiles of O_2 , temperature, chlorophyll *a* (Chl *a*) and nutrients in combination with measurements of particulate organic matter (POM), dissolved organic carbon (DOC), biogenic silicate (BSi) and the distribution of phytoplankton functional types (PFTs) based on pigment compositions along an east-west transect at 10°S from the coastal upwelling area to the well-stratified open ocean in the south-eastern tropical Pacific off the coast of Peru.

2. Material and methods

2.1. Study area and sampling

During the M77/3 cruise on board of *R/V Meteor* from Guayaquil/Ecuador to Callao/Peru between December 27, 2008 and January 21, 2009, hydrographic data and a range of biogeochemical parameters were collected. The study site extended from 4°S to 18°S and from 72°W to 84°W (Fig. 1.1) and was characterized by strong vertical and horizontal gradients in hydrography and biogeochemistry.

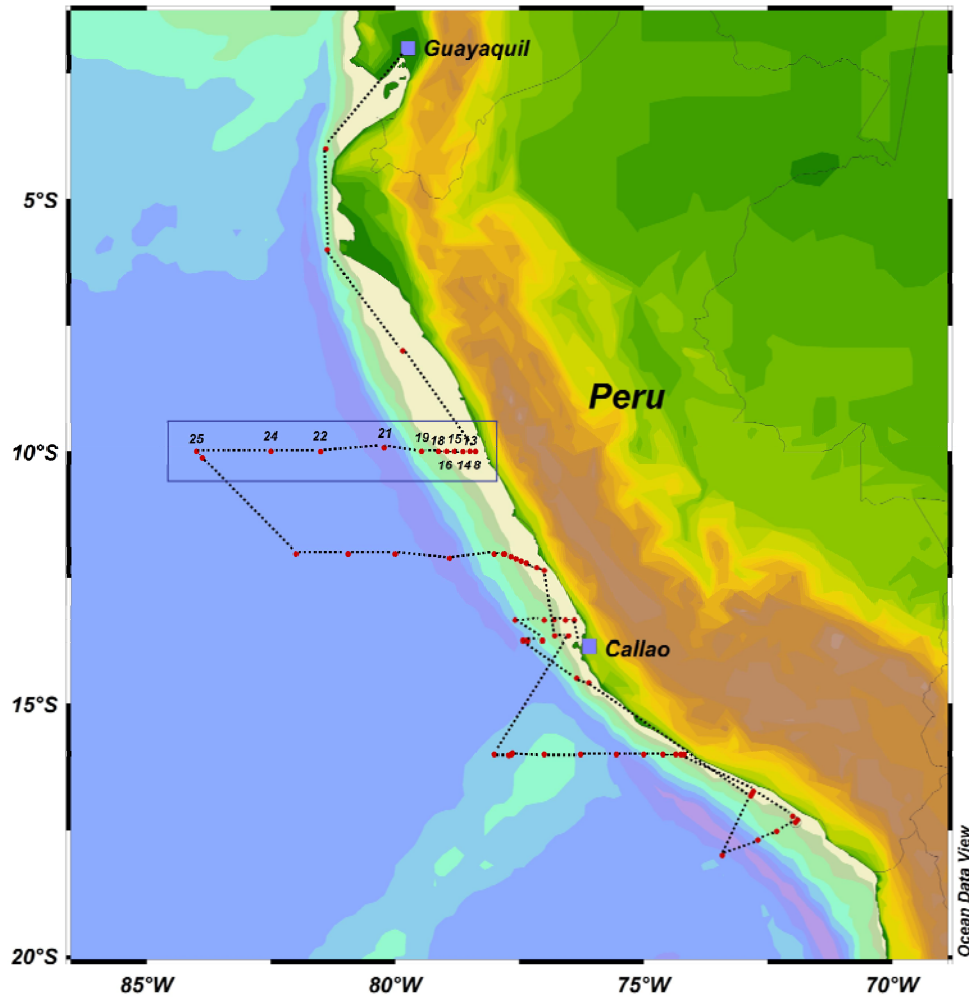


Figure 1.1. Cruise track of M77/3 cruise with all CTD stations denoted in red and the investigated transect along 10°S indicated by the blue frame off the Peruvian coast. Data of hydrographic parameters, nutrients and Chl *a* was collected along the complete length of the transect from the coast to 84.5°W (station 8-25), whereas POM, DOC, BSi and phytoplankton pigments were only determined up to 82.5°W (station 8, 14, 21, 22 and 24). In addition bathymetric characteristics of the study site like the narrow continental shelf and the steep shelf break are displayed.

Our focus was on the physical and biogeochemical sampling of a 10°S transect stretching from the upwelling area on the Peruvian continental shelf at 78.38°W, across the steep continental slope to the open ocean of the eastern boundary regime at 84°W (hydrography, nutrients and Chl *a* measured at station 8-25) and 82.50°W (POM, DOC, BSi, PFTs measured at station 8, 14, 21, 22 and 24), respectively. Location of the cruise track, sampled stations and bathymetric characteristics of the study area are shown in Fig. 1.1.

For collecting hydrographic (O₂, temperature) and Chl *a* data as well as water samples for biogeochemical analyses, vertical casts were conducted using a rosette device equipped with a Seabird 9 plus CTD (conductivity-temperature-depth), dual Seabird O₂ sensors and a Dr. Haardt

fluorescence sensor. Water samples were collected in 24 x 10-L Niskin bottles. Calibration of the O₂ sensors was based on O₂ data gained from bottle samples and determined according to Winkler (1888).

2.2. Nutrient analyses

Water samples for analyses of nitrate (NO₃⁻), ammonium (NH₄⁺), phosphate (PO₄³⁻) and silicate (Si(OH)₄) were stored frozen (-20°C) until processing at the Max-Planck Institute in Bremen, Germany. NO₃⁻, PO₄³⁻ and Si(OH)₄ were measured with an autoanalyzer (TRAACS 800, Bran & Lubbe, Hamburg, Germany) according to Hansen and Koroleff (1999). NH₄⁺ was determined applying the salicylate-hypochlorite method by Bower and Holm-Hansen (1980).

2.3. POM

Water samples for particulate organic carbon (POC) and particulate organic nitrogen (PON) were filtered onto combusted (450°C for 5 h) Whatman GF/F filters (0.7 µm pore size; 25 mm diameter) at low vacuum pressure (<200 mbar) and stored frozen (-20°C). Filters were fumed with hydrochloric acid (37%) for ~15 h to remove all inorganic carbon, dried at 60°C for 12 h and finally wrapped in tin cups (8 x 8 x 15 mm) for combustion. Measurements were made according to Sharp (1974) using an elemental analyzer (EURO EA Elemental Analyzer) coupled to an EUROVECTOR gas chromatograph.

Particulate organic phosphorus (POP) was measured using a modified method according to Hansen and Koroleff (1999) by applying the oxidation reagent Oxisolv (Merck) to the defrosted filters plus 40 ml of ultrapure water. 30 min of cooking converted all POP components into orthophosphate. Addition of 1.25 ml of ascorbic acid and 1.25 ml of a mixed reagent (4.5 M H₂SO₄ + NH₄⁺-molybdate + potassium antimonyl tartrate) formed a blue complex, which was measured colorimetrically against ultrapure water at a wavelength of 882 nm with a Hitachi U-2000 spectrophotometer.

2.4. DOC

Glass vials (24 ml), caps and septa for DOC sampling were soaked in a Decon bath (2%; for min. 12 h), rinsed with ultrapure water, soaked in an HCl bath (10%; for min. 12 h) and rinsed very thoroughly again with ultrapure water. The cleaned glass vials were wrapped into aluminum foil and combusted at 450°C for 12 h to destroy all remaining organic material. Water samples for DOC were taken immediately from the CTD-Niskin bottles into the prepared

sampling vials and stored at -20°C. Samples were thawed, filtrated through combusted (450°C for 6 h) GF/F filters, acidified by adding 20 µl HCl (32%) to each sample and stored at 4°C until measurement. Filtration was performed in a solvent-free clean laboratory on land, because similarly controlled conditions, that are required to minimize contamination of DOC samples, were not available on board. Precipitates were not observed after thawing of the samples and the release of DOC from cells that may have broken during freezing was negligible. This is because POC concentration was on average only 11% of the DOC concentration, and systematic patterns of DOC could not be explained by corresponding shifts in POC. Systematic errors introduced by our filtration procedure are therefore negligible in the context of our study. Analysis of DOC was conducted using the HTO method (high-temperature catalytic oxidation) (Wurl and Min Sin, 2009) on a Shimadzu TOC-V analyzer. The accuracy of the DOC analysis was validated several times a day with DOC deep-sea reference material provided by the University of Miami.

2.5. BSi

Particulate biogenic silica was collected by filtration of water samples onto filters made of cellulose acetate (0.65 µm pore size; 25 mm diameter) at low vacuum pressure (<200 mbar) and stored frozen at -20°C. For analysis, the sample filters were incubated each with 25 ml NaOH (0.1 M) in Nalgene bottles at 85°C for 2h 15 min in a shaking water bath. After cooling of the incubated samples, analysis was conducted according to the method for determination of Si(OH)₄ by Hansen and Koroleff (1999).

2.6. Phytoplankton pigment analysis

Samples for phytoplankton pigment analysis via HPLC (High Pressure Liquid Chromatography) were filtered onto Whatman GF/F filters (0.7 µm pore size; 25 mm diameter) at low vacuum pressure and immediately stored frozen at -20°C. For pigment extraction, each filter was covered with approximately 3 g of glass beads (2 mm + 4 mm) and 2 ml of acetone. After homogenisation in a cell mill (Edmund Bühler GmbH) for 5 min and centrifugation for 10 min at 5000 rpm, the supernatant was filtered through a 0.2 µm Teflon filter and the extract stored at -80°C. The HPLC measurement was conducted by a Waters 600 controller in combination with a Waters 996 photodiode array detector (PDA) and a Waters 717plus auto sampler. The applied method was modified after Barlow et al. (1997).

Classification and quantification of the phytoplankton pigments was carried out using the software EMPOWERS (Waters GmbH, Eschborn, Germany). Phytoplankton class abundances were calculated with CHEMTAX (Mackey et al., 1997).

Table 1.1. Input and output matrix for CHEMTAX. Pigment to chlorophyll a_1/a_2 ratios for the selected phytoplankton groups. Modified input matrix after Mackey et al. (1996) and Veldhuis & Kraay (2004).

	chl c_3	chl c_1+c_2	peri	but	fuco	hex	neo	viola	diad	pras	allo	diat	zea	chl b_1	chl b_2	chl a_2	chl a_1	α -ca	β -ca
Input matrix																			
Diatoms	0.000	0.110	0.000	0.000	0.272	0.000	0.000	0.000	0.065	0.000	0.000	0.032	0.000	0.000	0.000	0.000	0.506	0.000	0.015
<i>Synechococcus</i>	0.000	0.000	0.000	0.000	0.000	0.000	0.000	0.000	0.000	0.000	0.000	0.000	0.301	0.000	0.000	0.000	0.615	0.000	0.084
<i>Prochlorococcus</i> HL	0.000	0.008	0.000	0.000	0.000	0.000	0.000	0.000	0.000	0.000	0.000	0.000	0.400	0.000	0.078	0.448	0.000	0.065	0.000
<i>Prochlorococcus</i> LL	0.000	0.013	0.000	0.000	0.000	0.000	0.000	0.000	0.000	0.000	0.000	0.000	0.210	0.000	0.359	0.322	0.000	0.097	0.000
Dinoflagellates	0.000	0.165	0.330	0.000	0.000	0.000	0.000	0.000	0.113	0.000	0.000	0.075	0.000	0.000	0.000	0.000	0.309	0.000	0.007
Haptophytes	0.100	0.077	0.000	0.004	0.128	0.182	0.000	0.000	0.055	0.000	0.000	0.023	0.000	0.000	0.000	0.000	0.427	0.003	0.001
Chrysophytes	0.055	0.055	0.000	0.207	0.154	0.000	0.000	0.000	0.032	0.000	0.000	0.026	0.000	0.000	0.000	0.000	0.456	0.014	0.000
Chlorophytes	0.000	0.000	0.000	0.000	0.000	0.000	0.036	0.029	0.000	0.000	0.000	0.000	0.000	0.260	0.000	0.000	0.629	0.018	0.027
Cryptophytes	0.000	0.053	0.000	0.000	0.000	0.000	0.000	0.000	0.000	0.000	0.154	0.000	0.000	0.000	0.000	0.000	0.750	0.002	0.040
Prasinophytes	0.000	0.026	0.000	0.000	0.000	0.000	0.042	0.014	0.000	0.108	0.000	0.000	0.000	0.351	0.000	0.000	0.445	0.014	0.002
<i>Trichodesmium</i>	0.000	0.000	0.000	0.000	0.000	0.000	0.000	0.000	0.000	0.000	0.000	0.000	0.133	0.000	0.000	0.000	0.760	0.107	0.000
Output matrix																			
Diatoms	0.000	0.155	0.000	0.000	0.279	0.000	0.000	0.000	0.029	0.000	0.000	0.016	0.000	0.000	0.000	0.000	0.509	0.000	0.013
<i>Synechococcus</i>	0.000	0.000	0.000	0.000	0.000	0.000	0.000	0.000	0.000	0.000	0.000	0.000	0.204	0.000	0.000	0.000	0.626	0.000	0.170
<i>Prochlorococcus</i> HL	0.000	0.008	0.000	0.000	0.000	0.000	0.000	0.000	0.000	0.000	0.000	0.000	0.400	0.000	0.078	0.448	0.000	0.065	0.000
<i>Prochlorococcus</i> LL	0.000	0.014	0.000	0.000	0.000	0.000	0.000	0.000	0.000	0.000	0.000	0.000	0.117	0.000	0.480	0.284	0.000	0.105	0.000
Dinoflagellates	0.000	0.165	0.330	0.000	0.000	0.000	0.000	0.000	0.113	0.000	0.000	0.075	0.000	0.000	0.000	0.000	0.309	0.000	0.007
Haptophytes	0.084	0.078	0.000	0.004	0.130	0.189	0.000	0.000	0.056	0.000	0.000	0.022	0.000	0.000	0.000	0.000	0.434	0.003	0.001
Chrysophytes	0.054	0.054	0.000	0.218	0.152	0.000	0.000	0.000	0.032	0.000	0.000	0.026	0.000	0.000	0.000	0.000	0.450	0.013	0.000
Chlorophytes	0.000	0.000	0.000	0.000	0.000	0.000	0.035	0.029	0.000	0.000	0.000	0.000	0.000	0.271	0.000	0.000	0.621	0.018	0.026
Cryptophytes	0.000	0.053	0.000	0.000	0.000	0.000	0.000	0.000	0.000	0.000	0.154	0.000	0.000	0.000	0.000	0.000	0.751	0.002	0.040
Prasinophytes	0.000	0.026	0.000	0.000	0.000	0.000	0.042	0.014	0.000	0.108	0.000	0.000	0.000	0.351	0.000	0.000	0.445	0.014	0.002
<i>Trichodesmium</i>	0.000	0.000	0.000	0.000	0.000	0.000	0.000	0.000	0.000	0.000	0.000	0.000	0.133	0.000	0.000	0.000	0.760	0.107	0.000

Abbreviations: chl c_3 : chlorophyll c_3 ; chl c_1+c_2 : chlorophyll c_1+c_2 ; peri: peridinin; but: 19'-butanoyloxyfucoxanthin; fuco: fucoxanthin; hex: 19'-hexanoyloxyfucoxanthin; neo: neoxanthin; viola: violaxanthin; diad: diadinoxanthin; pras: prasinoxanthin; allo: alloxanthin; diat: diatinoxanthin; zea: zeaxanthin; chl b_1 : chlorophyll b ; chl b_2 : divinylchlorophyll b ; chl a_2 : divinylchlorophyll a ; chl a_1 : chlorophyll a ; α -ca: α -carotene; β -ca: β -carotene.

This matrix factorizing program aims at estimating the contributions of individual phytoplankton groups to the microalgal community based on the detected concentrations of marker pigments and the theoretical ratios of individual pigments to Chl *a* for each taxonomic class. The applied pigment ratios are representative for species of the tropical/equatorial ocean (Mackey et al., 1996), with modifications according to Veldhuis & Kraay (2004) concerning the *Prochlorococcus* population (Tab. 1.1). This group was divided into a high-light (surface) and a low-light (deep-water) adapted strain, based on the concentrations of divinylchlorophyll *a* and divinylchlorophyll *b* (Penno et al., 2000). The chlorophyll degradation product phaeophorbide was also determined via the HPLC method.

2.7. Data processing

Section plots of the 10°S transect were prepared with the MATLAB program. Ocean Data View 3.4. and 4.3. was used for production of a cruise map and for plotting nutrient data from World Ocean Atlas 2009 (Garcia et al., 2010b). Topographic contours in all plots were generated with ETOPO1 Global Relief Model (Amante and Eakins, 2009).

3. Results

3.1. Hydrographic structure

Hydrographic characterization of the water column along the east-west transect at 10°S in the East Pacific was accomplished by analyzing the distribution of temperature (Fig. 1.2A) and O₂ (Fig. 1.2B). Both parameters revealed significant gradients along the transect owing to along-shore currents and upwelling (Czeschel et al., 2011). In the area of the inner shelf between 78.3 and 79°W (station 8-18) upwelling of cold (<15°C) and O₂-deficient (<5 μmol kg⁻¹) intermediate water originating from 100-150 m towards the surface occurred. This water mass, supplied by the poleward flowing Peru-Chile Undercurrent, prevented the formation of a prominent stratification and shifted the upper boundary of the OMZ (O₂ <20 μmol kg⁻¹) into surface waters up to 10-20 m water depth. The impact of vertical advection was predominantly restricted to the narrow inner shelf section while a pronounced thermo- and oxycline occurred above the continental slope and in the open ocean. In consequence a sharp horizontal gradient of O₂ was generated due to a drop of the upper limit of the OMZ from surface waters above the inner shelf to almost 100 m depth in the water body above the steep shelf break.

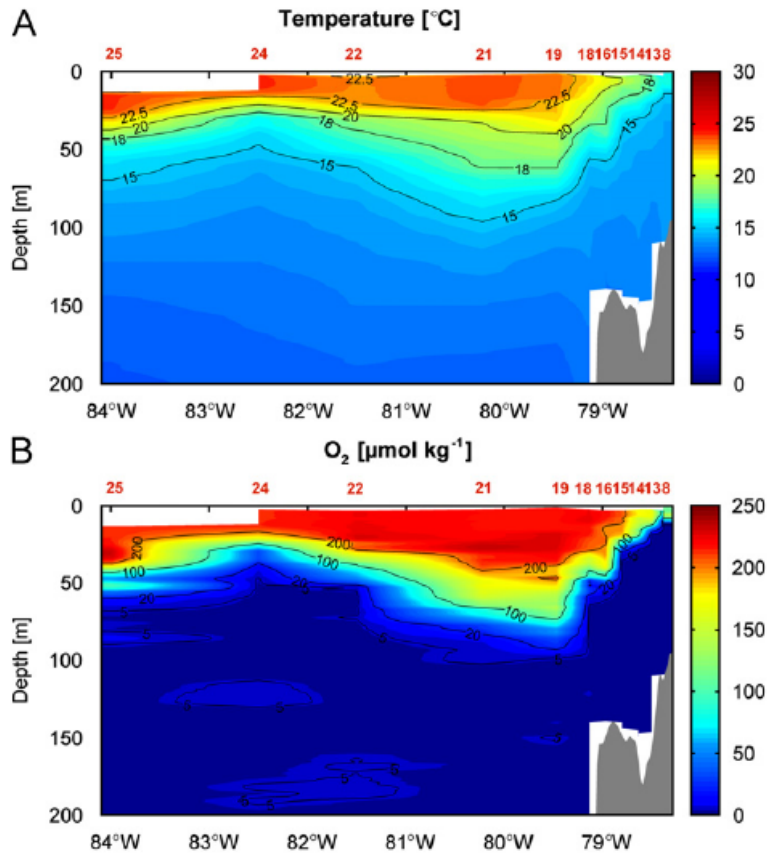


Figure 1.2. Spatial distribution of (A) temperature and (B) O₂ from 0 to 200 m depth in the water column along the complete 10°S section. Station numbers are denoted in red on top of the section plot.

The vertical extent of the oxycline was elevated over the continental shelf break, possibly caused by enhanced mixing of along-shore currents, and decreased west of the continental slope area towards the open ocean. In the open ocean the upper boundary of the OMZ reached about 50 m water depth. Based on the hydrographic data it can be concluded that physical forcing processes dominate the study area and establish various physico-chemical conditions for nutrient cycling and primary production.

3.2. Nutrient distribution

Distribution of the macronutrients NO₃⁻ (Fig. 1.3A), PO₄³⁻ (Fig. 1.3C) and Si(OH)₄ (Fig. 1.3D) showed a strong correlation with the hydrographic structure of the water column. For instance, temperature closely correlated with NO₃⁻ concentration ($r^2 = 0.84$; $n = 114$; $p < 0.0001$), with the exception of very low NO₃⁻ concentrations in close vicinity to the shelf bottom. A ‘high N loss’ sector was defined around the shelf bottom (station 8 and 13: 40 m - bottom; station 14, 15 and 16: 130 m – bottom) and the data excluded from the NO₃⁻/T regression.

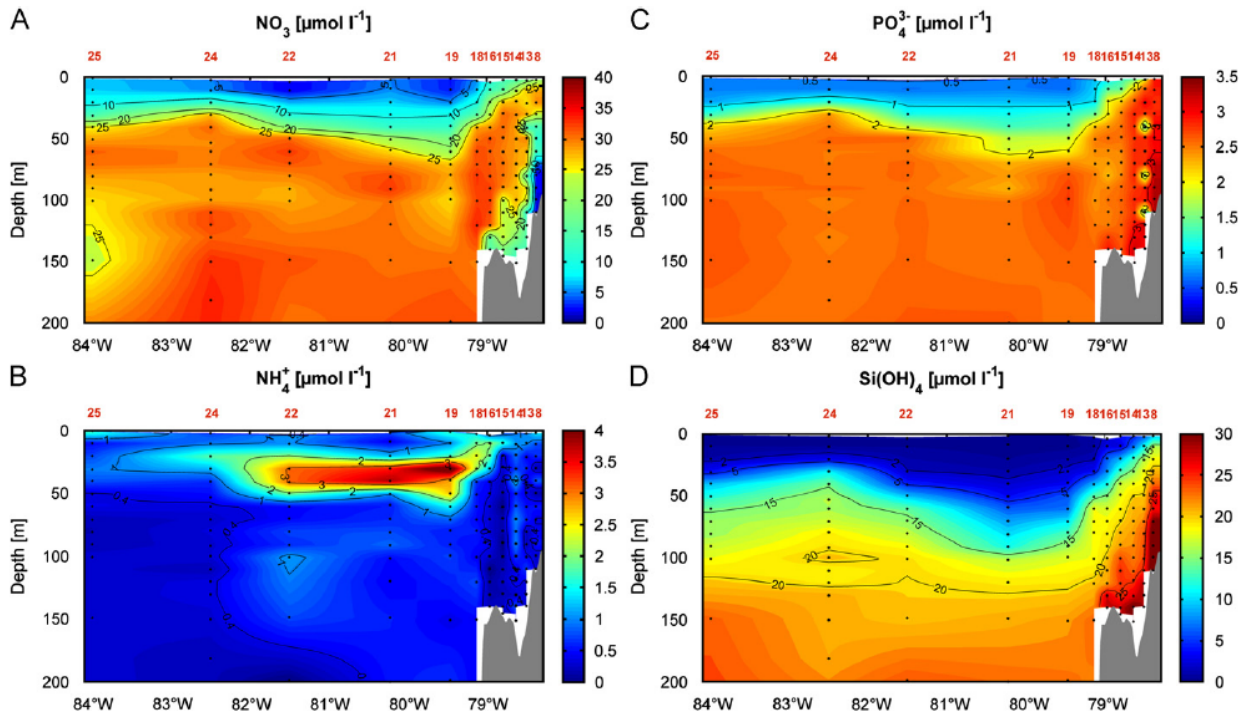


Figure 1.3. Spatial distribution of the major nutrients (A) NO_3^- , (B) NH_4^+ , (C) PO_4^{3-} and (D) Si(OH)_4 from 0 to 200 m depth along the complete transect. Style code as in Fig. 1.2.

Upwelling of intermediate waters in contact with the shelf sediment supplied high concentrations of PO_4^{3-} (up to $2 \mu\text{mol l}^{-1}$), Si(OH)_4 ($>15 \mu\text{mol l}^{-1}$) and NO_3^- ($>20 \mu\text{mol l}^{-1}$) to the surface layer of the inner shelf area, whereas nutrient concentrations were lower with $<1 \mu\text{mol PO}_4^{3-} \text{ l}^{-1}$ and $<2 \mu\text{mol Si(OH)}_4 \text{ l}^{-1}$ in the upper 25 m west of the inner shelf. Along the entire transect surface concentrations of NO_3^- and PO_4^{3-} ranged generally above $5 \mu\text{mol N l}^{-1}$ and $0.5 \mu\text{mol P l}^{-1}$, respectively, with a minimum of $2.7 \mu\text{mol NO}_3^- \text{ l}^{-1}$ above the shelf slope. While the NO_3^- to Si(OH)_4 ratio was <1 in the bottom waters of the inner shelf (Fig. 1.4), it ranged between 3-5 in the surface layer of the shelf and increased further to >10 towards the open ocean.

The distribution of NH_4^+ deviated significantly from the other macronutrients and displayed in some parts a converse pattern (Fig. 1.3B) as demonstrated by a negative correlation between NH_4^+ and NO_3^- within 20 to 150 m from station 18 to 24 ($r^2 = 0.64$; $n = 40$; $p < 0.0001$). A distinct maximum of NH_4^+ with concentrations up to $4 \mu\text{mol l}^{-1}$ was located in the broad pycnocline west of the inner shelf.

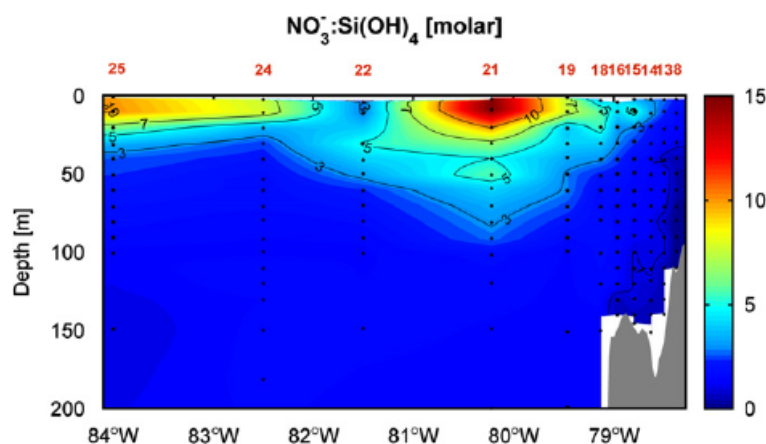


Figure 1.4. Ratio of NO_3^- to Si(OH)_4 from 0 to 200 m in the water column along the complete 10°S transect. Style code as in Fig. 1.2.

The ratio of total inorganic N (including NO_3^- , NO_2^- and NH_4^+) to P (PO_4^{3-}) was below Redfield proportions along the entire 10°S transect (Fig. 1.5A), with values generally ranging between 10-14. Lower values of 4-10 were measured in waters close to the shelf sediment and the upper 20 m along most of the transect. The observed low N:P ratios correspond to high concentrations of excess phosphate ($\text{P}^* = \text{inorg. P} - \text{inorg. N}/16$; after Deutsch et al., 2007) (Fig. 1.5B), with peak concentrations $>1 \mu\text{mol l}^{-1}$ in waters close to the shelf sediment and concentrations ranging between 0.2-0.5 $\mu\text{mol l}^{-1}$ in the upper 50 m west of 79°W (station 18). The ubiquitous existence of P^* within and above the OMZ emphasizes the relative deficiency in NO_3^- along the entire transect.

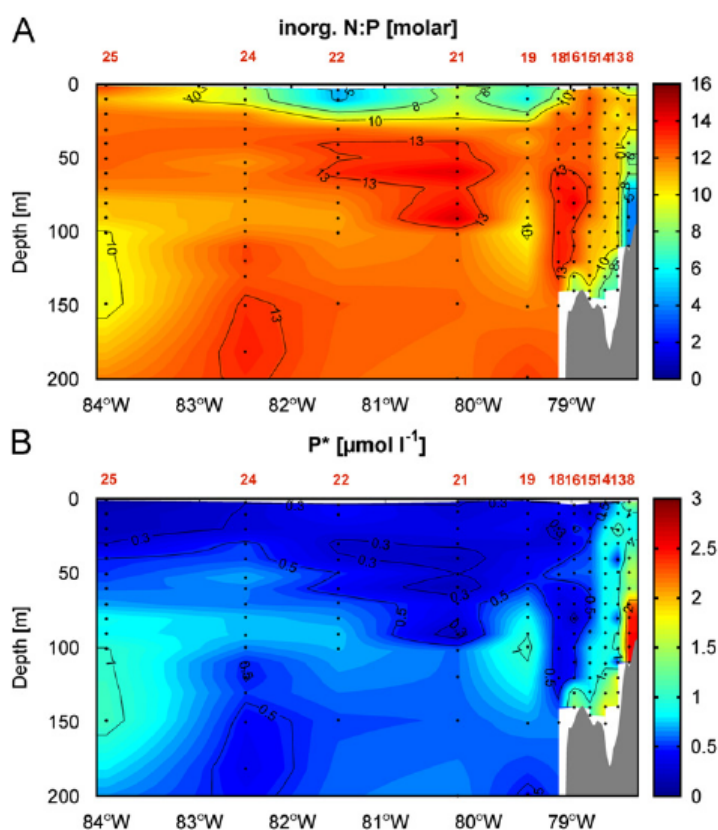


Figure 1.5. (A) Inorganic N:P stoichiometry and (B) excess P (P^*) according to the Redfield ratio of 16:1 along the complete transect. Style code as in Fig. 1.2.

3.3. Organic matter distribution and stoichiometry

Particulate organic carbon (POC), nitrogen (PON), and phosphorus (POP) (Fig. 1.6A-C), and chlorophyll *a* (Chl *a*, Fig. 1.7) reached maximum concentrations in the nutrient-replete surface waters of the inner shelf (see Fig. 1.3). High concentrations of organic matter (POC >12.5 $\mu\text{mol l}^{-1}$, PON >1.5 $\mu\text{mol l}^{-1}$, POP >0.1 $\mu\text{mol l}^{-1}$, DOC >120 $\mu\text{mol l}^{-1}$) concomitant with the absence of Chl *a* in the area of the shelf bottom water indicate the accumulation of detrital organic matter, which may have originated from particle sinking or resuspension of sedimentary material. DOC concentrations along the transect ranged generally around 100 $\mu\text{mol l}^{-1}$ (Fig. 1.6D). Strongly elevated DOC concentrations (>250 $\mu\text{mol l}^{-1}$) in the upper layer of the inner shelf and the shelf break coincided with maximum concentrations of microalgal biomass. An extremely high value of DOC >250 $\mu\text{mol l}^{-1}$ was recorded at station 8 in 10 m depth, where concentrations of particulate organic material were large as well. Maximum concentrations of particulate organic compounds at that station occurred however in the very surface (2 m water depth) above the DOC peak.

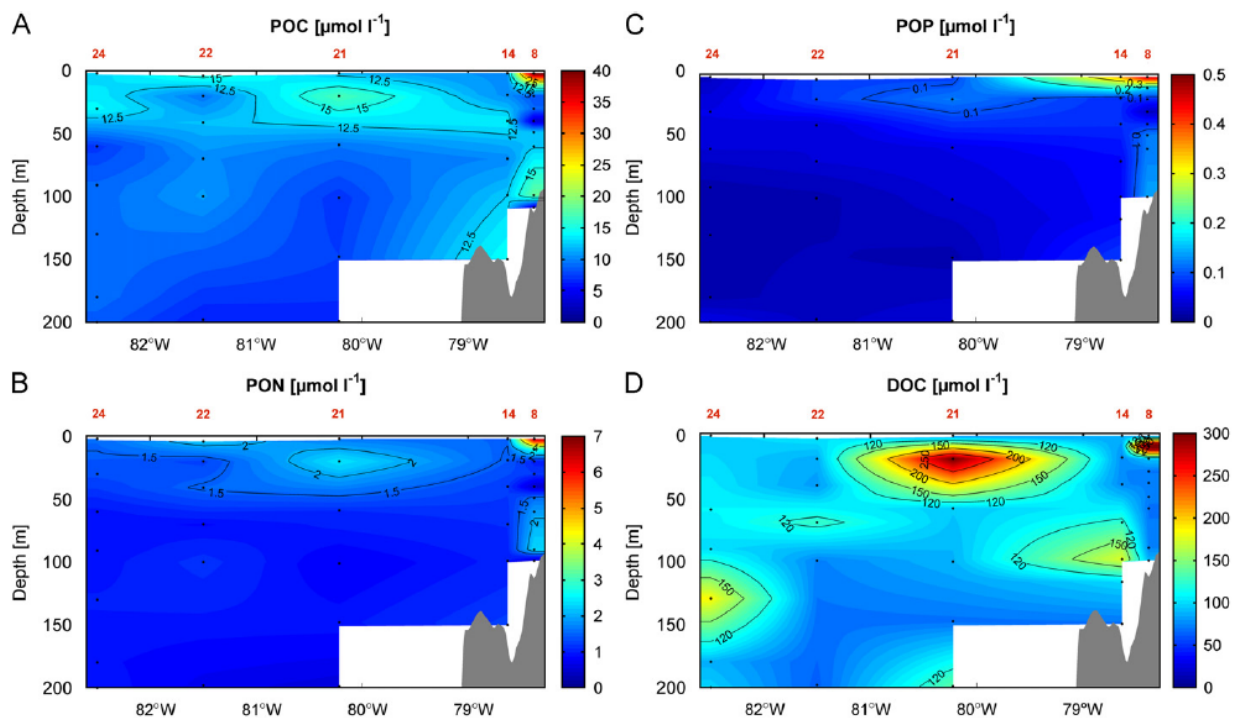


Figure 1.6. Spatial distribution of particulate organic matter with (A) POC, (B) PON, (C) POP and (D) DOC from 0 to 200 m at stations 8, 14, 21, 22 and 24. Style code as in Fig. 1.2.

While the inner shelf waters contained the largest amount of plankton biomass, elevated concentrations of organic matter (POC, PON, POP, DOC) and Chl *a* were also detected within the widely expanded and NH_4^+ -enriched pycnocline (see Fig. 1.2A, 1.3B) in the subsurface shelf break area. In addition, elevated concentrations of POC and Chl *a* occurred in the upper 50 m west of 82°W at station 24 and 25, respectively. Detection of Chl *a* between 80-100 m, even if

concentrations were quite low, indicate the presence of photoautotrophic organisms in the apparently still photic water layer.

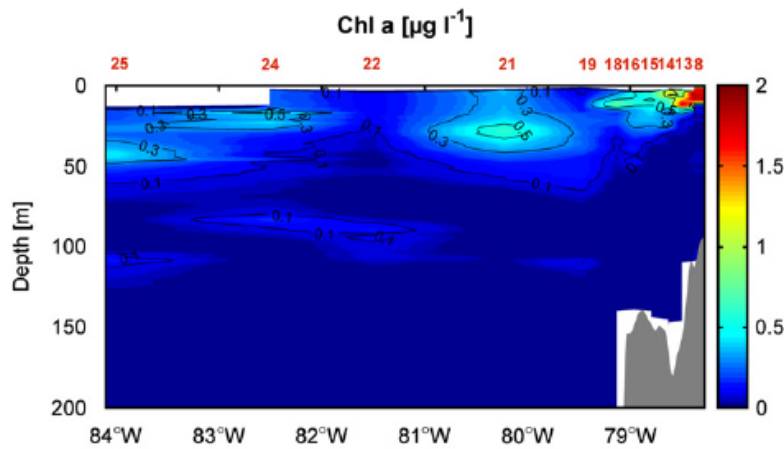


Figure 1.7. Spatial distribution of Chl a along the complete transect (0-200 m). Style code as in Fig. 1.2.

POP concentrations west of station 21 decreased to nanomolar levels which are below the detection limit of the method of analysis. This extremely low P content of organic matter led to a strongly increased PON:POP stoichiometry (20-50:1) (Fig. 1.8). Only in the waters above the inner shelf N:P composition of POM approached or fell below the 16:1 Redfield ratio. The water column down to 100 m above the continental slope displayed intermediate PON:POP ratios of 16-20. Considering the relatively high concentrations of NO_3^- and PO_4^{3-} along the entire transect, particulate organic matter concentrations were overall comparatively low.

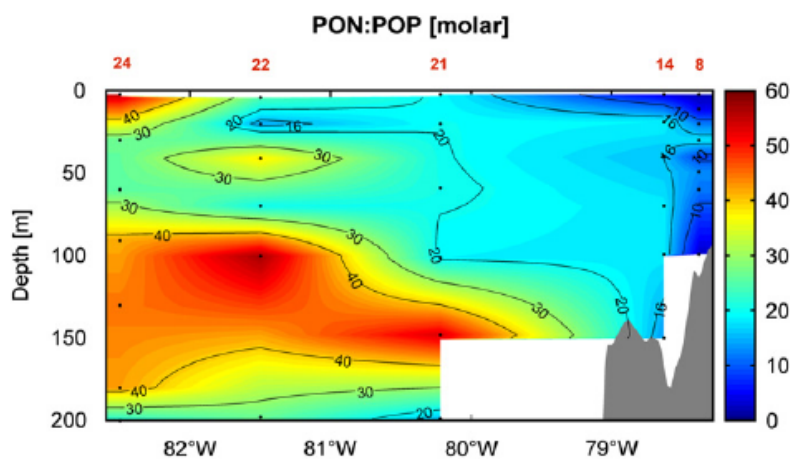


Figure 1.8. N:P stoichiometry of particulate organic matter at station 8, 14, 21, 22 and 24 along the transect (0-200 m). Style code as in Fig. 1.2.

3.4. Distribution of phytoplankton functional types (PFTs)

The abundance of phytoplankton groups along the 10°S section was determined on the basis of their pigment composition with the matrix factorization program CHEMTAX (Mackey et al., 1997). Diatoms, characterized amongst others by the pigment fucoxanthin, were in terms of Chl *a* normalized biomass the most dominant group of phytoplankton along the 10°S transect (Fig. 1.9A). Yet, high diatom abundance was primarily restricted to the nutrient-rich upper 20 m of the coastal upwelling area, with lower concentrations stretching into the shelf break waters. These lower values between station 14 and 21 were however a product of interpolation due to a low sample resolution in this area. Diatom biomass in the shelf surface layer matched with the distribution of BSi (Fig. 1.10), which in the majority originates from diatom silica frustules and therefore serves as an indicator for diatom abundance.

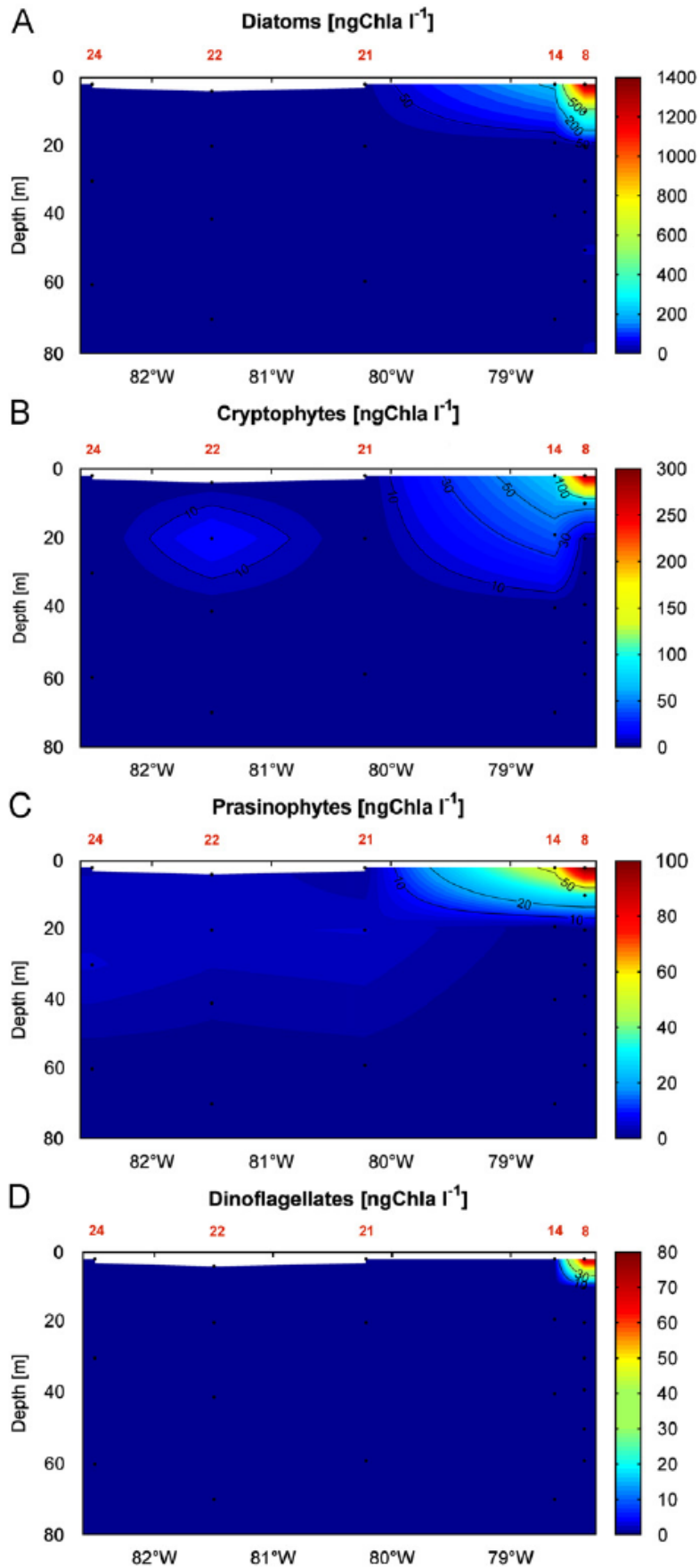


Figure 1.9. Abundance of PFTs at station 8, 14, 21, 22 and 24, which inhabited mainly the surface layer in the realm of the inner shelf from 0 to 80 m. (A) Diatoms, (B) cryptophytes, (C) prasinophytes and (D) autotrophic dinoflagellates. Style code as in Fig. 1.2.

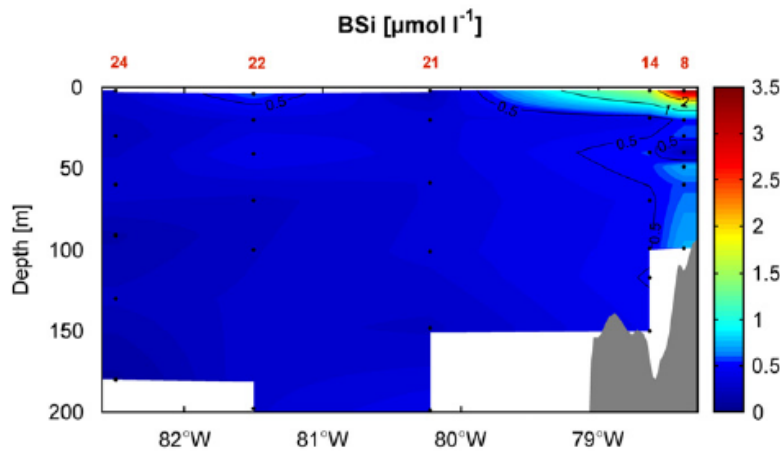


Figure 1.10. Concentrations of diatom-derived BSi from 0 to 200 m water depth at station 8, 14, 21, 22 and 24 along the transect. Style code as in Fig. 1.2.

Major occurrences of crypto- and prasinophytes, the latter being a subclass of the chlorophytes detectable via the diagnostic accessory pigment prasinoxanthin, occurred in the surface layer off the coast, but in terms of Chl *a* normalized biomass were less prominent than diatoms (Fig. 1.9B and 1.9C). Dinoflagellates, which can be identified precisely by the pigment peridinin exclusively produced by this group (see Tab. 1.1), played a negligible role in terms of biomass during our observations off the Peruvian coast, with a small population occurring in the surface water close to the coast (Fig. 1.9D). As mentioned before, no direct data exists for classification of phytoplankton functional types (PFT) between station 14 and 21. Considering the comparatively high Chl *a* fluorescence signal of $>0.5 \mu\text{g l}^{-1}$ in this section (see Fig. 1.7), interpolation of pigment data between stations 14 and 21 therefore may have led to an underestimation of PFT values within the shelf area of the transect.

The chlorophyll derivative phaeophorbide can be used as an indicator for herbivorous grazing (Shuman and Lorenzen, 1975). Concentrations of this phaeopigment occurred only in the water column above the continental shelf at station 8 and 14, and reached there quite high levels up to 700 ng l^{-1} (Fig. 1.11). No phaeophorbide was detected at station 21, 22 and 24.

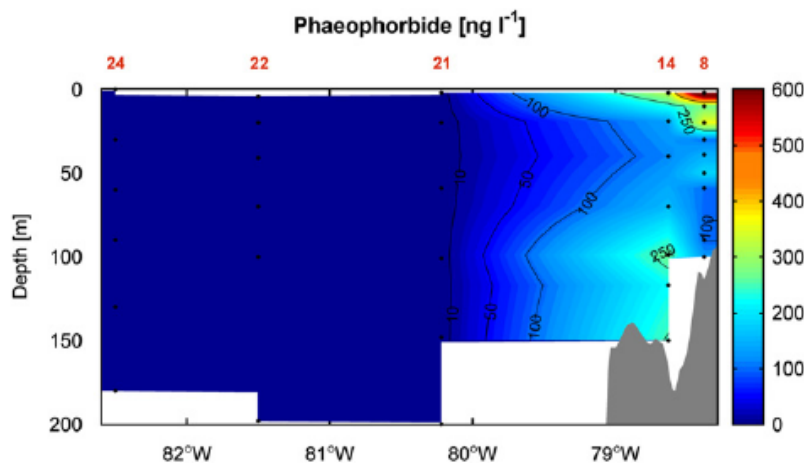


Figure 1.11. Distribution of the chlorophyll degradation product phaeophorbide along the transect at station 8, 14, 21, 22 and 24 from 0 to 200 m. Style code as in Fig. 1.2.

Chlorophytes, haptophytes, chrysophytes, and the unicellular pico-cyanobacterium *Synechococcus* also occurred in the surface waters (0-30 m) of the inner shelf area. In contrast to the larger phytoplankton mentioned above, these groups were not restricted to the nutrient-rich waters of the inner shelf area but were additionally present in the subsurface water layers west of the shelf (Fig. 1.12A-D). The population of haptophytes at 10°S consisted in large parts presumably of the colonial algae *Phaeocystis globosa*. *Phaeocystis* and coccolithophores contain the same marker pigments (chlorophyll c_3 , 19'-butanoyloxyfucoxanthin and 19'-hexanoyloxyfucoxanthin), but synthesize them in different proportions. Consequently, both groups of haptophytes cannot be distinguished from each other by pigment analysis. Microscopic counting of samples taken during on-deck incubation experiments on the same cruise revealed no indications of coccolithophores, instead large numbers of *Phaeocystis* were observed (Hausse et al., submitted for publication). Haptophyte communities in the tropics and subtropics are recently known to comprise also a significant fraction of picoplanktonic species (<3 μm) that are difficult to identify microscopically (e.g. Lepère et al., 2009; Liu et al., 2009). Based on all these facts we assume that the discovered populations of haptophytes along 10°S consisted of *Phaeocystis* as well as of picoeukaryotes. These haptophytes formed together with chlorophytes, chrysophytes and the prokaryote *Synechococcus* a subsurface photoautotrophic assemblage within the high NH_4^+ -containing pycnocline west of the inner shelf, also reflected in elevated Chl *a* concentrations (see Fig. 1.7). The picoplanktonic species *Synechococcus*, represented by the diagnostic pigment zeaxanthin (see Tab. 1.1), dominated this deep Chl *a* maximum in terms of Chl *a* normalized biomass.

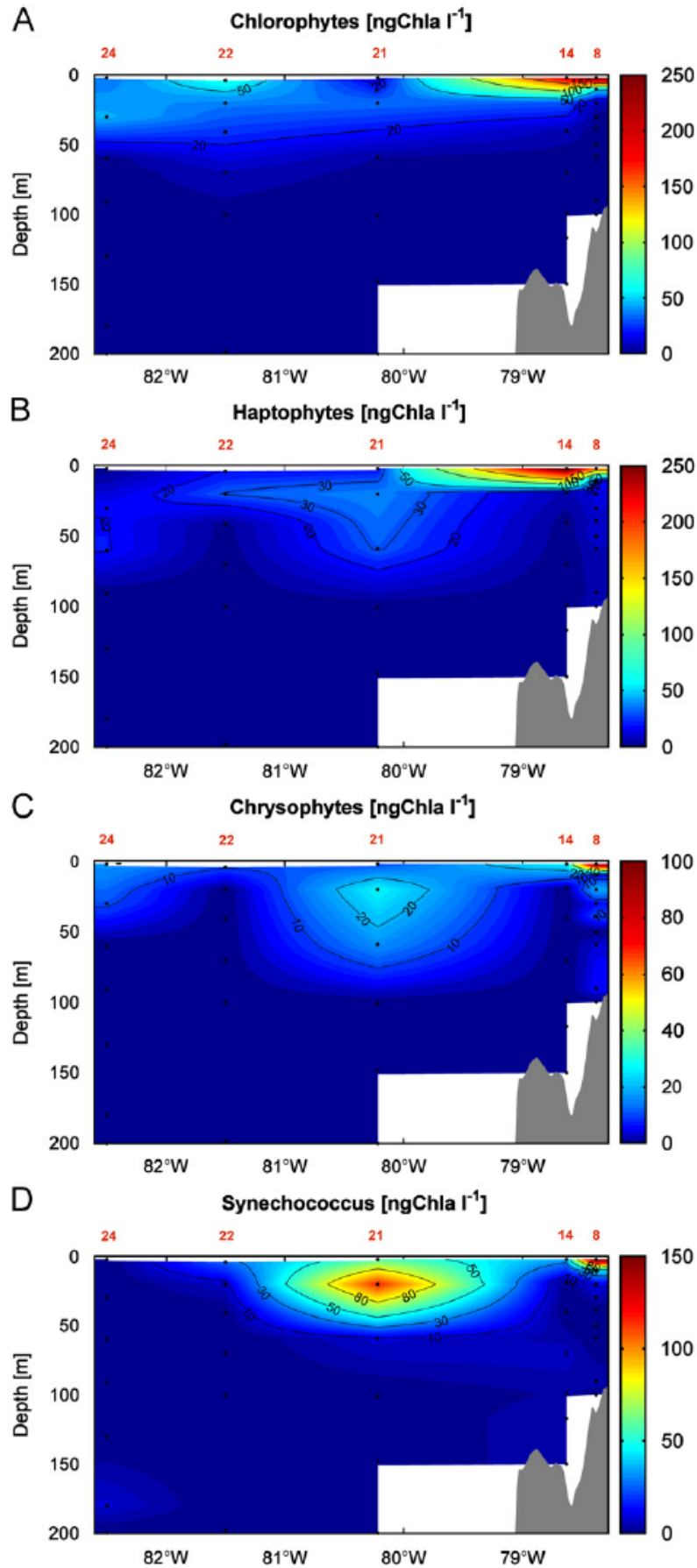


Figure 1.12. Abundance of PFTs growing in the surface layer of the inner shelf region and in the subsurface waters above the shelf slope at station 8, 14, 21, 22 and 24 (0-200 m). (A) Chlorophytes, (B) haptophytes, (C) chrysophytes and (D) the unicellular picocyanobacteria *Synechococcus*. Style code as in Fig. 1.2.

All PFTs mentioned so far produce monovinylchlorophyll *a* as their major photosynthetic active pigment. The genus *Prochlorococcus*, which belongs to the phylum cyanobacteria but lacks the ability of N-fixation, is an exception as it is the only photoautotrophic organism synthesizing divinylchlorophyll. Detection of this pigment allows an explicit classification of the small *Prochlorococcus* cells in the sample. By using the ratio of divinylchlorophyll *a* to divinylchlorophyll *b*, *Prochlorococcus* populations can be further distinguished into high- and low-light adapted strains. Very low concentrations (5 ng Chl *a* l⁻¹) of a high-light strain were detected in the upper 50 m at 82.5°W (station 24) (Fig. 1.13A). Higher concentrations of a low-light adapted population were observed in the intermediate water west of the shelf which increased going further west (Fig. 1.13B). Interpolation over a large depth (100-198 m) produced concentrations of this strain down to 170 m at station 22 as presented in the section plot. This might have led to an overestimation of the *Prochlorococcus* abundance in these waters. Presumably the lower margin of the low-light adapted *Prochlorococcus* population was in the range of 100 m and its occurrence coincided with the oxic/anoxic transition zone (see Fig. 1.2B and Tab. 1.1), representing the only photoautotroph on the transect growing in water below the pycnocline.

It has to be noted that no photosynthetic accessory pigments indicating the presence of N-fixing cyanobacteria (i.e. myxoxanthophyll, aphanizophyll, echinenone) were found at the stations that were sampled for PFT abundance.

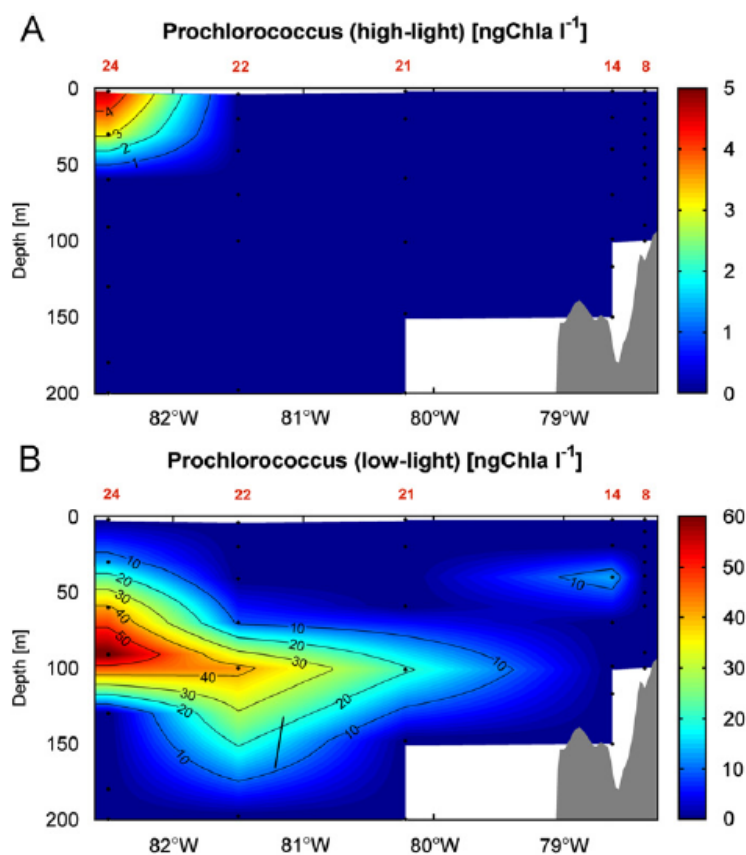


Figure 1.13. Abundance of two strains of the pico-cyanobacteria *Prochlorococcus*, (A) a high-light and (B) a low-light adapted population at station 8, 14, 21, 22 and 24 (0-200 m). Style code as in Fig. 1.2.

4. Discussion

4.1. HNLC conditions

Our observations showed upwelling of cold, O₂-depleted and nutrient-rich intermediate water in progress in the narrow inner shelf region of the transect between 78.3°W and 79°W (station 8-18), providing optimal growth conditions for phytoplankton. However, observed maximum concentrations of Chl *a* were low compared to common values for this extremely productive area (Chavez, 1995; Pennington et al., 2006). A large discrepancy existed between nutrient availability and particulate organic matter concentrations in the surface layer, with PON and POP levels up to an order of magnitude lower than inorganic NO₃⁻ and PO₄³⁻. Mean surface concentrations of NO₃⁻ and PO₄³⁻ in the tropical South East Pacific for January 2009 approximated by World Ocean Atlas data (Garcia et al., 2010b) show that the waters along 10°S were in the center of a massive upwelling plume, originating from the Peruvian shelf (Fig. 1.14A and 1.14B). Repressed uptake of these upwelled nutrients in surface waters enabled the expansion of nutrient plumes far into the oligotrophic Pacific open ocean to 115°W.

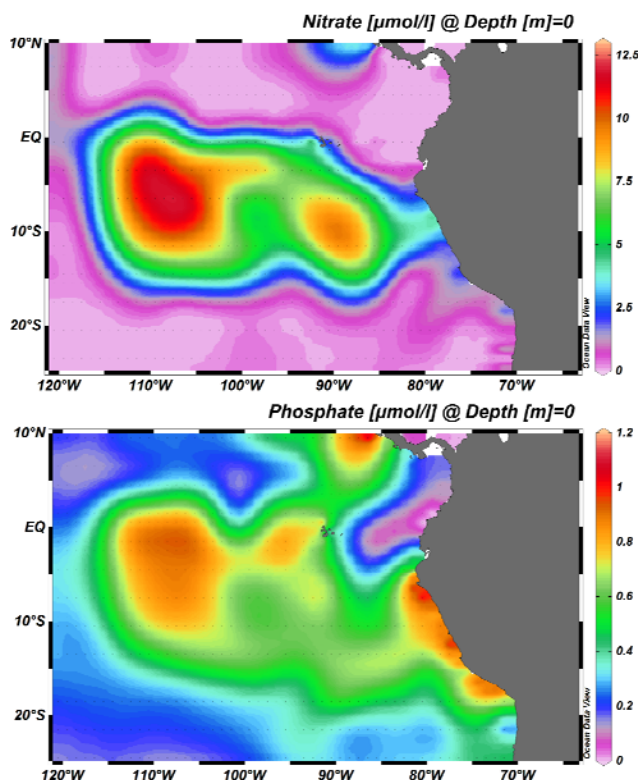


Figure 1.14. Mean surface concentrations of (A) NO₃⁻ and (B) PO₄³⁻ in the tropical South East Pacific for January 2009 (from World Ocean Atlas 2009; Garcia et al., 2010).

These high-nutrient, low-chlorophyll (HNLC) conditions have been reported previously for the Peruvian upwelling system (i.e. Thomas, 1979; Strickland et al., 1969; Minas and Minas, 1992). Iron limitation of phytoplankton, especially of diatoms, has been discussed as a possible explanation (Bruland et al., 2005). However, measured iron concentrations were not limiting

along the transect (C. Schlosser, personal communication). Very high ratios of NO_3^- to Si(OH)_4 of over 10:1 in the surface layer west of the inner shelf indicate that dissolved silica is ultimately limiting the build-up of diatom biomass (Conley and Malone, 1992; Dugdale et al., 1995). In fact, surface Si(OH)_4 concentrations of $<2 \mu\text{mol l}^{-1}$ west of the inner shelf are likely to cause Si(OH)_4 limitation stress for diatoms growing under NO_3^- replete conditions. But if blooming of diatoms was impeded by Si(OH)_4 limitation, other non-silicifying phytoplankton could have taken over. The fact that this was not observed points to herbivorous grazing by meso- and microzooplankton controlling phytoplankton standing stocks (Minas et al., 1986; Cullen et al., 1992). Most copepods avoid O_2 -depleted intermediate water layers and are forced to remain in the ventilated upper part of the water column (Boyd and Cowles, 1980). The resulting 'concentrated' grazing pressure may have contributed to keeping microalgal biomass low. High abundance of the chlorophyll derivative phaeophorbide in surface waters of the shelf area supports this assumption. Grazing on phytoplankton by herbivores produces this phaeopigment, which serves thus as a suitable indicator for zooplankton feeding activity. Complete absence of phaeophorbide at station 21 may imply that the NH_4^+ maximum at this station was mainly a product of bacterial decomposition rather than of zooplankton excretion (Smith and Whittedge, 1977).

4.2. Non-'Redfieldian' primary production

Dominance of phytoplankton communities by diatoms is a common characteristic of coastal upwelling systems and large phytoplankton generally prosper in nutrient-rich waters. In particular diatoms can take advantage of nutrient replete conditions through high levels of maximum specific uptake rates and a quick metabolic response after vertical intrusions of nutrient-rich water (Fawcett and Ward, 2011). As already pointed out these 'bloomers' are adapted to exponential growth with fast cell division and accordingly their metabolism requires the synthesis of large amounts of RNA, which is generally low in N:P. Nutrient requirements based on the specific growth strategy of the phytoplankton are therefore responsible for its cellular N:P composition (Arrigo, 2005). Particulate organic matter in the water column above the inner shelf had rather low N:P ratios $<16:1$, consistent with increased abundances of large diatoms, dinoflagellates and cryptophytes, which are all originating phylogenetically from the red plastid superfamily featuring low cellular N:P quotas (Quigg et al., 2003; Falkowski et al., 2004). According to Mills and Arrigo (2010) low N:P uptake of exponentially growing phytoplankton in eutrophic systems may be the main reason for a reduced availability of P^* for diazotrophic phytoplankton. This point is however addressed in more detail in the next section.

Prasinophytes and chlorophytes, both belonging to the green plastid superfamily, plus the unicellular cyanobacterium *Synechococcus*, also contributed to primary production in the

surface water layer of the inner shelf. Their cells commonly exhibit a relatively high N:P composition >20:1 (Quigg et al., 2003; Bertilsson et al., 2003), implying that N:P ratios of the inner shelf waters would have been even lower without the occurrence of this generally smaller phytoplankton.

Nutrient conditions for the phytoplankton community changed between the inner shelf and the steep shelf break due to a drastic shift in the hydrographic structure from intense coastal upwelling to the formation of a pronounced pycnocline. Accumulation of NH_4^+ in subsurface layers associated with strong density gradients is a common phenomenon in well-stratified waters, where a sufficient source of organic material is available from sinking organic matter 'trapped' within the pycnocline (Fogg, 1991; Holmedal and Utnes, 2006). The resulting long residence time of organic particles within this layer is generating optimal conditions for regeneration by zooplankton grazing and/or heterotrophic bacteria (Saino et al., 1983; Brzezinski, 1988). But since the absence of phaeophorbide at station 21 indicate a minor relevance of herbivorous grazing, this nutrient recycling system was presumably sustained by microbial degradation.

Even though NO_3^- and PO_4^{3-} were present at non-limiting concentrations in off-shelf waters, biomass of large blooming PFTs was significantly lower compared to the near-shore surface waters. The phytoplankton community west of the inner shelf consisted to a large part of nano- and picophytoplankton, which is characteristic for systems of regenerative primary production (Malone, 1980). As discussed in Section 4.1, diatom growth was likely inhibited by Si(OH)_4 limitation outside the center of upwelling. Size-selective grazing by mesozooplankton on large microalgae and microzooplankton may have suppressed build-up of the microphytoplankton community and relieved grazing pressure on the nano- and picoplankton communities (Richardson et al., 2004).

According to its marker pigment concentration the pico-cyanobacterium *Synechococcus* was the most abundant phytoplankton in the NH_4^+ -enriched subsurface layer. With its small cell size and a metabolism adapted to low nutrient concentrations, *Synechococcus* is a typical representative of the 'survivalists'. Cellular N:P is high owing to large amounts of proteins for nutrient uptake which permit maintaining net growth even under low nutrient availability (Bertilsson et al., 2003).

Chlorophytes, as part of the green plastid superfamily, are also characterized by a high N:P quota exceeding by far Redfield proportions. In the shelf slope area this group co-occurred with the abundant haptophytes and low numbers of microphytoplanktonic species, both characterized by low N:P ratios. Thus, the co-occurrence of 'bloomers' and 'survivalists' in this transition zone between shelf and oceanic waters resulted in the observed intermediate N:P ratios and can be seen as an example for the multi-specific composition of the intermediate Redfield ratio of 16:1 (Klausmeier et al., 2004a).

The oceanic section of the 10°S transect at station 22 and 24 west of 81°W was almost exclusively inhabited by one phytoplankton species, the unicellular pico-cyanobacterium *Prochlorococcus*, which is known to dominate photosynthetic biomass in the oligotrophic ocean (e.g. Campbell et al., 1994; Liu et al., 1997). A low-light adapted strain was distributed along the lower part of the thermo- and oxycline. Due to its photosynthetic apparatus *Prochlorococcus* can absorb photons at very high efficiency even at extremely low irradiances, allowing growth in waters below the nutricline down to 150-200 m depth. This is probably an essential feature of this non-diazotrophic phytoplankton to satisfy its nutrient demands for surviving in the highly stratified oligotrophic ocean (Partensky et al., 1993; Moore et al., 1995).

The high PON:POP stoichiometry (>20:1) in the open ocean section west of 80°W indicates a pronounced N-rich nutrient-acquisition machinery of the phytoplankton cells, although nutrients in the seawater were still available in sufficient quantities. Particularly high ratios (>40:1) were observed in the surface layer at 82.5°W (station 24) and in the intermediate water body between 80 and 170 m, correlating with the occurrence of the two *Prochlorococcus* strains. As the dominating photoautotrophic species of the oligotrophic ocean, this picoplanktonic organism is also featuring a high N:P- containing functional machinery (Bertilsson et al., 2003), allowing generally exploitation of the impoverished nutrient pools of the stratified ocean. Replete nutrient conditions even in the off-shelf waters did apparently not initiate a shift in allocation of cellular resources towards production of growth machinery in *Prochlorococcus*. In the course of ocean warming and the associated strengthening of water column stratification, oligotrophic regions are likely to expand and will promote growth of this high N:P assimilating picoplankton (Irwin et al., 2009). Increased uptake of N compared to P by expanding distributions of *Prochlorococcus* may enhance the inorganic N-deficit and generate elevated amounts of P* which could promote N-fixation (Mills and Arrigo, 2010).

4.3. Does P* control N-fixation?

A concept introduced by Deutsch et al. (2007) hypothesizes a tight spatial coupling between processes of N loss via denitrification and N gain via N-fixation. In their model simulations of global N-fixation rates Deutsch et al. (2007) assume an N:P uptake by non-diazotrophic phytoplankton according to Redfield. Bioavailable N lost via denitrification is estimated to range between 200-300 Tg yr⁻¹ (Codispoti, 1995; Galloway et al., 1995), generating excess PO₄³⁻ and thus favouring growth of N-fixing cyanobacteria. OMZs such as off the Peruvian coast represent particularly large sinks of inorganic N. In fact, low inorganic N:P ratios <10:1 in the vicinity of the shelf sediment indicate that a significant amount of remineralized NO₃⁻ is consumed by the microbial processes of denitrification (e.g. Codispoti and Packard, 1980) and/or DNRA (Lam et al., 2009), the latter subsequently providing NH₄⁺ for anammox, before reaching the euphotic

zone. As a result of this microbially induced N loss and the concomitant gain of P from anoxic shelf sediments, N has the potential to run into depletion before P does (Harrison et al., 1981), generating excess amounts of P available for the autotrophic community. Especially large phytoplankton in OMZ-influenced coastal upwelling areas takes advantage of the low inorganic N:P stoichiometry and removes a large portion of the P^* generated in O_2 -depleted intermediate shelf waters from surface shelf waters before it reaches oceanic waters (see Fig. 1.5B). This non-Redfield nutrient assimilation by non-diazotrophic phytoplankton counteracts the replenishment of the local N-deficit by decoupling the microbial processes of N loss and N gain in OMZ-influenced waters.

Despite the fact that positive values of P^* were present throughout the entire transect, based on the phytoplankton pigment analysis we could not detect photoautotrophic diazotrophic cyanobacteria at any of the stations sampled for PFT abundance. *Trichodesmium* and *Crocospaera*, representing presumably the most dominant species of nitrogen-fixing cyanobacteria in the tropical ocean, both contain the carotenoid myxoxanthophyll (Carpenter et al., 1993; Mohamed et al., 2005), which was not detected at any of the stations along 10°S. Molecular data collected during the same cruise detected genes expressing the N-fixation catalyzing enzyme nitrogenase concentrated within the OMZ on the 10°S transect (Löscher et al., unpublished results). These N-fixers were identified primarily as new clusters of probably heterotrophic bacteria. The recently discovered unicellular 'Group A' cyanobacteria is reported to lack photosystem II as well as photosynthetic accessory pigments (Zehr et al., 2008). Pigment fingerprinting can consequently not be applied for identification of this exceptional group of diazotrophs. However, Löscher et al. (unpublished results) did not detect any gene copies by representatives of 'Group A' along 10°S. Considering this finding and on the basis of the distribution of phytoplankton marker pigments along 10°S, we conclude that no phototrophic N-fixers occurred along the transect. This implies that the ubiquitous presence of excess concentrations of P in the upper 200 m along the transect did not result in growth of N-fixing cyanobacteria and conflicts with the hypothesis by Deutsch et al. (2007). Apparently it is not possible to deduce the distribution of diazotrophic phytoplankton solely from the N:P stoichiometry of dissolved nutrients without considering non-Redfield uptake of phytoplankton. Further crucial factors such as N availability, iron supply (Berman-Frank et al., 2001) and temperature distribution (reviewed by Stal, 2009) also have to be taken into account.

In fact, NO_3^- concentrations hardly dropped below $5 \mu\text{mol l}^{-1}$ even in the surface layer along 10°S. An ecological niche for N-fixers to enrich these waters with further N was thus not really given. Even though the low N:P supply ratio would have favoured growth of diazotrophic cyanobacteria, relatively high concentrations of NO_3^- (and also NH_4^+) in the off-shelf surface waters may have repressed their expansion.

As already mentioned, phytoplankton growth along 10°S was not limited by the micronutrient iron (C. Schlosser, personal communication). Yet, several studies reported on a tight correlation between water temperature and the distribution of N-fixing cyanobacteria (e.g. Falcón et al., 2005; Staal et al., 2007). In particular *Trichodesmium*, but also unicellular diazotrophs common in warmer waters appear to have a narrow temperature range for growth and N-fixation. Regions in the tropical and subtropical ocean characterized by water temperatures below 25°C were in most of the cases devoid of diazotrophic cyanobacteria, even with nutrient conditions (low inorganic N:P) favourable for their growth (Staal et al., 2007). Surface temperatures along 10°S never exceeded 25°C, but ranged mainly between 20-24°C in the off-shelf waters, which may have precluded the development of diazotrophic cyanobacteria despite the abundance of excess phosphate.

5. Conclusions

Our observations showed that the large oceanographic variability in the South East Pacific provides the habitat for a multitude of phytoplankton communities, forming a highly diverse photoautotrophic ecosystem from large diatoms in the near-shore upwelling areas to small picoplankton in the open ocean. Total phytoplankton biomass was kept low probably by zooplankton grazing in combination with an offshore Si(OH)_4 limitation of diatoms. Horizontal as well as vertical gradients in hydrography and nutrient distribution have a crucial impact on the taxonomical composition of the phytoplankton community by selecting for different types of growth strategies. Associated differences in specific nutrient requirements caused strong deviations in biomass elemental composition from the Redfield ratio, emphasizing non-‘Redfieldian’ nutrient assimilation by phytoplankton as a major driver in ecological stoichiometry. In order to evaluate the role of P^* as a control for the abundance of N-fixing cyanobacteria in the eastern boundary current areas further field data, including especially rates of N-fixation, are necessary. Even though P^* serves as the primary driver promoting growth of diazotrophic cyanobacteria on a global scale, its presence is a necessary but not sufficient condition for its development locally. Additional factors influencing the distribution of N-fixers on a local scale, such as N availability, iron supply and temperature, have to be considered.

Acknowledgments

We gratefully acknowledge technical assistance and support by Peter Fritsche, the CTD-Team and the Crew of *R/V Meteor* on-board the M77/3 cruise. Thanks also to Kai G. Schulz for help preparing the section plots. This work is a contribution of the Sonderforschungsbereich 754 "Climate-Biogeochemistry Interactions in the Tropical Ocean" (www.sfb754.de) which is supported by the German Science Foundation (DFG).

Study 2.**Changes in N:P stoichiometry influence taxonomic composition and nutritional quality of phytoplankton in the Peruvian upwelling**

Helena Hauss, Jasmin M.S. Franz and Ulrich Sommer

Helmholtz Centre for Ocean Research Kiel (GEOMAR), Düsternbrooker Weg 20, 24105 Kiel, Germany

*corresponding author:

Helena Hauss, Helmholtz Centre for Ocean Research (GEOMAR), Düsternbrooker Weg 20, 24105 Kiel, Germany, hhauss@geomar.de, Phone: +49 431 6004017, Fax: +49 431 6004402

Abstract

Inorganic dissolved macronutrient (nitrogen, N, and phosphorus, P) supply to surface waters in the eastern tropical South Pacific is influenced by expanding oxygen minimum zones, since N loss occurs due to microbial processes under anoxic conditions while P is increasingly released from the shelf sediments. To investigate the impact of decreasing N:P supply ratios in the Peruvian Upwelling, we conducted nutrient manipulation experiments using a shipboard mesocosm setup with a natural phytoplankton community. In a first experiment, either N or P or no nutrients were added with mesozooplankton present or absent. In a second experiment, initial nutrient concentrations were adjusted to four N:P ratios ranging from 2.5 to 16 using two “high N” and two “high P” levels in combination (i.e. +N, +P, +N and P, no addition). Over six and seven days, respectively, microalgal biomass development as well as nutrient uptake was monitored. Phytoplankton biomass strongly responded to N addition, in both mesozooplankton-grazed and not grazed treatments. The developing diatom bloom in the “high N” exceeded that in the “low N” treatments by a factor of two. No modulation of the total biomass by P-addition was observed, however, species-specific responses were more variable. Notably, some organisms were able to benefit from low N:P fertilization ratios, especially *Heterosigma* sp. and *Phaeocystis globosa* which are notorious for forming blooms that are toxic or inadequate for mesozooplankton nutrition. After the decline of the diatom bloom, the relative contribution of unsaturated fatty acid to the lipid content of seston was positively correlated to diatom biomass in the peak bloom, indicating that positive effects of diatom blooms on food quality of the protist community to higher trophic levels remain even after the phytoplankton biomass was incorporated by grazers. Our results indicate an overall N-limitation of the system, especially in the case of dominating diatoms, which were able to immediately utilize the available nitrate (within two days) and develop a biomass maximum within three days of incubation. After the decline of diatom biomass, detection of the cyanobacterial marker pigment aphanizophyll indicated the occurrence of diazotrophs, especially in those enclosures initially provided with high N supply. This was surprising, as diazotrophs are thought to play a role in compensating to some extent the N deficit above OMZs in the succession of phytoplankton after an upwelling event.

1. Introduction

Coastal upwelling systems are immensely productive, contributing an estimated 11% to the annual new production while covering only 1% of the world's oceans (Chavez and Toggweiler, 1995; Pennington et al., 2006). In the eastern tropical South Pacific, the high productivity in the photic zone leads to an extensive oxygen minimum zone (OMZ) at depth, reaching suboxic and in some regions anoxic oxygen (O_2) levels (Fiedler and Talley, 2006). Recent observations indicate that this OMZ is expanding in the course of global climate change (Stramma et al., 2008). Besides direct effects of low O_2 concentrations on metazoan life (Vaquer-Sunyer and Duarte, 2008), the biogeochemistry of both water column and sediments are highly influenced by concentrations of dissolved O_2 : under anaerobic conditions, massive losses of dissolved inorganic nitrogen (N) occur through denitrification (Deutsch et al., 2001) and anammox (Kuypers et al., 2005). In contrast, anoxic shelf sediments are a source for dissolved inorganic phosphate (P) as, under reducing conditions, P bound to metal oxides or biogenic apatite in fish debris is released into the water column (Van Cappellen and Ingall, 1994; Lenton and Watson, 2000). Thus, water masses that are already significantly below the canonical N:P Redfield ratio of 16 are transported by upwelling processes into the productive surface layer (Franz et al., 2012). Since changes in the nutrient stoichiometry have been observed to affect phytoplankton in respect of its community structure (Sommer et al., 2004), its elemental composition (Gervais and Riebesell, 2001) and its nutritional value for higher trophic levels (Kiørboe, 1989; Sterner and Schulz, 1998), changes in the upwelled nutrient stoichiometry may have strong impacts on the primary and secondary production as well as the biogeochemical cycling off Peru. It has been accepted for decades that the overall productivity in the Peruvian coastal upwelling is limited by new nitrogen (Dugdale, 1985). While it is largely assumed that especially large-celled phytoplankton communities on the shelf rely on the vertical supply of nitrate as opposed to offshore pico- and nanoplankton dominated assemblages that take advantage of regenerated ammonium and urea (Probyn, 1985), tracer uptake experiments conducted off Peru indicate that ammonium (NH_4) regenerated in surface waters can contribute up to 50% of total assimilated dissolved inorganic nitrogen (DIN; Fernández et al., 2009). However, the effect of non-Redfield N and P supply dynamics on the shelf phytoplankton assemblage has not been well studied yet, and field data describing the changes in community structure with increasing distance from the coastal upwelling are scarce (DiTullio et al., 2005; Franz et al., 2012). Traditionally, upwelling areas are considered to be regions of short energy transfer across few trophic levels, with diatoms, calanoid copepods and small pelagic fish feeding on zoo- and partly phytoplankton as key players (Cushing, 1989; Alheit and Niquen, 2004). Furthermore, diatoms are considered the main drivers of export flux due to their large cell sizes, high sinking velocities and rapid flocculation (Buesseler, 1998), thus channelling biomass into the OMZ. A plethora of studies exists describing the response of marine phytoplankton to nutrient

enrichment experiments (see Downing et al., 1999 and references therein) in terms of biomass or chlorophyll-a (Chl-a) change relative to an unamended control. Although the use of batch assays has been criticized in low-nutrient environments (Hutchins et al., 2003), they have contributed pivotally to our understanding of nutrient limitation in many systems and are considered suitable to simulate pulsed nutrient supply in coastal upwelling areas. While a number of studies have been conducted in the eastern North Pacific (Kudela and Dugdale, 2000; Wetz and Wheeler, 2003; Fawcett and Ward, 2011), little information is available on phytoplankton biomass regulation off Peru (Hutchins et al., 2002). Furthermore, no detailed studies exist that examine phytoplankton succession following an upwelling event in this area. The ability to fix elemental N by diazotrophic cyanobacteria is a major advantage in ecosystems prone to N limitation. Thus, it is argued that excess P in the euphotic zone as a result of N losses within the OMZ in the tropical eastern South Pacific could facilitate considerably higher N_2 -fixation rates than previously assumed (Deutsch et al., 2007). This is well in line with observations reporting that the role of unicellular cyanobacteria in the nutrient cycle has been underestimated (Zehr et al., 2001; Montoya et al., 2004; Moisaner et al., 2010) compared to the extensive surface blooms of *Trichodesmium* spp. in the warm surface waters of the oligotrophic ocean (Breitbarth et al., 2007).

The transfer of primary to secondary production (i.e. zooplankton growth) is driven by various factors, among which the quality of prey can be of equal or higher relevance than its quantity (Kleppel, 1993). Within the biochemical composition of microalgae, the proportion of polyunsaturated fatty acids (PUFAs) in relation to saturated and monounsaturated fatty acids (SAFA and MUFA, respectively) form an integral part of the food quality of a primary producer to higher trophic levels (Müller-Navarra et al., 2000). PUFAs such as 20:5n3 (eicosapentanoic acid, EPA) and 22:6n3 (docosahexanoic acid, DHA) cannot be synthesized *de novo* by most metazoan consumers and are thus considered essential (Brett and Müller-Navarra, 1997). It was demonstrated that PUFA content in the particulate matter can enhance secondary production of marine zooplankton (e.g. Jónasdóttir et al., 1995; Vargas et al., 2006). While carbon accumulation in nutrient-limited monoalgal phytoplankton cultures results in cells that are rich in lipids (Malzahn et al., 2010), N limitation may have a negative effect on relative PUFA content, as shown by Klein Breteler et al. (2005). Furthermore, changes in the taxonomic composition of a phytoplankton assemblage under nutrient limitation may influence the availability of PUFAs depending on the physiology of the species involved (Mayzaud et al., 1989; Vargas et al., 2006).

We hypothesized that changes in inorganic N and P supply as well as their ratio would influence the community composition and total biomass development of the phytoplankton, in turn affecting the quality to higher trophic levels. To investigate this, nutrient limitation experiments

were conducted using an *in situ* phytoplankton assemblage and meso-scale shipboard experimental containers.

2. Materials and Methods

2.1. Experimental setup

Two short-term (6 and 7d) growth experiments were conducted during cruise M77/3 on the German RV “Meteor” from Guayaquil (Ecuador) to Callao (Peru) from Dec 26, 2008 to Jan 21, 2009 (Table 2.1). The experimental setup comprised twelve 70L mesocosm bags afloat in four gimbals-mounted cooling water baths connected to a flow-through system that allowed a complete water exchange of the water bath with surface seawater within 10 to 15 min (Fig. 2.1 A). Surface water for the initial filling was obtained from repeated casts (10m depth) using Niskin bottles mounted on a CTD-rosette at 12°02.05’S, 077°47.33’W for experiment 1 and at 16°0.01’S, 074°37.04’W for experiment 2 (Fig. 2.1 B). The collected water from individual Niskin bottles was mixed in large barrels before filling the individual bags. Temperatures within the mesocosms varied with sea surface temperature and ranged from 19.0 to 23.0°C in experiment 1 and from 18.0 to 25.6°C in experiment 2. The water baths were shaded with nets to reduce light intensity to approximately 30% of surface irradiation. Daytime light intensity within the water baths ranged from 700 to 2600 $\mu\text{E s}^{-1} \text{m}^{-2}$. As an experimental treatment, inorganic N and P levels were manipulated by initial fertilization using ammonium nitrate (NH_4NO_3) and monopotassium phosphate (KH_2PO_4) to the respective target DIN:DIP ratios (Table 1), where DIN includes NH_4 and NO_3 . Equal SiO addition ($10\mu\text{mol L}^{-1}$) to all mesocosms using sodium metasilicate penta-hydrate ($\text{Na}_2\text{SiO}_3 \cdot 5\text{H}_2\text{O}$) as well as Provasoli PII metal mix (6ml) prevented co-limitation by Si or by trace elements. In experiment 1, either N or P (or none) was added in the presence or absence of mesozooplankton (removed by a 200 μm mesh screen), while experiment 2 was aimed at a closer investigation of N:P impact, and thus encompassed four N:P treatments, of which one (N:P=5) received no nutrient addition and thus represents the ambient nutrient conditions at the filling station. During experiment 2, the bottom plate construction failed in two mesocosms in the course of the experiment, thus these were omitted from subsequent analyses. Due to the limited water volume in this first application of the setup and the volume requirements of sampling (4-5L d^{-1}), mesocosms had to be restocked (i.e. diluted to initial volume) on days 3 (14L in experiment 1, 20L in experiment 2) and 5 (8L in experiment 1, 15L in experiment 2) using 5 μm -filtered surface seawater. In experiment 2, SiO was also restocked to $10\mu\text{mol L}^{-1}$ on day 5. However, due to the large differences in biomass and nutrient concentrations between sampling days, we did not attempt to calculate growth

rates and correcting the data for the dilution as we concluded that an extrapolation of growth rates in the sampled water would introduce a considerable error.

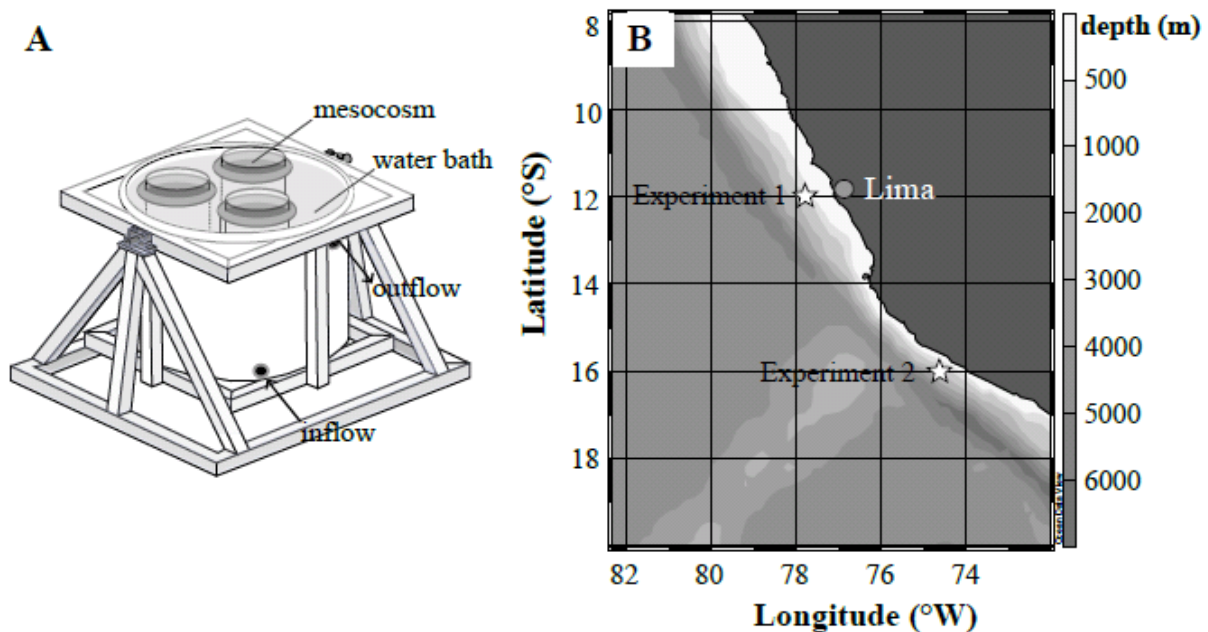


Figure 2.1. Sketch of three mesocosms within gimbals-mounted water bath with flow-through cooling using surface seawater (panel A). Four water baths with a total of twelve mesocosms were used. Locations of initial filling of the two experiments are indicated by stars on panel B.

Table 2.1. Overview of the initial and adjusted conditions of the two experiments.

	Experiment 1			Experiment 2			
initial conditions							
Latitude	12°02.05'S			16°0.01'S			
Longitude	077°47.33'W			074°37.04'W			
T (°C)	20.3			18.2			
DIN	5.5			5.0			
DIP	1.6			1.0			
SiO	3.2			3.7			
experimental conditions							
treatment	+N	none	+P	+N	+N&P	none	+P
N:P	20	3.4	2.8	16	8	5	2.5
N level	high	low	low	high	high	low	low
P level	low	low	high	low	high	low	high
adjusted DIN	32	5.5	5.5	16.0	16.0	5.0	5.0
adjusted DIP	1.6	1.6	2	1.0	2.0	1.0	2.0
adjusted SiO	10	10	10	10	10	10	10
replicates							
	2x zooplankton removed			3x			
	2x zooplankton						

2.2. Analyses

All samples except for fatty acid composition were taken on a daily basis after gentle mixing of each mesocosm by up-and-down stirring. Samples for dissolved inorganic nutrients (NO_3^- , NO_2^- , PO_4^{3-} , SiO) were filtered through 5 μm cellulose acetate filters (\varnothing 25mm) and immediately analyzed on board according to Hansen and Koroleff (1999) using a Hitachi U-2000 spectrophotometer. For determination of NO_2^- , 0.2ml sulphonamide and 0.2ml naphthylethyldiamine were added to 10ml of sample, incubated 30min at room temperature, and absorbance was measured at 542nm against double deionized water. To calculate the amount of NO_3^- in the sample, all NO_3^- compounds were reduced to NO_2^- using a cadmium reductor with the reagents sulphanilamide and N-1-naphthylethyldiamine dihydrochloride and incubating for 20min at room temperature before measuring. NH_4^+ analysis was conducted according to Holmes et al. (1999). Immediately after sampling, 10ml of unfiltered sample was mixed with 2.5ml of working reagent (WR) and incubated in the dark for 2h 15min, and its emission measured at 422nm. The WR consisted of 2L borate-buffer (80g $\text{Na}_2\text{B}_4\text{O}_7 \cdot 10\text{H}_2\text{O}$ + 2L double deionized water), 10ml of sodium sulfite (1g Na_2SO_3 in 125ml double deionized water) and 100ml of OPA-solution (4g orthophthaldialdehyde in 100ml ethanol).

For the analysis of PO_4^{3-} , 0.3ml of a mixed reagent (4.5M H_2SO_4 + ammonium molybdate + potassium antimonyl tartrate) and 0.3ml ascorbic acid were added to 10ml sample, incubated at room temperature for 10min and the absorbance measured at 882nm against double deionized water.

Analysis of $\text{Si}(\text{OH})_4$ was performed according to Hansen and Koroleff (1999). 0.3ml of a mixed reagent (molybdate solution + 3.6M H_2SO_4 in the ratio 1:1) was added to 10ml of unfiltered sample. After 10-20 min of incubation, 0.2ml oxalic acid and 0.2ml of ascorbic acid were added, and after another 30min, absorption was measured against double deionized water at 810nm wavelength in a spectrophotometer.

Cell counts of Lugol-stained microplankton were conducted daily on board using the inverted microscope method after Utermöhl (1958). Sedimentation volume was 50ml. At least 100 cells per category were counted when possible. Biovolumes were calculated after approximation to geometric shapes (Hillebrand et al. 1999) and converted to biomass ($\mu\text{g C L}^{-1}$) using the carbon to volume relationships described in Menden-Deuer and Lessard (2000). Nanoplankton and bacterial abundance were assessed using a flow cytometer (FACScalibur, Becton Dickinson, San Jose, CA, USA). Samples (5ml) were fixed with 2% formaldehyde, frozen at -80°C , transported to the laboratory and measured at a flow rate of $50.6\mu\text{l min}^{-1}$. Cells were distinguished by forward scatter (relative cell size) and fluorescence of Chl-a, phycoerythrin, and allophycocyanin. Biovolume was estimated assuming spherical shapes. For bacterial abundance, samples were diluted 1:3, stained with SYBR-Green and counted at lower flow rate ($13.9\mu\text{l min}^{-1}$).

The fatty acids of bulk seston were measured as fatty acid methyl esters (FAMES). 250 or 500ml water, depending on the concentration of phytoplankton, were filtered on precombusted 0.2µm GF/F filters at the start (duplicate sample) and the end of the experiment (one sample per mesocosm) and frozen at -80°C. Lipids were extracted from the samples with dichloromethane:methanol:chloroform (1:1:1 volume ratios), and C23:0 standard added. After centrifugation, water-soluble fractions were removed by washing with a 1M KCl solution and dried by addition of NaSO₄. The solvent was evaporated to dryness in a rotaryfilm evaporator (150-200mbar) and the remainder transferred with 200µl chloroform into a glass cocoon. Esterification was done over night using 2% H₂SO₄ in methanol at 50°C. The FAMES were washed from the H₂SO₄ using n-hexane, transferred into a new cocoon, and evaporated to dryness using nitrogen gas. N-hexane was added to a final volume of 100µl. All chemicals used were GC grade. FAMES were analyzed by gas chromatography using a Varian CP 8400 gas chromatograph equipped with a DB-225 column (JandW Scientific, 30m length, 0.25mm inner diameter, 0.25mm film). The carrier gas was helium at a pressure of 82.737Pa. Sample aliquots (1µl) were injected splitless. The injector temperature was set to 250°C. The column oven was set to 60°C for 1min after injection, after which it was heated to 150°C at 15°C min⁻¹, then to 170°C at 3°C min⁻¹, and finally to 220°C at 1°C min⁻¹, which was held for 21 min. The flame ionization detector was set to 300°C. FAMES were quantified using calibrations set up for each fatty acid separately.

Samples for High Pressure Liquid Chromatography (HPLC) were vacuum-filtered (150mbar) onto Whatman GF/F filters (25 mm) and immediately stored at -20°C until analysis in the laboratory. Filters were homogenized for 5min with 2mm and 4mm glass beads and 2ml acetone (90%). The supernatant was filtered through a 0.2µm teflon filter and stored at -80°C. The HPLC measurement was conducted by a Waters 600 controller in combination with a Waters 996 photodiode array detector (PDA) and a Waters 717plus auto sampler (modified after Barlow et al. 1997). Classification and quantification of the various phytoplankton pigments was performed with the software EMPOWERS (Waters).

2.3. Statistics

In order to estimate nutrient uptake rates, linear regressions were fitted to DIN and DIP over time in experiment 1. To be able to estimate nutrient drawdown dynamics in the different treatments in experiment 2, where the decrease in nutrient concentrations was nonlinear, three-parameter logistic regressions were fitted to nutrient concentrations over time:

$$(1) \quad [N] = \frac{a}{1 + \left(\frac{t}{t_{50}} \right)^b}$$

where $[N]$ is the concentration ($\mu\text{Mol L}^{-1}$) of the respective nutrient, t is time (days), and a , b , and t_{50} are regression parameters, so that t_{50} represents the time where half of the initially available nutrient concentration is consumed. Only values up to day four were included, as post-bloom conditions resulted in slight increase in detected concentrations of N and P.

Diatom biomass was described using a lognormal function

$$(2) \quad BM = BM_{MAX} * e^{-0.5 * \left(\frac{\ln(t / t_{BM_{MAX}})}{b} \right)^2}$$

Where BM is the observed biomass at time t (d), BM_{MAX} is the maximum biomass reached during bloom development and $t_{BM_{MAX}}$ is the time when maximum biomass is reached.

A factorial ANOVA with time, initial N level and P level as factors as used to explore differences between treatments in the biomass of individual species as well as aphanizophyll. A correlation matrix was used to explore the relationships between total diatom biomass (maximum of the respective mesocosm during the entire experiment) and individual fatty acids and their ratios determined at termination of the experiment (i.e. after the bloom). Data were square-root transformed to approximate normality.

3. Results

3.1. Nutrients

In situ nutrient concentrations at the filling stations were 5.5 and 5 $\mu\text{mol L}^{-1}$ total DIN, 1.6 and 1.0 $\mu\text{mol L}^{-1}$ DIP, and 3.2 and 3.7 $\mu\text{mol L}^{-1}$ SiO in experiment 1 and 2, respectively. This translates into molar N:P ratios of 3.4 and 5 in experiment 1 and 2, respectively (Tab 2.1).

After the start of the experiment, nutrient drawdown of the three macronutrients (DIN, DIP, SiO) began after a time lag of 1-2 days in experiment 1 and immediately in experiment 2. Generally, nutrient drawdown in experiment 1 (Fig. 2.2) was slower than in experiment 2 (Fig. 2.3), in which the initial phytoplankton assemblage contained more diatoms, with a mean (\pm SD) proportion of 6.9 \pm 3.8% and 60.2 \pm 7.4% of total microplankton biomass on day 1 in experiment 1 and 2, respectively. No significant differences in nutrient drawdown were detected within experiment 1 between the mesocosms with zooplankton present as opposed to the ones that were mesh-screened, therefore, data were pooled into four replicates of the three nutrient treatments. Until the termination of the experiment, dissolved nutrients were detected in all mesocosms. The drawdown of DIN in the “high N” treatment was significantly faster (ANCOVA, $p < 0.001$) than in the two “low N” treatments, with a mean (\pm SE) uptake rate of 2.9(\pm 0.3) $\mu\text{mol N d}^{-1}$ in the +N treatment, 0.40(\pm 0.12) $\mu\text{mol N d}^{-1}$ in the +P and 0.40(\pm 0.13) $\mu\text{mol N d}^{-1}$ in the ambient treatment, respectively (Fig. 2.2A). Similarly, DIP uptake rates were similar in the two

“low P” treatments over the course of the experiment, with $0.09(\pm 0.02)\mu\text{mol P d}^{-1}$ in the ambient and +N treatment, respectively, and significantly higher (ANCOVA, $p < 0.001$) in the +P treatment with $0.12(\pm 0.03)\mu\text{mol P d}^{-1}$. No continuous removal of SiO could be observed (Fig. 2.2C). In contrast to experiment 1, the DIN pool was completely depleted on the third day in experiment 2. Mean half consumption times $t_{50}(\pm \text{SE})$ of DIN were significantly longer in the “high N” treatments ($p = 0.014$), with $1.84(\pm 0.07)$ and $1.9(\pm 0.08)$ days in the N:P=16 and 8, and $1.32(\pm 0.18)$ and $1.41(\pm 0.15)$ days in N:P=5 and 2.5 treatments, respectively. For DIP, mean half consumption times were significantly longer in the “high P” treatments ($p = 0.009$), with $1.23(\pm 0.07)$ and $1.73(\pm 0.09)$ days in the N:P=16 and N:P=8, and $1.34(\pm 0.2)$ and $2.23(\pm 0.3)$ days in the N:P=5 and 2.5 treatments, respectively. In the N:P=2.5 treatment, supplied P uptake was incomplete and a concentration of approximately $0.5\mu\text{mol L}^{-1}$ remained until termination of the experiment. The ratio of drawdown velocity, expressed as $t_{50}\text{N}:t_{50}\text{P}$, was positively related to initial N:P supply (Fig. 2.3, insert on panel B).

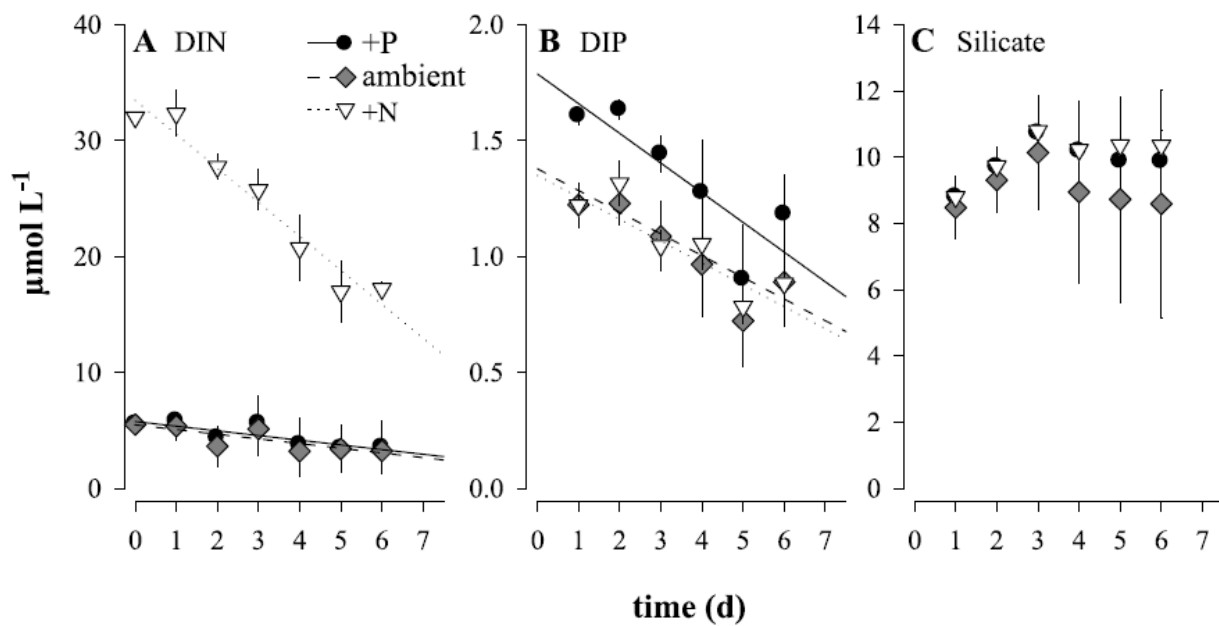


Figure 2.2. Dissolved inorganic nutrient (DIP, panel A, DIN, panel B, and SiO, panel C) concentrations ($\mu\text{mol L}^{-1}$) in experiment 1 over time. Values are treatment means (\pm standard deviation). Data from mesocosms with mesozooplankton removed and not removed were pooled because of insignificant differences, hence $n=4$ for all treatments.

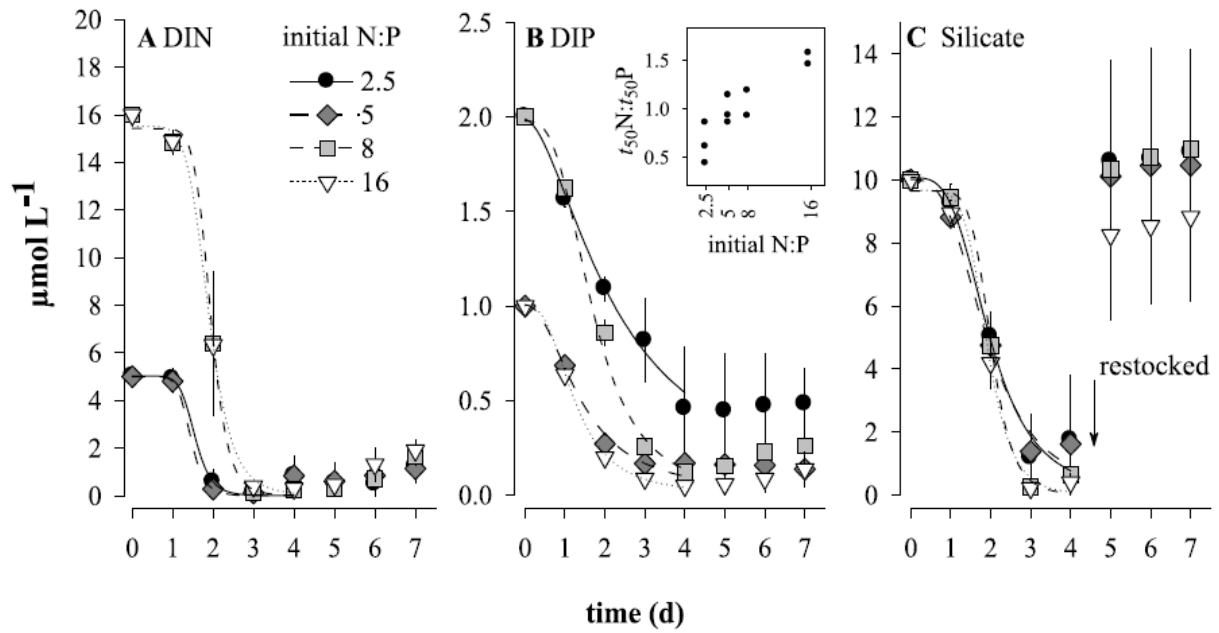


Figure 2.3. Dissolved inorganic nutrient (DIP, panel A, DIN, panel B, and SiO, panel C) concentrations ($\mu\text{mol L}^{-1}$) in experiment 2 over time. Values are treatment means (\pm standard deviation, $n=2-3$). Lines are sigmoid regressions fitted through individual mesocosm values up to day four (indicated by dashed line). Insert on panel B indicates relationship between half consumption times ($t_{50N}:t_{50P}$) and initial N:P supply ratio.

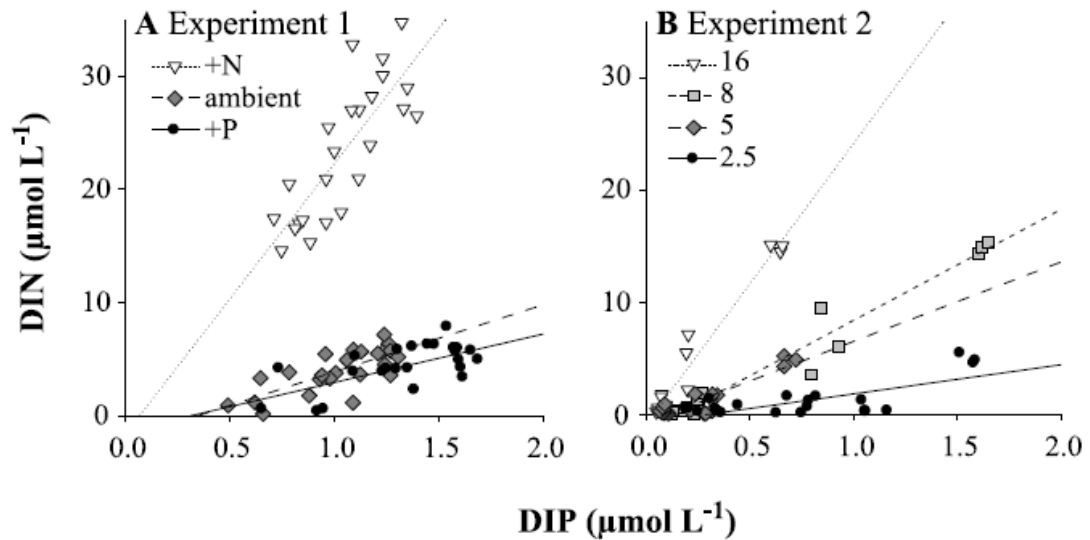


Figure 2.4. Uptake ratios of inorganic nitrogen and phosphorus in experiment 1 (panel A) and experiment 2 (panel B). Values are individual data, slopes of linear regressions correspond to uptake ratios.

The uptake ratios of inorganic N and P in the different experimental treatments determined by linear regressions (Fig. 2.4) were closely related to the initial N:P ratio provided in both experiments. In experiment 1, the regression slopes (\pm SE, $p < 0.001$) were 23.92(\pm 1.73), 5.9(\pm 1.15) and 4.28(\pm 1.05) in the +N (N:P=32), ambient (N:P=3.4) and +P (N:P=2.8) treatments, respectively. In experiment 2, the regression slopes (\pm SE, $p < 0.001$) were 25.01(\pm 1.48), 9.88(\pm 0.56), 7.07(\pm 0.75) and 2.59(\pm 0.56) in the +N (N:P=16), + N&P (N:P=8), ambient (N:P=5) and +P (N:P=2.5) treatments, respectively.

3.2. Total diatom biomass

In experiment 1, the removal of mesozooplankton larger than 200 μ m resulted in about two-fold increase in diatom biomass development within the respective nutrient addition treatments (Fig. 2.5). Nevertheless, diatom biomass was always higher in the +N treatments than in the other two. In experiment 2, diatom biomass was also higher in the two “high N” treatments (N:P=16 and N:P=8) than in the two “low N” treatments (N:P=5 and N:P=2.5) whereas no differences could be detected among the “high P” and “low P” treatments (Fig. 2.6A). The peak bloom was reached slightly earlier in the “low N” treatments.

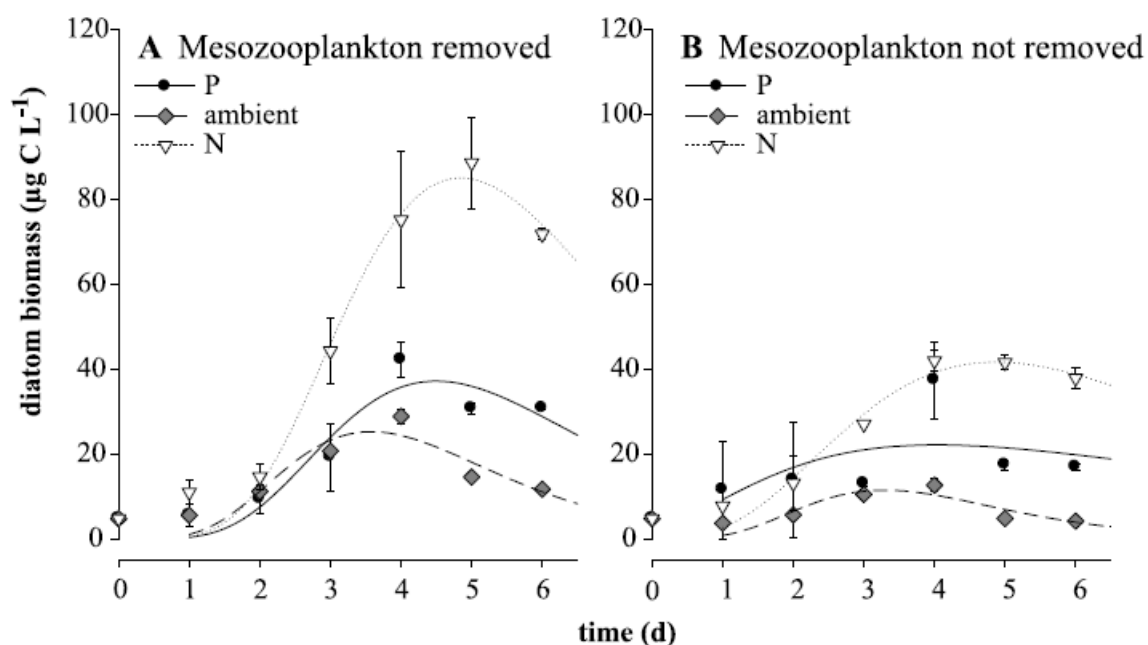


Figure 2.5. Summed diatom biomass (µg C L⁻¹) in experiment 1 over time in mesocosms with mesozooplankton removed (Panel A) and not removed (Panel B). Values are means (\pm standard deviation, $n=2$) of the fertilization treatments (+N, +P, ambient). Lines are lognormal regressions fitted through individual mesocosm data over the entire time period.

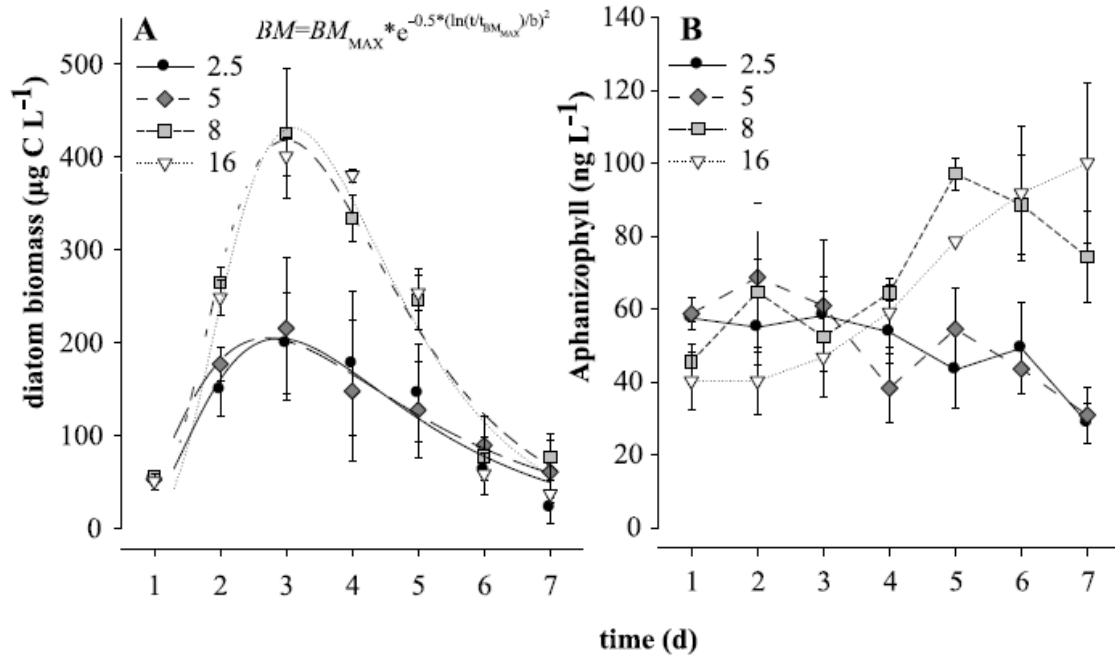


Figure 2.6. Summed diatom biomass (µg C L⁻¹) in experiment 2 over time (Panel A) and Aphanizophyll concentration (ng L⁻¹) as determined by HPLC over time (Panel B). Values are treatment means (±standard deviation). Lines in Panel A are lognormal regressions fitted through individual mesocosm data over the entire time period. Values are treatment means (±standard error).

3.3. Cyanobacterial marker pigment

During the first three days of experiment 2, no significant differences in the amount of aphanizophyll between the different treatments could be detected (Fig. 2.6B). However, after day 3, two diverging trends in the distribution of the pigment were monitored in the “high N” and “low N” treatments. Initial DIN concentration had a significant impact ($p < 0.0001$) on the production of aphanizophyll (factorial ANOVA with N-level, P-level and time as factors), whereas neither initial P nor the interaction between the two were significant and Tukey’s HSD post-hoc comparison ($p < 0.01$) revealed a significant separation of the aphanizophyll concentration between the two N-levels on days 6 and 7. In the two “high N” treatments (16:1 and 8:1), aphanizophyll increased continuously up to maximum mean (±SE) concentration of $168.2(\pm 37.7)$ and $163.9(\pm 13.8)$ ng L⁻¹ in the 16:1 and 8:1 treatment, respectively. Only minor changes over time were detected in those tanks treated with initial “low N”, with final mean (±SE) values of $66.8(\pm 7.7)$ and $54.7(\pm 10.0)$ in the 5:1 and 2.5:1 treatment, respectively.

Table 2.2. Summary of maximum biomass and *p*-values of an ANOVA comparing biomass of individual taxa over the entire experiment 1.

Nutrient treatment	initial	maximum biomass (µgC L ⁻¹)					p-value			
		ambient	+N	+P	ambient	+N	+P	time	zoo	nutrient
Nanoplankton										
<i>Prochlorococcus</i> -like mixed phototroph nanoplankton	1.5	0.8	0.8	0.8	2.0	6.0	6.4	<0.001	0.041	0.699
	16.1	164.9	193.8	198.1	193.7	256.9	239.0	<0.001	0.001	0.391
	0.0	2.8	2.3	2.1	3.9	5.5	6.2	<0.001	0.001	0.461
<i>Synechococcus</i> -like										
Ciliates										
<i>Laboea</i> sp.	6.0	3.0	7.5	6.9	2.1	7.7	3.0	<0.001	0.331	0.001
	0.1	1.2	4.9	3.6	1.2	4.1	6.0	<0.001	0.451	<0.001
	0.3	1.2	1.2	1.1	1.0	1.3	0.5	<0.001	<0.001	0.001
	0.4	1.2	5.0	1.0	0.4	0.7	1.5	<0.001	<0.001	<0.001
Dinoflagellates										
<i>Ceratium tripos</i>	1.1	0.3	5.3	0.7	0.7	5.1	1.8	<0.001	0.386	<0.001
	14.8	4.5	19.8	6.8	6.2	19.3	8.5	<0.001	0.500	<0.001
	7.9	35.6	199.4	24.9	12.3	137.7	17.6	<0.001	<0.001	<0.001
	0.3	0.5	2.0	0.6	0.6	0.7	0.4	0.016	<0.001	<0.001
<i>Protoperidinium depressum</i>	2.0	7.3	10.9	25.5	2.2	1.3	12.1	<0.001	<0.001	<0.001
	10.1	9.1	4.4	2.4	11.2	6.8	13.5	<0.001	0.009	0.142
	1.3	2.1	2.0	2.4	2.6	2.1	4.4	<0.001	0.034	<0.001
	28.6	145.7	233.6	151.9	72.2	164.3	64.6	<0.001	<0.001	<0.001
<i>Prorocentrum triestinum</i>										
Diatoms										
<i>Thalassiosira</i> sp.	2.3	4.6	7.1	3.2	1.3	3.6	16.9	0.161	0.902	0.180
	0.0	19.2	33.8	37.5	8.4	11.9	24.6	<0.001	<0.001	<0.001
	1.1	4.3	12.5	70.2	10.4	30.6	37.5	<0.001	0.023	<0.001
	0.1	3.9	64.9	3.7	2.5	36.4	2.3	<0.001	<0.001	<0.001
	1.1	3.6	5.8	5.8	12.5	7.4	4.5	0.977	0.165	0.924
	0.1	3.1	2.1	2.9	1.2	1.7	2.1	<0.001	0.023	0.935
	0.0	1.9	0.4	0.9	1.6	0.4	0.8	<0.001	0.036	<0.001
	0.1	166.4	195.2	114.8	151.0	175.9	146.4	<0.001	0.197	<0.001
<i>Pseudonitzschia</i> sp.										
other										
<i>Heterosigma</i> sp.	0.0	36.7	213.3	50.0	13.3	147.6	37.0	<0.001	<0.001	<0.001
	2.2	12.5	72.8	31.1	20.5	39.6	20.5	<0.001	0.970	<0.001
	8.8	36.1	213.0	29.2	18.1	147.4	25.2	<0.001	<0.001	<0.001
	1.6	7.1	15.5	12.6	4.2	11.9	10.6	<0.001	<0.001	<0.001
<i>Pyramimonas</i> sp.										

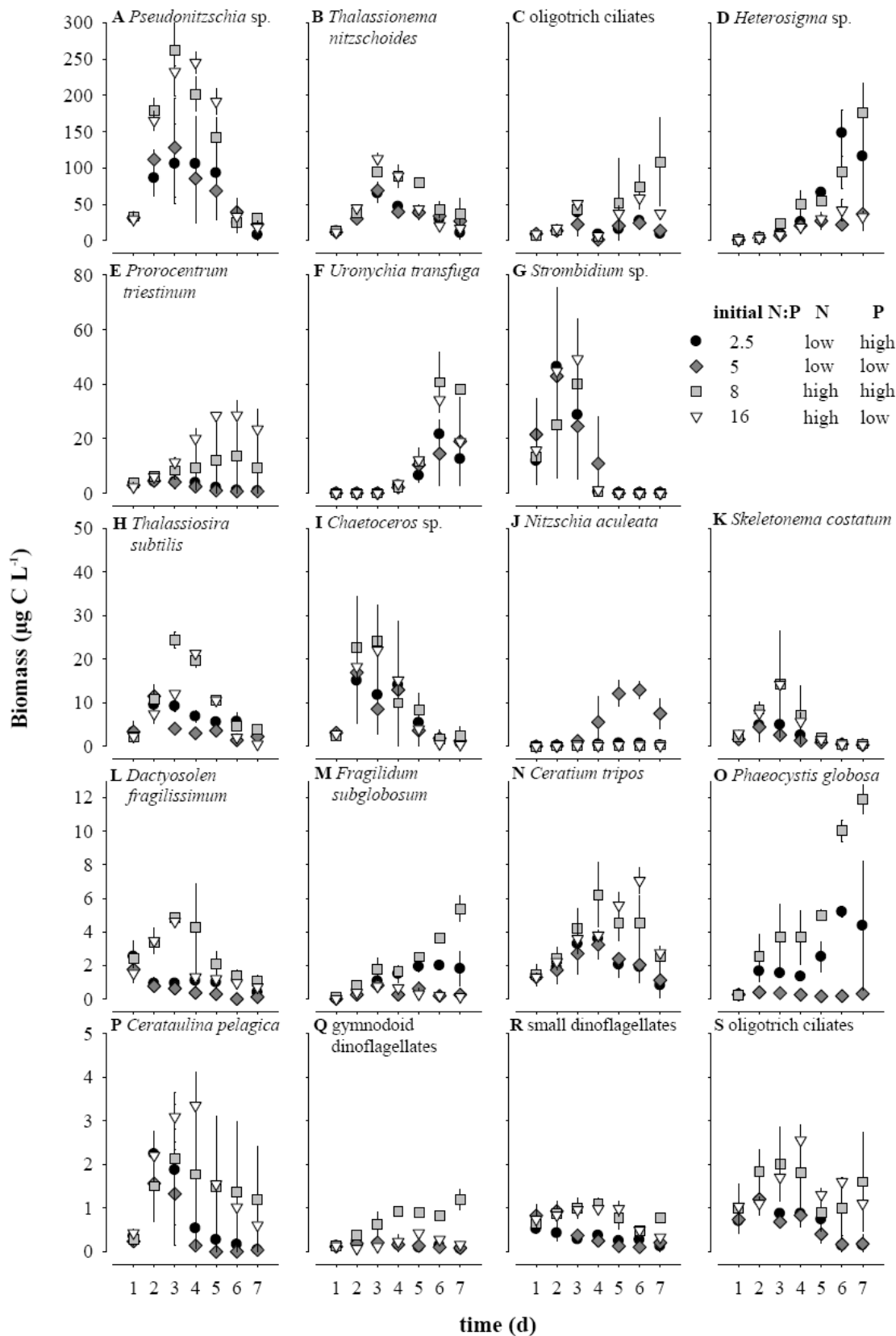


Figure 2.7. Microplankton biomass ($\mu\text{g C L}^{-1}$) derived from microscopic counts in experiment 2. Diatoms: panels A,B,H,I,J,K,L and P, dinoflagellates (all mixotrophic): panels E,M,N,Q,R, ciliates: panels C,G,S, haptophytes: panel O and raphidophytes: panel D. Note different scaling on y-axis, with the taxa reaching the highest biomass in the top row, and lowest in the bottom row. Values are treatment means (\pm standard deviation).

3.4. Individual taxa

In experiment 1, there were taxon-specific differences in the response to nutrient treatments and presence of mesozooplankton. Tab. 2.2 summarizes maximum biomasses of individual taxa as well as ANOVA significance levels of time (days), nutrient treatment (+N, + P, no addition) and zooplankton presence. Both zooplankton and nutrient supply significantly affected several microplankton species (Tab. 2.2). The presence of zooplankton resulted in many (but not all) of the larger organisms reaching lower biomasses. For example, the dominant diatom group (*Pseudonitzschia* sp.) was not negatively affected by higher grazing pressure ($p=0.197$). In contrast, nanoplankton biomass was significantly ($p<0.001$) higher in the mesh-screened treatments, indicating a trophic cascade effect. Nutrient addition resulted in higher biomass in most groups, with N-addition having a larger impact than P-addition (compare Fig. 2.5). The three dominant (biomass-based) dinoflagellate species (*Prorocentrum triestinum*, *Dinophysis caudata* and *Ceratium furca*) were all positively affected by N-addition, while P addition did not result in a biomass increase relative to the unamended control. Likewise, the two diatom groups contributing the largest proportion of biomass dominant diatoms (*Pseudonitzschia* sp. and *Chaetoceros* spp.) were positively affected by N ($p<0.001$), but not by P addition; however, in *Thalassiosira subtilis* and *Dactylosolen fragilissimum* the biomass response to P addition was significantly higher ($p<0.001$) than in the “ambient” treatment, while the two nutrient addition treatments (+N and +P) were not significantly different from each other. Likewise, in experiment 2, the dinoflagellate *Prorocentrum triestinum* (Fig. 2.7E) and diatoms of the genus *Pseudonitzschia* (Fig. 2.7A) were favoured by N-addition, while *Heterosigma* sp. (Fig. 2.7D) and *Phaeocystis globosa* (Fig. 2.7O) benefitted from increased P levels. The only species that reached significantly higher biomass in mesocosms with no nutrient addition was the diatom *Nitzschia aculeata* (Fig. 2.7J).

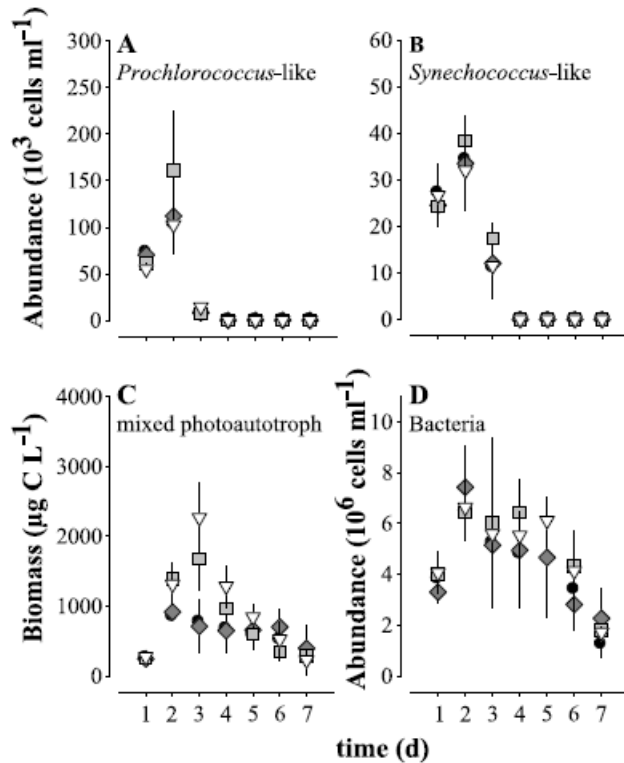


Figure 2.8. Nanoplankton abundance (panels A and B, no. ml^{-1}) and biomass (panel C, $\mu\text{g C L}^{-1}$) and bacterial abundance (Panel D, cells ml^{-1}) over time as detected by flow cytometry.

At the start of the experiment, a cluster with small ($<5\mu\text{m}$) cells containing very little Chl-a, and phycoerythrin likely *Prochlorococcus* (Fig. 2.8A), and one of similar size with slightly more Chl-a and especially phycoerythrin, likely *Synechococcus* (Fig. 2.8B), were identified and initially increased in number, but disappeared after day 4, with no differences between treatments. As the forward scatter to size conversion is inaccurate for cells smaller than $5\mu\text{m}$, we were not able to convert their abundance data into biomass by measured cell sizes. However, assuming a cellular carbon content of 50 and 200fg C cell^{-1} for *Prochlorococcus*- and *Synechococcus*-like cells (Bertilsson et al., 2003) would result in a maximum biomass of approximately 8.0 and $7.6\mu\text{g C L}^{-1}$, respectively. Mixed photoautotrophic nanoplankton comprised a considerable amount of the total calculated biomass (mean diameter $7.7\mu\text{m}$, Fig. 2.8C), with a similar temporal development of biomass as the microplankton (estimated from microscopic counts), however exceeding its biomass. Again, a significant difference between the two N-levels, but not between P-levels, was detected ($p < 0.001$). The highest biomass was reached on day 3 with $2266(\pm 498)$ and $1680(\pm 441)\mu\text{g C L}^{-1}$ in the N:P=16 and N:P=8 treatments, respectively, and on day 2 with $916(\pm 126)$ and $847(\pm 33)\mu\text{g C L}^{-1}$ in the N:P=5 and N:P=2.5 treatments, respectively. Bacterial abundance developed in parallel with the phytoplankton bloom, reaching a maximum abundance on day 2 and declining afterwards (Fig. 2.8D). No treatment effects could be detected in bacterial abundance.

3.5. Fatty acid composition

No significant correlation between maximum diatom biomass and total lipid content or individual fatty acid components could be detected. Both EPA (20:5n3) and DHA proportion (22:6n3) decreased slightly in both experiments during the course of the experiments. EPA contributed a mean (\pm SD) proportion of 4.39(\pm 0.49) and 5.13(\pm 0.06)% of total FA at the start, and 2.47(\pm 0.6) and 4.23(\pm 2.14)% at the end of experiment 1 and 2, respectively, while DHA contributed a mean (\pm SD) proportion of 10.38(\pm 0.68) and 5.37(\pm 0.01)% of total FA at the start, and 4.89(\pm 0.78) and 5.15(\pm 1.74)% at the end of experiment 1 and 2, respectively. However, a significant correlation ($r=0.69$, $p<0.05$) existed between the relative amount of unsaturated fatty acids ($FA_{\text{unsat/sat}}$) and maximum diatom biomass (Fig. 2.9).

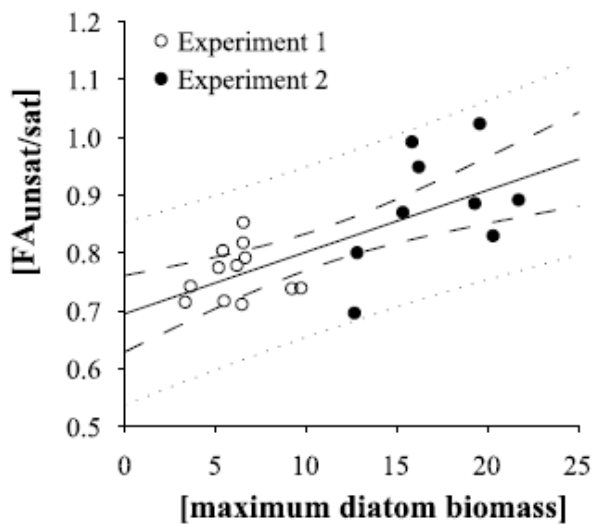


Figure 2.9. Positive correlation ($r=0.69$) of the proportion of unsaturated fatty acids ($FA_{\text{unsat/sat}}$) at final day of the two experiments with the maximum diatom biomass during the experiment. Values are square-root transformed single mesocosm data. Dashed line indicates 95% confidence band, dotted line indicates 95% prediction band.

4. Discussion

The Peruvian upwelling system is characterized by strong spatial gradients in surface nutrient concentrations, both in absolute concentrations and relative to each other (Bruland et al., 2005; Franz et al., 2012), indicating that several macro- and micronutrients can potentially limit primary productivity. Particularly iron can limit phytoplankton growth (Hutchins et al., 2002), while silicate limitation of diatoms becomes more crucial further offshore (Franz et al., 2012). However, under low O_2 conditions on the shelf, the high solubility of iron supplies high concentrations of Fe(II) to surface waters along with P (Bruland et al., 2005), rendering N the macronutrient in shortest supply if OMZs are expanding. Phytoplankton counts revealed a considerable effect of nutrient availability on the community structure of the primary producers, and N addition significantly increased the total biomass of protists (Fig. 2.5 and 2.6), indicating an overall N-limitation of the system. Under N-repletion, diatom biomass doubled and biomass

of autotrophic dinoflagellates increased up to 4-fold compared to the treatments with relatively low concentrations of N, implying that an increasing N-deficit in the O₂-deficient waters of the eastern South Pacific can induce a shift in the taxa dominating the phytoplankton community at the expense of diatoms and dinoflagellates. Given the response of bulk diatom biomass, it becomes evident that biomass production at the primary producer level depends solely on the supply of inorganic N. This is surprising, as we expected at least a modulation of the response by P availability. Diatoms are frequently characterized as “bloomers” (Klausmeier et al., 2004b; Arrigo, 2005) that keep a high-rRNA growth machinery adapted to rapid exponential growth and, thus, display low N:P requirements (Loladze and Elser, 2011) and are able to efficiently utilize excess P. Mills and Arrigo (2010) employed a dynamic ecosystem model to explore the relationship between nutrient uptake ratios of phytoplankton and marine nitrogen fixation. They suggested that by non-Redfield uptake stoichiometry, fast-growing phytoplankton (i.e. diatoms) in upwelling areas utilize excess P and therefore ultimately control new nitrogen flux by N-fixation into the ocean, as then excess P would not be available to diazotrophs further offshore. However, the plasticity of uptake stoichiometry (i.e. N:P < Redfield, Fig. 2.4) indicates that it is impossible to classify growth modes and uptake ratios of certain functional types of phytoplankton without taking into account that both growth and uptake ratio strongly depend on the limiting nutrient. This is partly reflected in the particulate matter (POM) pool (Franz et al., *subm.*), but also linked to higher release of dissolved organic phosphate (DOP; Franz et al., *subm.*). The partitioning of phytoplankton-derived organic matter between its dissolved and particulate fractions as a response to changes in nutrient supply has also been described by Conan et al. (2007), hence, we cannot conclude that the observed uptake ratios described in the present study are directly translated to phytoplankton or POM.

Wetz and Wheeler (2003) observed complete depletion of NO₃ by diatoms within three to five days, while SiO and PO₄ were still available, in deck incubation experiments off Oregon where deep water was seeded with a surface inoculum. Interestingly, the N:P uptake ratio before N depletion ranged from 13 to 15.6 in their study. N:P uptake ratios observed in yet another eastern boundary current system, the Benguela current, in microcosm incubations conducted by Pitcher et al. (1993) ranged from 13.5 to 19.8. Hence, it can be concluded that uptake ratios of diatom-dominated phytoplankton assemblages in upwelling areas are not necessarily low in N:P as suggested by Mills and Arrigo (2010); rather, the observed uptake ratios are directly related to supply. This can also be seen from the relative uptake velocity (estimated as “half consumption times” in our study) for the limiting and non-limiting nutrient, respectively. The ability of blooming diatoms to immediately utilize DIN and outcompete smaller size fractions of phytoplankton has recently been demonstrated in a simulated upwelling mesocosm experiment in Monterey Bay by Fawcett and Ward (2011). If the immediate growth response of fast-growing large diatoms to such upwelling events is directly related to the vertical supply of dissolved

inorganic nitrogen across into the photic zone, this might further intensify this imbalanced nutrient budget in the Peruvian upwelling.

While Fawcett and Ward (2011) observed a succession of diatom species from “ubiquitous” *Pseudonitzschia* spp.-dominated to “upwelling” *Chaetoceros* spp.-dominated, we found quite the contrary, *Pseudonitzschia* spp. contributing substantially to the total developing biomass, which in parts may be due to their protection against grazing. It has to be noted that some species within the genus *Pseudonitzschia* are known to produce the neurotoxin domoic acid, although it is questionable whether this is harmful to copepods (Lincoln et al., 2001). As can be seen from results in Experiment 1, presence of mesozooplankton did not significantly influence biomass development in *Pseudonitzschia* spp. Their relative proportion of microplankton biomass thus increased when grazing pressure on other algal groups was increased in the unscreened treatments (Tab. 2.2). However, since *Pseudonitzschia* numbers decreased after depletion of nutrients in both experiments, they apparently are consumed by microzooplankton. Their dominance might therefore also be caused by allelopathic effects that negatively affect the growth of other microalgae (Granéli and Hansen, 2006). Further, *Pseudonitzschia pseudodelicatissima* has been reported to grow particularly well following high ammonium concentrations (Seeyave et al., 2009), making it a good competitor in both upwelling and post-upwelling conditions. In the California Current, *Pseudonitzschia* was found to be associated with the beginning or end of strong upwelling periods, when nutrients are elevated but declining (Kudela et al., 2002).

In our experiment, *Phaeocystis globosa* (although never dominating algal biomass) was clearly profiting from P addition. This is in line with a study by Riegman et al. (1992) in the southern North Sea, who observed a positive effect of decreasing dissolved N:P in riverine discharge on biomass development of *P. globosa*. The authors hypothesized that *P. globosa* is a good competitor under N-limitation and tested this hypothesis in laboratory competition experiments. They found that *P. globosa*, while being outcompeted at high N:P by the coccolithophore *Emiliania huxleyi* and the diatom *Chaetoceros socialis*, quickly became the dominant species under N limitation (N:P=1.5). Interestingly, *P. globosa* growth was also found to be enhanced under increased Fe supply in the eastern tropical South Pacific (Hutchins et al., 2002); it may thus be one of the “winners” of elevated P/Fe and low N conditions on the shelf under ocean deoxygenation. *P. globosa* is thought to be of comparably low nutritional value to zooplankton consumers, as experimental studies using calanoid copepods and a mono-specific diet of *Phaeocystis* resulted in low egg production rates (Tang et al., 2001; Turner et al., 2002). However, since adult survivorship and egg hatching success were high throughout these feeding experiments, the authors conclude that the low food quality is due to the lack of essential constituents rather than the content of chemical compounds that act as mitotic

inhibitors (Turner et al., 2002). Moreover, its fatty acid composition was determined to be low in n3 PUFAs (Tang et al., 2001).

Within the biochemical make-up of primary producers, the fatty acid composition is recognized as one of the key factors of food quality. To metazoan consumers, particularly long-chained polyunsaturated fatty acids (PUFAs), such as eicosapentaenoic acid (EPA; 20:5n3) and docosahexaenoic acid (DHA; 22:6n3) are considered essential, as they usually cannot be synthesized *de novo* and thus have to be ingested in adequate amounts. In natural food webs, these components influence the growth and reproduction of zooplankton as well as trophic transfer efficiency (Kainz et al., 2004). Although a persistent effect on the bulk fatty acid composition could be detected at the end of the experiments (Fig. 2.9), no differences were found in the relative amounts of essential PUFAs such as EPA and DHA. Although the relative contribution of these components decreased during the experiments, they still contributed substantially to total lipids. It is therefore unlikely that consumers will be limited by PUFAs as a consequence of nitrogen-limited diatom growth in this assemblage. It has to be noted that the fatty acid analysis took place at the termination of the experiment, when a large proportion of the primary producers' biomass constituting the peak bloom was transferred to protozoan grazers such as various ciliates (Fig. 2.7C) and mixotroph dinoflagellates such as *Fragilidium subglobosum* (see Fig. 1.7M). For copepods, it has been demonstrated that protozoans contribute relatively more to the diet in oligotrophic ocean regions or under post-bloom conditions when phytoplankton concentrations are low (Calbet and Saiz, 2005). While it is generally accepted that marine ciliates contribute to the availability of phytoplankton biomass to mesozooplankton by repackaging of cells that are too small to be consumed directly (Sherr and Sherr, 1988), they are considered incapable of synthesizing PUFAs beneficial to higher trophic levels, a process dubbed "trophic upgrading" (Klein Breteler et al., 1999).

While nitrogen fixing cyanobacteria may be able to partially compensate the lack of available nitrogen, this appears to happen in a distinct succession rather than a direct response to P availability. Several studies in limnetic (Smith, 1983; Vrede et al., 2009), brackish (Niemi, 1979) and marine (Michaels et al., 1996) environments have reported on cyanobacterial blooms triggered by low inorganic N:P stoichiometry. Analysis of the pigment inventory by HPLC revealed that the photosynthetic accessory pigment aphanizophyll increased considerably after the complete depletion of both inorganic N and P after the diatom bloom in those tanks that received high initial N load (Fig. 2.6B). This xanthophyll is solely produced by cyanobacterial phytoplankton (Hertzberg and Jensen, 1966), but not by all cyanobacterial genera. It is even regarded indicative of N-fixing cyanobacteria (Hall et al., 1999) in freshwater systems, which is supported by the negative correlation between $\delta^{15}\text{N}$ in particulate organic matter (low $\delta^{15}\text{N}$ characterizes atmospheric fixed N) and the concentration of aphanizophyll in lakes (Patoine et al., 2006). Nevertheless, since aphanizophyll has also been detected in *Microcystis aeruginosa*

(Soma et al., 1993), a freshwater species which lacks the ability to fix dinitrogen, its detection might not necessarily imply the abundance of diazotrophic cyanobacteria. However, up to now there is no marine non-diazotroph cyanobacterium known to synthesize aphanizophyll. The widely abundant oceanic non-diazotrophs picoautotrophs *Prochlorococcus* and *Synechococcus* lack this pigment. No filamentous cyanobacteria such as *Trichodesmium* were detected by microscopic inspection, which is not surprising as they are not recorded in the nutrient-rich waters of the Peruvian Shelf. In general, *Trichodesmium* is encountered in oligotrophic waters with sea surface temperatures $>20^{\circ}\text{C}$ (Breithbarth et al., 2007). However, in contrast to filamentous species that often reach lengths of $200\mu\text{m}$ and form dense colonies, unicellular diazotrophic cyanobacteria with sizes of approximately $1\text{--}8\mu\text{m}$ cannot be identified using light microscopy, neither could they be distinguished from other photoautotrophs by flow cytometry. Only little is known about the pigment composition of N-fixing cyanobacteria such as the lately found “Group A” (Zehr et al., 2001) or diatom-diazotroph associations (DDAs) such as the endosymbiotic *Richelia intracellularis*. According to Řezanka and Dembitsky (2006), pigments from *Richelia* have not yet been isolated. However, their phylogeny (order Nostocales, family Nostocaceae) could indicate that they might be able to synthesize this pigment. DDAs have been found to substantially contribute to the diazotroph community in subtropical and tropical waters. Their occurrence has been reported from ocean areas as different as the Amazon River plume (Foster et al., 2007), the eastern tropical Atlantic (Foster et al., 2009), the southwest Indian Ocean (Poulton et al., 2009) and the southern California Current (Kimor et al., 1978). Since we did not assess N_2 -fixation rates in this study, and could not concomitantly detect other diazotroph carotenoids such as myxoxanthophyll, we cannot conclude whether the cyanobacteria present in the experiment were diazotrophic. Furthermore, even if diazotrophs were present in our experiment, N_2 -fixation might be down-regulated due to preferential uptake of DIN (Holl and Montoya, 2005). Further studies to investigate this succession pattern are recommended, preferably applying molecular techniques and N_2 -fixation rate assays, as it might be an important driver of the onshore-offshore differences in dominating algal functional groups.

Acknowledgments

We would like to thank the crew of RV “Meteor” for excellent support, Peter Fritsche for on-board nutrient measurements, and Thomas Hansen and Arne Malzahn for help in the lab. We thank Dr. Rainer Kiko and two anonymous reviewers for critically commenting on an earlier version of the manuscript. This work is a contribution of the DFG-supported project SFB754 (www.sfb754.de).

Study 3.**Effect of variable nutrient enrichment on the functional composition of a phytoplankton community in the eastern tropical Atlantic**

Jasmin M.S. Franz^{1*}, Helena Hauss¹, Carolin R. Löscher² and Ulf Riebesell¹

¹Helmholtz Centre for Ocean Research Kiel (GEOMAR), Düsternbrooker Weg 20, 24105 Kiel, Germany

²Institut für Allgemeine Mikrobiologie, Christian-Albrechts Universität zu Kiel, Am Botanischen Garten 1-9, 24118 Kiel, Germany

*corresponding author:

Jasmin M.S. Franz, Helmholtz Centre for Ocean Research Kiel (GEOMAR), Düsternbrooker Weg 20, 24105 Kiel, Germany, jfranz@geomar.de, Phone: +49-431-600-4290, Fax: +49-431-600-4446

Abstract

Results from previous bioassays conducted in the oligotrophic Atlantic Ocean determined availability of inorganic nitrogen (N) as the proximal limiting control of primary production, but additionally displayed a synergistic growth effect of combined N and P addition. To identify the primary limiting nutrient of coastal phytoplankton in the tropical ocean, we performed an 11-day nutrient enrichment experiment with a natural phytoplankton community from shelf waters off Northwest Africa in shipboard mesocosms. We used pigment and gene fingerprinting together with flow cytometry for classification and quantification of the taxa-specific photoautotrophic response on variable nutrient supply. Total phytoplankton biomass was solely controlled by the level of N supply, while combined high enrichment of N and P did not induce a further increase in phytoplankton abundance compared to high N enrichment alone. Extreme dominance of the photoautotrophic assemblage by N-limited diatoms in conjunction with the absence of any P-limited phytoplankton species prevented an additive effect of combined N and P addition on total phytoplankton biomass. Furthermore, succession of diatoms and nitrogen-fixing cyanobacteria occurred after nutrient exhaustion following to fertilization. The response of phytoplankton succession to the simulated upwelling event suggests that, in addition to the common distribution of nitrogen-fixing algae in the oligotrophic open ocean, shelf waters in the tropical East Atlantic may support growth of diazotrophic cyanobacteria such as *Trichodesmium* subsequent to upwelling pulses.

1. Introduction

Various theories are circulating about the nature of nutrient limitation in the pelagic tropical Atlantic. Bioassay approaches including additions of inorganic nitrogen (N), phosphorus (P) and dissolved iron (Fe) in the eastern Atlantic determined N as the key limiting nutrient for total primary production (e.g. Graziano et al., 1996; Mills et al., 2004; Moore et al., 2008). Some of these experiments indicated however also an apparent co-limitation of N and P (Moore et al., 2008), or Fe and P (Mills et al., 2004), both on a more species-specific level. In particular Fe and surplus P are assumed to provide a niche for diazotrophic phytoplankton (Mills et al., 2004). The gradient in nutrient N:P stoichiometry from Redfield conditions ($\sim 16:1$) in the eastern Atlantic to relatively high ratios ($>30:1$) in the West Atlantic implies a transition from slight N to severe P limitation (Fanning et al., 1992; Wu et al., 2000; Moore et al., 2008). In combination with the apparent absence of significant pelagic N loss in the eastern tropical North Atlantic (ETNA) (Ryabenko et al., 2011), the lower N:P signature appears to be rather conflicting with regard to the high supply of N to this area via dinitrogen (N_2)-fixation (e.g. Falc3n et al., 2004; Voss et al., 2004), riverine discharge (Nixon et al., 1996) and dust deposition (Talbot et al., 1986). Compared to the severely O_2 -deficient waters in the eastern Pacific and the Arabian Sea, minimum concentrations in the underlying oxygen minimum zone (OMZ) of the ETNA are generally too high ($40\text{--}50\text{ }\mu\text{mol kg}^{-1}$; Karstensen et al., 2008) to enable water column denitrification as a large-scale N loss process. But O_2 concentrations down to zero have meanwhile been detected in the core of spin-off eddies at the Cape Verde time-series station in the ETNA (Karstensen, pers. comm.). Moreover, recent publications indicate benthic N loss via denitrification and anaerobic ammonium oxidation (anammox) within the sediment of the Northwest African continental shelf (Trimmer and Nicholls, 2009; Jaeschke et al., 2010). Consequently, intermediate waters with reduced N:P stoichiometry are transported via coastal upwelling into the euphotic zone, forcing primary production towards N limitation. Along with high Fe supply by dust deposition from the African continent (Gao et al., 2001), such nutrient conditions are generally favouring development of N_2 -fixing cyanobacteria. As a result, diazotrophic phytoplankton like the filamentous cyanobacterium *Trichodesmium* (Capone et al., 1997; Tyrrell et al., 2003) and several groups of lately discovered unicellular diazotrophs (e.g. *Crocospaera*, Group A cyanobacteria, diatom-symbionts) (Falc3n et al., 2002; Langlois et al., 2008) are highly abundant throughout the tropical and subtropical Atlantic and contribute significantly to the input of N via biological N_2 -fixation.

Closer to the coast in the realm of the Northwest African upwelling, phytoplankton communities are primarily dominated by typical representatives of eutrophic systems such as diatoms, the haptophyte *Phaeocystis* and dinoflagellates (Margalef, 1978). Growth of diatoms and dinoflagellates are controlled by N availability (Ryther and Dunstan, 1971; Hauss et al., *subm.*), while *Phaeocystis globosa* has been reported to favour low N:P supply ratios (Riegman et al.,

1992; Hauss et al., subm.). Especially diatoms are, based on their low cellular N:P stoichiometry (Quigg et al., 2003; Arrigo, 2005), suspected to exploit a considerable fraction of freshly upwelled P on the shelf by non-Redfield production, reducing potentially the availability of P for diazotrophs further offshore (Mills and Arrigo, 2010; Franz et al., 2012).

Production of organic matter as a response to different nutrient supply conditions in that same experiment (Franz et al., subm.) indicated a proximate N limitation of total primary production. In this study, we address in detail the taxon- or even species-specific response of the phytoplankton community by identification and quantification of phytoplankton through pigment and gene fingerprinting and flow cytometry.

2. Material & Methods

2.1. Mesocosm experimental set-up

A nutrient limitation experiment in shipboard mesocosms was conducted using a natural phytoplankton community during R/V *Meteor* cruise M83-1 from Las Palmas (Gran Canary/Spain) to Mindelo (São Vicente/Cape Verde) in Oct./Nov. 2010 (Fig. 3.1).

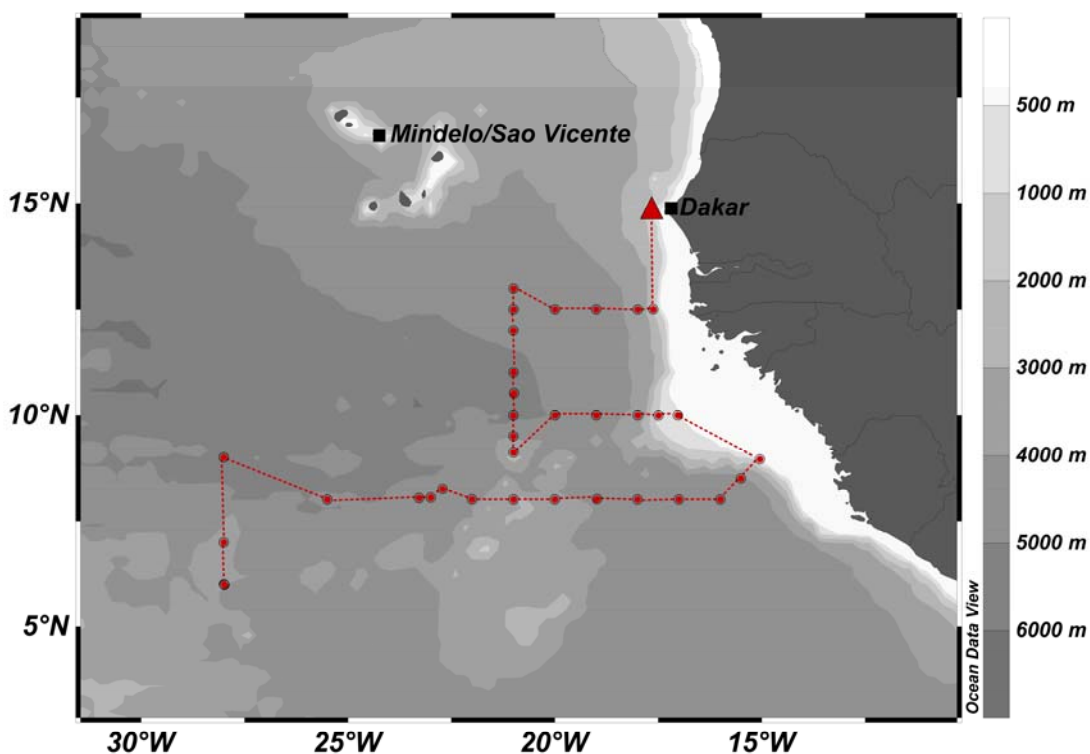


Figure 3.1. Map of the ETNA showing the mesocosm filling station on the Northwest African Shelf off Dakar (red triangle) and the following cruise track (red dots) during the 11-day nutrient enrichment experiment on RV *Meteor* cruise M83-1.

Twelve mesocosms in four flow-through gimbals-mounted water baths on deck of the ship (see Fig. 3.2) were filled each with 150 L of natural seawater from about 5 m water depth (15°0.01'N, 17°45.00'W; see Fig. 3.1) using a peristaltic pump. The individual mesocosm enclosure is a cylindrical plastic bag fixed to a floating tire and with a plexiglass bottom. Continuous flow of ambient surface seawater through the water baths via in- and outflow provided *in situ* temperature conditions (<2°C above sea surface temperature).

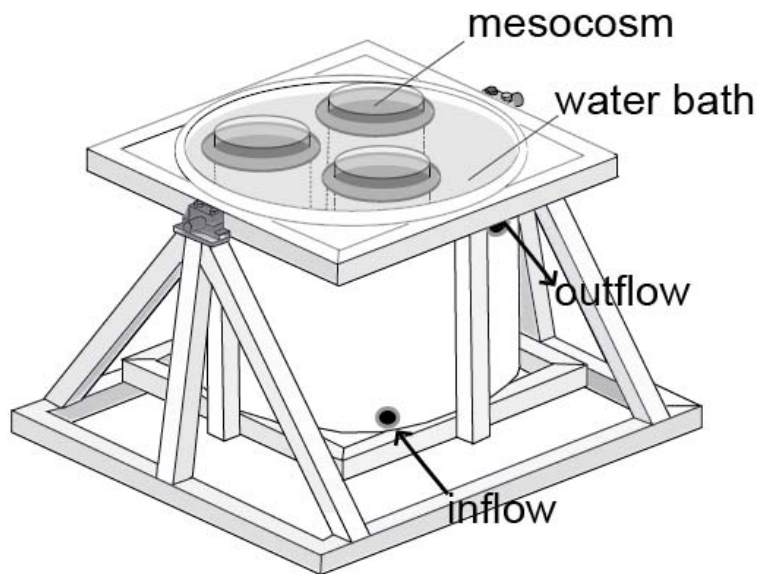


Figure 3.2. Schematic draft of three shipboard mesocosms floating in a gimbals-mounted water bath.

Surface irradiance in the mesocosms was reduced by 60% to $100 - 600 \mu\text{E m}^{-2} \text{s}^{-1}$ by covering the water baths with solid white lids. Initially, inorganic nutrients (ammonium (NH_4^+), nitrite (NO_2^-), nitrate (NO_3^-), phosphate (PO_4^{3-}), silicate ($\text{Si}(\text{OH})_4$)) of the natural seawater medium were determined and four different N:P treatments (in triplicates) were adjusted by nutrient additions (NaNO_3 and KH_2PO_4). Treatment replicates were distributed over the different water baths. Initial molar N:P supply ratios ranged between 16:1 and 2.8:1. Addition of $15 \mu\text{mol L}^{-1}$ $\text{Na}_2\text{SiO}_3 \cdot 5\text{H}_2\text{O}$ and 10 ml of a trace metal mix (Provasoli II trace metal mix; West and McBride, 1999) to all treatments should prevent other nutrient limitation effects than by N or P (Tab. 3.1). Sampling for biogeochemical and taxonomical analyses was conducted on a daily basis for a period of 11 days. Technical issues during filling of mesocosm #8 (5.5:1 treatment) resulted in its exclusion from the experiment analysis. N:P treatment 5.5:1 was therefore only represented by duplicate mesocosms.

Table 3.1. Overview of mesocosm filling site, initial and experimental conditions during the M83-1 cruise.

initial conditions				
Latitude	15°0.01'N			
Longitude	17°45.00'W			
T(°C)	27.6			
DIN	0.3			
DIP	0.1			
Si(OH) ₄	1.4			
experimental conditions				
N supply level	high N	high N	low N	low N
N:P	16	8	5.5	2.8
DIN supply (μmol L ⁻¹)	12	12	4.13	4.13
DIP supply (μmol L ⁻¹)	0.75	1.5	0.75	1.5
Si(OH) ₄ supply (μmol L ⁻¹)	15	15	15	15

2.2. Inorganic nutrients

Water samples for inorganic nutrients were pre-filtered through 5 μm cellulose acetate filters (26 mm) and measured immediately after sampling with a Quattro autoanalyzer (Seal Analytical) and an external fluorometer (Jasco FP-2020). Analysis of NO₃⁻, NO₂⁻, PO₄³⁻ and Si(OH)₄ was performed according to Hansen and Koroleff (1999), and NH₄⁺ was analyzed according to the method by Holmes et al. (1999).

2.3. Flow cytometry (FCM)

Cell counts for phytoplankton and bacterial abundance were obtained using a flow cytometer (FACScalibur, Becton Dickinson, San Jose, CA, USA). Samples (5 ml) were fixed with 2% formaldehyde and frozen at -80°C. Samples were filtered through a 64 μm syringe filter prior to measurement at a flow rate of 50.6 μl min⁻¹. Cells were distinguished by size (front scatter) and fluorescence of chlorophyll *a*, phycoerythrin, and allophycocyanin. Biovolume was estimated assuming spherical shapes from a front scatter to size calibration and converted to biomass (μmol C L⁻¹) using the carbon to volume relationships described in Menden-Deuer and Lessard (2000). However, as the calibration is only valid for cells >3 μm, we assumed 50 and 200 fg C cell⁻¹ for *Prochlorococcus* and *Synechococcus*-like cells, respectively (Bertilsson and Berglund, 2003). For bacterial abundance, samples were diluted 1:3, stained with SYBR-Green and counted at lower flow rate (13.9 μl min⁻¹). Unfortunately, 38 samples for bacterial abundance were lost due to inappropriate dilution.

2.4. Biogenic silica

Particulate biogenic silica was collected by filtration of water samples onto filters made of cellulose acetate (0.65 µm pore size; 25 mm diameter) at low vacuum pressure (<200 mbar) and stored frozen at -20°C. For analysis, the sample filters were incubated each with 25 ml NaOH (0.1 M) in Nalgene bottles at 85°C for 2h 15 min in a shaking water bath. After cooling of the incubated samples, analysis was conducted according to the method for determination of Si(OH)₄ by Hansen and Koroleff (1999).

2.5. Phytoplankton pigments

Samples for phytoplankton pigment analysis via HPLC (High Pressure Liquid Chromatography) were filtrated onto Whatman GF/F filters (0.7 µm pore size; 25 mm diameter) at low vacuum pressure and immediately stored frozen at -80°C. For pigment extraction, each filter was covered with approximately 3 g of glass beads (2 mm + 4 mm) and 2 ml of acetone. After homogenisation in a cell mill (Edmund Bühler GmbH) for 5 min and centrifugation for 10 min at 5000 rpm, the supernatant was filtered through a 0.2 µm Teflon filter and the extract stored at -80°C. The HPLC measurement was conducted by a Waters 600 controller in combination with a Waters 996 photodiode array detector (PDA) and a Waters 717plus auto sampler. The applied method was modified after Barlow et al. (1997). Classification and quantification of the phytoplankton pigments involving chlorophylls, carotenoids and degradation products was carried out using the software EMPOWERS (Waters).

2.6. *nifH*-gene detection

Samples for DNA purification were taken by filtering a volume of 1 L seawater through 0.2 µm polyethersulfon membrane filters (Millipore, Billerica, MA, USA). The filters were immediately frozen and stored at -80°C. Nucleic acids were extracted using the Qiagen DNA/RNA All prep Kit (Qiagen, Hilden, Germany) according to the manufacturer's protocol. *NifH* was amplified by PCR with primers as described in Zani et al. (2000) followed by Topo TA cloning (Invitrogen, Carlsbad, CA) and Sanger sequencing (carried out by the Institute of Clinical Molecular Biology, Kiel). Detected *nifH* clusters were quantified by quantitative Real Time PCRs as previously described by Langlois et al. (2008) and Foster et al. (2007). TaqMan® qPCRs were set up in 25 µl reactions containing 12.5 µl TaqMan® buffer (Applied Biosystems), 8.0 µl of nuclease-free water, 0.5 µmol L⁻¹ of the forward and reverse primers, 0.25 µmol L⁻¹ TaqMan probe, and 1 µl of template DNA. Reactions were performed in technical duplicates in an ABI 7300 qPCR system (Applied Biosystems). For each primer and probe set, standard curves were obtained from

dilution series ranging from 10^7 to 1 gene copies per reaction; standards were made using plasmids containing the target *nifH* gene.

3. Results

3.1. Nutrient drawdown

Drawdown of the macronutrients DIN, DIP and Si(OH)_4 was fast after initiation of the experiment (Fig. 3.3). DIN inventories were already exhausted in all treatments on day 3 (Fig. 3.3A). P concentrations, with the exception of the 2.8:1 mesocosms, reached the detection limit of the applied method of $\sim 0.2 \mu\text{mol L}^{-1}$ on day 3 (Fig. 3.3B). DIP drawdown in the 2.8:1 treatment was comparatively slow, and residual concentrations of $\sim 0.2 \mu\text{mol L}^{-1}$ were measured until the end of the experiment. Substantial consumption of $\sim 11 \mu\text{mol Si(OH)}_4 \text{ L}^{-1}$ occurred in the ‘high N’ treatments (treatments 16:1 and 8:1 supplied with $12 \mu\text{mol N L}^{-1}$) between day 2 and 3 (Fig. 3.3C). ‘Low N’ (treatments 5.5:1 and 2.8:1 supplied with $4.13 \mu\text{mol N L}^{-1}$) phytoplankton utilized with $\sim 5 \mu\text{mol L}^{-1}$ less than 50% Si(OH)_4 in the same period.

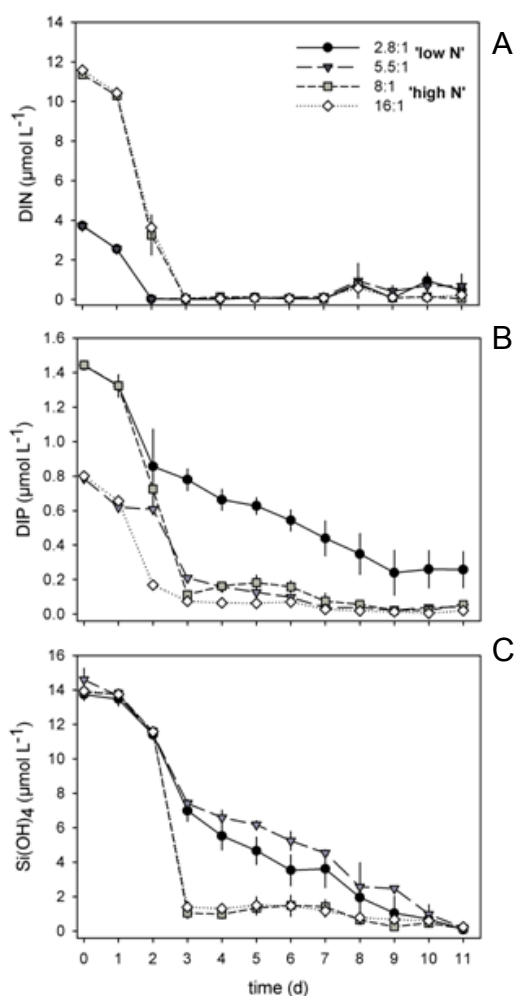


Figure 3.3. Temporal development of (A) DIN (including NH_4^+ , NO_2^- and NO_3^-), (B) DIP and (C) Si(OH)_4 within the four N:P treatments. Values are treatment means and vertical error bars denote the standard error of replicates within each N:P treatment.

3.2. Biomass of phyto- and bacterioplankton via flow cytometry (FCM)

Total phytoplankton biomass quantified via FCM was significantly affected by N supply (Fig. 3.4A; Tab. 3.2). During the primary bloom (day 2-4), maximum biomass concentration was increased four-fold by high N supply, as 'high N' mesocosms accumulated $150\text{--}200\ \mu\text{mol C L}^{-1}$ compared to $\sim 50\ \mu\text{mol C L}^{-1}$ in the 'low N' treatments.

Bacterial abundance was also significantly affected by initial N supply (Tab. 3.2), even though the effect was less pronounced compared to the phytoplankton biomass (Fig. 3.4B). Approximately $200 \times 10^5\ \text{cells ml}^{-1}$ accumulated until day 6 in the 'high N' treatments, while cell numbers achieved $150 \times 10^5\ \text{cells ml}^{-1}$ in the 'low N' treatments. Data points between day 7 and 9 are missing due to complications during measurement.

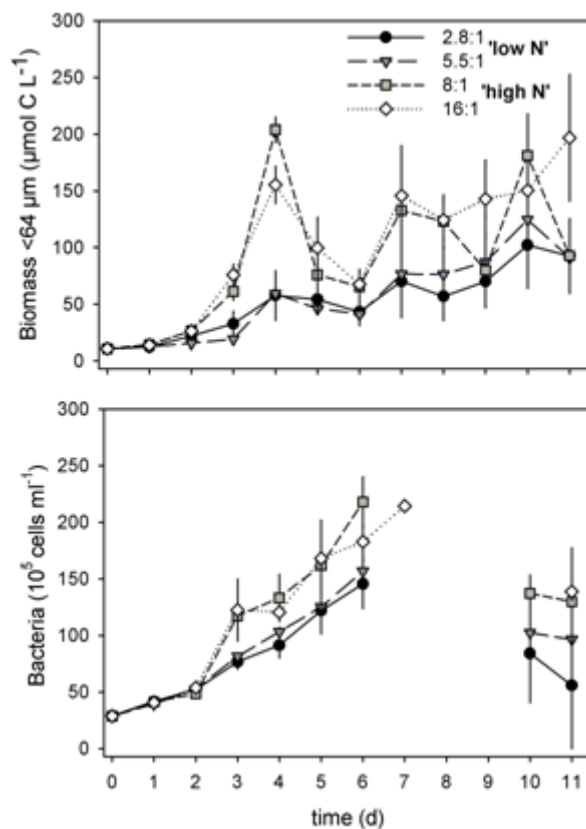


Figure 3.4. Temporal development of (A) phytoplankton biomass ($<64\ \mu\text{m}$) and (B) bacterial abundance derived from flow cytometry within the four N:P treatments. Style code following to Fig. 3.3.

Table 3.2. Summary of *p*-values of non-parametric Mann-Whitney-U tests comparing the significance of DIN and DIP supply on the development of the detected phytoplankton pigments, BSi, total phytoplankton biomass and bacterial cell abundance. Statistical significant effects ($p < 0.05$) are denoted in bold.

	N supply	P supply
total phytoplankton biomass	<0.0001	0.233
bacteria abundance	<0.05	0.546
Chl <i>a</i>	<0.0001	0.082
BSi	<0.05	0.318
Fucoxanthin	<0.0001	0.173
Chlorophyll <i>c</i> ₁₊₂	<0.0001	0.198
Diadinoxanthin	<0.0001	0.553
Diatoxanthin	<0.0001	0.075
β -Carotene	<0.0001	<0.05
Zeaxanthin	0.054	<0.05
Chlorophyll <i>c</i> ₃	0.064	0.080
19'-Hexanoyloxyfucoxanthin	0.055	0.766
Peridinin	<0.0001	0.665
Aphanizophyll	<0.05	0.907
Myxoxanthophyll	<0.0001	0.665
Alloxanthin	0.209	0.994
Chlorophyll <i>b</i>	0.710	0.953
Violaxanthin	0.610	0.560
19'-Butanoyloxyfucoxanthin	0.274	0.801
<i>Trichodesmium nifH</i> -gene	0.647	0.824

3.3 Proxys for taxonomical phytoplankton composition (phytopigments, BSi and *nifH*)

The temporal development of Chl *a*, a proxy for total photoautotrophic biomass, was, in agreement with phytoplankton abundance determined via FCM, significantly affected by N supply (Fig. 3.5A; Tab. 3.2). Chl *a* in the 'high N' treatments exceeded with up to 4.5 $\mu\text{g L}^{-1}$ maximum concentrations in the 'low N' treatments ($\sim 2.5 \mu\text{g L}^{-1}$) in particular during the bloom peak (day 2-3). However, maximum concentrations of Chl *a* and FCM-derived biomass (i.e. cell numbers) showed a temporal discrepancy of two days.

Accumulation of BSi mirrored the uptake of Si(OH)_4 in the individual treatments, as maximum values of $\sim 24 \mu\text{mol BSi L}^{-1}$ occurred in the 'high N' mesocosms (Fig. 3.5B). In contrast, BSi did only slightly accumulate in the 'low N' treatments, hardly surpassing concentrations of 10 $\mu\text{mol L}^{-1}$ throughout the experiment. Thus, production of BSi was significantly affected by the initial N supply, whereas initial P enrichment did not have any effect (Tab. 3.2).

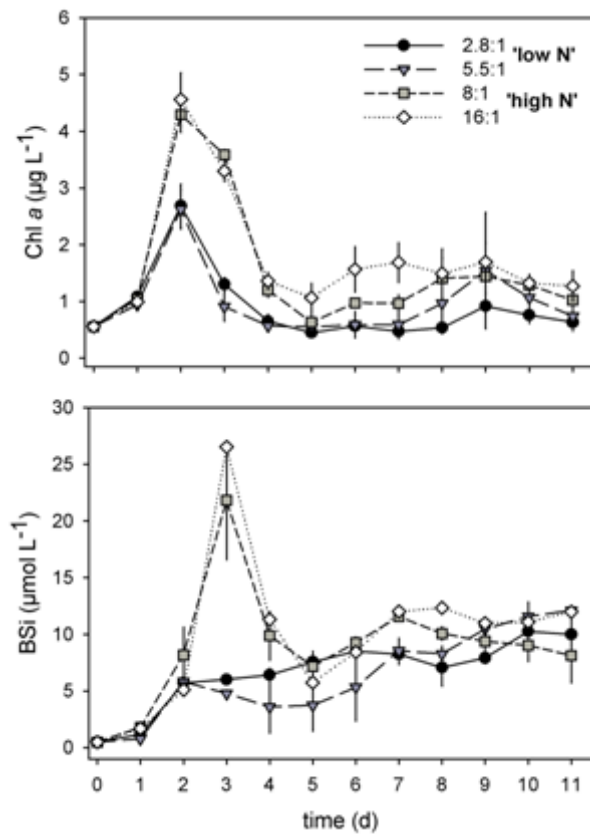


Figure 3.5. Temporal development of (A) Chl a and (B) BSi within the four treatments. Style code following to Fig. 3.3.

Fucoxanthin, chlorophyll c_{1+2} and diadinoxanthin represented in terms of concentration the most dominant phytopigments (Fig. 3.6). Together with diatoxanthin and β -carotene, they function as marker pigments for diatom abundance. These five pigments displayed a similar pattern of distribution in the individual treatments, significantly controlled by N supply and only differing in their concentration level (Tab. 3.2). Equally high concentrations of the individual pigment in the 'high N' treatments faced equally low contents in the 'low N' treatments. This effect was most pronounced during the exponential phase (day 2-3), differing in concentration by a factor of 2.

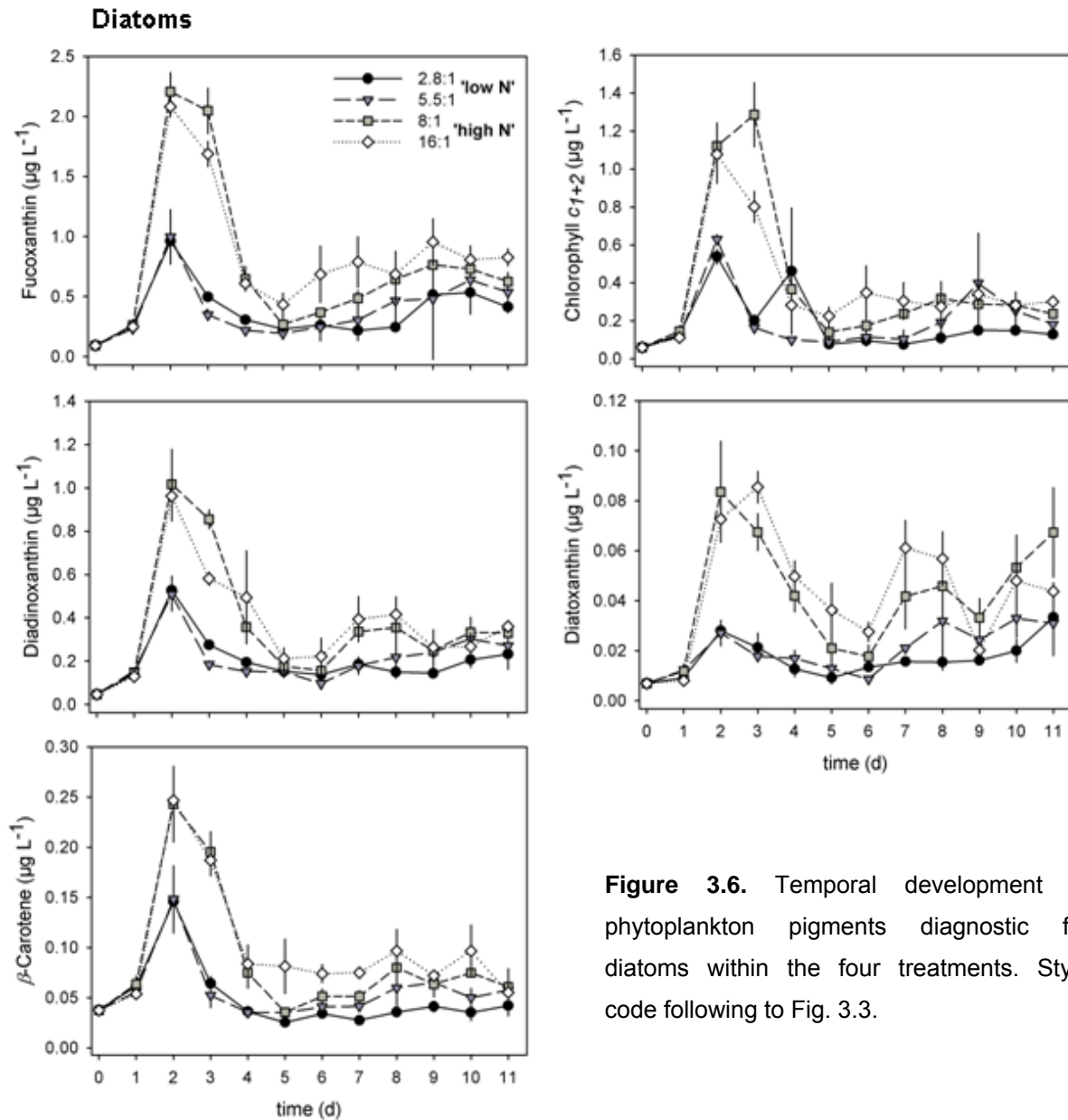


Figure 3.6. Temporal development of phytoplankton pigments diagnostic for diatoms within the four treatments. Style code following to Fig. 3.3.

Production of the xanthophylls aphanizophyll and myxoxanthophyll, both occurring only in cyanobacteria, was strongly affected by N supply (Fig. 3.7A; Tab. 3.2). They hardly accumulated in the 'low N' treatments (e.g. $>0.05 \mu\text{g L}^{-1}$ aphanizophyll), whereas concentrations reached maximum levels between day 4-6 in the 'high N' treatments (e.g. $\sim 0.17 \mu\text{g L}^{-1}$ aphanizophyll).

Chlorophyll c_3 and the carotenoid 19'-hexanoyloxyfucoxanthin are mainly synthesized by the taxonomic group of haptophytes. Both pigments did not respond to specific nutrient supply according to statistical testing (Tab. 3.2). However, peaks of 19'-hexanoyloxyfucoxanthin were slightly higher in the 'high N' compared to the 'low N' treatments and chlorophyll c_3 accumulated stronger in the 'high N' mesocosms from day 6 on (Fig. 3.7B).

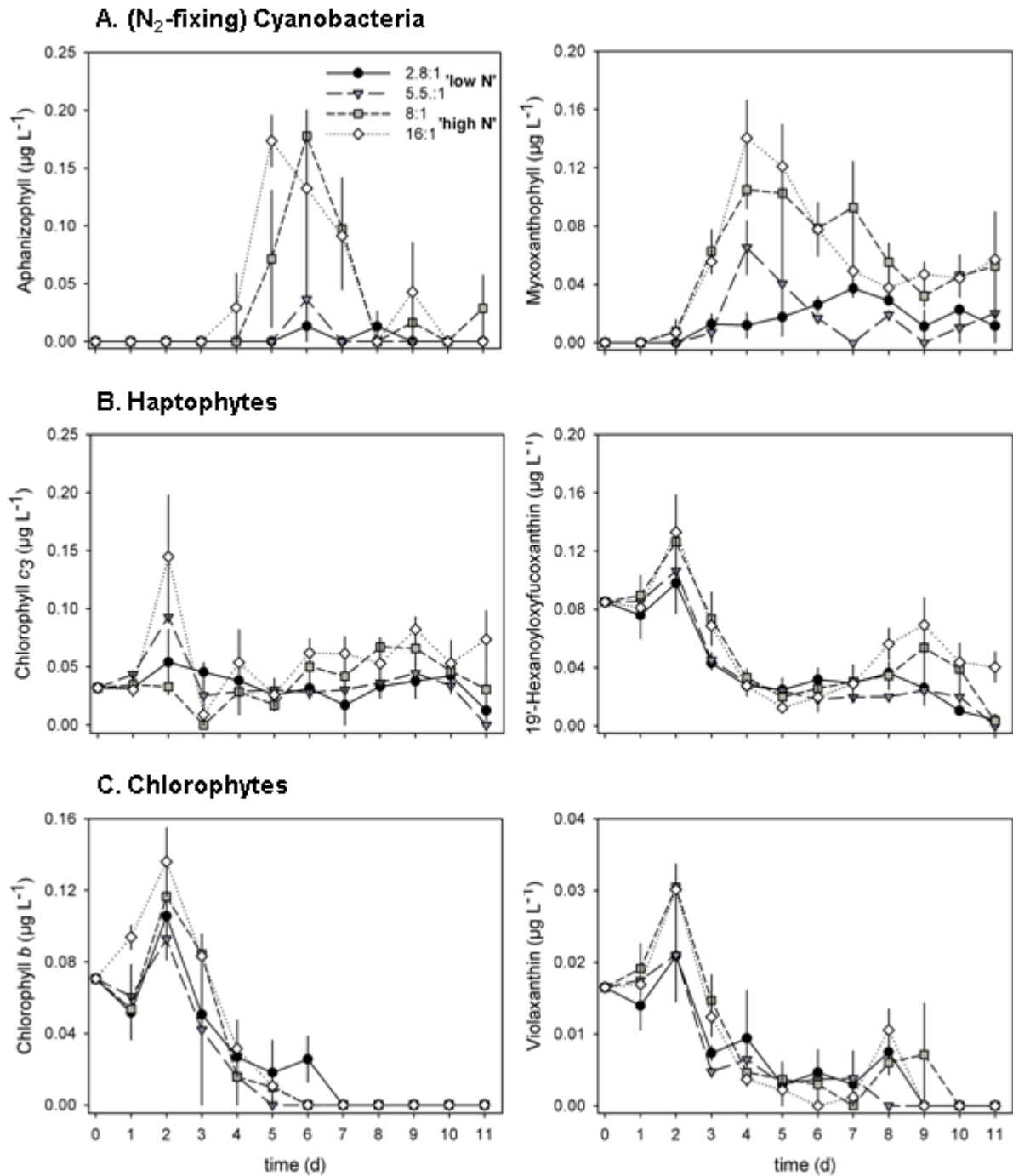


Figure 3.7. Temporal development of phytoplankton pigments diagnostic for (A) (N₂-fixing) cyanobacteria, (B) haptophytes and (C) chlorophytes within the four treatments. Style code following to Fig. 3.3.

Chlorophyll *b* and the carotenoid violaxanthin are indicators for the occurrence of chlorophytes. No significant effect of nutrient supply on both pigments was found (Tab. 3.2), yet maximum concentrations on day 2 and 3 were larger in the 'high N' mesocosms (Fig. 3.7C).

Concentration of the picocyanobacterial marker zeaxanthin was highest in the 16:1 treatment (Fig. 3.8A), though the standard error within this treatment was rather large throughout the experiment due to accumulation of higher concentrations in one of the three replicate

mesocosms. For that reason we suspect that this represents an outlier and zeaxanthin production was not affected by variable nutrient supply.

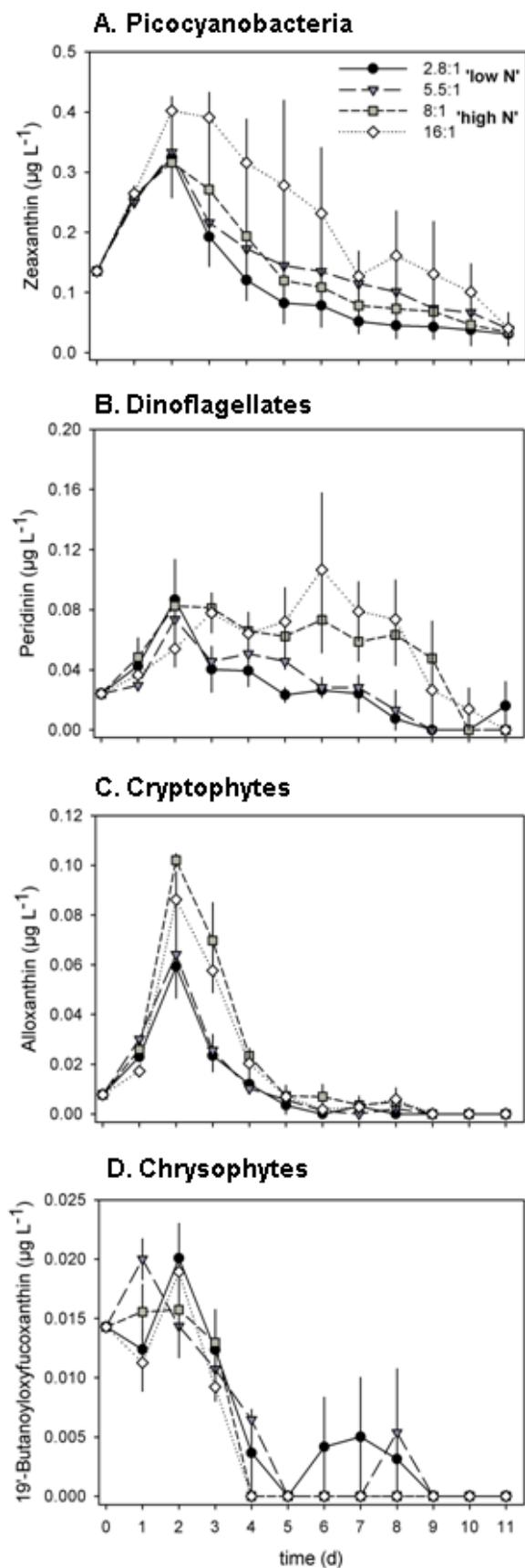


Figure 3.8. Temporal development of phytoplankton pigments diagnostic for (A) picocyanobacteria (e.g. *Synechococcus*), (B) dinoflagellates, (C) cryptophytes and (D) chrysophytes within the four treatments. Style code following to Fig. 3.3.

In contrast to many other carotenoids, peridinin is exclusively produced by dinoflagellates, thus representing an unambiguous indicator for the abundance of this phytoplankton group. Concentration of peridinin between the treatments was significantly influenced by N supply (Fig. 3.8B; Tab. 3.2).

Alloxanthin is a diagnostic pigment for the abundance of cryptophytes. Statistical analysis did not reveal a significant effect of nutrient supply on alloxanthin development (Tab. 3.2). But alloxanthin levels were higher in the 'high N' than in the 'low N' treatments during the peak phase from day 2-4 (Fig. 3.8C).

Development of 19'-butanoyloxyfucoxanthin, predominantly produced by chrysophytes, did not follow any significant pattern between the treatments and concentrations were extremely low throughout the experiment (Fig. 3.8D; Tab. 3.2).

Detection of group-specific *nifH*-gene copies in the mesocosms revealed high abundance of filamentous *Trichodesmium* (Fig. 3.9), along with scarce abundance of unicellular *Crocospaera*-like species, γ -proteobacteria, Group A and diatom-diazotroph associations (data not shown). *Trichodesmium*-specific *nifH*-gene copy numbers did not respond to N or P supply (Tab. 3.2) and increased exponentially over time, displaying the largest amplification towards the end of the experiment between day 8-11. Abundance of *Trichodesmium nifH*-genes and distribution of the cyanobacterial marker pigments myxoxanthophyll and aphanizophyll (Fig. 3.7A) neither agreed over time nor between treatments.

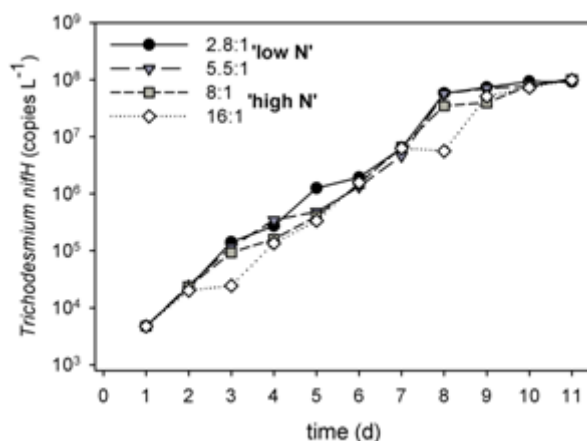


Figure 3.9. Temporal development of *Trichodesmium nifH*-gene abundance within the four N:P treatments on a log-scale. Style code following to Fig. 3.3.

4. Discussion

4.1. N supply controls phytoplankton growth

Chl *a* concentrations from HPLC measurements and phytoplankton biomass detected via FCM were significantly affected by the level of N supply but not by the N:P supply ratio, which is consistent with the response by POC and PON production in this experiment shown in a further work (Franz et al., unpubl. data). Combined high addition of N and P did not provoke an additional increase in algal biomass compared to the high N and low P enrichment. Hence, growth of bulk phytoplankton was solely controlled by the availability of N, a response that has been previously observed in association with coastal upwelling communities (Thomas et al., 1974; Hauss et al., *subm.*). Yet, the majority of nutrient enrichment experiments performed in marine environments reported a seemingly synergistic limitation effect of N and P on primary production (Graziano et al., 1996; Davey et al., 2008; Moore et al., 2008; Tang et al., 2009). Such a multiplicative control of growth by N and P is rather common in oligotrophic lakes (e.g. White and Payne, 1977; Elser et al., 1990). During low nutrient concentrations, neutralization of the proximate nutrient limitation by enrichment of this nutrient is assumed to quickly cause limitation by the secondary limiting nutrient. The above listed marine enrichment experiments were also performed in nutrient-impoverished waters of the tropical and subtropical ocean, which suggests a general close dependence of the primary and secondary limiting nutrient under low nutrient availability. However, results from Droop (1974) and Rhee (1978) confirmed Liebig's law of the minimum, which says that growth is solely controlled by the most limiting nutrient (Liebig, 1855). Rhee (1978) explained the additive effect of combined N and P addition with a competitive exclusion and coexistence of populations either limited by N or by P. Combined enrichment of N and P would stimulate growth of the N- and the P-limited species, resulting in a higher biomass yield than single addition of N or P. Hence, photoautotrophic communities in the oligotrophic ocean are presumably composed beside of N- also of P-limited species, which are jointly defining the response of the total algal assemblage. In contrast to that, diatoms extremely dominated phytoplankton biomass in this study and distribution of the specific marker pigments indicated no P-limitation of any phytoplankton group (see Tab. 3.2). Accordingly, total phytoplankton showed a pattern of single N-limitation. The strong dominance of N-controlled blooming phytoplankton in coastal upwelling areas seems to exclude the apparent additive growth effect of combined N and P enrichment observed in oligotrophic regions.

4.2. Phytoplankton community dominated by diatoms

Comparison of the distribution of Chl *a*, BSi and diatom marker pigments demonstrate a strong dominance of the microalgal assemblage in all treatments by diatoms, which is in agreement with the response of phytoplankton in a similar enrichment experiment conducted in the Peruvian upwelling (Hauss et al., subm.). Artificial nutrient addition, comparable to an episodic upwelling event, represented the trigger for fast nutrient drawdown and exponential growth by diatoms. Diatom metabolism is known to react promptly on sudden pulses of nutrient input with extremely high rates of nutrient uptake and cell division (Fawcett and Ward, 2011). This quick metabolic response may be the crucial advantage of diatoms to outcompete other phytoplankton groups in high nutrient regimes such as upwelling areas. Especially picoplanktonic species are inferior competitors under nutrient saturation. Small cells are highly beneficial under nutrient depletion (Chisholm, 1992), but they have no chance to prosper in coexistence with large blooming species in a eutrophic environment (Wilkerson et al., 2000; Wetz and Wheeler, 2003). Under high N supply conditions, diatom accumulation can even escape a top-down control by mesozooplankton grazing, as copepods are constrained by their longer development cycle (Goericke, 2002).

Blooming and dominance of diatoms is certainly influenced by the availability of Si(OH)_4 and Fe. Sufficient supply of Si(OH)_4 to diatoms is vital for building their silica-containing cell walls (Lewin, 1962). In addition, particularly coastal diatoms seem to have high Fe requirements (Sunda and Huntsman, 1995; Bruland et al., 2001) and their growth has been reported to be limited by Fe supply (Hutchins and Bruland, 1998; Hare et al., 2005). Si(OH)_4 and Fe were both initially provided to the phytoplankton community in adequate concentrations, to prevent limitation by other nutrients than by N and P.

4.3. Diatom-diazotroph succession

The single-pulse nutrient addition experiment in this study simulates an upwelling event. Following the characteristic succession of functional groups in such experiments can therefore help to explain their spatial distribution patterns, both in respect to the vertically stratified water column and in the shelf – slope - open ocean transect typical of eastern boundary current systems. It has been hypothesized before, following observations by Margalef (1973) and model predictions by Hood et al. (2004), that the succession sequence diatoms – cyanobacteria - flagellates might be characteristic of the ETNA. Traditionally, large-scale N input by N_2 -fixation has been largely attributed to the central and western part of the North Atlantic based upon the dominance of *Trichodesmium* and the high N:P export ratio in this regions (Capone et al., 2005). More recently, the role of unicellular cyanobacteria as well as diatom-diazotroph

associations (DDAs) has been increasingly acknowledged in the tropical North Atlantic (Montoya et al., 2007; Langlois et al., 2008; Foster et al., 2009).

Episodic pulses of upwelling on the shelf facilitate blooming of large primary producers, initiating rapid drawdown of the vertically supplied N in the surface layer. N depletion following to upwelling events may create a niche for N₂-fixing cyanobacteria. In this study, exhaustion of initially supplied N on day 3 (Fig. 3.3A) terminated a diatom-dominated bloom (see Fig. 3.5 and 3.6), thereby providing favouring conditions for the onset of diazotrophic development. Temporal distribution of the cyanobacterial marker pigments myxoxanthophyll and aphanizophyll was directly opposed to the development of the diatom bloom, as maximum pigment concentrations occurred between day 4 to 6 (Fig. 3.7A). The highest increase in the abundance of the *Trichodesmium*-specific *nifH*-gene, the functional gene expressing the N₂-fixation catalyzing enzyme nitrogenase, occurred also after termination of the diatom bloom from day 7 on. Termination of the diatom bloom seems to be a prerequisite for extensive growth of diazotrophic cyanobacteria. *Trichodesmium* is able to grow on NO₃⁻ (Holl and Montoya, 2005), but coexistence of diatoms and N₂-fixers under nutrient saturation is eliminated by the fact that cyanobacteria cannot compete with diatoms for the available P (Tilman, 1982). Based on high abundance of the *Trichodesmium*-specific *nifH*-gene in combination with only scarce copy numbers of *nifH*-genes from unicellular cyanobacteria and DDAs, we suppose that aphanizophyll and myxoxanthophyll can be considered as primarily *Trichodesmium*-derived. Consequently, *Trichodesmium* developed under nutrient depletion subsequent to the diatom-dominated phytoplankton bloom, supporting the hypothesis (see Margalef, 1973, and Hood et al., 2004) that N₂-fixers are growing in succession to diatoms in the upwelling area on the West African continental shelf.

Many observations support the general assumption that low N:P conditions are stimulating growth of N₂-fixers (e.g. Niemi, 1979; Vrede et al., 2009). But neither increased production of cyanobacterial marker pigments in the 'high N' treatments, a response that has already been observed in the mesocosm study by Hauss et al. (subm.), nor similar abundance of the *Trichodesmium*-specific *nifH*-gene across all treatments (Fig. 3.9; Tab. 3.2) indicate a stimulation of diazotrophic cyanobacteria by low N:P supply ratios. In contrast, production of myxoxanthophyll and aphanizophyll was lowest in the 2.8:1 treatment, which was the only treatment with residual amounts of DIP throughout the entire experiment. Likewise excess P did not induce an enhancement in *nifH*-gene abundance compared to the other treatments, implying that growth of diazotrophic algae was not limited by P availability. The discrepancy in the distribution of marker pigments and *nifH*-gene abundance precludes though a definite conclusion about the effect of variable nutrient supply on N₂-fixing cyanobacteria in the experiment. Nonetheless, the analogy in the increased production of cyanobacterial marker pigments in the 'high N' treatments between this study and Hauss et al. (subm.) suggests a

particular pattern behind this response, which we are not able to identify with the available dataset.

Furthermore, the disagreement between cyanobacterial diagnostic pigments and *nifH*-gene abundance exposes that our present comprehension of the correlation between different microalgal indicators is rather incomplete. Owing to this inconsistency and the associated uncertainty of the cyanobacterial proxies, and simply because we did not perform rate measurements of N₂-fixation, we are not able to evaluate the input of N via N₂-fixation during the experiment. Given that a secondary weaker diatom bloom developed after day 7, which showed the same pattern of N control, we suspect that an effective remineralization of nutrients must have occurred between the first and second bloom.

4.4. Ecological implications

Results from this simulated upwelling experiment indicate that phytoplankton in the ETNA may occur in a successional sequence as proposed by the model of Hood et al. (2004). Following to upwelling pulses and drawdown of nutrients by bloom forming species, coastal shelf areas can offer favouring growth conditions for N₂-fixers, provided that the vertical supply of nutrients occurs only episodically. The common non-consideration of upwelling regions as potential habitats for diazotrophic phytoplankton may have caused an underestimation of total N input by N₂-fixation into the tropical Atlantic Ocean. Furthermore, N₂-fixation in shelf areas may counteract the N-deficit of OMZ-influenced waters. So far, results indicate an absence of large-scale N loss via anammox or denitrification in the water column off Northwest Africa (Ryabenko et al., 2011), because relatively high minimum O₂ concentrations of about 40 µmol kg⁻¹ preclude these microbial pathways. But studies based on models (Matear and Hirst, 2003) and time-series analysis (Stramma et al., 2008) consider the ETNA as the region with the largest potential for expansion of low-oxygen environments. As a consequence, N loss processes may gradually establish in the deoxygenating waters of the tropical East Atlantic, enhancing the necessity for compensation of the N-deficit through biological N₂-fixation. Especially N-controlled primary production by blooming, non-diazotrophic species would benefit from the N supply via N₂-fixation, if upwelled N stocks are reduced due to microbial N loss processes in oxygen-deficient intermediate layers.

Acknowledgments

The authors would like to thank Kerstin Nachtigall, Martina Lohmann and the crew of R/V *Meteor* for their great support during the cruises. This work is a contribution of the Sonderforschungsbereich 754 "Climate - Biogeochemistry Interactions in the Tropical Ocean" (www.sfb754.de) which is supported by the German Science Foundation (DFG).

Study 4.**Production, partitioning and stoichiometry of organic matter under variable nutrient supply during mesocosm experiments in the tropical Pacific and Atlantic Ocean**

Jasmin M.S. Franz¹, Helena Hauss¹, Ulrich Sommer¹, Thorsten Dittmar² and Ulf Riebesell¹

¹GEOMAR | Helmholtz Centre for Ocean Research Kiel, Düsternbrooker Weg 20, 24105 Kiel, Germany

²Max Planck Research Group for Marine Geochemistry, University of Oldenburg, Institute for Chemistry and Biology of the Marine Environment, Carl-von-Ossietzky-Str. 9–11, 26129 Oldenburg, Germany

corresponding author:

Jasmin M.S. Franz GEOMAR | Helmholtz Centre for Ocean Research Kiel, Düsternbrooker Weg 20, 24105 Kiel, Germany, jfranz@geomar.de, Phone: +49-431-600-4290, Fax: +49-431-600-4446

Abstract

Oxygen-deficient waters in the ocean, generally referred to as oxygen minimum zones (OMZ), are expected to expand as a consequence of global climate change. Poor oxygenation is promoting microbial loss of inorganic nitrogen (N) and increasing release of sediment-bound phosphate (P) into the water column. These intermediate water masses, nutrient-loaded but with an N deficit relative to the canonical N:P Redfield ratio of 16:1, are transported via coastal upwelling into the euphotic zone. To test the impact of nutrient supply and nutrient stoichiometry on production, partitioning and elemental composition of phytoplankton-derived dissolved (DOC, DON, DOP) and particulate (POC, PON, POP) organic matter, three nutrient enrichment experiments were conducted with natural phytoplankton communities in shipboard mesocosms, during research cruises in the tropical waters of the South East Pacific and the North East Atlantic. Maximum accumulation of POC and PON was observed under high N supply conditions, indicating that primary production was controlled by N availability. The stoichiometry of photoautotrophic biomass was unaffected by nutrient N:P supply during exponential growth under nutrient saturation, while it was highly variable under conditions of nutrient limitation and closely correlated to the N:P supply ratio, although PON:POP of accumulated phytoplankton generally exceeded the supply ratio. Phytoplankton N:P composition was constrained by a general lower limit of 5:1. Channelling of assimilated P into DOP appears to be the mechanism responsible for the consistent offset of cellular stoichiometry relative to inorganic nutrient supply and nutrient drawdown, as DOP build-up was observed to intensify under decreasing N:P supply. Low nutrient N:P conditions in coastal upwelling areas overlying O₂-deficient waters seem to represent a net source for DOP, which may stimulate growth of diazotrophic phytoplankton. These results demonstrate that microalgal nutrient assimilation and partitioning of phytoplankton-derived organic matter between the particulate and the dissolved phase are controlled by the N:P ratio of upwelled nutrients, implying substantial consequences for nutrient cycling and organic matter pools in the course of decreasing nutrient N:P stoichiometry.

1. Introduction

Oxygen minimum zones (OMZs) of the tropics and subtropics occur in conjunction with highly productive eastern boundary upwelling systems, e.g. the Peru Current in the Eastern Tropical South Pacific (ETSP) and the Canary Current in the Eastern Tropical North Atlantic (ETNA). Nutrient-rich deep water is transported by wind-driven upwelling vertically into the euphotic zone, ensuring high rates of primary production. Large amounts of sinking microalgal biomass enhance consumption of dissolved oxygen (O_2) in the mesopelagic zone indirectly via microbial degradation of organic matter (Helly and Levin, 2004). Beside these loss processes, deoxygenation is further promoted by a pronounced stratification of the upper water column off the upwelling centers, impeding ventilation of the O_2 -depleted intermediate water body (Reid, 1965; Luyten et al., 1983). Climate change-induced warming of the surface layer leads to an intensified stratification of the upper tropical ocean and rising sea surface temperatures impede the uptake of atmospheric O_2 by lowering its solubility (Keeling and Garcia, 2002; Matear and Hirst, 2003).

The impact of low O_2 levels on redox-sensitive nutrient cycling is immense. Sub- or anoxia creates niches for the microbial processes of denitrification (Codispoti and Christensen, 1985) and anaerobic ammonium oxidation (anammox) (Thamdrup and Dalsgaard, 2002; Kuypers et al., 2003), both contributing to the deficit of biologically available inorganic nitrogen (N) by converting it to nitrous oxide and/or dinitrogen (N_2). Decreasing oxygenation has also implications on phosphorus cycling. If bottom water and sediment become depleted in O_2 , buried metal oxide complexes are reduced and the associated dissolved inorganic phosphorus (P) is released back into the water column. A further source of P is the dissolution of apatite-containing fish debris in the sediments of the continental shelf areas. This process supplies additional P to the dissolved reactive P pool especially in the fish-rich waters of the ETSP (Suess, 1981; Van Cappellen and Berner, 1988).

These deoxygenation-induced changes in nutrient cycling are generating intermediate water masses with a low nutrient N:P signature relative to the Redfield ratio of 16:1 (Redfield, 1958). Via coastal upwelling, these are transferred into the surface layer, fuelling primary production. An open question is how primary production will respond to OMZ-induced shifts in nutrient availability and the associated decline in nutrient N:P stoichiometry. The prevailing N limitation of phytoplankton within coastal upwelling systems suggests a decreasing trend of photoautotrophic production in the course of expanding OMZs (Dugdale, 1985). Modifications in the concentration of supplied nutrients are known to further affect the biochemical composition of phytoplankton (Gervais and Riebesell, 2001). Sterner and Elser (2002) introduced the 'they are what they eat' theory, implying that phytoplankton N:P generally mirrors N:P supply. In contrast, studies involving dynamic nutrient models or field surveys claimed the specific growth strategy of phytoplankton being the key control of its elemental stoichiometry (Klausmeier et al.,

2004a; Arrigo, 2005; Franz et al., 2012). This hypothesis is based on the fact that the different functional compartments within a phytoplankton cell are varying in their individual nutrient demands (Falkowski, 2000; Geider and LaRoche, 2002). Cellular stoichiometry varies as a function of the specific functional machinery that dominates in a species' metabolism, i.e. cell assembly or resource acquisition. Furthermore, partitioning of phytoplankton-derived organic matter between its dissolved and particulate fractions might be influenced by changes in the nutrient supply (Conan et al., 2007). This response is relevant in respect of DON and DOP as substitute nutrient sources for phytoplankton in waters that are deficient in inorganic nutrient compounds (reviewed by Karl and Björkman, 2002, and Bronk et al., 2007).

Our major objective was to test experimentally the response of natural phytoplankton communities taken from the euphotic zone above the OMZs off Peru and West Africa to variable combinations of N and P supply concentrations and their ratios. Production of particulate and dissolved organic matter as well as elemental composition of the bulk phytoplankton community were determined in order (i) to identify the key nutrient controlling phytoplankton growth, (ii) to unravel whether nutrient N:P supply is reflected in the PON:POP composition of accumulated phytoplankton biomass and (iii) to detect potential shifts in the partitioning of accumulated organic matter between dissolved and particulate fractions under different types of nutrient enrichment.

2. Material & Methods

2.1. Mesocosm experimental set-up

This study is based on the results of three nutrient enrichment experiments conducted in shipboard mesocosms during RV *Meteor* cruises M77-3 in the Peruvian Upwelling (PU) region from Guayaquil (Ecuador) to Callao (Peru) in Dec./Jan. 2008/09, M80-2 in the ETNA from Mindelo (São Vicente/Cape Verde) to Dakar (Senegal) in Nov./Dec. 2009 and M83-1 off the coast of West Africa (WA) from Las Palmas (Gran Canary/Spain) to Mindelo (São Vicente/Cape Verde) in Oct./Nov. 2010 (Fig. 4.1).

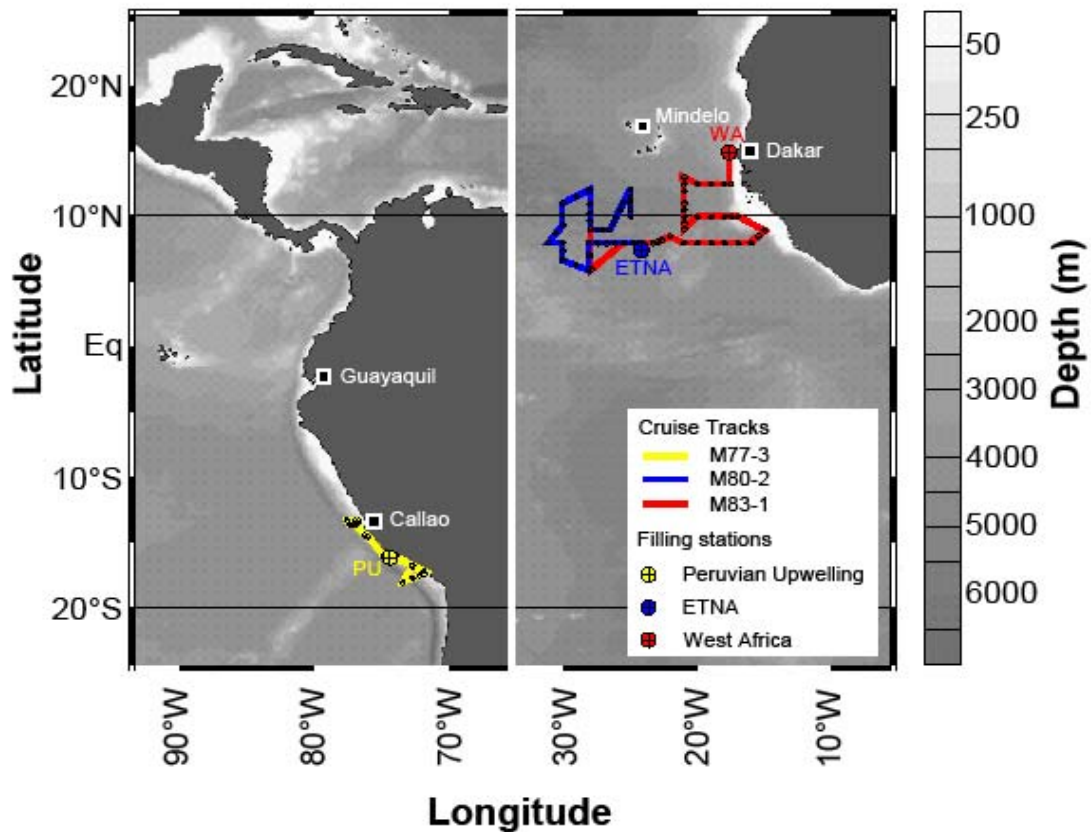


Figure 4.1. Map of the tropical Pacific and Atlantic showing filling stations of the mesocosms (crossed circles) plus the following cruise track during the time of experiments (dots) at the respective cruise. Yellow markers denote cruise M77-3 (PU), blue M80-2 (ETNA) and yellow M83-1 (WA).

For each experiment, twelve mesocosms with a volume of 70 L (PU) or 150 L (ETNA and WA) were distributed over four flow-through gimbals-mounted water baths on deck of the ship (Fig. 4.2). The single mesocosm enclosure was a cylindrical plastic bag with a plexiglass bottom fixed to a floating tire. On the PU cruise, the mesocosms were filled with 70 L each, using natural seawater from 10 m depth (Niskin bottles from CTD-casts), which was pre-screened (200 μ m mesh size) to remove mesozooplankton. On the ETNA cruise, mesocosm bags were each filled with 130 L of natural seawater from 5 m water depth using a peristaltic pump. Additionally, a 20 L inoculum from the chlorophyll *a* maximum at around 50 m depth taken with the CTD-rosette was added to each mesocosm. On the PU cruise, mesocosms were each filled completely with 150 L of seawater from 5 m depth with the peristaltic pump. As surface mesozooplankton abundance was low at the study site, no pre-screening of the medium was done in this case. Continuous flow of ambient surface seawater through the water baths provided *in situ* temperature conditions ($<2^{\circ}\text{C}$ above sea surface temperature).

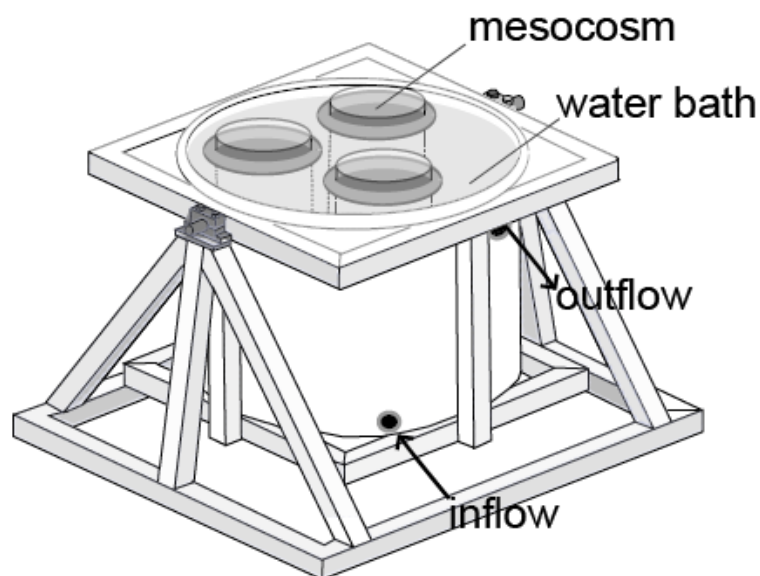


Figure 4.2. Schematic draft of three shipboard mesocosms floating in a gimbal-mounted water bath.

Surface irradiance in the mesocosms on the Pacific cruise ($700\text{--}2600\ \mu\text{mol photons m}^{-2}\ \text{s}^{-1}$) was reduced to approximately 30% by covering the water baths with camouflage nets, whereas solid white lids shaded the tanks on the Atlantic cruises. The solid lids reduced surface light intensity by approximately 50%, resulting in mesocosm light conditions between 100 to $1000\ \mu\text{mol photons m}^{-2}\ \text{s}^{-1}$. Initially, inorganic nutrients (ammonium (NH_4^+), nitrite (NO_2^-), nitrate (NO_3^-), phosphate (PO_4^{3-}), silicate (Si(OH)_4)) of the natural seawater medium were determined and four different N:P treatments in each experiment were adjusted by nutrient additions (Tab. 4.1). Nutrient concentrations of the initial medium on the PU cruise were increased due to upwelling on the shelf. For adjustment of the four N:P treatments, either N (+N), P (+P), N combined with P (+NP) or nothing (control) was added. In contrast, surface nutrient concentrations were extremely low on the West African shelf. To adjust similar nutrient concentrations and N:P supply ratios to the PU experiment, N and P were added to all four treatments, but in variable concentrations. Enrichment with high N and low P (+N), low N and high P (+P), high N and high P (+NP), low N and low P (control) represented the four treatments. For simplification we use 'enrichment', including high addition, or 'no enrichment', including low addition, for both experiments.

Initial molar N:P supply ratios ranged between 20 and 2.5 in all three experiments. Si(OH)_4 and a trace metal mix (Provasoli II trace metal mix; West and McBride, 1999) were added to all treatments (Tab. 4.1). Sampling for biogeochemical analyses was conducted on a daily basis for a period of 7 (PU), 9 (ETNA) and 11 days (WA). Because of their smaller volume during the PU cruise, all mesocosms had to be restocked on sampling days 3 and 5 with filtered ($5\ \mu\text{m}$) natural surface seawater provided by the internal ship's pump (dilution factors: 0.4 and 0.27, respectively). Nutrient concentrations of this medium were on average $5.5\ \mu\text{mol l}^{-1}$ DIN, $0.5\ \mu\text{mol l}^{-1}$ DIP and $8.6\ \mu\text{mol l}^{-1}$ Si(OH)_4 . Nutrient inventories in the mesocosms were partially

restocked through the dilution. Since this was conducted already after the biomass peak and in equal amounts to all twelve mesocosms, we exclude a significant influence on the outcome of the experiment which was mainly driven by the initial nutrient supply.

Table 4.1. Overview of mesocosm filling sites, initial and experimental conditions during the three cruises.

M77-3 (PU)					M80-2 (ETNA)				M83-1 (WA)			
initial conditions												
Latitude	16°0.01'S				7°41.37'N				15°0.01'N			
Longitude	74°37.04'W				24°13.50'W				17°45.00'W			
T(°C)	18.2				27.9				27.6			
DIN	5				0.3				0.3			
DIP	1				0.1				0.1			
Si(OH) ₄	3.7				0.7				1.4			
experimental conditions												
(high) enrichment	+N	+NP	control	+P					+N	+NP	control	+P
N:P supply	16	8	5	2.5	20	15	10	5	16	8	5.5	2.8
DIN supply (μmol L ⁻¹)	16	16	5	5	9	7.5	7.5	7.3	12	12	4.13	4.13
DIP supply (μmol L ⁻¹)	1	2	1	2	0.5	0.5	0.7	1.6	0.75	1.5	0.75	1.5
Si(OH) ₄ supply (μmol L ⁻¹)	10	10	10	10	6	6	6	6	15	15	15	15

2.2. Inorganic nutrients

Analysis of the nutrients NO₂⁻, NO₃⁻, PO₄³⁻ and Si(OH)₄ was conducted on board immediately after sampling according to Hansen and Koroleff (1999). Prior to measurement, samples were pre-filtered through 5 μm cellulose acetate filters (26 mm). A Hitachi U-2000 spectrophotometer was used for all colorimetric measurements on the PU cruise, while they were carried out with a Quattro autoanalyzer (Seal Analytical) during the experiments in the ETNA and WA. NH₄⁺ analysis during PU was conducted according to Holmes et al. (1999), and according to Kerouel and Aminot (1997) with a Jasco FP-2020 fluorometer in the Atlantic.

The utilized abbreviation DIN (dissolved inorganic nitrogen) includes the inorganic nitrogen compounds NO₂⁻, NO₃⁻ and NH₄⁺, DIP (dissolved inorganic phosphorus) includes PO₄³⁻ and all other forms of ortho-phosphate.

2.3. POM

Water samples from the mesocosms for particulate organic carbon (POC) and nitrogen (PON) and for particulate organic phosphorus (POP) were filtered onto pre-combusted (450°C for 5 h) Whatman GF/F filters (0.7 μm pore size; 25 mm diameter) at low vacuum pressure (200 mbar) and stored frozen at -20°C until analysis. Filters for POC/PON were fumed with hydrochloric acid (37%) for ~15 h to remove the inorganic carbon, dried at 60°C for 12 h and wrapped in tin

cups (8 x 8 x 15 mm) for combustion. Final measurements of POC and PON were made according to Sharp (1974) using an elemental analyzer (EURO EA Elemental Analyser) coupled to an EUROVECTOR gas chromatograph.

POP was measured using a modified method according to Hansen and Koroleff (1999) by incubating the defrosted filters with the oxidation reagent Oxisolv (Merck) and 40 mL of ultrapure water for 30 min in a household pressure cooker.

2.4 DOM

For the analysis of dissolved organic nitrogen (DON) and phosphorus (DOP) water samples were pre-filtered through combusted (450°C for 5 h) Whatman GF/F filters (25 mm; 0.7 µm) on the PU and ETNA cruise. No pre-filtration was conducted during the cruise off WA, thus yielding total nitrogen (TN) and phosphorus (TP) instead of total dissolved nitrogen (TDN) and phosphorus (TDP), respectively.

Analysis was accomplished according to Koroleff (1977). Initially, one portioning spoon of the oxidation reagent Oxisolv (Merck) was dissolved in 40 mL of sample and autoclaved in a pressure cooker for 30 min. 10 mL of the oxidized sample was added to 0.3 mL of a mixed reagent (4.5 M H₂SO₄ + NH₄⁺- molybdate + potassium antimonyl tartrate) and 0.3 mL of ascorbic acid, incubated for 10 min and finally TDP (PU, ETNA) or TP (WA) was determined colorimetrically at 882 nm against ultrapure water. Detection limit of the method was 0.2 µmol L⁻¹ and analytical precision was ±8.3%. The DOP concentration was calculated as follows:

$$\text{DOP} = \text{TDP} - \text{DIP} \quad (1)$$

$$\text{DOP} = \text{TP} - (\text{DIP} + \text{POP}) \quad (2)$$

DON was analyzed by pumping the oxidized sample through a reductor containing cadmium, resulting in the reduction of all dissolved organic nitrogen compounds to NO₂⁻. After an incubation of 30 min, TDN (PU, ETNA) or TN (WA) was measured with a spectrophotometer at a wavelength of 542 nm against ultrapure water. Detection limit of the method was 0.1 µmol L⁻¹ and analytical precision was ±0.1 µmol L⁻¹. The DON concentration was obtained as follows:

$$\text{DON} = \text{TDN} - \text{DIN} \quad (3)$$

$$\text{DON} = \text{TN} - (\text{DIN} + \text{PON}) \quad (4)$$

Measurement of TDN from the WA experiment was carried out in combination with the DOC analysis (PU and WA). Water samples for TDN and DOC were collected in ultra-clean and pre-combusted (450°C for 12 h) glass vials and stored at -20°C. In a solvent-free clean laboratory

on land, thawed samples were filtrated through combusted (450°C for 6 hours) GF/F filters and acidified by adding 20 µl HCl (32%) to each sample. Analysis of TDN (detection limit: 2 µmol L⁻¹; AP: ±1 µmol L⁻¹) and DOC (DL: 5 µmol L⁻¹; AP: ±1 µmol L⁻¹) was conducted using the HTCO method (high-temperature catalytic oxidation) (Wurl and Min Sin, 2009) on a Shimadzu TOC-V analyzer. The accuracy of the analysis was validated several times a day with deep-sea reference material provided by the University of Miami. Concentrations of DON were calculated using Eq. (3).

2.5. Calculations

Build-up of dissolved and particulate organic matter in the three experiments was determined based on the time period of exponential growth from the initial sampling day until the first day after nutrient exhaustion. The first day after complete DIN exhaustion in all treatments plus the subsequent day (in order to compensate temporal fluctuation of individual maxima of organic matter) were defined for each experiment as the time of maximum organic matter accumulation (PU: day 4 and 5; ETNA: day 6 and 7; WA: day 4 and 5). The difference in concentration between the initial sampling day and the respective day of maximum accumulation represented the build-up of organic matter. It was not possible to calculate a build-up of DOP during the WA experiment as measured concentrations were in large part close to or even below the detection limit of 0.2 µmol L⁻¹ throughout the experiment, and the associated large daily variability in the data precluded a determination of accumulating DOP for each treatment.

Drawdown of nutrients was determined in accordance with the accumulation of organic matter, i.e. it is defined as the difference in DIN or DIP, respectively, from initial sampling until the maximum of organic matter accumulation (PU: day 4 and 5; ETNA: day 6 and 7; WA: day 4 and 5). To highlight differences in nutrient drawdown at variable N:P supply, treatments were united into four N:P supply groups: ~16:1 (including N:P treatments of 15:1 and 16:1), ~8:1 (including N:P treatments of 8:1 and 10:1), ~5:1 (including N:P treatments of 5:1 and 5.5:1), ~2:1 (including N:P treatments of 2.5:1 and 2.8:1).

Effects of nutrient enrichment on production of POM and DOM compounds were identified using the effect size metric response ratio RR_x , calculated as follows:

$$RR_x = \ln(E/C) \quad (5)$$

where E denotes the build-up of the respective organic compound in the enriched treatment (+N, +P or +NP), whereas C represents the build-up of the variable in the control (see Tab. 1). Since it was impossible to determine an accumulation of DOP during the WA cruise, absolute concentrations of DOP were used for calculating RR_x .

2.6. Statistical analyses

Relationships of pelagic community response variables to the inorganic N:P supply ratio and drawdown ratios of DIN and DIP were determined using regression analyses (SigmaPlot, Systat). Effects of the three nutrient enrichment treatments (+N, +P, or +NP) on RR_x of the accumulated dissolved and particulate organic compounds during the experiments in the PU and off WA were compared using one-way ANOVA, followed by Tukey's post-hoc test to compare specific combinations of factors (Statistica 8, StatSoft). A significance level of $p < 0.05$ was applied to all statistical tests.

3. Results

3.1. Nutrient uptake

Removal of DIN and DIP per biomass unit from the medium was closely related to the N:P supply ratio over all three experiments (Fig. 4.3). Drawdown ratios determined through the regression slopes of DIN versus DIP reflected the N:P supply. N:P drawdown in the ~16:1 N:P treatments was $17.18(\pm 0.49)$, $8.42(\pm 0.30)$ in the ~8:1 treatments, $6.21(\pm 0.48)$ in the ~5:1 treatments and $2.93(\pm 3.21)$ in the treatments with an N:P supply of about 2:1.

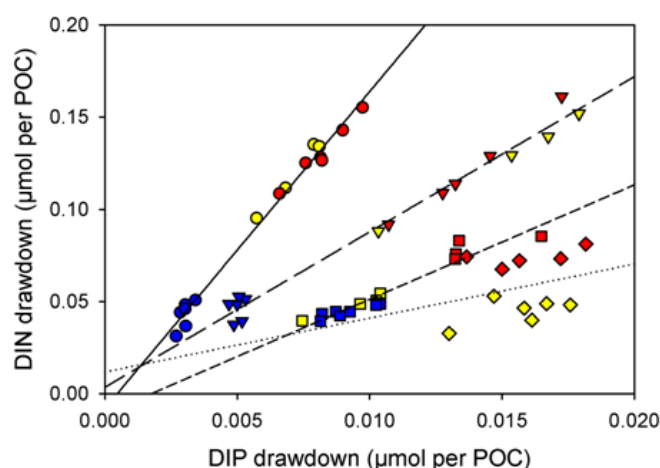


Figure 4.3. Drawdown of DIN versus DIP (both normalized to per POC unit) during the PU (yellow), ETNA (blue) and WA (red) experiments. Linear regressions were fitted to the nutrient drawdown in the treatments supplied with N:P~16:1 (circles; straight line: $y = 17.18(\pm 0.49)x - 0.01(\pm 0.003)$, $r^2 = 0.989$, $p < 0.0001$), N:P~8:1 (triangles; long-dashed line: $y = 8.42(\pm 0.30)x + 0.004(\pm 0.004)$, $r^2 = 0.984$, $p < 0.0001$), N:P~5:1 (squares; short-dashed line: $y = 6.21(\pm 0.48)x - 0.01(\pm 0.01)$, $r^2 = 0.923$, $p < 0.0001$) and N:P~2:1 (diamonds; dotted line: $y = 2.93(\pm 3.21)x + 0.01(\pm 0.05)$, $r^2 = 0.085$, $p = 0.386$).

3.2. Nutrient enrichment and build-up of organic matter

Our data show that the phytoplankton community was limited by N within the PU and WA experiments. This effect was noticeably stronger in the experiment carried out in the Atlantic (WA) (Fig. 4.4; Tab. 4.2). N addition induced strong responses of POC and PON build-up compared to the P enriched treatment, whether through fertilization by N alone ($p_{\text{POC}}=0.001$; $p_{\text{PON}}=0.002$) or in combination with P ($p_{\text{POC}}=0.002$; $p_{\text{PON}}=0.001$) (Fig. 4.4A and B).

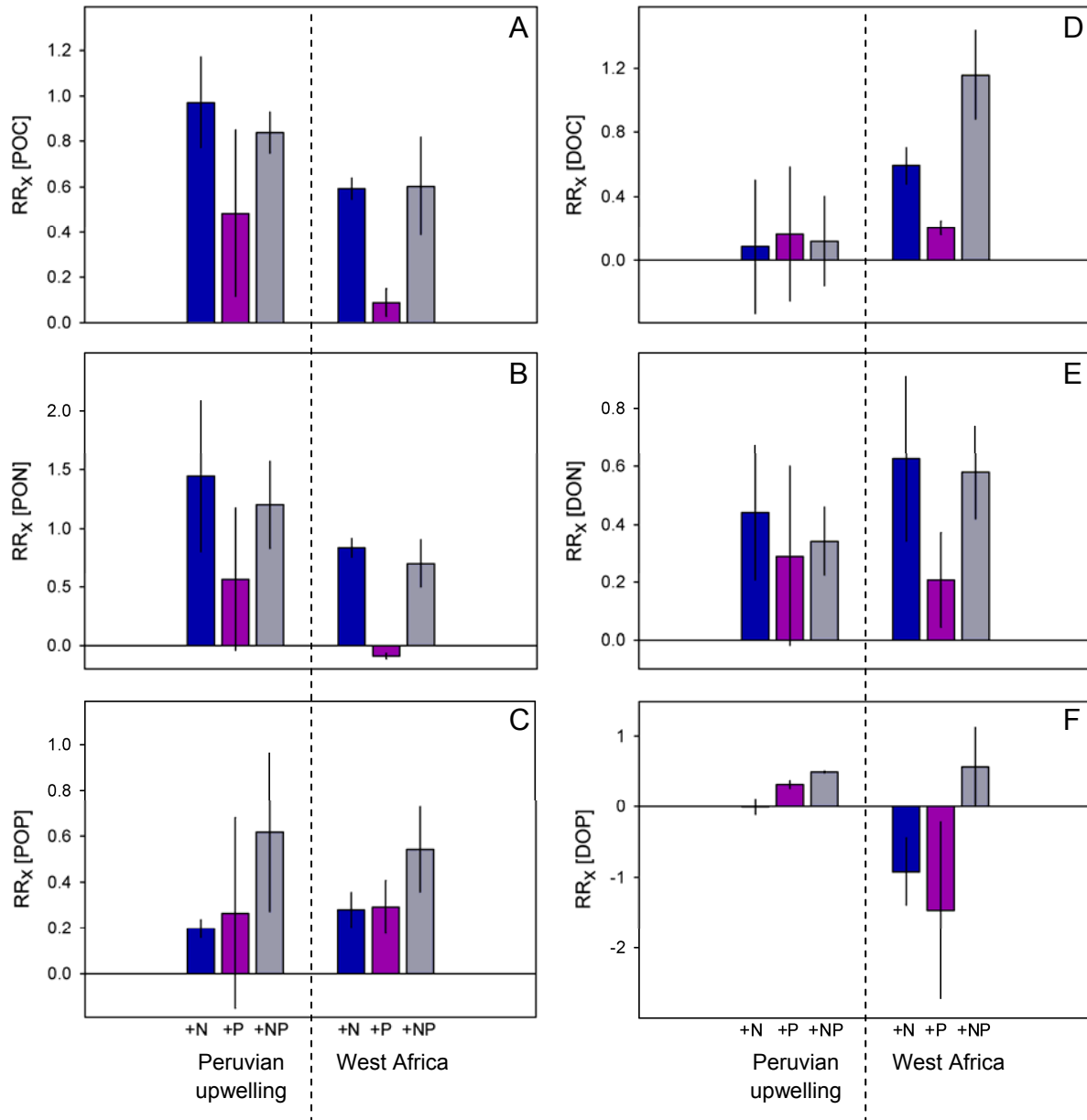


Figure 4.4. Relative responses (RR_x) of the autotrophic communities to enrichment in high N (+N, blue), high P (+P, purple) or to combined high N and high P (+NP, grey), during the PU (Peruvian upwelling) and the WA (West Africa) experiments. Response variables are build-up of (A) POC, (B) PON, (C) POP, (D) DOC and (E) DON. (F) Since no accumulation of DOP could be determined for the WA experiment, absolute concentrations of DOP were used to evaluate RR_x . For detailed calculation of RR_x see Sect.

4.2.5. Values are treatment means and the error bars denote the standard deviation for two consecutive days of production within each treatment of high nutrient enrichment.

P supply provoked only a minor increase in the response of POC production relative to the control treatment, and PON build-up was even negatively affected by P supply. The same trend was observed for the mesocosm experiment in the PU, but effects were not significant due to large standard deviations within the three treatments.

In both experiments, combined supply of N and P generated increased accumulation of POP compared to addition of N (PU: $p=0.314$; WA: $p=0.054$) or P (PU: $p=0.277$; WA: $p=0.066$) alone (Fig. 4.4C).

DOC and DON production displayed no statistically significant difference in the RR_x between the three treatments during the PU cruise ($p=0.577$) (Fig. 4.4D and E). In the WA experiment, build-up of DOC and DON responded in a similar way to N fertilization like POC and PON, although the response for DOC in the +NP treatment was two-fold increased compared to the RR_x in the +N treatment ($p=0.001$). Nonetheless, N enrichment caused a significantly elevated DOC accumulation in contrast to P supply (+N: $p=0.006$; +NP: $p=0.0002$). DON production appeared to be also promoted by N supply, but no significant effect between the three treatments could be detected due to high variability among replicates and sampling days ($p=0.205$).

Table 4.2. Summary of p -values obtained from ANOVA comparing the effects of the three high nutrient enrichment treatments (+N, +P, or +NP) on build-up (POC, PON, POP, DOC, DON) or concentration (DOP) of organic elemental compounds during the PU and WA experiment. Statistical significant effects ($p<0.05$) are denoted in bold.

Experiment	Factor	+N vs. +P	+N vs. +NP	+P vs. +NP	treatment
PU	RR_x [POC]	0.134	0.975	0.193	0.106
	RR_x [PON]	0.162	0.987	0.210	0.120
	RR_x [POP]	0.998	0.314	0.277	0.243
	RR_x [DOC]	0.652	0.996	0.665	0.577
	RR_x [DON]	0.629	0.886	0.908	0.654
	RR_x [DOP]	0.225	0.039	0.398	0.047
WA	RR_x [POC]	0.001	0.994	0.002	0.0005
	RR_x [PON]	0.0002	0.473	0.0005	<0.0001
	RR_x [POP]	0.993	0.054	0.066	0.036
	RR_x [DOC]	0.006	0.0009	0.0002	<0.0001
	RR_x [DON]	0.188	0.804	0.464	0.205
	RR_x [DOP]	0.621	0.321	0.065	0.074

Absolute concentrations of DOP were used to assess the effect of nutrient enrichment on DOP, since no detectable accumulation of DOP occurred within the WA experiment. The strong variation of DOP within the treatments caused strong negative responses to single high N or P supply and positive RR_x in the +NP mesocosms (Fig. 4.4F). The measured fluctuation of DOP stocks around the detection limit of $0.2 \mu\text{mol L}^{-1}$ suggest a high uncertainty in DOP data. In the experiment off Peru, DOP was affected by high P addition, as RR_x was increased in the +P and +NP treatment, whereas DOP showed on average no response to N fertilization. In particular the combined addition of N and P resulted in increased concentrations of DOP in relation to the +N treatment ($p=0.039$).

3.3. Elemental stoichiometry of particulate organic matter

Over all three mesocosm experiments, the PON:POP ratio of biomass build-up correlated positively with the inorganic N:P supply ratio ($p<0.0001$) (Fig. 4.5). Thus, the supplied N:P stoichiometry did influence the PON:POP production ratio of phytoplankton, although the PON:POP of produced biomass exceeded the N:P of nutrient supply in most cases. This deviation between the inorganic and organic N:P ratio slightly increased with decreasing supply ratios, denoted by the slope of linear regression of $0.90(\pm 0.07)$. No PON:POP values lower than 5:1 were observed, although some treatments were provided with even lower nutrient N:P ratios of 2.8 and 2.5.

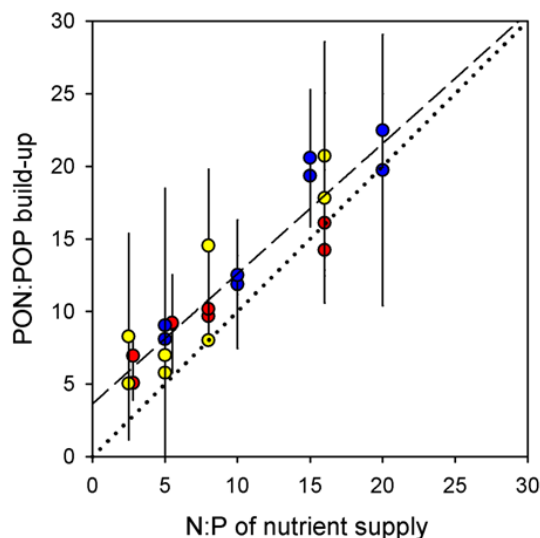


Figure 4.5. Positive linear correlation (dashed line: $y=0.90(\pm 0.07)x+3.64(\pm 0.08)$, $r^2=0.875$, $p<0.0001$) between N:P of nutrient supply and the PON:POP of produced biomass until day one and two after DIN limitation in the PU (yellow), ETNA (blue) and WA (red) experiment. Dotted line indicates PON:POP build-up equal to N:P supply. Values are treatment means and the vertical error bars denote the standard deviation of replicates within each N:P treatment.

During exponential growth under nutrient-saturated conditions, PON:POP across all experiments fluctuated between a range of 11:1 to 21:1, regardless of the respective N:P supply ratio (Fig. 4.6A). PON:POP composition within the individual experiments only slightly varied between the treatments. When phytoplankton entered the stationary growth phase due to exhaustion of N, their PON:POP began to diverge between the treatments and towards their respective N:P supply ratio (Fig. 4.6B). N:P supply conditions $<16:1$, indicating N-limitation of the autotrophic community according to Redfield, caused in general a decrease in the PON:POP. Redfield- or P-limited conditions, induced by an initial $N:P \geq 16:1$, entailed an increase of the phytoplankton N:P stoichiometry. These effects were strong in the ETNA and WA experiments, and more weakly pronounced in the PU approach. Overall, PON:POP composition of the phytoplankton ranged between 6:1 to 24:1 over all experiments during the stationary phase.

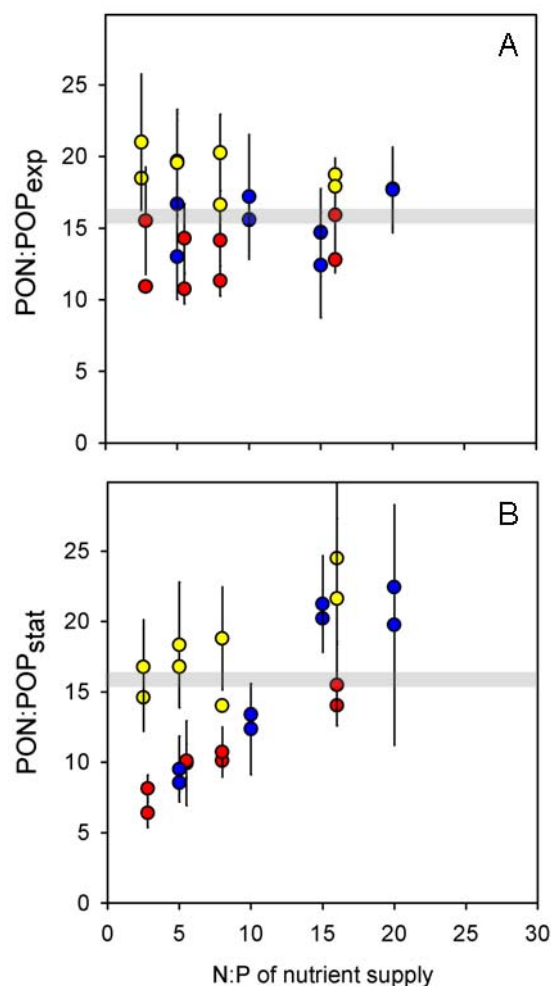


Figure 4.6. PON:POP stoichiometry during (A) exponential and (B) stationary growth phase. Greyish bars signify the N:P Redfield ratio of 16:1. Style and color-coding according to Fig. 4.5.

The relation between nutrient uptake and the production of biomass is demonstrated in Tab. 4.3. In general, initial inventories of N and P were consumed completely and N:P uptake closely matched the N:P supply in all experiments. But the uptake ratio of N:P exceeded the supply ratio in the lowest N:P treatments of the PU (2.5:1) and the WA (2.8:1) trial, as unused P was left in the medium during both experiments (data not shown). Values <1 of the quotient of N:P uptake and build-up display that PON:POP production was, with a few exceptions, higher than N:P drawdown. This discrepancy in the ratio of nutrient consumption and particulate matter production increased in each experiment with decreasing N:P supply and is therefore congruent to the offset between PON:POP build-up and the N:P supply ratio shown in Fig. 4.5.

Table 4.3. Summary of the N:P uptake and the stoichiometry of particulate organic matter build-up within each experiment. The quotient of N:P drawdown and PON:POP build-up describes the analogy of N:P uptake and produced PON:POP.

	N:P supply	N:P drawdown (\pm SD) ($\mu\text{mol L}^{-1}$)	PON:POP build-up (\pm SD) ($\mu\text{mol L}^{-1}$)	N:P drawdown/ PON:POP build- up
PU	16	17.0(\pm 0.3)	19.3(\pm 6.4)	0.88
	8	8.8(\pm 0.4)	11.3(\pm 4.9)	0.78
	5	5.7(\pm 0.8)	8.8(\pm 7.4)	0.65
	2.5	3.9(\pm 0.9)	6.2(\pm 2.7)	0.62
ETNA	20	20.2(\pm 0.9)	21.6(\pm 3.9)	0.94
	15	14.2(\pm 1.9)	10.5(\pm 3.6)	1.35
	10	9.2(\pm 1.3)	21.5(\pm 3.6)	0.43
	5	4.8(\pm 0.1)	10.3(\pm 2.6)	0.46
WA	16	16.0(\pm 0.4)	15.2(\pm 2.6)	1.05
	8	8.8(\pm 0.3)	9.9(\pm 1.5)	0.88
	5.5	5.7(\pm 0.4)	7.6(\pm 3.0)	0.75
	2.8	4.7(\pm 0.5)	6.0(\pm 1.4)	0.77

3.4. Partitioning of organic matter

Changes occurred in the partitioning of N- and P-containing organic matter between the dissolved and the particulate fraction in relation to nutrient supply. Build-up of PON decreased with decreasing N:P supply in the PU (slope of regression (SR=0.46(\pm 0.19), $p=0.053$) and WA (SR=0.50(\pm 0.11), $p=0.005$) trial, whereas PON accumulation was unaffected by nutrient supply in the ETNA experiment (SR=0.07(\pm 0.04), $p=0.094$) (Fig. 4.7A; Tab. 4.4). DON production showed no significant response to the N:P supply ratio in the ETNA (SR=0.03(\pm 0.05), $p=0.625$) and the PU experiment (SR=0.20(\pm 0.12), $p=0.129$) (Fig. 4.7B). Like PON, DON build-up was also significantly reduced with lower N:P supply off West Africa (SR=0.19(\pm 0.07), $p=0.040$).

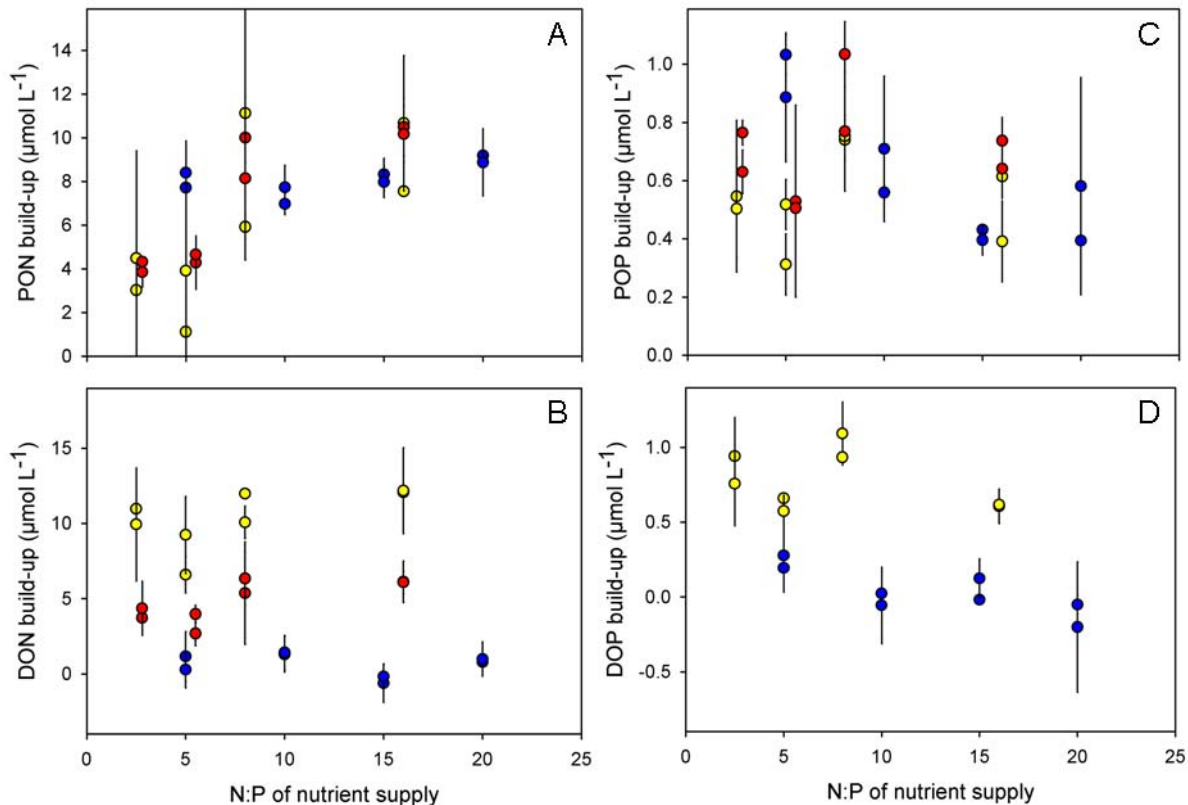


Figure 4.7. Build-up of (A) PON, (B) DON, (C) POP and (D) DOP until day one and two after DIN limitation as a function of N:P stoichiometry of the supplied nutrients during three (PON, DON, POP) or two experiments (DOP). Style and color-coding according to Fig. 4.5.

The nutrient N:P stoichiometry did not have an effect on POP production in the PU ($\text{SR}=0.002(\pm 0.012)$, $p=0.897$) and WA trial ($\text{SR}=0.004(\pm 0.013)$, $p=0.771$), while POP accumulation was significantly higher at low N:P supply in the ETNA trial ($\text{SR}=0.033(0.009)$, $p=0.011$) (Fig. 4.7C). Build-up of DOP was stimulated by lowered N:P supply off Peru ($\text{SR}=-0.012(\pm 0.014)$, $p=0.411$) and in the ETNA experiment ($\text{SR}=-0.020(\pm 0.007)$, $p=0.020$) (Fig. 4.7D). The influence of the nutrient N:P stoichiometry on DOP production in the WA experiment could not be determined, since DOP did not accumulate in this experiment.

Table 4.4. Summarizing the effect of decreasing N:P supply on accumulation of PON, DON, POP and DOP within each experiment. Statistical significance of the individual effect ($p < 0.05$; denoted by *) was tested with linear regression analysis and p -values are given in brackets.

	PON build-up	DON build-up	POP build-up	DOP build-up
PU	↓ ($p=0.053$)	↔ ($p=0.129$)	↔ ($p=0.897$)	↑ ($p=0.411$)
ETNA	↔ ($p=0.094$)	↔ ($p=0.625$)	↑* ($p=0.011$)	↑* ($p=0.020$)
WA	↓* ($p=0.005$)	↓* ($p=0.040$)	↔ ($p=0.771$)	?

↑ increase; ↓ decrease; ↔ unaffected

4. Discussion

4.1. Nutrient limitation of mesocosm phytoplankton

In the mesocosm experiments conducted in the upwelling areas off Peru (PU) and Northwest Africa (WA), microalgal growth responded with enhanced growth to the addition of N, while combined fertilization of N and P did not induce a further increase in biomass production compared to N-alone enrichment (Fig. 4.4). The effect that N was the critical element controlling photoautotrophic production was primarily driven by diatoms, as they dominated mesocosm phytoplankton communities during both experiments (Hauss et al., subm.; Franz et al., unpubl. results). This diatom dominance can likely be attributed to their fast metabolic reaction including high maximum uptake rates and fast cell division after input of new N (Fawcett and Ward, 2011). A comparable reaction was already recorded by Rhyther and Dunstan (1971), where NH_4^+ enrichment induced strong growth of the diatom *Skeletonema costatum*, while P addition resulted in equally poor growth of this species compared to the unamended control. Primary production in coastal upwelling areas, to a major part accomplished by diatoms, has been known for decades to be limited by ‘newly’ supplied N from the deep (Dugdale, 1985). Thus, it is not surprising that the phytoplankton community in the mesocosm experiments, provided with replete amounts of Si(OH)_4 and iron, was regulated by the macronutrient N. Yet, since the cellular assembly machinery of blooming species like diatoms are requiring in addition large quantities of P molecules for RNA synthesis, we expected highest growth rates in the 8:1 N:P treatments, which were enriched in N and P. However, total production of phytoplankton biomass was solely controlled by N supply and showed no reaction to P fertilization. Similar responses of natural phytoplankton communities were recorded in another nutrient enrichment experiment performed in the upwelling area off Southern California (Thomas, 1974). A multitude of nutrient fertilization studies were conducted in oligotrophic regions and showed patterns of N

as well as of P limitation (e.g. Graziano et al., 1996; Moore et al., 2008). Although N was the primary limiting nutrient (see also meta-analysis by Downing et al., 1999), combined additions of N and P induced larger increases in phytoplankton biomass compared to providing N alone. Summarizing results from all these nutrient enrichment experiments, including this study, we can deduce that under the premise that no other nutrient (e.g. Fe, Si) limits primary production, picoplanktonic communities from nutrient-poor waters tend to be limited by N and P, whereas microalgal assemblages from upwelling areas are exclusively limited by N. Yet, we have to be careful with generalizing these responses to the bulk of marine non-diazotrophic photoautotrophs, since there is a wide variability among different phytoplankton groups concerning their optimal nutrient conditions (Geider and LaRoche, 2002). For instance, growth of some rare photoautotrophs during the PU experiment was favoured by low N:P nutrient ratios (Haus et al., *subm.*).

Considering the response of the phytoplankton community as a whole, this study gives indications of the key nutrient controls of primary production in coastal upwelling areas and how nutrient assimilation and photoautotrophic production of organic matter responds to changes in nutrient inventories.

4.2. Relationship between N:P supply and phytoplankton N:P

Redfield (1958) discovered the average elemental composition of seston and of seawater nutrients to be remarkably similar and suggested a tight coupling between organic matter and nutrient stoichiometry. However, beside the ratio of nutrient supply (Rhee, 1978; Sterner and Elser, 2002), phytoplankton stoichiometry is influenced considerably by growth rate (Goldman et al., 1979). Numerous studies discussed the relation between the physiological growth state and the cellular N:P ratio of phytoplankton (Sterner and Elser, 2002; Klausmeier et al., 2004a, 2004b; Arrigo, 2005). Exponential growth requires an assembly machinery rich in ribosomes, which are characterized by low N:P. In contrast, equilibrium growth under nutrient limitation is maintained by a metabolism optimized for resource acquisition, consisting mainly of N-rich proteins. Hence, the growth strategy of the cell affects nutrient requirements and ultimately its biochemical composition substantially.

In addition, the growth phase defined by nutrient availability is regulating phytoplankton elemental stoichiometry (Klausmeier et al., 2004b and 2008). Elemental ratios of organic matter within the individual experiments showed only minor deviations from each other during exponential growth under high nutrient availability, regardless of the respective N:P supply ratio (Fig. 4.6A). Nutrient saturation allowed cells to “eat what they need” (after Sterner and Elser, 2002), closely matching their specific optimal uptake ratio and constraining phytoplankton N:P to a relatively narrow range around Redfields’ 16:1. Under nutrient depletion during the

stationary phase, cells consume nearly the entire pool of supplied nutrients, and consequently their elemental composition approached the respective N:P input ratio, generating a much wider PON:POP range (Fig. 4.6B). N:P drawdown ratios obtained from regression analysis also showed that nutrient uptake kinetics of the cells were strongly influenced by the N:P supply ratio (Fig. 4.3). The tight positive correlation between ratios of nutrient supply and organic biomass after nutrient exhaustion indicates a high flexibility of phytoplankton stoichiometry to changes in nutrient supply ratios when absolute nutrient concentrations are low. This response has already been described by culture experiments (Rhee, 1978; Goldman et al., 1979) and model based data (Klausmeier et al., 2004a). An extremely high or low PON:POP stoichiometry under conditions of nutrient limitation are likely to be caused by luxury consumption and intracellular storage of the nutrient (N or P) that is not limiting (Goldman et al., 1979; Geider and LaRoche, 2002). Nonetheless, the flexibility of cellular N:P is ultimately restricted. Phytoplankton elemental composition seemed to be constrained by a lower ratio of 5:1, as biomass was not produced with a PON:POP composition <5:1 (Fig. 4.5). Using a compilation of published data on the biochemical composition of phytoplankton, Geider and LaRoche (2002) identified also a lower limit for microalgal N:P stoichiometry of 5:1. Unused residual amounts of DIP in the medium (data not shown) and exudation of excess P (Fig. 4.7D) are conform with the concept that limits to the cellular storage capacity for nutrients are causing the decoupling of nutrient supply ratio and microalgal elemental composition (Geider and LaRoche, 2002).

A consistent offset between the PON:POP ratio of produced biomass and the N:P supply ratio occurred over the entire gradient of N:P, yet approaching the 1:1 line with increasing N:P supply (Fig. 4.5). Thus, the largest offset occurred at the lowest N:P supply tested. This deviating trend is partly a result of the unused DIP left in the medium in the 2.5:1 and 2.8:1 N:P treatments during the PU and WA trials. Our data indicate that the increased deviation between organic N:P build-up and inorganic N:P uptake under low N:P supply was caused by enhanced transfer of DIP into the DOP pool. Decreasing N:P supply ratios may thereby induce a shift in the partitioning of organic P from the particulate to the dissolved phase. The lower the nutrient N:P supply ratio, the more phosphorus may be channeled into DOP instead of being utilized for particulate biomass build-up. With excess P in the medium (excess $P = DIP - DIN/16$), Conan and colleagues (2007) detected also a significant part (around 80%) of assimilated P in the dissolved organic fraction. Already in 1974, Banse highlighted the high importance of dissolved organic compounds in nutrient cycling and in changes of phytoplankton N:P, as removal of inorganic substances from the medium does not necessarily imply their exclusive incorporation into particulate biomass. For instance, exudation of dissolved fractions of organic material by healthy non-senescent cells is not uncommon (Mague et al., 1980; Mykkestad et al., 1989) and may influence organic matter cycling significantly.

4.3. Effect of different nutrient enrichment on organic matter partitioning

Changes in the N:P supply ratios affected the production of organic nitrogen and phosphorus and their partitioning between the particulate and the dissolved fraction. In the experiment off Peru, decreasing N:P supply entailed a reduction in PON accumulation, whereas DON build-up varied only marginally along the gradient of N:P supply. Excess P resulting from decreasing N:P supply ratios was transferred into DOP, while POP production remained rather unaffected by an increasing P availability. Changes in the PON:POP composition of phytoplankton under variable nutrient supply in this experiment on the Peruvian shelf were caused by the pools of PON and DOP responding to changing nutrient supply.

In the ETNA experiment, organic nitrogen, neither in the particulate nor in the dissolved phase, was affected by nutrient supply. PON:POP of biomass build-up was solely controlled by changes in the production of POP and DOP in response to variable N:P supply ratios. Like in the PU trial, DOP accumulation increased with decreasing N:P supply and declined under rising N:P conditions, respectively. Phytoplankton cells confronted with P-starvation activate expression of extracellular enzymes such as alkaline phosphatase which are catalyzing hydrolysis of organic phosphorus compounds (Dyhrman and Ruttenberg, 2006; Dyhrman et al., 2006; Ranhofer et al., 2009). Alkaline phosphatase expression and activity is generally stimulated by P-deficiency at concomitant N-repletion. Increases in excess P may consequently diminish production of this hydrolytic enzyme, as the need for using DOP as a substitute source for nutrition is vanishing. Poor DOP consumption would even allow an enhanced accumulation of organic phosphorus in the dissolved phase, as observed in the Peruvian upwelling. Beside low removal rates, accelerated DOP production via microalgal exudation, cell lysis and zooplankton grazing (Karl and Björkman, 2002) may be the reason for increasing DOP accumulation with decreasing N:P supply. For example, protozoan grazing has been linked to the transfer of organic phosphorus from the particulate to the dissolved fraction (Dolan et al., 1995). However, more reasonable in conjunction with changes in nutrient inventories seems to be an increased exudation of DOP induced by a form of luxury consumption of P by the microalgal cells under growing P availability. Luxury uptake of the non-limiting nutrient by phytoplankton typically occurs under nutrient saturation to refill cellular reservoirs for upcoming events of nutrient starvation (Healey, 1973; Geider and LaRoche, 2002; Sarthou et al., 2005). Yet, intracellular accumulation of phosphorus is quantitatively confined and an excess in intracellular phosphorus is disposed via exudation.

Unfortunately, we could not assess the effect of variable nutrient supply on DOP build-up in the experiment conducted on the West African shelf. But since PON production was significantly reduced under low N:P supply together with no effect on POP build-up, the growing offset between PON:POP stoichiometry and inorganic N:P was likely induced by enhanced channelling of P into the DOP pool. The general absence of DOP accumulation in the WA

experiment may be due to several reasons. Low concentrations could be caused by low DOP release via exudation, grazing or cell lysis. Alternatively, enhanced or reduced removal of DOP could have also affected the magnitude of DOP accumulation. Photoautotrophic microorganisms can utilize certain DOP compounds as an additional P source (reviewed by Cembella et al., 1984, and by Karl and Björkman, 2002), and especially the filamentous cyanobacterium *Trichodesmium* is known to grow largely on DOP (e.g. Dyhrman et al., 2002; Sohm and Capone, 2006). The presence of *Trichodesmium* in the WA experiment and the fact that its abundance increased under exhaustion of DIP (Franz et al., unpubl. results) indicates that DOP exuded from blooming diatoms (Franz et al., unpubl. results) was immediately assimilated by the cyanobacteria. Differences in the taxonomical composition of the phytoplankton communities can therefore strongly influence DOP dynamics. It must be further taken into account that DOP can include a multitude of organic compounds that differ considerably in their molecular configuration (Karl and Björkman, 2002). This entails differences in the bioavailability of the various DOP compounds. Small nucleotides (e.g. Adenosinetrifosphat) can be easily assimilated, whereas polymers (DNA, RNA) are characterized by long turnover times, resulting in accumulation of DOP in the water column (Thingstad et al., 1993; Björkman and Karl, 1994). Consequently, the biochemical composition of the individual DOP pool determines its bioavailability and is pivotal for its removal by bacteria and microalgae.

In contrast to the PU and ETNA experiments, DON accumulation increased with increasing N:P supply off West Africa. This can either be attributed to an enhanced deposition or an impaired removal of DON at high N supply, or a combination of both. Even though N was the critical nutrient, saturation presumably stimulated luxury uptake of N by phytoplankton cells, resulting in a restocking of the intracellular N reservoirs, but causing also enhanced exudation of DON. High phytoplankton biomass in the N-rich treatments induced development of a large protozoan community, which increased the DON pool via grazing and excretion additionally. DON may have also accumulated due to an impeded removal by phytoplankton. In fact, DON serves as a nitrogen source for some phytoplankton groups under DIN depletion and especially labile forms of DON are frequently assimilated by photoautotrophs (reviewed by Bronk et al. 2007). But under high DIN availability the autotrophic cells preferred assimilation of the more bioavailable forms of DIN, promoting accumulation of DON in the medium.

The artificial nutrient enrichment to natural phytoplankton communities from eastern boundary current systems in the ship-board mesocosms can be regarded as a simulated upwelling event, facilitating development of a typical phytoplankton bloom subsequent to nutrient pulses from the deep. Considerations about shifts of N and P between the inorganic, organic particulate and organic dissolved fraction are therefore based on the dominant autotrophic community and protozoa. But heterotrophic bacteria are also known to feed on

inorganic and dissolved organic nutrient compounds (Kirchman, 1994), and will certainly influence in particular pools of DON and DOP. Nonetheless, we presume that significant effects in these pools are primarily induced by the response of phytoplankton to variable nutrient supply. Hence, we could show that pools of DON and DOP are indeed affected by the magnitude of N:P supply and may thus play an important role in coastal upwelling biogeochemistry under decreasing N:P supply ratios.

Conclusions

Against the background of expanding OMZs and the associated increase in N loss, biogeochemistry of high-productivity upwelling areas overlying O₂-deficient intermediate waters may face severe changes in the future. Our results indicate a decline in organic matter production of coastal phytoplankton as a result of decreasing N supply. The observed high flexibility of phytoplankton elemental stoichiometry to variations in the N:P supply ratio suggests a general decrease in the N:P composition of primary producers in the upwelling regime in the course of decreasing seawater N:P. However, phytoplankton N:P seems to have a critical lower limit of about 5:1. DIP in excess of this ratio is likely to be transferred into the DOP pool or remains unused in shelf waters. Surface waters departing from the shelf would thus be enriched in DIP and DOP, and might fuel growth of diazotrophic phytoplankton in the oceanic off-shelf regions. High-quality *in situ* measurements of DOP in surface waters above the OMZ on the continental shelf and adjacent to the upwelling area are necessary to confirm this hypothesis. Modifications in the cellular N:P composition also entails a change in the nutritional value of coastal microalgae as a food source. Effects of changing N:P supply may therefore also involve higher trophic levels of the pelagic food web.

Acknowledgments

The authors would like to thank technicians Peter Fritsche, Thomas Hansen, Kerstin Nachtigall, Martina Lohmann and the crew of *R/V Meteor* for their great support during the cruises. We thank Matthias Friebe for technical assistance with DOC and TDN analysis. This work is a contribution of the Sonderforschungsbereich 754 "Climate - Biogeochemistry Interactions in the Tropical Ocean" (www.sfb754.de) which is supported by the German Science Foundation (DFG).

III. Synthesis and future perspectives

Acidification and warming of the ocean, both induced by the increase in anthropogenic carbon dioxide (CO₂), are commonly regarded as the two major stressors for marine systems in the course of global change. Since recent years, ocean deoxygenation has been increasingly recognized as an additional stress factor with the potential to significantly impact the ocean (reviewed by Keeling et al., 2009, and by Gruber, 2011). The projected expansion of OMZs in the tropical ocean (Matear and Hirst, 2003; Stramma et al., 2008) may have profound implications for marine biogeochemistry on a global scale, as these O₂-deficient zones are closely connected to highly productive eastern boundary current systems. Coastal upwelling areas comprise merely a tiny fraction of the global ocean, but account for a substantial part of global marine primary and secondary production (Ryther, 1969; Pauly and Christensen, 1995). The productivity of these ecosystems relies primarily on the physically-mediated vertical nutrient supply to the surface. Inventories and cycling of inorganic nutrients are thought to react highly sensitive to an expansion and intensification of O₂-deficiency, with unknown implications for the autotrophic as well as the heterotrophic community. In order to elucidate the effects of proceeding ocean deoxygenation on primary production in coastal upwelling domains, biogeochemical field surveys as well as nutrient enrichment experiments with natural phytoplankton communities in shipboard-mesocosms were conducted during three cruises to the eastern margins of the tropical Pacific and Atlantic Ocean.

Aquatic mesocosms, namely meso-scale enclosures that allow controlled manipulation of certain environmental factors under close to natural conditions, are popular tools to study biogeochemical processes and elemental cycling in aquatic systems. Mesocosms can be regarded as experimental ecosystems, since they represent a compromise between highly controlled but small-scale, mostly mono-cultural lab experiments and *in situ* field surveys. The possibility to study the response of a complete natural community to specifically manipulated factors, with all its mutual interactions and indirect effects, represents the major advantage of the mesocosm approach. In the framework of this thesis, natural plankton communities from the tropical ocean were confronted with different concentrations and ratios of N and P in shipboard mesocosms, to examine the effect of deoxygenation-induced changes in nutrient inventories and stoichiometry on phytoplankton.

Nitrogen as primary limiting nutrient for phytoplankton growth

The experimental design of the mesocosm experiments was, in the context of decreasing N:P supply ratios, solely aimed at resolving the question whether N or P, or a combination of both nutrients is controlling primary production in tropical eastern boundary regions. To preclude any nutrient limitation other than by N or P, all experimental treatments were equally supplied with replete amounts of Fe and Si(OH)_4 . Indeed, Fe is known to limit phytoplankton growth in coastal upwelling areas (Hutchins et al., 2002), a response that is mainly driven by dominating large diatoms which seem to have an exceptionally high demand for this micronutrient (Sunda and Huntsman, 1995; Hutchins and Bruland, 1998). Fe supply to the euphotic zone via upwelling probably increases with expanding OMZs, as continental shelf sediments are significant sources for this trace metal (Johnson et al., 1999) and anoxic conditions in bottom waters are promoting release of Fe from the sediment (Ingall and Jahnke, 1994). Enhancement in Fe supply to the euphotic zone would affect primary production and microalgal community composition (DiTullio et al., 2005; Hare et al., 2005).

Replete concentrations of Fe (Schlosser, pers. comm.), NO_3^- , and PO_4^{3-} , in conjunction with relatively low concentrations of Si(OH)_4 in the off-shelf waters on the 10°S transect in Study 1 suggest that diatom growth was limited by Si(OH)_4 availability adjacent to the Peruvian inner shelf. Diatom-dominated microalgal assemblages in upwelling areas are known to react particularly sensitive to changes in Si(OH)_4 concentrations (Dugdale and Wilkerson, 1998), since diatoms require this nutrient for their silica cell walls (Lewin, 1962). Regeneration of biogenic silicate has been linked to the colonization by bacteria, which degrade the organic coating used to prevent dissolution of the silica shell of living diatoms (Biddle and Azam, 1999; Demarest et al., 2011). Still, it remains entirely unclear if and how Si(OH)_4 recycling will be affected by an intensification of low O_2 waters on the continental shelf.

Thus, availability of Fe and Si(OH)_4 can each limit primary production, particularly in the diatom-dominated upwelling areas, and may possibly both be influenced by changes in the ocean's redox-state. Nonetheless, this thesis exclusively aims at investigating the effect of variable N:P supply on phytoplankton growth, community structure and biomass stoichiometry.

Three nutrient enrichment experiments, conducted in shipboard mesocosms (Study 2, 3 and 4) in eastern boundary regions of the Pacific and Atlantic Ocean, revealed N compared to P as the primary limiting nutrient for primary production. This response is generally in agreement with the majority of nutrient addition experiments performed in marine ecosystems (e.g. Vince and Valiela, 1973; Graziano et al., 1996; Davey et al., 2008; Moore et al., 2008; Tang et al., 2009). But although phytoplankton growth was significantly stimulated by N fertilization in these previous experiments, it was fuelled even further by combined addition of N and P; an effect that did not apply to the experiments completed in upwelling areas within the framework of this thesis (see Fig. III.1, right panel). The apparent synergistic effect of combined N and P

enrichment was likewise observed in a global meta-analysis that compiled results from a multitude of nutrient enrichment experiments conducted in a variety of marine systems (see Fig. III.1, left panel; Elser et al., 2007), whereof only one study was accomplished in an upwelling region (Thomas et al., 1974). Primary production in this nutrient fertilization experiment run off the Californian coast was, similar to Study 2, 3 and 4, solely controlled by N availability. The response of phytoplankton communities common in nutrient-rich tropical upwelling areas was hence highly underrepresented in the large-scale meta-analysis by Elser et al. (2007).

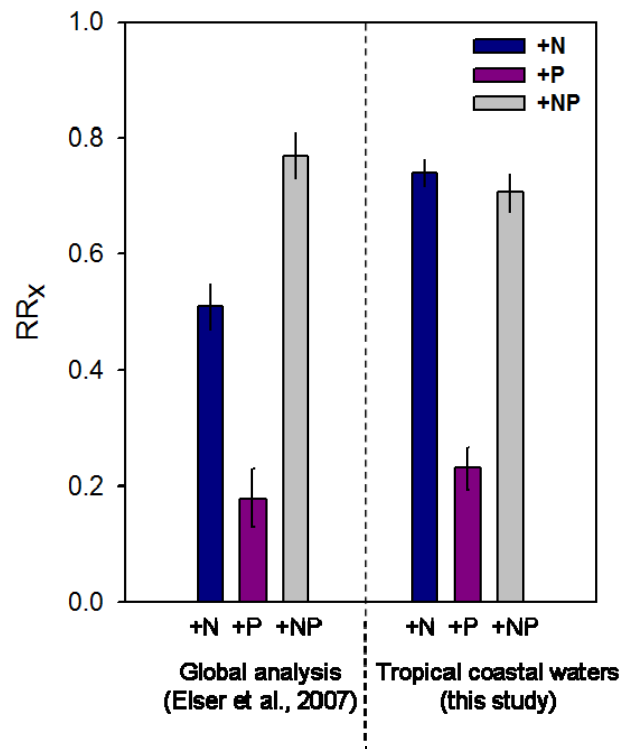


Figure III.1. Relative responses (RR_x) of phytoplankton to enrichment in N (+N), P (+P) or to combined addition in N and P (+NP). The left panel shows RR_x from a global meta-analysis by Elser et al. (2007), including results of nutrient enrichment experiments from different marine areas. The right panel shows mean RR_x (of POC build-up) from enrichment experiments conducted in the Peruvian upwelling and off the coast of NW Africa (Study 4). For detailed calculation of RR_x see section 2.5. in Study 4. Values are treatment means and error bars denote the standard error.

Provided that no further nutrient is limiting (e.g. Fe, Si(OH)_4), it can be differentiated between exclusive N limitation of bulk phytoplankton in coastal shelf waters (this study; Thomas et al., 1974; Downing et al., 1999) and a multiplicative limitation effect of N and P on primary production in the oligotrophic open ocean (Graziano et al., 1996; Davey et al., 2008; Moore et al., 2008; Tang et al., 2009). Yet, Liebig's law of the minimum, declaring that growth is solely controlled by the primary limiting nutrient, has been confirmed to hold in either way (Droop, 1974; Rhee, 1978). The seemingly synergistic growth effect of simultaneous N and P addition is assumed to be a result of competitive exclusion and coexistence of populations either limited by

N or by P in natural communities. Combined addition of N and P favours growth of both N- and P-limited species, resulting in a higher biomass yield compared to single N or P fertilization. Based on this hypothesis, phytoplankton assemblages in bioassays conducted in the oligotrophic ocean may be equally composed of N- and P-limited species, which are jointly controlling the response of the total algal community. Primary production in coastal upwelling areas is largely dominated by diatoms and dinoflagellates, which are both limited by N availability (Ryther and Dunstan, 1971; Smetacek, 1999; Study 2 and 3). Hence, bulk phytoplankton shows only patterns of N-limitation (Fig. III.1; right panel). The effect of single N-limitation was less pronounced during the experiment in the Peruvian upwelling, because responses on nutrient enrichment were more variable on a species-specific level (Study 2). Growth of flagellate autotrophs such as the haptophyte *Phaeocystis globosa* and the chrysophyte *Heterosigma* sp. was favoured by the addition of P (Study 2). Low nutrient N:P has already been demonstrated to promote development of colony-forming *Phaeocystis globosa*, as it represents a good competitor under N-limitation (Riegman et al., 1992). Still, biomass of the P-limited species was too low compared to the N-limited diatoms and dinoflagellates to have a significant effect on total primary production.

In the context of future decreasing diapycnal N:P supply, evaluation of these findings implies a possible shift in the community structure of phytoplankton in coastal upwelling areas from large species to smaller nanoplankton, since diatoms and dinoflagellates are disadvantaged while certain flagellates appear to benefit from low N:P supply conditions. Picoplanktonic species such as *Synechococcus* and *Prochlorococcus* were however completely unaffected by variable nutrient enrichment (Study 2 and 3).

N₂-fixation in the realm of coastal upwelling areas

The potential of N₂-fixation to counteract the growing N-deficit represents a central issue within the scope of expanding OMZs. Based on numerous observations in aquatic environments (e.g. Niemi, 1979; Vrede et al., 2009), low nutrient N:P ratios are widely believed to stimulate the development of N₂-fixing cyanobacteria. The universal N-deficit in conjunction with excess P in OMZ-influenced waters may thus provide an ecological niche for N₂-fixers (Deutsch et al., 2007). Quite the contrary, cyanobacterial marker pigments mainly accumulated within the N-enriched treatments during the mesocosm experiments (Study 2 and 3), while abundance of the *Trichodesmium*-specific *nifH*-gene was not affected by variable nutrient supply (Study 3). The occurred discrepancy in the distribution of diagnostic pigments and the *nifH*-gene impedes a definite conclusion about the effect of low N:P supply ratios on diazotrophic growth. Yet, residual amounts of DIP left throughout the experiment in the lowest N:P treatment during Study 2 and 3, indicate that P availability was not crucial for the development of N₂-fixing

cyanobacteria. The analogy in the responses of cyanobacterial marker pigments to nutrient supply in the experiments off Peru (Study 2) and on the West African shelf (Study 3) suggests a particular pattern behind this reaction, whose clarification should be subject to future research. Results from the field survey off Peru reconfirm the insignificant effect of excess P on growth of diazotrophic cyanobacteria, as no marker pigments indicating N₂-fixing cyanobacteria were detected in the low N:P waters overlying the OMZ (Study 1). P availability is certainly an important factor for the development of N₂-fixers (Sañudo-Wilhelmy et al., 2001; Dyhrman et al., 2002), but it is apparently not possible to predict growth of diazotrophic phytoplankton solely on the basis of a low nutrient N:P stoichiometry. Factors such as iron availability (Berman-Frank et al., 2001) and sea surface temperature (reviewed by Stal, 2009) have to be considered, as they are likely to further influence occurrence of N₂-fixing cyanobacteria. Replete concentrations of Fe (Schlosser, pers. comm.) and PO₄³⁻ on the transect off Peru (Study 1) indicate that growth of diazotrophic algae was not limited by P or Fe. Abundance of N₂-fixing cyanobacteria has been demonstrated to be highly constrained by water temperature (e.g. Falcón et al., 2005; Staal et al., 2007). Relatively low sea surface temperatures along the transect between ~17-23°C as a consequence of strong upwelling on the shelf, may thus have precluded development of photoautotrophic N₂-fixers *a priori*.

Diazotrophic cyanobacteria are typically prospering in the stratified oligotrophic open ocean adjacent to the dynamic and nutrient-rich waters on the continental shelf. N₂-fixing cyanobacteria are also able to grow on NO₃⁻ (Holl and Montoya, 2005), but they are in general inferior competitors for P uptake compared to diatoms under replete nutrient conditions (Tilman, 1982), which basically eliminates a successful coexistence of both algal groups. Nonetheless, field observations (Margalef, 1973), models (Hood et al., 2004) and results from Study 2 and 3 suggest growth of diazotrophs in a successional sequence to diatoms following to upwelling events in shelf waters. Termination of diatom blooms by N starvation in coastal upwelling areas provides apparently a further niche for N₂-fixation that has hardly been considered so far. This succession of functional phytoplankton groups would particularly apply to the shelf waters off Northwest Africa, where high Fe concentrations frequently occur due to deposition of dust originating from the Saharan desert (Gao et al., 2001). Beside the prevalent oceanic N₂-fixation, a significant amount of N₂ might be already fixed within coastal waters, as cyanobacteria take advantage of N depletion between two upwelling events. Thus, cyanobacterial N₂-fixation may partially compensate the N-deficit of upwelled, OMZ-derived water immediately on the continental shelf.

N₂-fixation in the open ocean next to the Peruvian upwelling may be, despite the general excess in P, impeded by low water temperatures. However, constantly warm water, high Fe input via dust deposition and the depletion of inorganic nutrients after diatom blooms induced by episodic

upwelling events seem to stimulate development of diazotrophic cyanobacteria in shelf waters off Northwest Africa.

Multiple controls of cellular N:P stoichiometry

Changes in macronutrient availability may additionally affect cellular composition of phytoplankton cells. Alfred Redfield (1958) proposed a tight coupling between the concentration of nutrients in seawater and the elemental composition of phytoplankton biomass, based on the observed similarity between them. Since then, oceanographers have been seeking after the key control of phytoplankton stoichiometry.

Indeed, in agreement with culture experiments by Rhee (1978) and Goldman et al. (1979), a strong correlation occurred between the N:P supply ratio and the microalgal N:P composition in all three nutrient enrichment experiments (Study 4). Yet, high flexibility of cellular N:P was confined to the stationary growth phase after nutrient exhaustion, a pattern already described in a model-based study by Klausmeier et al. (2004b). Once phytoplankton growth is limited by low external nutrient concentrations, cells consume the residual nutrients in the medium and biomass is finally matching the supply ratio. Compared to this “they are what they eat” situation, cells are free to “eat what they need” under nutrient saturation (see Sterner and Elser, 2002). They incorporate nutrients in a fixed ratio which approximates their optimal uptake ratio, regardless of the medium N:P. Hence, phytoplankton N:P stoichiometry is not adjusting towards the nutrient supply ratio during high nutrient availability, as the intracellular elemental composition is then controlled by species-specific nutrient requirements rather than by external nutrient concentrations (Klausmeier et al., 2004b). Extreme deviations from the optimal cellular elemental stoichiometry under nutrient starvation are most likely achieved by intracellular storage of the non-limiting nutrient (Goldman et al., 1979; Geider and LaRoche, 2002).

Phytoplankton N:P stoichiometry and the taxa-specific growth strategy correlated on the east-west transect at 10°S in the Pacific (Study 1). The plankton N:P ratio increased successively from the Peruvian shelf towards the open ocean on the transect. In the nutrient-rich shelf waters, blooming phytoplankton such as diatoms featured a low N:P composition (~10:1), based on their P-demanding cell assembly machinery (Klausmeier et al., 2004a; Arrigo, 2005; Loladze and Elser, 2011). Picoplankton like *Prochlorococcus*, typically abundant in the stratified oligotrophic oceanic section of the transect, pursues in general a strategy of sustaining net growth. Its metabolism is thus geared to acquisition of nutrients and/or light, and consequently cellular N:P is relatively high (>20:1) due to the large content of N-rich proteins. Horizontal and vertical gradients of hydrography and nutrient availability select for different types of growth, which seem to control biomass elemental composition considerably.

Based on these results, phytoplankton N:P stoichiometry is not at all affected by only one, but by several factors, including nutrient supply, the cellular growth phase and the specific growth strategy.

Ecological implications for coastal upwelling areas

Findings within this thesis demonstrate that changes in the nutrient N:P supply ratio could have substantial implications for the biogeochemistry of upwelling systems. Results from the nutrient enrichment experiments indicate a significant decline in total primary production as a result of reduced N supply (Study 2, 3 and 4). But high phytoplankton standing stocks are bottom-up controlling the food chain in the upwelling area and are essential for the high productivity of this ecosystem. A decline in phytoplankton biomass may thus affect all trophic levels, from microscopic primary consumers up to large predators. Reduced primary production under N-limited conditions was mainly induced by diatoms, as the most abundant primary producer in all mesocosm approaches. Diatoms represent the actual sustainers of the large fish production, since their large size enables extremely short food chains (Ryther, 1969; Cushing, 1989). Small planktivorous fish like anchoveta and sardines have specialized gills to filter large phytoplankton out of the water. Some colonial diatoms even form aggregates up to centimetres in diameter, and can be directly eaten by fish without special filter feeding adaptations (Ryther, 1969). A reduction in diatom biomass could presumably have a large direct effect on production of herbivores and zooplanktivores (e.g. small pelagic fishes, copepods, ciliates), associated with further consequences for the carnivorous consumers of the eastern boundary regime (e.g. whales, sea birds, piscivorous fishes, squids).

Yet, some autotrophic flagellates (*Heterosigma* sp., *Phaeocystis globosa*) seemed to be favoured by low seawater N:P ratios (Study 2), implying a potential shift in the taxonomical composition and size structure of the phytoplankton community in shelf waters influenced by the underlying OMZ. A tendency from large microalgae towards smaller nanoplankton in the course of a deoxygenation-caused decrease in N:P supply may be possible. Growth of the haptophyte *Phaeocystis globosa* has already been observed to be stimulated by low nutrient N:P stoichiometry (Riegman et al., 1992). *Phaeocystis* is generally of low food quality for zooplankton, leading to low egg production (Tang et al., 2001; Turner et al., 2002) and ultimately to a decrease in the abundance of copepods (Bautista et al., 1992). Similar to the general reduction in primary productivity, a shift in the taxonomical composition of the phytoplankton community could have profound implications for the entire food web of the upwelling area.

Low N:P supply ratios did unexpectedly not stimulate development of N₂-fixing cyanobacteria (Study 1, 2 and 3). Compensation of the N-deficit in eastern boundary current

systems by oceanic N₂-fixation as a response to low nutrient N:P supply from the nearby shelf seems therefore questionable. However, specific proxies (*nifH*-gene, phytopigments) indicate growth of diazotrophic cyanobacteria in succession to diatom blooms after pulses of nutrient enrichment (Study 2 and 3). N₂-fixers such as *Trichodesmium* appear to occupy the niche following to diatom blooms induced by episodic upwelling events, and may counteract the N-deficit via N₂-fixation in shelf waters.

Declining concentrations of phytoplankton biomass in general and diatom abundance specifically, may certainly have an impact on organic matter export to the deep ocean. The downward flux of POC is known to react highly sensitive to shifts towards or away from diatoms (Boyd and Newton, 1999), due to their large size and the ballast effect of the silica shell. Only recently, a tight link between high export rates and biominerals such as silica was shown for the upper ocean (Sanders et al., 2010). Hence, large-sized and silica-containing bloom forming phytoplankton facilitates high sinking rates of organic matter and an efficient transport of biologically fixed CO₂ to the ocean interior (Dugdale and Wilkerson, 1998; Buesseler, 1998). Declining rates of primary production in the euphotic zone along with a change in the size spectrum of phytoplankton towards smaller, non-silicifying cells may reduce the efficiency of the biological pump in the upwelling domain, weakening the ocean's capacity for sequestering atmospheric CO₂. Alterations in organic matter fluxes into and through the O₂-deficient layer may further influence microbial processes and O₂ fluxes within the OMZ.

Based on results from Study 4, a general decrease in phytoplankton N:P stoichiometry as a result of lower N:P supply ratios can be expected. The nutritional value of the phytoplankton for herbivorous grazers such as zooplankton may be reduced, since e.g. copepods feature a relatively high N:P composition of 25 to 30. Phytoplankton grown under N-limitation exhibit a reduced content of polyunsaturated fatty acids (Klein Breteler et al., 2005), which represent an essential component of metazoan nutrition for reproduction and growth (Brett and Müller-Navarra, 1997; Kainz et al., 2004).

Overall, results gained within this thesis indicate that a deoxygenation-induced decrease in the N:P supply ratio may have substantial implications for the biogeochemical system and the entire food web of coastal upwelling areas.

Perspectives

Observations during experiments and fields surveys within the framework of this thesis raised several further questions. In the following section, I will address some of these issues in more detail.

The observed discrepancy between cyanobacterial marker pigments and *nifH*-gene abundance in Study 3 demonstrates that our present comprehension of certain microalgal proxies is still incomplete. Pigment and gene fingerprinting are used as tools for distinguishing between various functional types of phytoplankton or even for determination of phytoplankton abundance on taxa or species level. Yet, detailed knowledge on functioning of these phytoplankton markers under variable conditions of e.g. nutrient supply, light intensity and temperature, is indispensable for quantitative evaluation of biomass estimates based on these parameters. On that purpose, ambiguous indicators for phytoplankton abundance such as phytopigments and functional genes, potentially variable under changing environmental conditions, have to be compared to microscopic counts. Especially nutrient availability can play a decisive role in the cellular composition of photosynthetic pigments. Henriksen and colleagues (2002) detected significant changes in the composition of accessory pigments between the exponential growth phase and nutrient limited conditions. Losses in the cellular pigment content were larger under N- than under P-limitation, owing to the close connection between pigment synthesis and the intracellular N metabolism (Latasa and Berdalet, 1994). Variability in pigment per cell quotas between nutrient saturation and nutrient depletion can be up to 3-fold, which may lead to significant uncertainties in the pigment-based biomass. In favour of correct application of taxa-specific pigments as phytoplankton proxies, it is necessary to improve understanding of the obvious flexibility of the pigment content per cell.

Investigations about phytoplankton nutrient limitation include in most cases merely the dissolved inorganic pool of N and P and do not account for dissolved organic compounds as further nutrient sources for photoautotrophs. But many studies already reported on the utilization of DON (reviewed by Bronk et al., 2007) and DOP (reviewed by Cembella et al., 1984, and by Karl and Björkmann, 2002) by phytoplankton. Results from Study 4 indicate an enhanced transfer of excess P into DOP. In the mesocosm experiments, P has been determined as the non-limiting nutrient in eastern boundary regions (Study 2, 3 and 4) and excess P possibly stimulated luxury uptake by phytoplankton and intracellular storage (Geider and LaRoche, 2002). A large fraction of this P was apparently transferred via exudation into the DOP pool. Exponential growing algae like diatoms own a P-rich metabolism (Arrigo, 2005), but cellular P requirements were presumably already met by excess DIP. Utilization of DOP by exponentially growing algae was consequently not given, as excess concentrations of the more favourable inorganic P were available. Offshore flowing surface currents would carry the DOP reservoir generated on the shelf to the open ocean, where it may promote growth of diazotrophic cyanobacteria. Hence,

enhanced DOP availability as a result of lowered N:P supply ratios could potentially replenish the large-scale N-deficit in OMZ-influenced waters via stimulation of N_2 -fixation in off-shelf waters. On that account, great demand exists in collecting further information about the channelling of excess P via coastal phytoplankton to DOP and about the fate of this DOP with regard to N_2 -fixation. In order to evaluate bioavailability of different phosphorus sources for photoautotrophic nutrition, diazotrophic phytoplankton could be supplied with various phosphorus compounds, including inorganic and organic molecules. Alternatively, cultures of N_2 -fixers could be supplied with a naturally DOP-enriched and orthophosphate-exhausted medium derived from a shelf phytoplankton culture or community (preferably with diatoms) cultivated at variable N:P stoichiometry. Results from this approach could give a confident answer whether diazotrophs grow on DOP-containing exudates from shelf phytoplankton. Measurement of the activity of extracellular hydrolytic enzymes such as alkaline phosphatase as well as radioactively labelled P substrates should be included, in order to elucidate processes and fluxes with respect to substrate preferences and assimilation costs.

The role of DOP in biogeochemical cycling of eastern boundary current systems attains further relevance with regard to the model-based study by Mills and Arrigo (2010), who proposed a tight regulation of oceanic N_2 -fixation by non-Redfield nutrient uptake of non-diazotrophic phytoplankton. Although N availability was determined as the primary limiting factor for growth of the upwelling plankton community, optimal N:P uptake ratios may be rather low during exponential growth under nutrient saturation. Low N:P consumption of inorganic nutrients by phytoplankton in shelf waters reduces the surplus in P (see Study 1) and its availability for N_2 -fixing cyanobacteria in off-shelf waters. Study 4 suggests that large parts of the consumed P are shifted into the DOP pool, probably via exudation, thereby attenuating drawdown of excess P by shelf phytoplankton. Consequently, increased availability of DOP could potentially fill the gap, and replenish the N-deficit by stimulating N_2 -fixation. Investigations about the production and fate of DOP may be combined with an experimental approach testing the theory by Mills and Arrigo (2010) via monitoring nutrient drawdown by a culture or community of coastal diatoms under saturated nutrient concentrations with variable N:P ratios. Such experiments could provide answers whether large coastal microalgae are constraining N_2 -fixation by exploiting excess P or rather facilitating N_2 -fixation via enhanced DOP exudation in low N:P waters.

Results from this thesis particularly show that our understanding of the ultimate controls of N_2 -fixation in the ocean is quite vague. If we want to reasonably estimate the role of biological N_2 -fixation in present and future N budgets of the tropical deoxygenated ocean, we have to define the actual drivers of this process.

However, remineralization of nutrients by bacteria represents a common problem of algal bloom experiments in enclosed systems, as detritus cannot sink out of the system and remineralized nutrient pools are affecting autotrophic production. The secondary bloom in Study 3 was most

likely enabled by decomposition of organic matter produced during the primary bloom. Sedimentation and export of organic matter during and after phytoplankton blooms should be embedded in the experimental set-up of nutrient enrichment experiments to prevent extensive remineralization processes that do not apply for systems with export production dominating like upwelling domains and to improve simulation of natural conditions in general. For example, sedimented material could be easily removed through a sediment trap at the bottom of the mesocosm (see KOSMOS- Kiel Off-Shore Mesocosms).

Eastern boundary upwelling systems are not only stressed by ocean deoxygenation, but represent as well hotspots for ocean warming and acidification (Gruber, 2011). OMZs below the euphotic zone of upwelling areas encounter naturally high CO₂ concentrations due to enhanced remineralization rates (Ianson et al., 2003; Paulmier et al., 2011). Uptake of anthropogenic CO₂ by the ocean since the onset of industrialization exacerbated CO₂ conditions within OMZs. Feely et al. (2008) described large-scale upwelling of such anthropogenic CO₂-enriched water into the surface on the Californian continental shelf. Reduced outgassing of CO₂ from such oversaturated surface waters as a consequence of future elevated atmospheric CO₂ concentrations will probably intensify these acidification events. Thus, phytoplankton communities in upwelling areas of the future ocean would face lower inorganic N:P ratios in conjunction with particularly high CO₂ concentrations. Mono-cultural lab experiments with diatoms, dinoflagellates and cyanobacteria demonstrated a stimulation of growth by increased CO₂ availability under nutrient saturation (reviewed by Riebesell et al., 2011). Tortell and colleagues (2002) provided evidence that CO₂ concentration can affect the taxonomic structure of a marine phytoplankton community. A significant community shift from *Phaeocystis* towards diatoms occurred under high CO₂ in the experiment conducted on the Peruvian shelf, while total phytoplankton biomass showed no response to CO₂ supply. This taxonomic shift appears particularly interesting with regard to the specific response of both algal groups to changing nutrient N:P supply ratios within Study 2 and 3, suggesting a shift in phytoplankton abundance from diatoms towards nanoflagellates such as *Phaeocystis* under lowered N:P supply conditions. The opposing tendency in the response of these typical representatives of upwelling phytoplankton assemblages to future increasing CO₂ concentrations and decreasing N:P stoichiometry leads to the question which types of primary producers will ultimately benefit and which will be disadvantaged in coastal upwelling areas under future conditions. Dedicated research efforts are necessary to illuminate combined effects of different aspects of global change (decreasing N:P, elevated CO₂ and warming) on upwelling ecosystems.

References

- Alheit, J., Niquen, M., 2004. Regime shifts in the Humboldt Current ecosystem. *Progress in Oceanography* 60, 201-222.
- Amante, C., Eakins, B.W., 2009. ETOPO1 1 Arc-Minute Global Relief Model: Procedures, Data Sources and Analysis. NOAA Technical Memorandum NESDIS NGDC-24, p. 19.
- Arrigo, K.R., 2005. Marine microorganisms and global nutrient cycles. *Nature* 437, 349-355.
- Banse, K., 1974. The nitrogen-to-phosphorus ratio in the photic zone of the sea and the elemental composition of the plankton. *Deep-Sea Research* 21, 767-771.
- Banse, K., 1974. The nitrogen-to-phosphorus ratio in the photic zone of the sea and the elemental composition of the plankton. *Deep-Sea Research* 21, 767-771.
- Barlow, R.G., Cummings, D.G., Gibb, S.W., 1997. Improved resolution of mono- and divinyl chlorophylls *a* and *b* and zeaxanthin and lutein in phytoplankton extracts using reverse phase C-8 HPLC. *Marine Ecology Progress Series* 161, 303-307.
- Bautista, B., Harris, R.P., Tranter, P.R.G., Harbour, D., 1992. In situ copepod feeding and grazing rates during a spring bloom dominated by *Phaeocystis* sp. in the English Channel. *Journal of Plankton Research*, 14, 691-703.
- Berman-Frank, I., Cullen, J.T., Shaked, Y., Sherrell, R.M., Falkowski, P.G., 2001. Iron availability, cellular iron quotas, and nitrogen fixation in *Trichodesmium*. *Limnology and Oceanography* 46, 1249-1277.
- Berman-Frank, I., Quigg, A., Finkel, Z.V., Irwin, A.J., Haramaty, L., 2007. Nitrogen-fixation strategies and Fe requirements in cyanobacteria. *Limnology and Oceanography* 52, 2260-2269.
- Bertilsson, S., Berglund, O., Karl, D.M., Chisholm, S.W., 2003. Elemental composition of marine *Prochlorococcus* and *Synechococcus*: Implications for the ecological stoichiometry of the sea. *Limnology and Oceanography* 48, 1721-1731.
- Biddle, K.D., Azam, F., 1999. Accelerated dissolution of diatom silica by marine bacterial assemblages. *Nature* 397, 508-512.
- Björkman, K., and Karl, D.M., 1994. Bioavailability of inorganic and organic phosphorus compounds to natural assemblages of microorganisms in Hawaiian coastal waters. *Marine Ecology Progress Series* 111, 265-273.
- Blackman, F.F., 1905. Optima and limiting factors. *Annals of Botany* 19, 281-298.
- Blain, S., Leynaert, A., Treguer, P., Chretiennot-Dinet, M.C., Rodier, M., 1997. Biomass, growth rates and limitation of equatorial Pacific diatoms. *Deep-Sea Research* 44, 1255-1275.
- Bopp, L., Le Quere, C., Heimann, M., Manning, A.C., and Monfray, P., 2002. Climate-induced oceanic oxygen fluxes: Implications for the contemporary carbon budget. *Global Biogeochemical Cycles* 16, 1022, doi:10.1029/2001GB001445.
- Bower, C.E., Holm-Hansen, T., 1980. Salicylate-hypochlorite method for determining ammonia in seawater. *Canadian Journal of Fisheries and Aquatic Sciences* 37, 794-798.

- Boyd, C.M., Cowles, T.J., 1980. Grazing patterns of copepods in the upwelling system off Peru. *Limnology and Oceanography* 25, 583–596.
- Boyd, P.W., Newton, P.P., 1999. Does planktonic community structure determine downward particulate organic carbon flux in different oceanic provinces? *Deep-Sea Research I* 46, 63–91.
- Breitbarth, E., Oschlies, A., LaRoche, J., 2007. Physiological constraints on the global distribution of *Trichodesmium* - effect of temperature on diazotrophy. *Biogeosciences* 4, 53–61.
- Brett, M.T., Müller-Navarra, D.C., 1997. The role of highly unsaturated fatty acids in aquatic foodweb processes. *Freshwater Biology* 38, 483–499.
- Bronk, D.A., See, J.H., Bradley, P., and Killberg, L., 2007. DON as a source of bioavailable nitrogen for phytoplankton. *Biogeosciences* 4, 283–296.
- Bruland, K.W., Rue, E.L., Smith, G.J., 2001. Iron and macronutrients in California coastal upwelling regimes: implications for diatom blooms. *Limnology and Oceanography* 46, 1661–1674.
- Bruland, K.W., Rue, E.L., Smith, G.J., DiTullio, G.R., 2005. Iron, macronutrients and diatom blooms in the Peru upwelling regime: brown and blue waters of Peru. *Marine Chemistry* 93, 81–103.
- Brzezinski, M.A., 1988. Vertical distribution of ammonium in stratified oligotrophic waters. *Limnology and Oceanography* 33, 1176–1182.
- Buesseler, K.O., 1998. The decoupling of production and particulate export in the surface ocean. *Global Biogeochemical Cycles* 12, 297–310.
- Calbet, A., Saiz, E., 2005. The ciliate-copepod link in marine ecosystems. *Aquatic Microbial Ecology* 38, 157–167.
- Campbell, L., Nolla, H.A., Vaultot, D., 1994. The importance of *Prochlorococcus* to community structure in the central North Pacific Ocean. *Limnology and Oceanography* 39, 954–961.
- Capone, D.G., Zehr, J.P., Paerl, H.W., Bergman, B., Carpenter, E.J., 1997. *Trichodesmium*, a globally significant marine cyanobacterium. *Science* 276, 1221–1229.
- Capone, D.G., Burns, J.A., Montoya, J.P., Subramaniam, A., Mahaffey, C., Gunderson, T., Michaels, A.F., Carpenter, E.J., 2005. Nitrogen fixation by *Trichodesmium* spp.: An important source of new nitrogen to the tropical and subtropical North Atlantic Ocean. *Global Biogeochemical Cycles* 19, GB2024, doi:10.29/2004GB002331.
- Carpenter, E.J., Romans, K., 1991. Major role of the cyanobacterium *Trichodesmium* in nutrient cycling in the North Atlantic Ocean. *Science* 254, 1356–1358.
- Carpenter, E.J., O'Neil, J.M., Dawson, R., Capone, D.G., Siddiqui, P.J.A., Roenneberg, T., Bergman, B., 1993. The tropical diazotrophic phytoplankton *Trichodesmium*: biological characteristics of two common species. *Marine Ecology Progress Series* 95, 295–304.
- Carpenter, E.J., Subramaniam, A., Capone, D.G., 1999. Biomass and productivity of the cyanobacterium *Trichodesmium* spp. in the tropical N Atlantic ocean. *Deep-Sea Research I* 51, 173–203.

- Cembella, A.D., Antia, N.J., Harrison, P.J., 1984. The utilization of inorganic and organic phosphorous compounds as nutrients by eukaryotic microalgae: A multidisciplinary perspective: Part 1. *Critical Reviews in Microbiology* 10, 317-391.
- Chavez, F.P., 1995. A comparison of ship and satellite chlorophyll from California and Peru. *Journal of Geophysical Research* 100, 24855-24862.
- Chavez, F.P., Toggweiler, J.R., 1995. Physical estimates of global new production: The upwelling contribution. In: Summerhayes, C.P., Emeis, K.C., Angel, M.V., Smith, R.L., Zeitzschel, B. (Eds.), *Upwelling in the ocean: Modern processes and ancient records*. Wiley, pp. 313-320.
- Chisholm, S.W., 1992. Phytoplankton size. In: Falkowski, W.G., Woodhead, A.D. (Eds.), *Primary Productivity and Biogeochemical Cycles in the Sea*, Plenum Press, New York, pp. 213-273.
- Coale, K.H., Johnson, K.S., Fitzwater, S.E., Gordon, R.M., Tanner, S., Chavez, F.P., Ferioli, L., Sakamoto, C., Rogers, P., Millero, F., Steinberg, P., Nightingale, P., Cooper, D., Cochlan, W.P., Landry, M.R., Constantinou, J., Rollwagen, G., Trasvina, A., Kudela, R., 1996. A massive phytoplankton bloom induced by an ecosystem-scale iron fertilization experiment in the equatorial Pacific Ocean. *Nature* 383, 495-501.
- Codispoti, L.A., Packard, T.T., 1980. On the denitrification rate in the eastern tropical South Pacific. *Journal of Marine Research* 38, 453-477.
- Codispoti, L.A., Christensen, J.P., 1985. Nitrification, denitrification and nitrous oxide cycling in the eastern tropical South Pacific Ocean. *Marine Chemistry* 16, 277-300.
- Codispoti, L.A., 1995. Is the ocean losing nitrate? *Nature* 376, 724.
- Codispoti, L.A., Brandes, J.A., Christensen, J.P., Devol, A.H., Naqvi, S.W.A., Paerl, H.W., Yoshinari, T., 2001. The oceanic fixed nitrogen and nitrous oxide budgets: Moving targets as we enter the anthropocene. *Scientia Marina* 65, 85-105.
- Conan, P., Søndergaard, M., Kragh, T., Thingstad, F., Pujo-Pay, M., Williams, P. le B., Markager, S., Cauwet, G., Borch, N.H., Evans, D., Riemann, B., 2007. Partitioning of organic production in marine plankton communities: The effects of inorganic nutrient ratios and community composition on new dissolved organic matter. *Limnology and Oceanography* 52, 753-765.
- Conley, D.J., Malone, T.C., 1992. Annual cycle of dissolved silicate in Chesapeake Bay: implications for the production and fate of phytoplankton biomass. *Marine Ecology Progress Series* 81, 121-128.
- Cullen, J.J., Lewis, M.R., Davis, C.O., Barber, R.T., 1992. Photosynthetic characteristics and estimated growth rates indicate grazing is the proximate control of primary production in the equatorial Pacific. *Journal of Geophysical Research* 97, 639-654.
- Cushing, D.H., 1989. A difference in structure between ecosystems in strongly stratified waters and in those that are only weakly stratified. *Journal of Plankton Research* 11, 1-13.
- Czeschel, R., Stramma, L., Schwarzkopf, F., Giese, B.S., Funk, A., Karstensen, J., 2011. Mid-depth circulation of the eastern tropical South Pacific and its link to the oxygen minimum zone. *Journal of Geophysical Research-Oceans* 116, C01015, doi:10.1029/2010JC006565.

- Davey, M., Tarran, G.A., Mills, M.M., Ridame, C., Geider, R.J., LaRoche, J., 2008. Nutrient limitation of picophytoplankton photosynthesis and growth in the tropical North Atlantic. *Limnology and Oceanography* 53, 1722-1733.
- Demarest, M.S., Brzezinski, M.A., Nelson, D.M., Krause, J.W., Jones, J.L., Beucher, C.P., 2011. Net biogenic silica production and nitrate regeneration determine the strength of the silica pump in the Eastern Equatorial Pacific. *Deep-Sea Research II* 58, 462-476.
- Deutsch, C., Gruber, N., Key, R.M., Sarmiento, J.L., Ganachaud, A., 2001. Denitrification and N_2 fixation in the Pacific Ocean. *Global Biogeochemical Cycles* 15, 483-506.
- Deutsch, C., Sarmiento, J.L., Sigman, D.M., Gruber, N., Dunne, J.P., 2007. Spatial coupling of nitrogen inputs and losses in the ocean. *Nature* 445, 163-167.
- DiTullio, G.R., Hutchins, D.A., Bruland, K. W., 1993. Interaction of iron and major nutrients controls phytoplankton growth and species composition in the tropical North Pacific Ocean. *Limnology and Oceanography* 38, 495-508.
- DiTullio, G.R., Geesey, M.E., Maucher, J.M., Alm, M.B., Riseman, S.F., Bruland, K.W., 2005. Influence of iron on algal community composition and physiological status in the Peru upwelling system. *Limnology and Oceanography* 50, 1887-1907.
- Dolan, J.R., Thingstad, T.F., Rassoulzadegan, F., 1995. Phosphate transfer between microbial size-fractions in Villefranche Bay (N. W. Mediterranean Sea), France in autumn 1992. *Ophelia* 41, 71-85.
- Downing, J.A., Osenberg, C.W., Sarnelle, O., 1999. Meta-analysis of marine nutrient-enrichment experiments: variation in the magnitude of nutrient limitation. *Ecology* 80, 1157-1167.
- Droop, M.R., 1974. The nutrient status of algal cells in continuous culture. *Journal of the Marine Biological Association of the United Kingdom* 54, 825-855.
- Dugdale, R.C., 1985. The effects of varying nutrient concentrations on biological production in upwelling regions. *CALCOFI Reports* 26, 93-96.
- Dugdale, R.C., Wilkerson, F.P., Minas, H.J., 1995. The role of a silicate pump in driving new production. *Deep-Sea Research I* 42, 697-719.
- Dugdale, R., Wilkerson, F., 1998. Silicate regulation of new production in the equatorial Pacific upwelling. *Nature* 391, 270-273.
- Dyhrman, S.T., Webb, E., Anderson, D.M., Moffett, J., Waterbury, J., 2002. Cell specific detection of phosphorus stress in *Trichodesmium* from the Western North Atlantic. *Limnology and Oceanography* 47, 1823-1836.
- Dyhrman, S.T., Ruttenberg, K.C., 2006. Presence and regulation of alkaline phosphatase activity in eukaryotic phytoplankton from the coastal ocean: Implications for dissolved organic phosphorus remineralization. *Limnology and Oceanography* 51, 1381-1390.
- Dyhrman, S.T., Chappell, P.D., Haley, S.T., Moffett, J.W., Orchard, E.D., Waterbury, J.B., Webb, E.A., 2006. Phosphonate utilization by the globally important marine diazotroph *Trichodesmium*. *Nature* 439, 68-71.
- Ekman, V.W., 1905. On the influence of the earth's rotation on ocean currents. *Arch. Math. Astron. Phys.* 2.

- Elser, J.J., Marzolf, E.R., Goldman, C.R., 1990. Phosphorus and nitrogen limitation of phytoplankton growth in the freshwaters of North America: a review and critique of experimental enrichments. *Canadian Journal of Fisheries and Aquatic Sciences* 47, 1468-1477.
- Elser, J.J., Bracken, M.E.S., Cleland, E.E., Gruner, D.S., Stanley Harpole, S., Hillebrand, H., Ngai, J.T., Seabloom, E.W., Shurin, J.B., Smith, J.E., 2007. Global analysis of nitrogen and phosphorus limitation of primary producers in freshwater, marine and terrestrial ecosystems. *Ecology Letters* 10, 1135-1142.
- Falcón, L.I., Cipriano, F., Chistoserdov, A.Y., Carpenter, E.J., 2002. Diversity of diazotrophic unicellular cyanobacteria in the tropical North Atlantic Ocean. *Applied and Environmental Microbiology* 68, 5760-5764.
- Falcón, L.I., Pluvinage, S., Carpenter, E.J., 2005. Growth kinetics of marine unicellular N₂-fixing cyanobacterial isolates in continuous culture in relation to phosphorus and temperature. *Marine Ecology Progress Series* 285, 3-9.
- Falkowski, P.G., 1997. Evolution of the nitrogen cycle and its influence on the biological sequestration of CO₂ in the ocean. *Nature* 387, 272-275.
- Falkowski, P.G., 2000. Rationalizing elemental ratios in unicellular algae. *Journal of Phycology* 36, 3-6.
- Falkowski, P.G., Katz, M.E., Knoll, A.H., Quigg, A., Raven, J.A., Schofield, O., Taylor, F.J.R., 2004. The evolution of modern eukaryotic phytoplankton. *Science* 306, 354-360.
- Fanning, K.A., 1992. Nutrient provinces in the sea- concentration ratios, reaction-rate ratios, and ideal covariation. *Journal of Geophysical Research-Oceans* 97, 5693-5712.
- Fawcett, S.E., Ward, B.B., 2011. Phytoplankton succession and nitrogen utilization during the development of an upwelling bloom. *Marine Ecology Progress Series* 428, 13-31.
- Feely, R.A., Sabine, C.L., Hernandez-Ayon, J.M., Ianson, D., Hales, B., 2008. Evidence for upwelling of corrosive "acidified" water onto the continental shelf. *Science* 320, 1490-1492.
- Ferris, M.J., Palenik, B., 1998. Niche adaption in ocean cyanobacteria. *Nature* 396, 226-228.
- Fernández, C., Farías, L., Alcaman, M.E., 2009. Primary production and nitrogen regeneration processes in surface waters of the Peruvian upwelling system. *Progress in Oceanography* 53, 159-168.
- Fiedler, P.C., Talley, L.D., 2006. Hydrography of the eastern tropical Pacific: A review. *Progress in Oceanography* 56, 143-180.
- Fogg, G.E., 1991. The phytoplanktonic ways of life. *New Phytologist* 118, 191-232.
- Foster, R.A., Zehr, J.P., 2006. Characterization of diatom-cyanobacteria symbioses on the basis of *nifH*, *hetR* and 16S rRNA sequences. *Environmental Microbiology* 8, 1913-1925.
- Foster, R.A., Subramaniam, A., Mahaffey, C., Carpenter, E.J., Capone, D.G., Zehr, J.P., 2007. Influence of the Amazon River plume on distributions of free-living and symbiotic cyanobacteria in the western tropical North Atlantic Ocean. *Limnology and Oceanography* 52, 517-532.
- Foster, R.A., Subramaniam, A., Zehr, J.P., 2009. Distribution and activity of diazotrophs in the Eastern Equatorial Atlantic. *Environmental Microbiology* 11, 741-750.

- Franz, J., Krahmann, G., Lavik, G., Grasse, P., Dittmar, P., Riebesell, U., 2012. Dynamics and stoichiometry of nutrients and phytoplankton in waters influenced by the oxygen minimum zone in the tropical eastern Pacific. *Deep-Sea Research I* 62, 20-31.
- Franz, J.M.S., Hauss, H., Sommer, U., Dittmar, T., Riebesell, U. Production, partitioning and stoichiometry of organic matter under variable nutrient supply during mesocosm experiments in the tropical Pacific and Atlantic ocean. *Biogeosciences*, submitted for publication.
- Franz, J.M.S., Hauss, H., Löscher, C.R., Riebesell, U. Effect of variable nutrient enrichment on the functional composition of a phytoplankton community in the eastern tropical Atlantic. Unpublished results.
- Fuenzalida, R., Schneider, W., Garcés-Vargas, J., Bravo, L., Lange, C., 2009. Vertical and horizontal extension of the oxygen minimum zone in the eastern South Pacific Ocean. *Deep-Sea Research II*, 56, 1027-1038.
- Galan, A., Molina, V., Thamdrup, B., Woebken, D., Lavik, G., Kuypers, M.M.M., Ulloa, O., 2009. Anammox bacteria and the anaerobic oxidation of ammonium in the oxygen minimum zone off northern Chile. *Deep-Sea Research II* 56, 1125–1135.
- Galloway, J.N., Schlesinger, W.H., Levy II, H., Michaels, A., Schnoor, J.L., 1995. Nitrogen fixation: anthropogenic enhancement-environmental response. *Global Biogeochemical Cycles* 9, 235–252.
- Gao, Y., Kaufman, Y.J., Tanré, D., Kolber, D., Falkowski, P.G., 2001. Seasonal distributions of aeolian iron fluxes to the global ocean. *Geophysical Research Letters* 28, 29-32.
- Garcia, H.E., Locarnini, R.A., Boyer, T.P. and Antonov, J.I., 2010a. World Ocean Atlas 2009, Volume 3: Dissolved Oxygen, Apparent Oxygen Utilization, and Oxygen Saturation. In: Levitus, S. (Ed.), NOAA Atlas NESDIS 70, U.S. Government Printing Office, Washington, D.C., 344 pp.
- Garcia, H.E., Locarnini, R.A., Boyer, T.P., Antonov, J.I., 2010b. World Ocean Atlas 2009, Volume 4: Nutrients (phosphate, nitrate, silicate). Levitus, S. (Ed.), NOAA Atlas NESDIS 71, U.S. Government Printing Office, Washington, D.C., 398 pp.
- Geider, R.J., LaRoche, J., 2002. Redfield revisited: variability of C:N:P in marine microalgae and its biochemical basis. *European Journal of Phycology* 37, 1-17.
- Gervais, F., Riebesell, U., 2001. Effect of phosphorus limitation on elemental composition and stable carbon isotope fractionation in a marine diatom growing under different CO₂ concentrations. *Limnology and Oceanography* 46, 497-504.
- Goericke, R., 2002. Top-down control of phytoplankton biomass and community structure in the monsoonal Arabian Sea. *Limnology and Oceanography* 47, 1307-1323.
- Goldman, J.C., McCarthy, J.J., Peavey, D.G., 1979. Growth rate influence on the chemical composition of phytoplankton in oceanic waters. *Nature* 279, 210-215.
- Granéli, E., Hansen, P.J., 2006. Allelopathy in harmful algae: a mechanism to compete for resources? In: Granéli, E., Turner, J.T. (Eds.), *Ecology of harmful algae*, Ecological Studies 189, pp. 189-201.
- Graziano, L.M., Geider R.J., Li, W.K.W., Olaizola, M., 1996. Nitrogen limitation of North Atlantic phytoplankton: Analysis of physiological condition in nutrient enrichment experiments. *Aquatic and Microbial Ecology* 11, 53-64.

- Gruber, N., Sarmiento, J.L., 1997. Global patterns of marine nitrogen fixation and denitrification. *Global Biogeochemical Cycles* 11, 235-266.
- Gruber, N., 2011. Warming up, turning sour, losing breath: ocean biogeochemistry under global change. *Philosophical Transactions of the Royal Society A* 369, 1980-1996.
- Hall, R.I., Leavitt, P.R., Dixit, A.S., Quinlan, R., Smol, J.P., 1999. Limnological succession in reservoirs: a paleolimnological comparison of two methods of reservoir formation. *Canadian Journal of Fisheries and Aquatic Sciences* 56, 1109-1121.
- Hall, S.P., Smith, V.H., Lytle, D.A., and Leibold, M.A., 2005. Constraints on primary producer N:P stoichiometry along N:P gradients. *Ecology* 86, 1894-1904.
- Hamersley, M.R., Lavik, G., Woebken, D., Rattray, J.E., Lam, P., Hopmans, E.C., Sinninghe Damsté, Krüger, S., Graco, M., Gutiérrez, Kuypers, M.M.M., 2007. Anaerobic ammonium oxidation in the Peruvian oxygen minimum zone. *Limnology and Oceanography* 52, 923-933.
- Hansen, H.P., Koroleff, F., 1999. Determination of nutrients. In: Grasshoff, K., Klaus Kremling, K., Ehrhardt, M. (Eds.), *Methods of seawater analysis*, Wiley-VCH Verlag GmbH, Weinheim, Germany, pp. 159-228.
- Hare, C.E., DiTullio, G.R., Trick, C.G., Wilhelm, S.W., Bruland, K.W., Rue, E.L., Hutchins, D.A., 2005. Phytoplankton community structure changes following simulated upwelled iron inputs in the Peru upwelling region. *Aquatic Microbial Ecology* 38, 269-282.
- Harrison, W.G., Platt, T., Calienes, R., Ochoa, N., 1981. Photosynthetic parameters and primary production of phytoplankton populations off the northern coast of Peru. In: Richards, F. (Ed.), *Coastal Upwelling*. American Geophysical Union, Washington, DC, pp. 303-311.
- Hasle, G.R., Syvertsen, E.E., 1997. Marine diatoms. In: Tomas, C.R. (Ed.), *Identifying marine phytoplankton*, pp. 5-385.
- Hauss, H.M., Franz, J., Sommer, U. Changes in N:P stoichiometry influences taxonomic composition and nutritional quality of phytoplankton in the Peruvian upwelling - a mesocosm experiment. *Journal of Sea Research*, submitted for publication.
- Healey, F.P., 1973. Inorganic nutrient uptake and deficiency in algae. *Critical Reviews in Microbiology* 3, 69-113.
- Helly, J.J., Levin, L.A., 2004. Global distribution of naturally occurring marine hypoxia on continental margins. *Deep-Sea Research* 51, 1159-1168.
- Henriksen, P., Riemann, B., Kaas, H., Sørensen, H.M., Sørensen, H.L., 2002. Effects of nutrient-limitation and irradiance on marine phytoplankton pigments. *Journal of Plankton Research* 24, 835-858.
- Hertzberg, S., Jensen, S.L., 1966. The carotenoids of blue-green algae II: The carotenoids of *Aphanizomenon flos-aquae*. *Phytochemistry* 5, 565-570.
- Hillebrand, H., Dürselen, C.D., Kirschtel, D., Pollinger, U., Zohary, T., 1999. Biovolume calculation for pelagic and benthic microalgae. *Journal of Phycology* 35, 403-424.
- Holl, C.M., Montoya, J.P., 2005. Interactions between nitrate uptake and nitrogen fixation in continuous cultures of the marine diazotroph *Trichodesmium* (Cyanobacteria). *Journal of Phycology* 41, 1178-1183.

- Holmedal, L.E., Utnes, T., 2006. Physical-biological interactions and their effect on phytoplankton blooms in fjords and near-coastal waters. *Journal of Marine Research* 64, 97–122.
- Holmes, R.M., Aminot, A., K  rouel, R., Hooker, B.A., Peterson, B.J., 1999. A simple and precise method for measuring ammonium in marine and freshwater ecosystems. *Canadian Journal of Fisheries and Aquatic Sciences* 56, 1801-1808.
- Hood, R.R., Coles, V.J., 2004. Modeling the distribution of *Trichodesmium* and nitrogen fixation in the Atlantic Ocean. *Journal of Geophysical Research* 109, C06006, doi:10.1029/2002JC001753.
- Howard, J.B., Rees, D.C., 1996. Structural basis of biological nitrogen fixation. *Chemical Reviews* 96, 2965-2982.
- Hutchins, D.A., Bruland, K.W., 1998. Iron-limited diatom growth and Si:N uptake ratios in a coastal upwelling regime. *Nature* 393, 561-564.
- Hutchins, D.A., Hare, C.E., Weaver, R.S., Zhang, Y., Firme, G.F., DiTullio, G.R., Alm, M.B., Riseman, S.F., Maucher, J.M., Geesey, M.E., 2002. Phytoplankton iron limitation in the Humboldt Current and Peru Upwelling. *Limnology and Oceanography* 47, 997-1011.
- Hutchins, D.A., Pustizzi, F., Hare, C.E., DiTullio, G.R., 2003. A shipboard natural community continuous culture system for ecologically relevant low-level nutrient enrichment experiments. *Limnology and Oceanography: Methods* 1, 82-91.
- Ianson, D., Allen, S.E., Harris, S.L., Orians, K.J., Varela, D.E., Wong, C.S., 2003. The inorganic carbon system in the coastal upwelling region west of Vancouver Island, Canada. *Deep-Sea Research I*, 50, 1023-1042.
- Ingall, E., Jahnke, R., 1994. Evidence for enhanced phosphorus regeneration from marine sediments overlain by oxygen depleted waters. *Geochimica et Cosmochimica Acta* 58, 2571-2575.
- IPCC: Climate Change 2007. The Physical Science Basis. In: Solomon, S., Qin, D., Manning, M., Chen, Z., Marquis, M., Averyt, K.B., Tignor, M., Miller, H.L. (Eds.), *Contribution of Working Group I to the Fourth Assessment Report of the Intergovernmental Panel on Climate Change*, Cambridge University Press, Cambridge, UK and New York, NY, USA, 2007.
- Irwin, A.J., Oliver, M.J., 2009. Are ocean deserts getting larger? *Geophysical Research Letters* 36, L18609.
- Jaeschke, A., Abbas, B., Zabel, M., Hopmans, E.C., Schouten, S., Sinninghe Damst  , J.S., 2010. Molecular evidence for anaerobic ammonium-oxidizing (anammox) bacteria in continental shelf and slope sediments off northwest Africa. *Limnology and Oceanography* 55, 365-376.
- Johnson, K.S., Chavez, F.P., Friederich, G.E., 1999. Continental-shelf sediment as a primary source of iron for coastal phytoplankton. *Nature* 398, 697-700.
- J  nasd  ttir, S.H., Fields, D., Pantoja, S., 1995. Copepod egg production in Long Island Sound, USA, as a function of the chemical composition of seston. *Marine Ecology Progress Series* 119, 87-98.
- Kainz, M., Arts, M.T., Mazumder, A., 2004. Essential fatty acids in the planktonic food web and their ecological role for higher trophic levels. *Limnology and Oceanography* 49, 1784-1793.

- Karl, D.M., Björkman, K.M., 2002. Dynamics of DOP. In: Hansell, D.A., Carlson, C.A. (Eds.), *Biogeochemistry of Marine Dissolved Organic Matter*, Academic Press, San Diego, pp. 250-366, 2002.
- Karstensen, J., Stramma, L., Visbeck, M., 2008. Oxygen minimum zones in the eastern tropical Atlantic and Pacific oceans. *Progress in Oceanography* 77, 331-350.
- Keeling, R.F., Garcia, H., 2002. The change in oceanic O₂ inventory associated with recent global warming. *Proceedings of the National Academy of Sciences* 99, 7848-7853.
- Keeling, R.F., Körtzinger, A., Gruber, N., 2009. Ocean deoxygenation in a warming world. *Annual Review in Marine Science* 2, 463-493.
- Kerouel, R., Aminot, A., 1997. Fluorometric determination of ammonia in sea and estuarine waters by direct segmented flow analysis. *Marine Chemistry* 57, 265-275.
- Kirchman, D.L., 1994. The uptake of inorganic nutrients by heterotrophic bacteria. *Microbial Ecology* 28, 255-271.
- Kimor, B., Reid, F.M.H., Jordan, J.B., 1978. An unusual occurrence of *Hemiaulus membranaceus* Cleve (Bacillariophyceae) with *Richelia intracellularis* Schmidt (Cyanophyceae) off the coast of Southern California in October 1976. *Phycologia* 17, 162-166.
- Kjørboe, T., 1989. Phytoplankton growth rate and nitrogen content: implications for feeding and fecundity in a herbivorous copepod. *Marine Ecology Progress Series* 55, 229-234.
- Klausmeier, C.A., Litchman, E., Daufresne, T., Levin, S.A., 2004a. Optimal nitrogen-to-phosphorus stoichiometry of phytoplankton. *Nature* 429, 171-174.
- Klausmeier, C.A., Litchman, E., Levin, S.A., 2004b. Phytoplankton growth and stoichiometry under multiple nutrient limitation. *Limnology and Oceanography* 49, 1463-1470.
- Klausmeier, C.A., Litchman, E., Daufresne, T., and Levin, S.A., 2008. Phytoplankton stoichiometry. *Ecological Research* 23, 479-485.
- Klein Breteler, W.C.M., Schogt, N., Baas, M., Schouten, S., Kraay, G.W., 1999. Trophic upgrading of food quality by protozoans enhancing copepod growth: role of essential lipids. *Marine Biology* 135, 191-198.
- Klein Breteler, W.C.M., Schogt, N., Rampen, S., 2005. Effect of diatom nutrient limitation on copepod development: role of essential lipids. *Marine Ecology Progress Series* 291, 125-133.
- Kleppel, G.S., 1993. On the diets of calanoid copepods. *Marine Ecology Progress Series* 99, 183-183.
- Koroleff, F., 1977. Simultaneous persulphate oxidation of phosphorus and nitrogen compounds in water. In: Grasshoff, K. (Ed.), *Report of the Baltic Intercalibration Workshop*, Annex Interim Commission for the Protection of the Environment of the Baltic Sea, pp. 52-53.
- Kudela, R.M., Dugdale, R.C., 2000. Nutrient regulation of phytoplankton productivity in Monterey Bay, California. *Deep Sea Research II* 47, 1023-1053.
- Kudela, R., Cochlan, W., Roberts, A., 2002. Spatial and temporal patterns of *Pseudo-nitzschia* species in central California related to regional oceanography. *Harmful Algae*, 347-349.

- Kuypers, M.M.M., Sliekers, A.O., Lavik, G., Schmid, M., Jorgensen, B.B., Kuenen, J.G., Sinninghe Damste, J.S., Strous, M., and Jetten, M.S.M., 2003. Anaerobic ammonium oxidation by anammox bacteria in the Black Sea. *Nature* 422, 608-611.
- Kuypers, M.M.M., Lavik, G., Woebken, D., Schmid, M., Fuchs, B.M., Amann, R., Jørgensen, B.B., Jetten, M.S.M., 2005. Massive nitrogen loss from the Benguela upwelling system through anaerobic ammonium oxidation. *Proceedings of the National Academy of Sciences* 102, 6478-6483.
- Lam, P., Lavik, G., Jensen, M.M., van de Vossenberg, J., Schmid, M., Woebken, D., Gutiérrez, D., Amann, R., Jetten, M.S.M., Kuypers, M.M.M., 2009. Revising the nitrogen cycle in the Peruvian oxygen minimum zone. *Proceedings of the National Academy of Sciences of the United States of America* 106, 4752-4757.
- Langlois, R.J., Hümmel, D., LaRoche, J., 2008. Abundances and distributions of the dominant *nifH* phylotypes in the Northern Atlantic Ocean. *Applied and Environmental Microbiology* 74, 1922-1931.
- Latasa, M., Berdalet, E., 1994. Effect of nitrogen and phosphorus starvation on pigment composition of cultured *Heterocapsa* sp. *Journal of Plankton Research* 16, 83-94.
- Lenton, T.M., Watson, A.J., 2000. Redfield revisited 1. Regulation of nitrate, phosphate, and oxygen in the ocean. *Global Biogeochemical Cycles* 14, 225-248.
- Lepère, C., Vaultot, D., Scanlan, D.J., 2009. Photosynthetic picoeukaryote community structure in the South East Pacific Ocean encompassing the most oligotrophic waters on Earth. *Environmental Microbiology* 11, 3105-3117.
- Levitus, S., Antonov, J.I., Boyer, T.P., Stephens, C., 2000. Warming of the world ocean. *Science* 287, 2225-2229.
- Lewin, J.C., 1962. Silicification. In: Lewin, J.C. (Ed.), *Physiology and biochemistry of the algae*, Academic Press, pp. 445-455.
- Liebig, J. von, 1855. Principles of Agricultural chemistry with special reference to the late researches made in England. 17-34. Reprinted in: Pomeroy, L.R., 1974. Cycles of essential elements. *Benchmark papers in Ecology* 1, Dowden, Hutchinson & Ross Inc., Stroudsburg, Pennsylvania, 11-28.
- Lincoln, J.A., Turner, J.T., Bates, S.S., Léger, C., Gauthier, D.A., 2001. Feeding, egg production, and egg hatching success of the copepods *Acartia tonsa* and *Temora longicornis* on diets of the toxic diatom *Pseudo-nitzschia multiseries* and the non-toxic diatom *Pseudo-nitzschia pungens*. *Hydrobiologia* 453, 107-120.
- Liu, H.B., Nolla, H.A., Campbell, L., 1997. *Prochlorococcus* growth rate and contribution to primary production in the equatorial and subtropical North Pacific Ocean. *Aquatic Microbial Ecology* 12, 39-47.
- Liu, H., Probert, I., Uitz, J., Claustre, H., Aris-Brosou, S., Frada, M., Not, F., deVargas, C., 2009. Extreme diversity in noncalcifying haptophytes explains a major pigment paradox in open oceans. *Proceedings of the National Academy of Sciences of the United States of America* 106, 12803-12808.
- Löscher, C.R., Großkopf, T., Gill, D., Schunck, H., Joshi, F., Pinnow, N., Lavik, G., Kuypers, M.M.M., LaRoche, J., Schmitz, R.A. Nitrogen fixation in the oxygen minimum zone off Peru. Unpublished results.

- Loladze, I., Elser, J.J., 2011. The origins of the Redfield nitrogen-to-phosphorus ratio are in a homeostatic protein-to-rRNA ratio. *Ecology Letters* 14, 244-250.
- Luyten, J.R., Pedlosky, J., and Stommel, H., 1983. The ventilated thermocline. *Journal of Physical Oceanography* 13, 292-309.
- Mackey, M.D., Mackey, D.J., Higgins, H.W., Wright, S.W., 1996. CHEMTAX—a program for estimating class abundances from chemical markers: application to HPLC measurements of phytoplankton. *Marine Ecology Progress Series* 144, 265–283.
- Mackey, M.D., Higgins, H.W., Mackey, D.J., Wright, S.W., 1997. CHEMTAX User's Manual: A Program for Estimating Class Abundances from Chemical Marker – Application to HPLC Measurements of Phytoplankton Pigments. CSIRO Marine Laboratories Report 229, Hobart, Australia, 47 pp.
- Mague, T.H., Friberg, E., Hughes, D.J., and Morris, I., 1980. Extracellular release of carbon by marine phytoplankton: A physiological approach. *Limnology and Oceanography* 25, 262-279.
- Malone, T.C., 1980. Algal size. In: Morris, I. (Ed.), *The Physiological Ecology of Phytoplankton*. Blackwell Scientific Publications, Oxford, pp. 433–463.
- Malzahn, A.M., Hantzsche, F., Schoo, K.L., Boersma, M., Aberle, N., 2010. Differential effects of nutrient-limited primary production on primary, secondary or tertiary consumers. *Oecologia* 162, 35-48.
- Margalef, R., 1973. Fitoplancton marino del la region de afloramiento del NW de Africa: II. Composition y distribucion del fitoplancton. *Res Exp Cient B/O Cornide* 2, 65–94.
- Margaelf, R., 1978. Phytoplankton communities in upwelling areas. The example of Northwest Africa. *Oecologia Aquatica* 3, 97-132.
- Matear, R.J., Hirst, A.C., 2003. Long-term changes in dissolved oxygen concentrations in the ocean caused by protracted global warming. *Global Biogeochemical Cycles* 17, 1125, doi:10.1029/2002GB001997.
- Mayzaud, P., Chanut, J.P., Ackman, R.G., 1989. Seasonal changes of the biochemical composition of marine particulate matter with special reference to fatty acids and sterols. *Marine Ecology Progress Series* 56, 189-204.
- Menden-Deuer, S., Lessard, E.J., 2000. Carbon to volume relationships for dinoflagellates, diatoms, and other protist plankton. *Limnology and Oceanography* 45, 569-579.
- Michaels, A.F., Silver, M.W., 1988. Primary production, sinking fluxes and the microbial food web. *Deep-Sea Research* 35, 473-490.
- Michaels, A.F., Olson, D., Sarmiento, J.L., Ammerman, J.W., Fanning, K., Jahnke, R., Knap, A.H., Lipschultz, F., Prospero, J.M., 1996. Inputs, losses and transformations of nitrogen and phosphorus in the pelagic North Atlantic Ocean. *Biogeochemistry* 35, 181-226.
- Mills, M.M., Ridame, C., Davey, M., LaRoche, J., Geider, R.J., 2004. Iron and phosphorus co-limit nitrogen fixation in the eastern tropical North Atlantic. *Nature* 429, 292-294.
- Mills, M.M., Arrigo, K.R., 2010. Magnitude of oceanic nitrogen fixation influenced by the nutrient uptake ratio of phytoplankton. *Nature Geoscience* 3, 412-416.

- Minas, H.J., Minas, M., Packard, T.T., 1986. Productivity in upwelling areas deduced from hydrographic and chemical fields. *Limnology and Oceanography* 31, 1182–1206.
- Minas, H.J., Minas, M., 1992. Net community production in “High Nutrient-Low Chlorophyll” waters of the tropical and Antarctic Oceans: grazing versus iron hypothesis. *Oceanologica Acta* 15, 145–162.
- Mohamed, H.E., van de Meene, A.M.L., Roberson, R.W., Vermaas, W.V.J., 2005. Myxoxanthophyll is required for normal cell wall structure and thylakoid organization in the cyanobacterium *Synechocystis* sp. strain PCC6803. *Journal of Bacteriology* 187, 6883–6892.
- Moisander, P.H., Beinart, R.A., Hewson, I., White, A.E., Johnson, K.S., Carlson, C.A., Montoya, J.P., Zehr, J.P., 2010. Unicellular cyanobacterial distributions broaden the oceanic N₂ fixation domain. *Science* 327, 1512–1514.
- Montoya, J.P., Holl, C.M., Zehr, J.P., Hansen, A., Villareal, T.A., Capone, D.G., 2004. High rates of N₂ fixation by unicellular diazotrophs in the oligotrophic Pacific Ocean. *Nature* 430, 1027–1032.
- Montoya, J.P., Voss, M., Capone, D.G., 2007. Spatial variation in N₂-fixation rate and diazotroph activity in the Tropical Atlantic. *Biogeosciences* 4, 369–376.
- Moore, L.R., Goericke, R., Chisholm, S.W., 1995. Comparative physiology of *Synechococcus* and *Prochlorococcus*: influence of light and temperature on growth, pigments, fluorescence and absorptive properties. *Marine Ecology Progress Series* 116, 259–275.
- Moore, J.K., Doney, S.C., 2007. Iron availability limits the ocean nitrogen inventory stabilizing feedbacks between marine denitrification and nitrogen fixation. *Global Biogeochemical Cycles* 21, GB2001, doi:10.1029/2006GB002762.
- Moore, C. M., Mills, M.M., Langlois, R., Milne, A., Achtberg, E.P., LaRoche, J., Geider, R.J., 2008. Relative influence of nitrogen and phosphorus availability on phytoplankton physiology and productivity in the oligotrophic sub-tropical North Atlantic Ocean. *Limnology and Oceanography* 53, 291–305.
- Müller-Navarra, D.C., Brett, M.T., Liston, A.M., Goldman, C.R., 2000. A highly unsaturated fatty acid predicts carbon transfer between primary producers and consumers. *Nature* 403, 74–77.
- Myklestad, S., Holm-Hansen, O., Vårum, K.M., and Volcani, B., 1989. Rate of release of extracellular amino acids and carbohydrates from the marine diatom *Chaetoceros affinis*. *Journal of Plankton Research* 11, 763–773.
- Needoba, J.A., Foster, R.A., Sakamoto, C., Zehr, J.P., Johnson, K.S., 2007. Nitrogen fixation by unicellular diazotrophic cyanobacteria in the temperate oligotrophic North Pacific Ocean. *Limnology and Oceanography* 52, 1317–1327.
- Niemi, A., 1979. Blue-green algal blooms and N:P ratio in the Baltic Sea. *Acta Botanica Fennica* 110, 57–61.
- Nixon, S.W., Ammerman, J.W., Atkinson, L.P., Berounsky, V.M., Billen, G., Boicourt, W.C., Boynton, W.R., Church, T.M., Ditoro, D.M., Elmgren, R., Garber, J.H., Giblin, A.E., Jahnke, R.A., Owens, N.J.P., Pilson, M.E.Q., Seitzinger, S.P., 1996. The fate of nitrogen and phosphorus at the land-sea margin of the North Atlantic Ocean. *Biogeochemistry* 35, 141–180.

- Okin, G.S., Baker, A.R., Tegen, I., Mahowald, N.M., Dentener, F.J., Duce, R.A., Galloway, J.N., Hunter, K., Kanakidou, Kubilay, N., prospero, J.M., Sarin, M., Surapipith, V., Uematsu, M., Zhu, T., 2011. Impacts of atmospheric nutrient deposition on marine productivity: Roles of nitrogen, phosphorus, and iron. *Global Biogeochemical Cycles* 25, GB2022, doi:10.1029/2010GB003858.
- Oschlies, A., Schulz, K.G., Riebesell, U., Schmittner, A., 2008. Simulated 21st century's increase in oceanic suboxia by CO₂-enhanced biotic carbon export. *Global Biogeochemical Cycles* 22, GB4008, doi:10.1029/2007GB003147.
- Paerl, H.W., Prufert-Bebout, L.E., Guo, C., 1994. Iron-stimulated N₂ fixation and growth in natural and cultured populations of the planktonic marine cyanobacteria *Trichodesmium* spp. *Applied and Environmental Microbiology* 60, 1044-1047.
- Partensky, F., Blanchot, J., Vaultot, D., 1999. Differential distribution and ecology of *Prochlorococcus* and *Synechococcus* in oceanic waters: a review. *Bulletin de l'Institut océanographique*, Monaco, spécial 19.
- Partensky, F., Hoepffner, N., Li, W.K., Ulloa, O., Vaultot, D., 1993. Photoacclimation of *Prochlorococcus* sp. (Prochlorophyta) strains isolated from the North Atlantic and the Mediterranean Sea. *Plant Physiology* 101, 295–296.
- Patoine, A., Graham, M.D., Leavitt, P.R., 2006. Spatial variation of nitrogen fixation in lakes of the northern Great Plains. *Limnology and Oceanography* 51, 1665-1677.
- Paulmier, A., Ruiz-Pino, D., Garçon, V., 2011. CO₂ maximum in the oxygen minimum zone (OMZ). *Biogeosciences* 8, 239-252.
- Pauly, D., Christensen, V., 1995. Primary production required to sustain global fisheries. *Nature* 374, 255-257.
- Pennington, J.T., Mahoney, K.L., Kuwahara, V.S., Kolber, D.D., Calienes, R., Chavez, F.P., 2006. Primary production in the eastern tropical Pacific: A review. *Progress in Oceanography* 69, 285-317.
- Penno, S., Campbell, L., Hess, W.R., 2000. Presence in phycoerythrin in two strains of *Prochlorococcus* (cyanobacteria) isolated from the subtropical North Pacific Ocean. *Journal of Phycology* 36, 723–729.
- Pitcher, G.C., Bolton, J.J., Brown, P.C., Hutchings, L., 1993. The development of phytoplankton blooms in upwelled waters of the southern Benguela upwelling system as determined by microcosm experiments. *Journal of Experimental Marine Biology and Ecology* 165, 171-189.
- Poulton, A.J., Stinchcombe, M.C., Quartly, G.D., 2009. High numbers of *Trichodesmium* and diazotrophic diatoms in the southwest Indian Ocean. *Geophysical Research Letters* 36, L15610.
- Probyn, T.A., 1985. Nitrogen uptake by size-fractionated phytoplankton populations in the southern Benguela upwelling system. *Marine Ecology Progress Series* 22, 249-258.
- Quigg, A., Finkel, Z.V., Irwin, A.J., Rosenthal, Y., Ho, T.-Y., Reinfelder, J.R., Schofield, O., Morel, F.M.M., Falkowski, P.G., 2003. The evolutionary inheritance of elemental stoichiometry in marine phytoplankton. *Nature* 425, 291–294.
- Rabalais, N.N., Diaz, R.J., Levin, L.A., Turner, R.E., Gilbert, D., Zhang, J., 2010. Dynamics and distribution of natural and human-caused hypoxia. *Biogeosciences* 7, 585-619.

- Ranhofer, M., Lawrenz, E., Pinckney, J., Benitez-Nelson, C., and Richardson, T., 2009. Cell-specific alkaline phosphatase expression by phytoplankton from Winyah Bay, South Carolina, USA. *Estuaries and Coasts* 32, 943-957.
- Redfield, A.C., 1958. The biological control of chemical factors in the environment. *American Scientist* 64, 205-221.
- Reid, J.L., Jr., 1965. Intermediate waters of the Pacific Ocean. *Johns Hopkins Oceanographic Studies* 2, 85.
- Řezanka, T., Dembitsky, V.M., 2006. Metabolites produced by cyanobacteria belonging to several species of the family Nostocaceae. *Folia Microbiologica* 51, 159-182.
- Rhee, G.-Y., 1978. Effects of N:P atomic ratios and nitrate limitation on algal growth, cell composition, and nitrate uptake. *Limnology and Oceanography* 23, 10-25.
- Richardson, T.L., Jackson, G.A., Ducklow, H.W., Roman, M.R., 2004. Carbon fluxes through food webs of the eastern equatorial Pacific: an inverse approach. *Deep-Sea Research I* 51, 1245-1274.
- Riebesell, U., Tortell, P.D., 2001. Effects of Ocean Acidification on Pelagic Organisms and Ecosystems. In: Gattuso, J.-P., Hansson, L. (Eds.), *Ocean Acidification*, Oxford University Press, Oxford, UK, pp. 99-121.
- Riebesell, U., Körtzinger, A., Oschlies, A., 2009. Sensitivities of marine carbon fluxes to ocean change. *Proceedings of the National Academy of Sciences of the United States of America* 106, 20602-20609.
- Riegman, R., Noordeloos, A.A.M., Cadée, G.C., 1992. *Phaeocystis* blooms and eutrophication of the continental coastal zones of the North Sea. *Marine Biology* 112, 479-484.
- Rojas de Mendiola, B., 1981. Seasonal phytoplankton distribution along the Peru coast. In: Richards, F.A. (Ed.), *Coastal Upwelling research*, American Geophysical Union, Washington, DC, pp. 345-356.
- Ryabenko, E., Kock, A., Bange, H.W., Altabet, M.A., Wallace, D.W.R., 2011. Contrasting biogeochemistry of nitrogen in the Atlantic and Pacific oxygen minimum zones. *Biogeosciences Discussions* 8, 8001-8039.
- Ryther, J.H., 1969. Photosynthesis and fish production in the sea. *Science*, 166, 72-76.
- Ryther, J.H., Dunstan, W.M., 1971. Nitrogen, phosphorus, and eutrophication in the coastal marine environment. *Science* 171, 1008-1013, 10.1126/science.171.3975.1008.
- Saino, T., Otake, H., Wada, E., Hattori, A., 1983. Subsurface ammonium maximum in the northern Pacific and the Bering Sea in summer. *Deep-Sea Research* 30, 1157-1171.
- Saito, M.A., Moffet, J.W., Chisholm, S.W., Waterbury, J.B., 2002. Cobalt limitation and uptake in *Prochlorococcus*. *Limnology and Oceanography* 47, 1629-1636.
- Saito, M.A., Goepfert, T.J., Ritt, J. T., 2008. Some thoughts on the concept of colimitation: Three definitions and the importance of bioavailability. *Limnology and Oceanography* 53, 276-290.

- Sanders, R., Morris, P.J., Poulton, A.J., Stinchcombe, M.C., Charalampopoulou, A., Lucas, M.I., Thomalla, S.J., 2010. Does a ballast effect occur in the surface ocean? *Geophysical Research Letters* 37, L08602, doi:10.1029/2010GL042574.
- Sañudo-Wilhelmy, S.A., Kustka, A.B., Gobler, C.J., Hutchins, D.A., Yang, M., Lwiza, K., Burns, J., Capone, D.G., Raven, J.A., Carpenter, E.J., 2001. Phosphorus limitation of nitrogen fixation by *Trichodesmium* in the central Atlantic Ocean. *Nature* 411, 66-69.
- Sarthou, G., Timmermans, K.R., Blain, S., Tréguer, P., 2005. Growth physiology and fate of diatoms in the ocean: a review. *Journal of Sea Research* 53, 25-42.
- Schneider, B., Engel, A., Schlitzer, R., 2004. Effects of depth- and CO₂-dependent C:N ratios of particulate organic matter (POM) on the marine carbon cycle. *Global Biogeochemical Cycles* 18, GB2015, doi:10.1029/2003GB002184.
- Seeyave, S., Probyn, T.A., Pitcher, G.C., Lucas, M.I., Purdie, D.A., 2009. Nitrogen nutrition in assemblages dominated by *Pseudo-nitzschia* spp., *Alexandrium catenella* and *Dinophysis acuminata* off the west coast of South Africa. *Marine Ecology Progress Series* 379, 91-107.
- Shaffer, G., Olsen, M.S., Pedersen, J.O.P., 2009. Long-term ocean oxygen depletion in response to carbon dioxide emissions from fossil fuels. *Nature Geoscience* 2, 105-109.
- Sharp, J.H., 1974. Improved analysis for particulate organic carbon and nitrogen from seawater. *Limnology and Oceanography* 19, 984-989.
- Sherr, E., Sherr, B., 1988. Role of microbes in pelagic food webs: a revised concept. *Limnology and Oceanography* 33, 1225-1227.
- Shuman, F.R., Lorenzen, C.J., 1975. Quantitative degradation of chlorophyll by a marine herbivore. *Limnology and Oceanography* 20, 580-586.
- Smetacek, V., 1999. Diatoms and the ocean carbon cycle. *Protist* 150, 25-32.
- Smith, S.L., Whittedge, T.E., 1977. The role of zooplankton in the regeneration of of nitrogen in a coastal upwelling system off northwest Africa. *Deep-Sea Research* 24, 49-56.
- Smith, V.H., 1983. Low nitrogen to phosphorus ratios favor dominance by blue-green algae in lake phytoplankton. *Science* 221, 669.
- Sohm, J.A., Capone, D.G., 2006. Phosphorus dynamics of the tropical and subtropical north Atlantic: *Trichodesmium* spp. versus bulk plankton. *Marine Ecology Progress Series* 317, 21-28.
- Soma, Y., Imaizumi, T., Yagi, K., Kasuga, S., 1993. Estimation of algal succession in lake water using HPLC analysis of pigments. *Canadian Journal of Fisheries and Aquatic Sciences* 50, 1142-1146.
- Sommer, U., Hansen, T., Stibor, H., Vadstein, O., 2004. Persistence of phytoplankton responses to different Si: N ratios under mesozooplankton grazing pressure: a mesocosm study with NE Atlantic plankton. *Marine Ecology Progress Series* 278, 67-75.
- Staal, M., te Lintel Hekkert, S., Brummer, G.J., Veldhuis, M., Sikkens, C., Persijn, S., Stal, L.J., 2007. Nitrogen fixation along a north-south transect in the eastern Atlantic Ocean. *Limnology and Oceanography* 52, 1305-1316.
- Stal, L.P., 2009. Is the distribution of nitrogen-fixing cyanobacteria in the oceans related to temperature? *Environmental Microbiology* 11, 1632-1645.

- Sterner, R.W., Schulz, K.L., 1998. Zooplankton nutrition: recent progress and a reality check. *Aquatic Ecology* 32, 261-279.
- Sterner, R.W., Elser, J.J., 2002. *Ecological stoichiometry: The biology of elements from molecules to the biosphere*. Princeton Univ. Press.
- Stevens, H., and Ulloa, O., 2008. Bacterial diversity in the oxygen minimum zone of the eastern tropical South Pacific. *Environmental Microbiology* 10, 1244–1259.
- Stewart, F.J., Ulloa, O., DeLong, E.F., 2011. Microbial metatranscriptomics in a permanent marine oxygen minimum zone. *Environmental Microbiology* 14, 23-40.
- Stramma, L., Johnson, G.C., Sprintall, J., Mohrholz, V., 2008. Expanding oxygen-minimum zones in the tropical oceans. *Science* 320, 655-658.
- Strickland, J.D.H., Eppley, R.W., de Mendiola, B.R., 1969. Phytoplankton populations, nutrients and photosynthesis in Peruvian coastal waters. *Bol. Inst. del Mar del Peru* 2, 4–45.
- Suess, E., 1981. Phosphate regeneration from sediments of the Peru continental margin by dissolution of fish debris. *Geochimica et Cosmochimica Acta* 45, 577-588.
- Sunda, W.G., Huntsman, S.A., 1995. Iron uptake and growth limitation in oceanic and coastal phytoplankton. *Marine Chemistry* 50, 189-206.
- Talbot, R.W., Harriss, R.C., Browell, E.V., Gregory, G.L., Sebach, D.I., Beck, S.M., 1986. Distribution and geochemistry of aerosols in the tropical North Atlantic troposphere: relationship to Saharan dust. *Journal of Geophysical Research* 91, 5173-5182.
- Tang, K.W., Jakobsen, H.H., Visser, A.W., 2001. *Phaeocystis globosa* (Prymnesiophyceae) and the planktonic food web: feeding, growth, and trophic interactions among grazers. *Limnology and Oceanography* 46, 1860-1870.
- Tang, S., Jiang, L., Wu, Z.J., 2009. Adding nitrate and phosphate separately or together in the Central Indian Ocean: a nutrient enrichment experiment. *Ocean Science Discussions* 6, 2649-2666.
- Thamdrup, B., Dalsgaard, T., 2002. Production of N₂ through anaerobic ammonium oxidation coupled to nitrate reduction in marine sediments. *Applied and Environmental Microbiology* 68, 1312-1318.
- Thingstad, T.F., Skjoldal, E.F., Bohne, R.A., 1993. Phosphorus cycling and algal-bacterial competition in Sandsfjord, western Norway. *Marine Ecology Progress Series* 99, 239-259.
- Thomas, W.H., 1969. Phytoplankton nutrient enrichment experiments off Baja California and in the eastern equatorial Pacific Ocean. *Journal of the Fisheries Research Board of Canada* 26, 1133-1145.
- Thomas, W.H., Seibert, D.L.R., Dodson, A.N., 1974. Phytoplankton enrichment experiments and bioassays in natural coastal sea water and in sewage outfall receiving waters off Southern California. *Estuarine and Coastal Marine Science* 2, 191-206.
- Thomas, W.H., 1979. Anomalous nutrient-chlorophyll interrelationships in the offshore eastern tropical Pacific Ocean. *Journal of Marine Research* 37, 327–335.
- Tilman, D., 1982. *Resource competition and community structure*. Princeton University Press, Princeton, New Jersey.

- Tortell, P.D., DiTullio, G.R., Sigman, D.M., Morel, F.M.M., 2002. CO₂ effects on taxonomic composition and nutrient utilization in an Equatorial Pacific phytoplankton assemblage. *Marine Ecology Progress Series* 236, 37-43.
- Trimmer, M., Nicholls, J.C., 2009. Production of nitrogen gas via anammox and denitrification in intact sediment cores along a continental to slope transect in the North Atlantic. *Limnology and Oceanography* 54, 577-589.
- Tripp, H.J., Bench, S.R., Turk, K.A., Foster, R.A., Desany, B.A., Niazi, F., Affourtit, J.P., Zehr, J.P., 2010. Metabolic streamlining in an open-ocean nitrogen-fixing cyanobacterium. *Nature* 464, 90-94.
- Turner, J.T., Ianora, A., Esposito, F., Carotenuto, Y., Miralto, A., 2002. Zooplankton feeding ecology: does a diet of *Phaeocystis* support good copepod grazing, survival, egg production and egg hatching success? *Journal of Plankton Research* 24, 1185-1195.
- Tyrrell, T., Marañón, E., Poulton, A.J., Bowie, A.R., Harbour, D.S., Woodward, E.M.S., 2003. Large-scale latitudinal distribution of *Trichodesmium* spp. in the Atlantic Ocean. *Journal of Plankton Research* 25, 405-416.
- Uitz, J., Claustre, H., Gentili, B., Stramski, D., 2010. Phytoplankton class-specific primary production in the world's oceans: Seasonal and interannual variability from satellite observations. *Global Biogeochemical Cycles* 24, GB3016, doi:10.1029/2009GB003680.
- Utermöhl, H., 1958. Zur Vervollkommnung der quantitativen Phytoplankton Methodik. *Mitteilungen der Internationalen Vereinigung für Theoretische und Angewandte Limnologie* 9, 263-272.
- Van Cappellen, P., Berner, R.A., 1988. A mathematical model for the early diagenesis of phosphorus and fluorine in marine sediments; apatite precipitation. *American Journal of Science* 288, 289-333.
- Van Cappellen, P., Ingall, E.D., 1994. Benthic phosphorus regeneration, net primary production, and ocean anoxia: A model of the coupled marine biogeochemical cycles of carbon and phosphorus. *Paleoceanography* 9, 677-692.
- Vaquier-Sunyer, R., Duarte, C.M., 2008. Thresholds of hypoxia for marine biodiversity. *Proceedings of the National Academy of Sciences* 105, 15452.
- Vargas, C.A., Escribano, R., Poulet, S., 2006. Phytoplankton food quality determines time windows for successful zooplankton reproductive pulses. *Ecology* 87, 2992-2999.
- Veldhuis, M.J.W., Kraay, G.W., 2004. Phytoplankton in the subtropical Atlantic Ocean: towards a better assessment of biomass and composition. *Deep-Sea Research I* 51, 507-530.
- Vince, S., Valiela, I., 1973. The effects of ammonium and phosphate enrichments on chlorophyll *a*, pigment ratio and species composition of phytoplankton of Vineyard Sound. *Marine Biology* 19, 69-73.
- Voss, M., Croot, P., Lochte, K., Mills, M., Peeken, I., 2004. Patterns of nitrogen fixation along 10°N in the tropical Atlantic. *Geophysical Research Letters* 31, doi:10.1029/2004GL020127.
- Vrede, T., Ballantyne, A., Mille Lindblom, C., Algesten, G., Gudas, C., Lindahl, S., Brunberg, A.K., 2009. Effects of N: P loading ratios on phytoplankton community composition, primary production and N fixation in a eutrophic lake. *Freshwater Biology* 54, 331-344.

- West, J.A., McBride, D.L., 1999. Long-term and diurnal carpospores discharge patterns in the Ceramiaceae, Rhodomelaceae and Delesseriaceae (Rhodophyta). *Hydrobiologia* 298/299, 101-113.
- Webb, E.A., Ehrenreich, I.M., Brown, S.L., Valois, F.W., Waterbury, J.B., 2009. Phenotypic and genotypic strains of the diazotrophic cyanobacterium, *Crocospaera watsonii*, isolated from the open ocean. *Environmental Microbiology* 11, 338-348.
- Wetz, M.S., Wheeler, P.A., 2003. Production and partitioning of organic matter during simulated phytoplankton blooms. *Limnology and Oceanography* 48, 1808-1817.
- White, E., Payne, G.W., 1977. Chlorophyll production, in response to nutrient additions, by the algae in Lake Taupo water. *New Zealand Journal of Marine and Freshwater Research* 11, 501-507.
- White, K.K., Dugdale, R.C., 1997. Silicate and nitrate uptake in the Monterey Bay upwelling system. *Continental Shelf Research* 17, 455-472.
- Wilkerson, F.P., Dugdale, R.C., Kudela, R.M., Chavez, F.P., 2000. Biomass and productivity in Monterey Bay, California: contribution of the large phytoplankton. *Deep-Sea Research II* 47, 1003-1022.
- Winkler, L.W., 1888. Die Bestimmung des im Wasser gelösten Sauerstoffes. *Ber. Dtsch. Chem. Ges.* 21, 2843-2855.
- Wu, J.F., Sunda, Boyle, E.A., Karl, D.M., 2000. Phosphate depletion in the western North Atlantic Ocean. *Science* 289, 759-762.
- Wurl, O., Min Sin, T., 2009. Analysis of dissolved and particulate organic carbon with the HTCO technique. In: Wurl, O. (Ed.), *Practical Guidelines for the Analysis of Seawater*. CRC Press, Boca Raton, pp. 33-48.
- Zehr, J.P., Waterbury, J.B., Turner, P.J., Montoya, J.P., Omoregie, E., Steward, G.F., Hansen, A., Karl, D.M., 2001. Unicellular cyanobacteria fix N₂ in the subtropical North Pacific Ocean. *Nature* 412, 635-637.
- Zehr, J.P., Bench, S.R., Carter, B.J., Hewson, I., Niazi, F., Shi, T., Tripp, J., Affourtit, J.P., 2008. Globally distributed uncultivated oceanic N₂-fixing cyanobacteria lack oxygenic photosystem II. *Science* 322, 1110-1112.
- Zani, S., Mellon, M.T., Collier, J.L., Zehr, J.P., 2000. Expression of *nifH* genes in natural microbial assemblages in Lake George, New York, detected by reverse transcriptase PCR. *Applied Environmental Microbiology* 66, 3119-3124.

Contributions of authors

Study 1.

Franz, J., Krahmann, G., Lavik, G., Grasse, P., Dittmar, T., Riebesell, U.: Dynamics and stoichiometry of nutrients and phytoplankton in waters influenced by the oxygen minimum zone in the tropical eastern Pacific, *Deep-Sea Research Part I* 62, 20-31, 2012.

Jasmin Franz performed sampling, analysis of the samples, evaluation of the data and wrote the manuscript. Gerd Krahmann provided CTD data and assisted with the hydrography of the study area. Gaute Lavik and Patricia Grasse provided nutrient data. Thorsten Dittmar provided data on dissolved organic carbon. Ulf Riebesell assisted with input to the manuscript and revision.

Study 2.

Hauss, H.M., **Franz, J.M.S.**, Sommer, U.: Changes in N/P stoichiometry influence taxonomic composition and nutritional quality of phytoplankton in the Peruvian upwelling, *under review, Journal of Sea Research*.

Helena Hauss and Jasmin Franz conducted the experiments and analysis of the samples. Helena Hauss furthermore evaluated the data and wrote the manuscript. Ulrich Sommer provided data on phytoplankton counts, assisted experiment performance and manuscript revision.

Study 3.

Franz, J.M.S., Hauss, H.M., Löscher, C.R., Riebesell, U.: Effect of different nutrient conditions on the taxonomical composition of a phytoplankton community in the eastern tropical Atlantic, *to be submitted*.

Jasmin Franz and Helena Hauss conducted the experiments and analysis of the samples. Jasmin Franz furthermore evaluated the data and wrote the manuscript. Carolin Löscher provided molecular data on gene copies. Ulf Riebesell assisted with input to the manuscript and revision.

Study 4.

Franz, J.M.S., Hauss, H.M., Dittmar, T., Sommer, U., Riebesell, U.: Production, partitioning and stoichiometry of organic matter under different nutrient supply during mesocosm experiments in the tropical Pacific and Atlantic Ocean, *submitted for peer-review to Biogeosciences*.

Jasmin Franz and Helena Hauss conducted the experiments and evaluated the data. Jasmin Franz furthermore analyzed the samples and wrote the manuscript. Thorsten Dittmar provided

data on dissolved organic matter. Ulrich Sommer assisted with experiment performance and manuscript revision. Ulf Riebesell assisted with input to the manuscript and revision.

In addition, I have contributed to the following publications and manuscripts in the framework of the SFB 754 (Climate-Biogeochemical Interactions in the Tropical Ocean):

Hauss, H.M., **Franz, J.M.S.**, Hansen, T., Struck, U., Sommer, U.: Relative contribution of upwelled and atmospheric nitrogen to zooplankton production in the eastern tropical North Atlantic: Spatial distribution and relation to dissolved nutrient dynamics, *submitted for peer-review to Deep-Sea Research Part I*.

Ehlert, C., Grasse, P., Mollier-Vogel, E., Bösch, T., **Franz, J.M.S.**, de Souza, G.F., Reynolds, B.C., Stramma, L., Frank, M.: Silicon isotope distribution in waters and surface sediments of the Peruvian coastal upwelling, *to be submitted*.

Danksagung

Ich danke meinem Betreuer Ulf Riebesell, dass er mir die Möglichkeit gegeben hat, an so einem spannenden Thema zu arbeiten, sowie für den wertvollen Input und die lehrreichen Tipps bei der Erstellung der Manuskripte.

Vielen Dank auch an Uli Sommer, besonders für den Einsatz und die Zusammenarbeit auf der Peru-Ausfahrt.

Liebe Leni, du bist einfach ne Wucht und es war mir eine Ehre und wahre Freude mit dir dieses Abenteuer „Mesokosmen auf großer Reise im tropischen Ozean“ inklusive aller Höhen und Tiefen bestreiten zu dürfen. Ob beim Kampf mit dem störrischen GS „Arizona“, beim nächtlichen Grübeln über Nährstoffeinwaagen, Nährstofflösungen, Nährstoffkonzentrationen, Nährstoffverhältnisse, Nährstoffzugaben, Nährstoffaufnahme, Nährstofflimitation usw., beim „Wie bastel ich mir einen Mesokosmos?“, beim „Wo zum Teufel ist der Boden des Mesokosmos geblieben?“, oder beim Turnen auf, zwischen oder unter Zargeskisten, dein zupackendes Naturell und dein unerschütterlicher (zynischer) Humor haben vieles erträglicher gemacht und mich in höchstem Maße amüsiert.

Ich möchte auch der ganzen Mannschaft des SFB 754 für vier Jahre in einem großartigen Projekt (finanziert durch die DFG) danken. Besonderer Dank geht an die Fahrtleiter der Meteor-Reisen (Martin Frank, Doug Wallace und Martin Visbeck), an die CTD-Teams (Gerd Krahmann, Rudi Link, Lothar Stramma) und an einen wirklich umwerfenden Haufen an Doktoranden, mit denen ich sehr schöne und vor allem lustige Zeiten verbringen durfte. Harry, Paddy, Caro, Tobi, Tim, Anna, Oli, es war mir wirklich ein großes Vergnügen!

Vielen Dank auch an die Crew der Meteor, die uns drei tolle und erfolgreiche Ausfahrten ermöglicht hat.

Liebe Kerstin und lieber Peter, was hätte ich nur ohne euch angestellt?! Ihr habt diese ganze Arbeit erst möglich gemacht, durch Einarbeiten in Messmethoden, durch Messen tausender Nährstoffproben, durch den erstaunlichen Überblick beim Packen (79! Packstücke lieber Peter für eine Ausfahrt) und letztendlich durch Weitergabe eines unerschöpflichen Erfahrungsschatzes. Vielen Dank euch beiden! Danke aber natürlich auch an Master Hansen, Aljoscha und Martina. Und was hätt ich nur ohne den unermüdlichen Laboreinsatz von dir, lieber Scarlett gemacht. Muchas gracias princessa, para tu trabajao y tu amistad!

Danke an meine BI-Arbeitsgruppe, vor allem an meine langjährigen Bürozimmer-Kollegas Lennart und Sarah, aber auch an Kai S. (Stichwort: Matlab), Joana, Signe, Kai L., Andrea, Jan B. und wen ich noch vergessen hab...Ihr seid spitze und habt mir die Arbeitszeit sehr versüßt.

Lieber Benni, danke dass ich mich immer beim Fussballschauen mit dir und deinem Beamer von der „Arbeit“ erholen konnte und einfach dass du so nen dufter Kumpel bist. Das gleiche gilt für Matze und Enrico.

Lieber Janni, dir möchte ich zuallererst für deine langjährige treue Freundschaft danken, dafür, dass du einfach immer für mich da warst! Zudem weiß ich deine kritischen Hinterfragungen und deinen Input zu meiner Arbeit durchaus sehr zu schätzen, auch wenn es manchmal nicht so den Anschein gemacht hat...Danke auch, dass ich mich auf den zahlreichen Segeltörns auf deinem Boot von meiner anstrengenden Doktorarbeit erholen durfte.

Liebe Family (vor allem natürlich Mama und Papa Franz), ihr seid sowieso die Allercoolsten! Vielen Dank für eure Liebe und Unterstützung.

Eidesstattliche Erklärung

Hiermit erkläre ich an Eides statt, dass die vorliegende Dissertation, abgesehen von der Beratung durch meinen Betreuer, nach Inhalt und Form meine eigene Arbeit ist und ich keine anderen als die angegebenen Quellen und Hilfsmittel verwendet habe. Ferner versichere ich, dass die vorliegende Dissertation weder im Ganzen noch zum Teil einer anderen Stelle im Rahmen eines Prüfungsverfahrens vorgelegen hat und unter Einhaltung der Regeln guter wissenschaftlicher Praxis der Deutschen Forschungsgemeinschaft entstanden ist.

Kiel, den

Jasmin Franz